DOCTOR OF PHILOSOPHY

The analysis of genome stability maintenance mechanisms in human cancer cells and stem cells

Alzahrani, Faisal

Award date:
2015

Awarding institution:
Bangor University

PRIFYSGOL
BANGOR
UNIVERSITY

THE ANALYSIS OF GENOME STABILITY MAINTENANCE MECHANISMS IN HUMAN CANCER CELLS AND STEM CELLS

Ph.D. Thesis

NOVEMBER 1, 2014

Faisal Abdulrahman ALZAHRANI

Declaration and Consent

Details of the Work

I hereby agree to deposit the following item in the digital repository maintained by Bangor University and/or in any other repository authorized for use by Bangor University.

Author Name: Faisal Abdulrahman ALZAHRANI

Title: The analysis of genome stability maintenance mechanisms in human cancer cells and stem cells

Supervisor/Department: Dr. Ramsay James McFarlane

Funding body (if any): King Abdulaziz University - Saudi Ministry of Education

Qualification/Degree obtained: PhD in Molecular Biology of Cancer and Stem cells

This item is a product of my own research endeavours and is covered by the agreement below in which the item is referred to as "the Work". It is identical in content to that deposited in the Library, subject to point 4 below.

Non-exclusive Rights

Rights granted to the digital repository through this agreement are entirely non-exclusive. I am free to publish the Work in its present version or future versions elsewhere.

I agree that Bangor University may electronically store, copy or translate the Work to any approved medium or format for the purpose of future preservation and accessibility. Bangor University is not under any obligation to reproduce or display the Work in the same formats or resolutions in which it was originally deposited.

Bangor University Digital Repository

I understand that work deposited in the digital repository will be accessible to a wide variety of people and institutions, including automated agents and search engines via the World Wide Web.

I understand that once the Work is deposited, the item and its metadata may be incorporated into public access catalogues or services, national databases of electronic

theses and dissertations such as the British Library's EThOS or any service provided by the National Library of Wales.

I understand that the Work may be made available via the National Library of Wales Online Electronic Theses Service under the declared terms and conditions of use (http://www.llgc.org.uk/index.php?id=4676). I agree that as part of this service the National Library of Wales may electronically store, copy or convert the Work to any approved medium or format for the purpose of future preservation and accessibility. The National Library of Wales is not under any obligation to reproduce or display the Work in the same formats or resolutions in which it was originally deposited.

Statement 1:

This work has not previously been accepted in substance for any degree and is not being concurrently submitted in candidature for any degree unless as agreed by the University for approved dual awards.

Signed …….. (candidate)

Date ……..

Statement 2:

This thesis is the result of my own investigations, except where otherwise stated. Where correction services have been used, the extent and nature of the correction is clearly marked in a footnote(s).

All other sources are acknowledged by footnotes and/or a bibliography.

Signed ……. (candidate)

Date …….

Statement 3:

I hereby give consent for my thesis, if accepted, to be available for photocopying, for inter-library loan and for electronic repositories, and for the title and summary to be made available to outside organisations.

Signed ……. (candidate)

Date …….

NB: Candidates on whose behalf a bar on access has been approved by the Academic Registry should use the following version of **Statement 3:**

Statement 3 (bar):

I hereby give consent for my thesis, if accepted, to be available for photocopying, for inter-library loans and for electronic repositories after expiry of a bar on access.

Signed …… (candidate)

Date ……

Statement 4:

Choose **one** of the following options

a) I agree to deposit an electronic copy of my thesis (the Work) in the Bangor University (BU) Institutional Digital Repository, the British Library ETHOS system, and/or in any other repository authorized for use by Bangor University and where necessary have gained the required permissions for the use of third party material.	
b) I agree to deposit an electronic copy of my thesis (the Work) in the Bangor University (BU) Institutional Digital Repository, the British Library ETHOS system, and/or in any other repository authorized for use by Bangor University when the approved **bar on access** has been lifted.	
c) I agree to submit my thesis (the Work) electronically via Bangor University's e-submission system, however I **opt-out** of the electronic deposit to the Bangor University (BU) Institutional Digital Repository, the British Library ETHOS system, and/or in any other repository authorized for use by Bangor University, due to lack of permissions for use of third party material.	

Options B should only be used if a bar on access has been approved by the University.

In addition to the above I also agree to the following:

1. That I am the author or have the authority of the author(s) to make this agreement and do hereby give Bangor University the right to make available the Work in the way described above.

2. That the electronic copy of the Work deposited in the digital repository and covered by this agreement, is identical in content to the paper copy of the Work deposited in the Bangor University Library, subject to point 4 below.

3. That I have exercised reasonable care to ensure that the Work is original and, to the best of my knowledge, does not breach any laws – including those relating to defamation, libel and copyright.

4. That I have, in instances where the intellectual property of other authors or copyright holders is included in the Work, and where appropriate, gained explicit permission for the inclusion of that material in the Work, and in the electronic form of the Work as accessed through the open access digital repository, *or* that I have identified and removed that material for which adequate and appropriate permission has not been obtained and which will be inaccessible via the digital repository.

5. That Bangor University does not hold any obligation to take legal action on behalf of the Depositor, or other rights holders, in the event of a breach of intellectual property rights, or any other right, in the material deposited.

6. That I will indemnify and keep indemnified Bangor University and the National Library of Wales from and against any loss, liability, claim or damage, including without limitation any related legal fees and court costs (on a full indemnity bases), related to any breach by myself of any term of this agreement.

Signature: …… Date : …….

Abstract

Maintaining genome stability is essential for all dividing cells and it promotes longevity. The centromere is one region where stability is critical, as this is where the kinetochore identifies and attaches the spindle microtubules so that each sister chromatid can faithfully segregate. Our knowledge of centromere mechanism has improved vastly over the last decade. A functional role for homologous recombination within centromeric DNA has been proposed whereby covalently closed DNA loops (CCLs) are formed. We examined this model by studying the sites of deposition of the centromere marker, CENP-A, in cells that accumulate Holliday structures throughout there chromosomes. Whilst we found no direct evidence for CENP-A deposition at Holliday junction, tools for further analysis of this important question were developed.

Embryonic stem cells (ESCs) are derived from the inner cell mass of the blastocyst. ESCs give rise to lineages leading to all the somatic cells of the developing embryo. Therefore, any epigenetic disturbances or genome defects that occur in the genome at this early stage would have detrimental consequences for the embryo as a whole. Hence, these cells are likely to possess high fidelity genome maintenance mechanisms.

It has been shown that human stem cells and embryonal carcinoma cells do not show the same checkpoint-dependent response to DNA replication inhibition. In the present study, we used the SW480 and HCT116 cancer cell lines as non-stem cell controls, with the expectation that these cells would behave like somatic cells. We also used these cells to derive so called colonospheres, which are a proliferating population arising from these cells lines that have some key characteristics of cancer stem cells. We clearly demonstrated that cancer cells appear to respond distinctly to certain chemotherapeutic genome damaging agents when they transition to a more stem cell-like state. A key observation was the dramatic reduction in BLM and GEN1 levels in parallel with the appearance of stem cell markers upon sphere formation. The implications for chromosomal instability following DNA replication stress were also explored and assessed. We also successfully generated induced pluripotent stem cells (iPSCs) from human fibroblasts using modified mRNA. We used these cells and their isogenic parental cells to determine whether these cells differ in responses DNA damaging agent from isogenic fibroblast and/or embryonic stem cells.

Acknowledgements

All praise is due to Allah for the blessing and strength he gave me to begin and complete this journey, which is probably one of the biggest challenges I have faced thus far in my life. The best and worst moments were shared with many to whom I will always be grateful as without their support, kindness, patience and guidance, this work may not have seen the light of day. It is to them, after God, that I owe my deepest appreciation.

My first debt of gratitude goes to my supervisor and our group leader, Dr. Ramsay McFarlane, who patiently provided the vision, encouragement and advice that helped me to advance through the program and complete my work. It was an honour to work and study under his guidance. His comments and suggestions throughout were instrumental to the success of this study. I thank him for his friendship, empathy and great sense of humour. I also extend my heartfelt thanks to Dr. Jane Wakeman for her patience and advice during my work on stem cells.

Special thanks go to my family. I will always be grateful to my parents for their love, prayers and sacrifice. It is under their watchful eye that I gained the drive and ability to tackle challenges head on. My beloved wife Asmaa Ramzi and my sons have been an amazing source of inspiration and encouragement. Thank you, Asmaa, for looking after me so well during the final writing up period and for listening to me talking about cancer and stem cells every night for the past four years. I extend my thanks also to my sisters and brothers for their invaluable support and prayers.

My friends and research colleagues (the D7 team in particular) also deserve my sincerest appreciation; their friendship and assistance have meant more to me than I can sufficiently express. It was a privilege to study in the Department of Biological Sciences of Bangor University; its staff will always remain dear to me.

I am obliged to the Saudi Government for its sponsorship through the King Abdullah Program for Higher Education and King Abdul-Aziz University.

Last, but not least, for those who helped make this an amazing experience, but whose names are too many to list, THANK YOU!

List of Abbreviations

132N1	Human brain astrocytoma
5-dRP	5-deoxyribose phosphate
ABC	ATP-binding cassette
AML	Acute myeloid leukemia
AP site	Apurinic/apyrimidinic site
APH	Aphidicolin
ATM	Ataxia telangiectasia mutated
BER	Base excision repair
BLM	Bloom
BrdU	5-bromo-2'-deoxyuridine
BRDU	Bromodeoxyurdine
BS	Bloom syndrome
CATD	CENP-A targeting domain
CCL	Covalently closed loop
CDK	Cyclin-dependent kinases
cDNA	Complementary DNA
CENP-A	Centromere protein A
CHK	Checkpoint kinase
CIS	Cisplatin
Cisplatin	*Cis*-diamminedichloroplatinum II
cnt	Central core
CO	Crossover
CPDs	Cyclobutane–pyrimidine dimers
CPT	Camptothecin
CSCs	Cancer Stem Cells
DAPI	4',6-diamidino-2-phenylindole
dHJ	Double Holliday junction
DmBlm	The *Drosophila* orthologue of BLM
DMEM	Dulbecco's Modified Eagle Medium
DMSO	Dimethyl sulfoxide
dNTPs	Four deoxynucleoside triphosphates
DPBS	Dulbecco's phosphate-buffered saline
DSBs	DNA double-strand breaks
ECACC	European Collection of Cell Cultures
EGFR	Epidermal growth factor receptor
EMT	Epithelial-mesenchymal transition
ESC	Embryonic stem cells
Exo1	Exonuclease 1
FA	Fanconi anaemia
FBS	Foetal bovine serum
GCT	Testicular germ cell tumour

GG-NER	Global genomic NER
H3K4	Histone H3 lysine 4
HAC	Human artificial chromosome
HAT	Histone acetyltransferases
hESC	Human ESC
HJURP	Holliday junction recognizing protein
HR	Homologous recombination
HRP	Horseradish peroxidase
imr	Inner most repeats
iPSC	Induced pluripotent stem cell
KCM	Chromosome medium buffer
LIF	Leukaemia inhibitory factor
LOH	Loss of heterozygosity
mAbs	Monoclonal antibodies
MEF	Mouse embryo fibroblast
MMR	The mismatch repair
MutSα	MSH2/MSH6
NER	Nucleotide excision repair
NHEJ	Non-homologous end-joining
NSCLC	Non-small-cell lung cancer
NTC	Non-tumorigenic cell
otr	Outer repeats
PB	*piggyback*
PCNA	Proliferating Cell Nuclear Antigen
PCR	Polymerase chain reaction
PFA	Paraformaldehyde
PI	Propidium Iodide
PTMs	Post-translational modifications
PVDF	The Immobilon-P Membrane
RFC	Replication factor C
ROS	Reactive oxygen species
RSS	The recombination signal sequences
RT-PCR	Reverse transcription-PCR
SAC	Spindle assembly checkpoint
SCE	Sister chromatid exchange
SCM	Stem cell medium
SCNT	Somatic cell nuclear transfer
SDS	Sodium dodecyl sulphate
SDSA	Synthesis-dependent strand annealing
SFM	Serum-free medium
siRNA	Small interfering RNA
SSB	Single strand break
ssDNA	Single-stranded DNA
TC-NER	Transcription coupled NER

TDR	Thymidine
tetO	Tetracycline operator
TIC	Tumour-initiating cell
TNP	Nanoparticles
Top 1	DNA topoisomerase I
tRNA	Transfer RNA
UFBs	Ultra-fine DNA bridges
UV	Ultraviolet light
V(D)J	Variable diversity and Joining coding segments
VEGF-A	Vascular endothelial growth factor-A

Key words

Apoptosis, BLM, Bloom Syndrome, Cell cycle, CENP-A, Centromere, DNA damage repair, GEN1, genome instability, H2AX, HJURP, Holliday Junction, Homologues recombination, iPSC, MUS81, SCE, Stem cells.

Contents

List of Figures

List of Tables

Chapter 1

Introduction

Chapter 1. Introduction

1.1 Overview of the mitotic cell cycle

Human bodies are made of billions of some 200 different types of cells that behave differently and carry out specific roles (Watt and Driskell, 2010). Each cell type has a distinct morphology and differs in size according to their sites and functions. Almost all of these cells divide continuously in a precise mechanism to produce more cells but at a controlled rate, depending on their purposes, such as for repairing, replacement and growth. Germ line cells may undergo meiosis to produce gametes, but somatic cell divisions occur via mitosis. During mitosis, cells undergo sequential steps to produce identical copies of their genetic information and pass them from one cell to another (Hejmadi, 2010).

The eukaryotic cell cycle process defines the two major phases which are S (synthesis) phase and M (mitosis) phase. S phase is the period during which chromosomes are duplicated. M phase is the shortest phase in the cell cycle though the cell undergoes four sub phases during this phase: prophase, metaphase, anaphase and telophase. (Brevini and Pennarossa, 2013).

These phases are separated by two main gaps known; Gap-1 (G1) and Gap-2 (G2) (Kronja and Orr-Weaver, 2011). There is an additional gap phase, a G0 phase or quiescent state, when cell conditions are unfavourable for replication. This quiescence is a common feature of adult metazoan cells when proliferation signals are not present (O'Farrell, 2011). Most of the cell cycle activities take place during G1, S and G2 phases which are together called interphase (Singh and Dalton, 2014).

The cell cycle process encompass some DNA damage and DNA replication checkpoints through which the cell ensures fidelity of the DNA. The cell will not progress through these checkpoints if the DNA is damaged. Cyclin-dependent kinases (CDK) and their respective regulatory cyclin subunits control the progression of the cell through these checkpoints. Activation of these proteins may causes cell-cycle arrest following DNA damage or replication stress (Williams and Stoeber, 2012). Their activity may also drive the cells to speed up or slow down the cell cycle (Sorensen and Syljuasen, 2012) (Figure 1.1).

1.2 Cancerous cell

Cancer is one of the major causes of death and a key cause of many health problems globally. It was originally thought that cancer was linked with the modern lifestyle. However, various team of archaeologists recently found a 3,000 years old skeleton that had developed cancer and showed lesions in the bones and metastases in different places in the body (Kelland, 2014). Despite the significant improvement in cancer survival rates, recent studies estimated that millions of cancer patients will face death in the coming years (Siegel et al., 2013). Cancer is cellular disease in which cells lose control of division and acquire invasiveness traits. Cancer starts in a cell with mutation or alteration to regulation of genes that control growth, division and cellular activity. The major groups of genes contribute to cancer are oncogenes, tumour suppressor genes and DNA repair genes (Larsson, 2011). For example, the significant role of *p53* in tumour suppression has been studied extensively over the last three decade (Brady and Attardi, 2010). Analyses from different types of cancer show mutations in *p53* led to cell cycle dysfunction (Muller and Vousden, 2013). On the other hand, reactivation of p53 protein has stimulated cancer regression in mouse model (Ventura et al., 2007) (Figure 1.1).

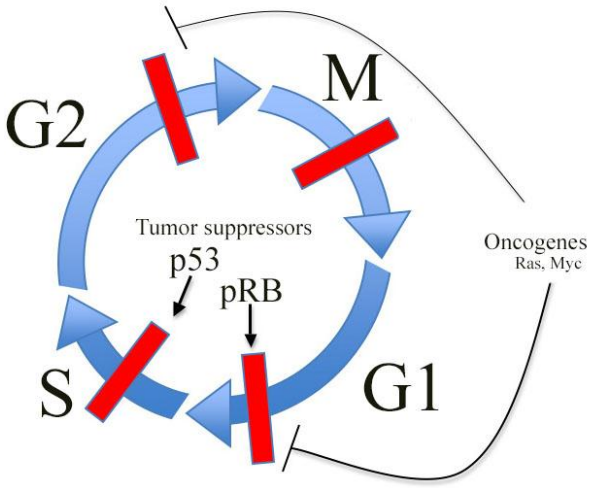

Figure 1:1 Checkpoints in Cell-Cycle Regulation

This digram shows four phases of cell cycle; G1: Gap 1, S: DNA synthesis, G2: Gap 2, and M: mitosis (blue arrow) along with the checkpoints between them (red bars). It indicates tumour supressors (black arrow) that act to maintain checkpoints such as pRB: the retinoblastoma protein and p53: Tumor protein p53. It also indicates oncogenes that let checkpoints to be overcome such as Ras and Myc. Adapted from (Chow, 2010).

1.3 The Hallmarks of Cancer

The field of cancer research is broad and comprehensive. Disparate ideas from divergent fields of study have been organized with underlying principles which Hanahan and Weinberg call cancer hallmarks. It has been proposed that there are six properties of cancer cells that are shared by most cancer cells and that defined neoplastic growth state (cancerous growth). These are: unlimited proliferation, lack of responsiveness to growth inhibitory signals, resistance to apoptosis, invasiveness, inducing angiogenesis and immortalizes proliferation (Hanahan and Weinberg, 2000). These features have been extended to include, the ability of deregulating cellular metabolism, evade immunological destruction, genomic instability and promoting inflammatory responses (Hanahan and Weinberg, 2011) (Figure 1.2). The linking of alteration in mRNA splicing factors with cancer progression has been observed frequently by a number of high-throughputs sequence programing (Oltean and Bates, 2013; Wu and Choudhry, 2013). This led recent studies to suggest that aberrant alternative splicing as an additional hallmark for cancer (Ladomery, 2013).

1.4 Targeted Therapies for Cancer

Cancer is not just one disease but a group of different diseases which vary according to the diversity of cell types, where the cancer is located in the body. Consequently, different strategies are required to tackle each type of cancer. Selected targeted therapies will be described briefly. The use of monoclonal antibodies (mAbs) has shown positive outcomes in cancer treatment. mAbs can be directed against cancer cells by several mechanism such as the binding to growth factor receptor that are overexpressed in some malignant condition (Scott et al., 2012). mAbs can also be used to manipulate the anticancer immune responses and induce apoptosis (Sliwkowski and Mellman, 2013). Epidermal growth factor receptor (EGFR) and HER2 are receptors tyrosine kinases among common targeted biomarker in certain tumour. These targets are involved in the development of personalized medicine strategies and early diagnosis of cancer (Wu et al., 2012).

Extraordinarily, nanotechnology-based therapeutics is employed for targeting cancer. It exhibits progressive effects compared with drug alone. For instance, recent work showed the effectiveness of nanoparticles (TNP) the chemotherapeutic docetaxel with prostate-specific membrane antigen at considerably lower dosages and obvious

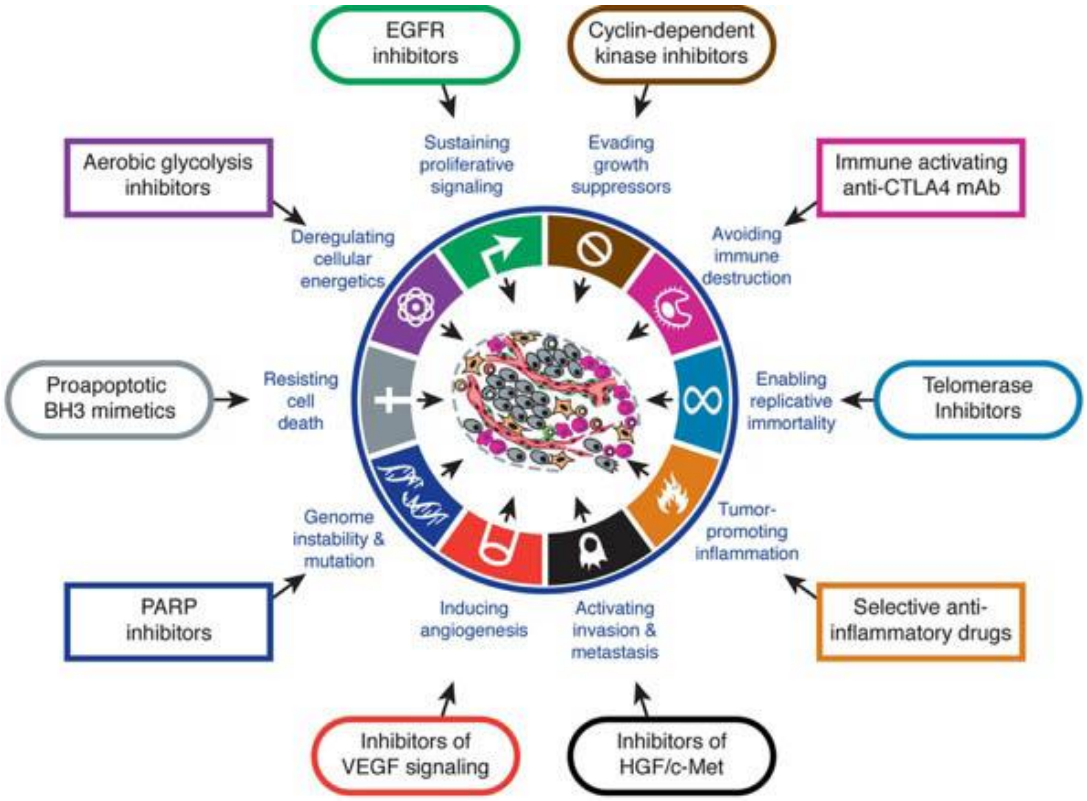

Figure 1:2 The summary of hallmarks of cancer and their therapeutic agents.

This shows examples of approaches that embayed in designing therapeutics targeted to the known and emerging hallmarks of cancer. (Hanahan and Weinberg, 2011)

improvement of accumulation in tumour (Hrkach et al., 2012). Nanotechnologies have also been applied in RNAi gene silencing in cancer targeting strategy. The main problem with the use of siRNAs was their intracellular delivery to their targets. However, gene silencing of certain genes in cancer tissue can be done by delivering small interfering RNA (siRNA) using nanoparticles delivery system (Nishimura et al., 2013).

1.5 Cancer Stem Cells (CSCs)

The phenomenon of cancer stem cells (CSCs) has received attention over the last 15 years. Our understanding of metastatic process has developed to reveal that tumours consist of heterogeneous cancer cells comprising a hierarchy of cells that is fueled by small population known as CSCs (Tirino et al., 2013). Primary tumours cause the minority of cancer deaths. Mainly, death is caused when the cancer cells confer malignant phenotypes traits such as invasiveness via re-activation a long silent embryonic programme is called the epithelial-mesenchymal transition (EMT) (Mani et al., 2008). When cancer cells pass through EMT and acquire aggressive traits, they also acquire many stem-cell like features (Maugeri-Sacca et al., 2012). This also confers the capability for the migration of cancer cells to distant tissue through blood vessels and the ability of seeding new secondary tumours (Brabletz, 2012). Acquiring of "stemness" by cancer cells is also supported by physiological microenvironment that present within niches, such as hypoxia and acidic conditions (Hjelmeland et al., 2010).

CSC possess key features including the ability to self-renew, proliferate and differentiate into secondary cell type with different phenotypes. CSCs exist as small population of cells that can be distinguished by their surface markers such as CD34+CD38– in leukaemia or +CD44+CD24– breast cancer (Yu et al., 2012). CSCs show high levels of expression of ATP-binding cassette (ABC) transporters family. ABCs improve cells resistance to drugs via reducing the intracellular accumulation of cytotoxic compounds (Elliott et al., 2010). CSCs also activate many of the pathways that originate during embryogenesis of stem cells such as Wnt/β-Catenin signalling and Notch (Takebe et al., 2011). Nonetheless more CSC markers still need to be identified to improve treatment and drug design. Several drugs in clinical trials are designed to specifically eliminate CSCs.

1.5.1 The Origin of CSCs

Tumours consist of different populations of cells that vary in their biological properties and potentials. Cancer tissues are heterogeneous and show different DNA profiling even if the sample was isolated from single tumour (Fisher et al., 2013). Cancer clonal evolution postulated that cancerous cell formation is a result of the accumulation of random mutation that arises during life. Applying this theory to understand cancer treatment strategies helps to understand the ineffectiveness of the main standard chemotherapies (Gil et al., 2008).

However, CSCs model hypothesised that the main cause of unsuccessful cancer treatment is a consequence of cancer initiating cells that have distinct features of CSCs such as, self-renewing, potential and resistance to cells death programme (Park et al., 2009). With the rising indication that CSCs are the main cause of cancer recurrence after chemotherapy, it is becoming increasingly important to understand the origin of such cells. The main proposed sources thought to be the root of CSCs are: 1. that they occur from stem cells existing in normal tissue, 2. progenitors (partly differentiated adult stem cells with limited properties), 3. They arise from differentiated cell that gains mutations that transfer them back to stem-like state (reprogramming-like mechanism). De-differentiation of somatic cells is supported by ability of reprograming differentiated cells to a pluripotency state by expressing the so called Yamanaka transcription factors which induce pluripotency (Friedmann-Morvinski and Verma, 2014).

Moreover, the formation of CSCs from normal adult stem cells is through the accumulation of genetic and epigenetic changes that led to switching on off some CSCs marker (Vincent and Van Seuningen, 2012). In Acute myeloid leukemia (AML) for instance, DNA methylation protects the hematopoietic stem-like state by reducing their differentiation through the overexpression of DNA methyltransferase, Dnmt1 (Munoz et al., 2012). Dnmt1 has also been seen to play similar role in CSCs of colon cancer (Im et al., 1997). Although the CSCs model has gained wide acceptance and recognition in cancer research, applying this hypothesis to all cancer types still represents a major challenge (Figure 1.3).

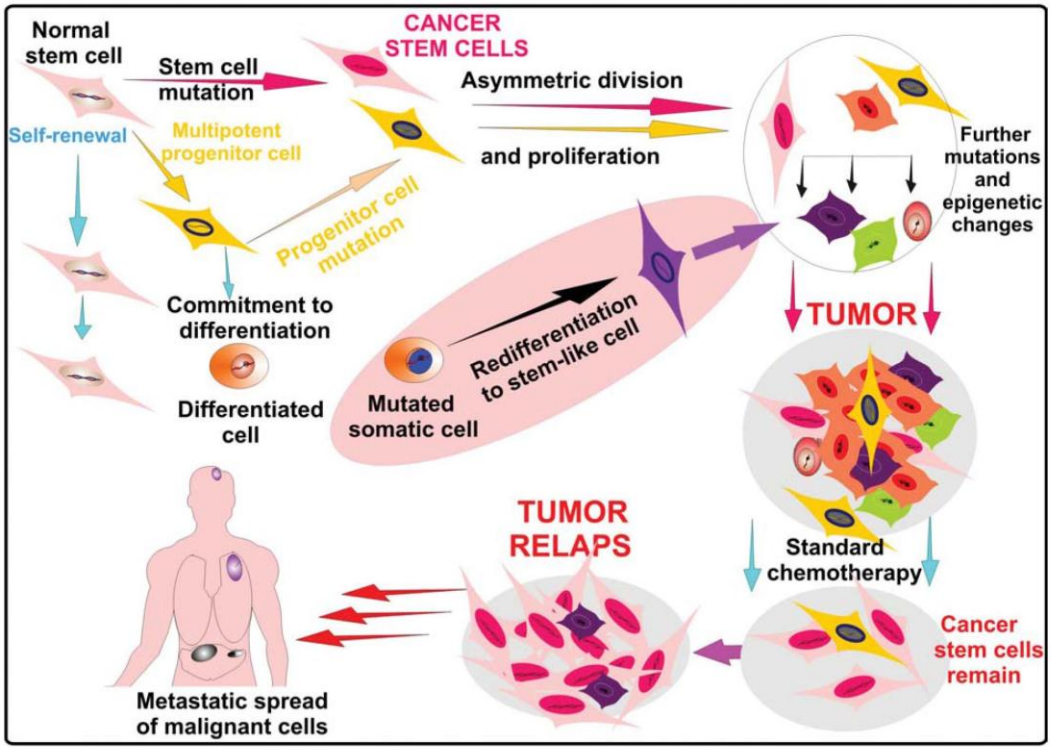

Figure 1:3 How cancer stem cells may orignate in the body ?

Stem cells exist in the human body naturally and divide asymmetrically for self-renewing and producing multipotent progenitor cell, which may differentiate to proginator cells and mature cells. This figure illustrates how cancer stem cells arise from mutated stem cell and/or from progenitor cells by genetic alteration. The cancer may originate sometime after its initial treatment by chemotherapy or radiotherapy. They can be resposible of metastatic spread of malignant cells in distanc sites of the body. They arise also from differmciated (somatic cell) that gains mutations transfering them back to stem-like state, mainly the capacity of renewal and propagation (Soltysova et al., 2005).

1.5.2 CSCs Implications for Tumor Therapy

Isolation and characterization of stem cells of leukemia and solid tumors have become essential in the study of cancer therapy (Clevers, 2011). A tumor consists of different clones that vary in their activity level of proliferation, differentiation, and tumor-initiation ability. In human leukemia, some of the cells have the capacity to divide indefinitely and maintain the tumor clone. It also gives rise to other leukemic cells that possess extensive proliferative and self-renewal potential and those cells that we called leukemia stem cells (Iwasaki, 2014; Soltysova et al., 2005). The ABC transporters are responsible for a common mechanism of drug resistance used by stem cells (Elliott et al., 2010). The efficiency of cytotoxic chemotherapy is limited to due cancer stem cells resistance to drugs and because of their limited replication.

Although those cells form a very small proportion of the tumor, their phenotype of being immortal is likely to be sufficient to allow tumor recurrence. The cancer may originate sometime after its initial treatment by chemotherapy or radiotherapy. It is proposed that if cancer cells rise from early stem cells or its progenitor cells, the metastases are formed readily with extensive genetic heterogeneity. Metastases resulting from a later stem cell are more homogenous with more limitation in metastatic capabilities. A tumor's heterogeneity and its growth in distant sites of the body under different environments may be derived from differentiation and/or dedifferentiation of cancer stem cells. Additional identification of cancer stem cells is required for differentiation therapy, which might become an improved therapeutic approach in the future. These improvements may foster the therapeutic potential of the CSC concept. Eventually, cancer treatment will involve elimination of all cells within a tumor; consequently, combination therapies that target both CSCs and the tumor mass are likely to emerge as particularly effective clinical strategies (Frank et al., 2010). Current targeting approaches to kill CSCs via targeting their properties are summarized in Figure 1.4. A successful therapy also requires deep understanding of the relationship between CSCs and the innate tumor microenvironment (associated host tissue) and the capability to interfere with this environment role to disrupt the tumor (Malanchi, 2013).

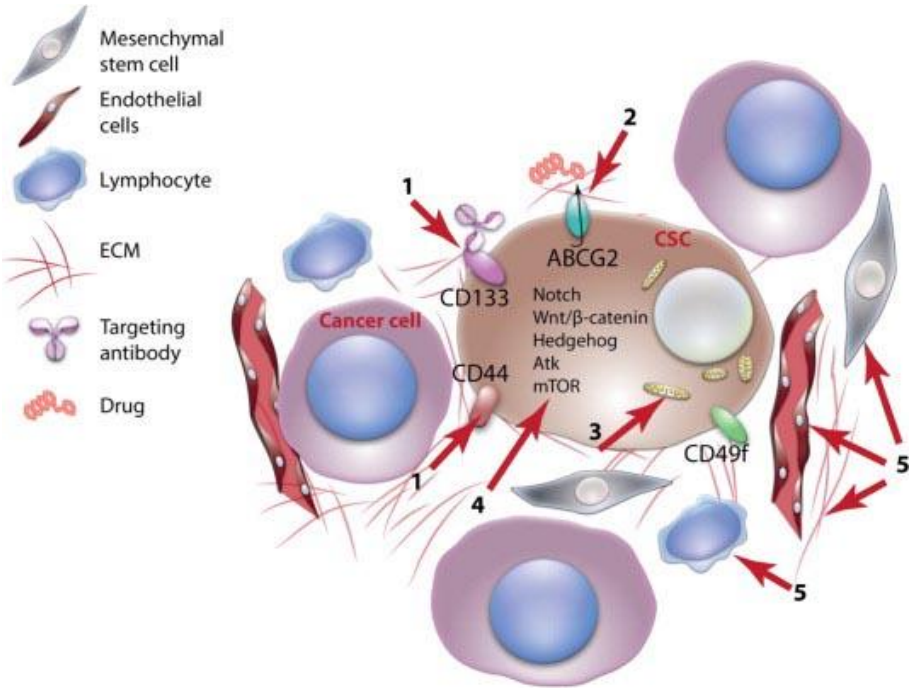

Figure 1:4: Possible therapeutic strategies for cancer stem cell elimination.

(1) Targeting surface proteins biomarker with the aim to develop CSCs-specific therapies such as CD133. (2) Inhibiting the role of efflux transporters to reduce drug resistant to cancer drugs. (3) Reprogramming CSCs to normal by altering its metabolism and induce it to differentiate. (4) Inhibiting essential pathways for CSCs proliferation such as Wnt/β-Catenin signalling (5) Affecting the vascular niche to impair micro environmental mechanisms that regulate GSC maintenance and function. (Zhao et al., 2013).

1.6 Types of DNA Damage and Repair Mechanisms

DNA replication is an essential mechanism for dividing cells. Each dividing cell carries out a complex operation to ensure that chromosomes are transferred identically from the parent cell to each daughter cell without introducing mistakes or mutations. DNA is damaged thousands of times during its replication by internal (spontaneously-derived) or external (exogenous agents) factors. Common DNA damage types include base and sugar lesions, single- or double-strand breaks, DNA crosslinking damage, and base mismatching (Lord and Ashworth, 2012). Failure of cells to cope with DNA damage results in genomic errors and can drive functional changes or eliminate essential cellular processes. If cells fail to produce the proteins of essential genes, the consequence is abnormal cell behaviour and the potential for genetic diseases such as cancer (Badura et al., 2012).

1.6.1 DNA damage sensing and signaling

The cellular system include mailman cells, have multiple DNA damage response (DDR) pathways that maintain its integrity in response to any genome defects or epigenetic disruptions. DDR pathways involve three main players, which are sensors, signal transducers, and effectors. At the heart of the entire DDR machinery are ATM (ataxia telangiectasia mutated) and ATR (ATM and Rad3 related), which are proteins that sense and detect aberrant DNA structures and trigger upstream DDR kinases (Marechal and Zou, 2013).

Conceptually, in respond to DNA stress, ATM and ATR are auto-phosphorylated and activate proteins involved in the DDR. The ATM-dependent phosphorylation of p53 via induction of p21 (also known as $p21^{WAF1/Cip1}$) are key steps for G1 cell-cycle checkpoint arrest following DNA insults(Delia et al., 2003)while the activation of Chk2 via ATM arrests the cell cycle at S-phase and G2 (Kastan and Bartek, 2004). Furthermore, ATM and ATR phosphorylation results in its rapid co-localization with MRN components and phosphorylates H2AX histone variant– subtype of H2A in event that take place in nuclear foci (Podhorecka et al., 2010).

Central to DDR events is the DNA damage mediator protein (MDC1), which in turn loads more MRN complexes via Nbs1, causing further recruitment of ATM and more phosphorylation of H2AX across the site of damage(Polo and Jackson, 2011). The

outcome of DDR pathways may differ according to the tissue that the cells originated from. Fibroblast for instance, prolonged cell cycle arrest in response to γ-radiation (Di Leonardo et al., 1994) while intestinal epithelial cells prefer apoptosis route. This could be explained by variances in p53 expression in different cells (Halacli et al., 2013).

1.6.2 Base Excision Repair (BER)

Base excision repair (BER) is the conserved mechanism required for the repair of DNA following base lesion removal by lesion-specific DNA glycosylases. These DNA glycosylases recognize and cleave the N-glycosidic linkage between a damaged base and its corresponding deoxyribose ring, generating an apurinic/apyrimidinic site (AP site). The formation of an AP site can also occur spontaneously by base loss. In both cases, AP sites are typically hydrolysed by DNA AP endonuclease (APE1), creating a single-strand gap flanked by 3-OH and 5-deoxyribose phosphate (5-dRP) termini. Alternatively, AP sites are cleaved by certain bifunctional glycosylases such as NEIL1 and NEIL2 that possess AP lyase activity. NEIL1 and NEIL2 catalyse successive β- and δ-elimination, leaving a 3′ phosphate at the resultant strand break. Following this DNA incision, DNA polymerase catalyses the addition of the correct nucleotide into the gap. Finally, a DNA ligase ends the BER process and restores the integrity of the helix via a nick-sealing step (Robertson et al., 2009) (Krokan and Bjoras, 2013) (Figure 1.5).

1.6.3 Nucleotide Excision Repair (NER)

Nucleotide excision repair (NER) is a highly versatile DNA repair mechanism that can remove and eliminate numerous types of DNA lesions. This is a fundamental repair system particularly for lesions caused by ultraviolet light (UV), such as cyclobutane–pyrimidine dimers (CPDs). Cisplatin-induced DNA interstrand crosslinks are also another typical substrate of NER.

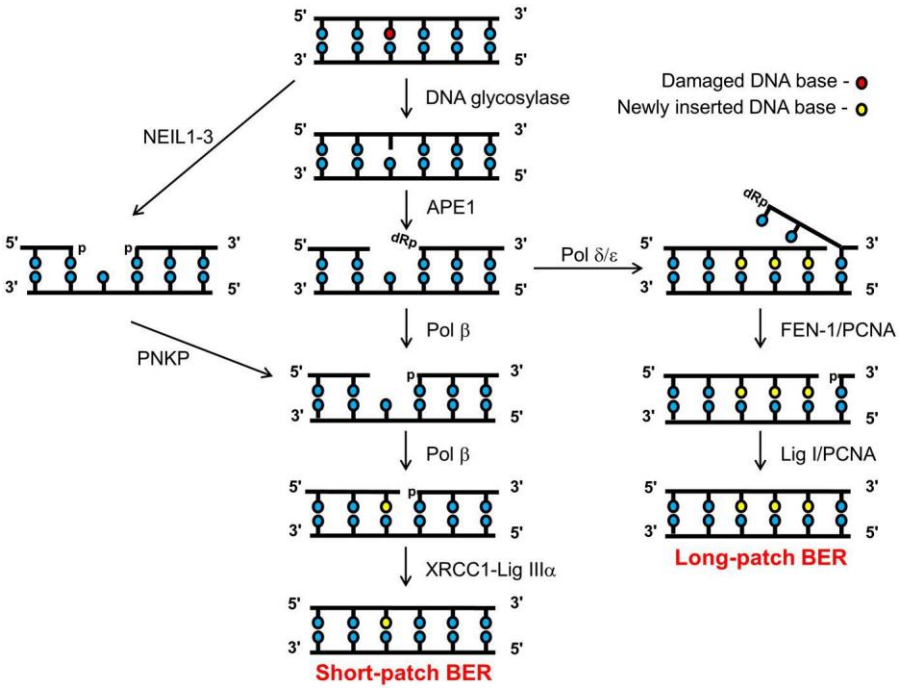

Figure 1:5 Schematic of the BER pathway.

The BER pathway starts with the recognition and removal of a damaged base, leaving the AP site, which is then removed by APE1 to form a DNA single strand break (SSB). The 5′-dRP moiety is then excised by Pol β and the correct nucleotide is inserted into the single-nucleotide break. The break end is then sealed by the XRCC1-Lig IIIα complex, thereby completing the short-patch BER pathway. The long-patch BER is regulated by Pol δ/ε, which inserts 2–8 more nucleotides into the gap to create a 5′-flap structure. This structure is removed by FEN1/PCNA and then sealed by Lig I to end the long-patch BER pathway. Alternatively, AP sites are cleaved by specific bifunctional glycosylases such as NEIL1 and NEIL2 that possess AP lyase activity (Nickson and Parsons, 2014).

Similar to the BER mechanism, NER involves a wide range of proteins that perform a multi-step 'cut-and-paste'-like pathway. The process involves the following stages: DNA damage recognition, unwinding of the double helix at the DNA lesion site, removal of the lesion containing the single stranded DNA segment; and single strand incision at either side of the lesion. These steps are followed by sequential repair synthesis and strand ligation of the remaining strand (Marteijn et al., 2014).

The NER system can be divided into two main subpathways: global genomic NER (GG-NER) and transcription coupled NER (TC-NER). GG-NER eliminates bulky damage throughout the genome in both transcribed and non-coding parts of the genome, while TC-NER is associated with actively transcribed genes and functions with high priority when lesions in a transcribed DNA strand confine the transcription activity. Both systems have a similar basic pathway except that each pathway utilizes different proteins during the initial damage recognition step (Petruseva et al., 2014).

Subsequent to the damage recognition step, both GG-NER and TC-NER progress through common 'core' NER reactions. The XPC complex in GG-NER or the CSB and CSA complexes in TC-NER cause conformational changes that render the DNA accessible for interaction with a multi-subunit (ten protein) complex and the multi-functional transcription factor TFIIH at the site of the lesion. Next, the main TFIIH helicase factors XPB and XPD separate the DNA helix, creating a bubble of about 30 nucleotides around the lesion. This is also coupled by the single stranded DNA binding protein RPA (replication protein A) that allows assembly of the so-called preincision complex. This step is mediated by two structure-specific endonucleases XPG and XPF/ERCC1 that cut the DNA on 3' and 5' sides of the lesion, respectively. Finally, an oligonucleotide spanning the lesion is removed and the resulting gap is resynthesized by DNA polymerase δ or ε using the undamaged strand as the template. This step is mediated by loading the Proliferating Cell Nuclear Antigen (PCNA) onto the DNA strand via Replication factor C (RFC). DNA ligase I and Flap endonuclease 1 or the Ligase-III and its partner XRCC1 then seal the nicks of the repaired strand, thereby completing the NER process (Lehmann, 2011) (Figure 1.6).

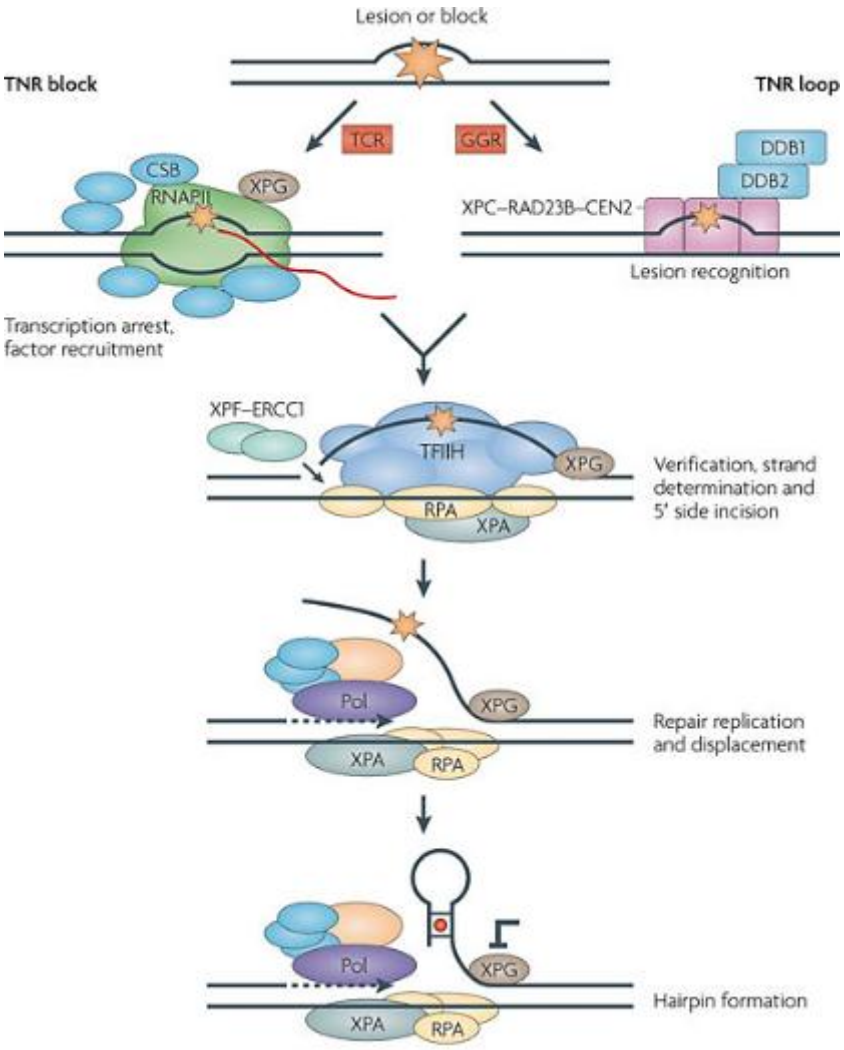

Figure 1:6 Schematic of the TC-NER and GG-NER pathways

The two major branches of the NER pathways: global genome repair (GGR) (left) and transcription-coupled repair (TCR) (right). GGR initiates by recognizing the damage with the XPC–RAD23B–centrin 2 (CEN2) complex. TCR is triggered by the blockage of RNA polymerase II (RNAPII) (red line) and then rescues the stalled polymerase via CSB proteins (blue). After that, the two pathways merge. The damaged strand is removed by the XPF–ERCC1 complex and the endonuclease XPG. The regulation of lesion verification is provided by helicase and ATPase activities within TFIIH, RPA and XPA. (McMurray, 2010). Finally, the resulting gap is resynthesized by DNA polymerase δ or ε using the undamaged strand as a template. This step is mediated by loading the Proliferating Cell Nuclear Antigen (PCNA) onto the DNA strand via Replication factor C (RFC).

1.6.4 Mismatch Repair (MMR)

The mismatch repair (MMR) mechanism has an important role in post-replication repair of wrongly incorporated bases as result of errors by the replication polymerases. MMR proteins also have a critical role in correcting insertion/deletion loops (IDLs) caused by polymerase slippage when a sequence of repetitive DNA is found at the replication site (Peña-Diaz and Jiricny, 2012). Therefore, this pathway is important for reducing the mutation rates in dividing cells, especially in parts of the genome with short repetitive nucleotide sequences (e.g. microsatellites). Clinically, carriers of MMR gene mutations are at high risk for a variety of cancers such as hereditary non-polyposis colon cancer (Win et al., 2012).

The MMR machinery carries out four principle steps: recognition of the strand containing mis-paired bases, digestion of the error-containing strand, gap filling by the DNA resynthesis and break sealing by DNA ligase. The MMR system is highly conserved from bacteria to mammalian cells. The basic MMR pathway initiates by two major MMR protein complexes, MutS and MutL in *E. coli* and their homologues in eukaryotes. Initially, MutS recognizes and binds the mismatch, with the accompanying MutL introducing an entry point for the downstream excision reaction. Two main MutS proteins that function as heterodimers can initiate mammalian MMR: the MSH2/MSH6 (MutSα) bound to base-base mismatches and short IDLs (one or two unpaired nucleotides), whereas MSH2/MSH3 (MutSβ) recognizes relatively larger IDLs. ATP binding induces mismatch-dependent activation of MutL in order to avoid nonspecific degradation of the genome. In humans, single-strand degradation is carried out by exonuclease 1 (Exo1) through the cooperation between MutLα and PCNA. DNA polymerase III then resynthesizes the gap left by Exo1. Lastly, the new strand is sealed by DNA ligase I to complete the repair (Fukui, 2010) (Figure 1.7).

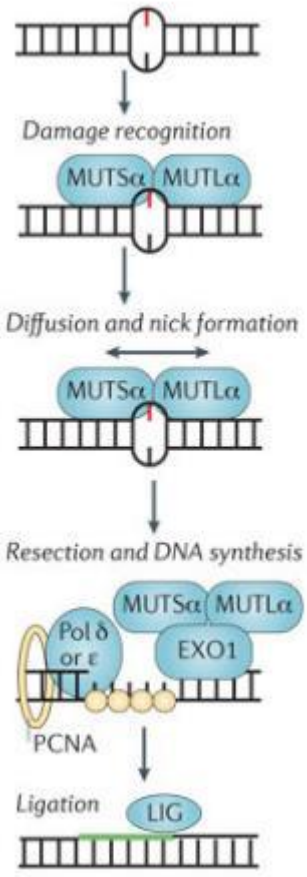

Figure 1:7 Schematic of the MMR pathway

The MMR machinery includes four principle stages: (1) Recognising the strand that contains mis-paired bases by MutS and MutL, (2) Digestion of the error-containing strand until the mismatched base is removed, (3) Gap filling by the DNA resynthesis, which adds the correct nucleotide, (4) Break sealing by DNA ligase (Fu et al., 2012).

1.6.5 DNA Double-Strand Break Repair

DNA double-strand breaks (DSBs) are amongst the most dangerous DNA lesions since a single unrepaired DSB is often sufficient to trigger cell death, while inaccurate repair potentially leads to mutations, deletions or chromosomal rearrangements events that can promote carcinogenesis and other genomic instability diseases. Therefore, faithful repair of DSBs is essential to maintain genome stability. Mammalian cells repair DSBs by two major pathways: homologous recombination (HR) and non-homologous end-joining (NHEJ). The main difference between these repair mechanisms is in their need for a homologous template DNA and in the fidelity of the repair process (Chapman et al., 2012).

HR is considered to be an error-free DSB repair mechanism that utilizes the genetic information from a homologous segment of DNA (for example; sister chromatids). NHEJ is generally error-prone in comparison to HR and it repairs DSBs by direct ligation of the broken ends. The NHEJ pathway operates throughout all phases of the cell cycle in mammalian cells, whereas HR is particularly important in the late S/G2 phases (Bee et al., 2013) (Figure 1.8).

1.6.5.1 DSB repair by Non-Homologous End-Joining (NHEJ)

The non-homologous end joining (NHEJ) mechanism is recruited by a relatively small number of essential enzymes that capture both ends of damaged DNA, join them in a synaptic DNA-protein structure and finally repair the broken DNA ends. The NHEJ process starts by the formation of a Ku70/Ku80 heterodimer complex surrounding the exposed DNA termini of the DSB. Ku is a conserved DNA end-binding protein that adopts a preformed ring-like shape molecule. It recognizes and encircles the duplex DNA ends at the DSB without sequence specificity. Another protein that binds to DSBs sites is DNA-dependent protein kinase catalytic subunit (DNA-PKcs) which forms a DNA-PK holoenzyme and triggers DNA-PKcs kinase activity. Ku also has the capability to translocate along the DNA molecule, allowing the interaction of DNA termini with DNA-PKcs. DNA-PKcs can also tether two DNA molecules via formation of a synaptic complex. Synapsis of DNA-PKs also undergoes autophosphorylation of DNA-PKcs, providing accessible DNA ends ***(Davis and Chen, 2013)*.**

The NHEJ mechanism may entail modification of DNA ends and sequence alteration before they can be rejoined by a ligation (error-prone rejoining) (Dahm-Daphi et al., 2005). Like most DNA repair pathways, resynthesis of missing nucleotides during NHEJ is required through the participation of DNA polymerases such as Pol μ and pol λ (Lieber et al., 2007). Alternatively, phosphorylation of the NHEJ-specific nuclease Artemis may also participate in end trimming via cleavage of 3' and 5' DNA overhangs. DNA end-processing proteins such as APE1, Tdp1 and PNKP are also required, together with the contribution of exonucleases Exo1 and WRN for restoring conventional 5′-phosphate and 3′-hydroxyl ends at the break position (Waters et al., 2014). Following processing of the DNA termini, DNA ligation is performed by DNA ligase IV via direct interaction of XRCC4 and coordination of XLF (XRCC4-like factor). The assembly of the XRCC4-XLF complex offers both DNA end protection and alignment and promotes DNA ligation (Mahaney et al., 2013) (Figure 1.8).

1.6.5.2 **Biological Functions of Homologous recombination (HR)**

HR is a fundamental cellular mechanism primarily required for the repair of chromosome breaks. It occurs either by replacement or the exchange of genetic material with its homologue on the sister chromatid or homologous chromosome (Oum et al., 2011). HR is involved in several biological processes such cell proliferation and genome stability (Moynahan and Jasin, 2010). It is also required for specialized programmes; for example, mating-type switching in budding yeast (Rusche and Rine, 2010). HR is also the main promoter of reproductive genetic diversity driving gamete formation (Choudhuri, 2014). Stern reported HR for the first time in somatic cells of *Drosophila* and called it somatic crossing over (Stern, 1936). All somatic cells require HR to repair DNA breakage induced by endogenous and exogenous sources. Unlike meiotic recombination, most mitotic recombination initiates in interphase (LaFave and Sekelsky, 2009).

Dysregulated homologous recombination is strongly associated with genome-destabilizing genetic diseases and syndromes. It causes chromosome aberrations that are observed in some cancers, such as chromosome translocation, which can occur due to errors in DNA replication, and telomere maintenance (Shammas et al., 2009). Down's syndrome is a common disorder caused by aberration of HR in meiosis that leads to an extra copy of Chromosome 21 (Ghosh et al., 2009). HR-related diseases

and syndromes also occur due to mutation of HR regulators; for example, Bloom's syndrome, where the HR intermediate processor, BLM, is lacking (Arora et al., 2014).

1.6.5.3 **DSB Repair by Homologous Recombination (HR)**

The homologous recombination (HR) repair mechanism is divided into three main phases: end resection, strand invasion and progress of DNA synthesis. During end resection, the DNA ends surrounding the DSB are recognized by the MRE11-RAD50-NBS1 (MRN) complex and CtIP (RBBP8), resulting in 3' single stranded (ss) DNA overhangs (Sartori et al., 2007). Resection processing is then accelerated by the combined action of BLM and Exo1 exonuclease (Nimonkar et al., 2008). Subsequently, single-stranded DNA tails are coated by RPA to remove disruptive secondary structures that can interfere with RAD51 (or its orthologue RecA in prokaryotes). Rad52 binds RPA to facilitate Rad51-mediated displacement of RPA, forming a presynaptic complex. In vertebrates, this event requires the action of Rad52, BRCA2 and Rad51 paralogues (RAD51B, RAD51C, RAD51D, XRCC2 and XRCC3) (Forget and Kowalczykowski, 2010). BRCA2 interacts with RAD51 to form presynaptic filaments on single-stranded DNA (ssDNA). These filaments seek out homologous sequences to the damaged strand and perform DNA strand invasion, which is the key step in this pathway. Afterward, DNA polymerases further extend DNA synthesis from the 3'-end of the invading strand to form a D-loop structure (Krejci et al., 2012) (figure 1.8).

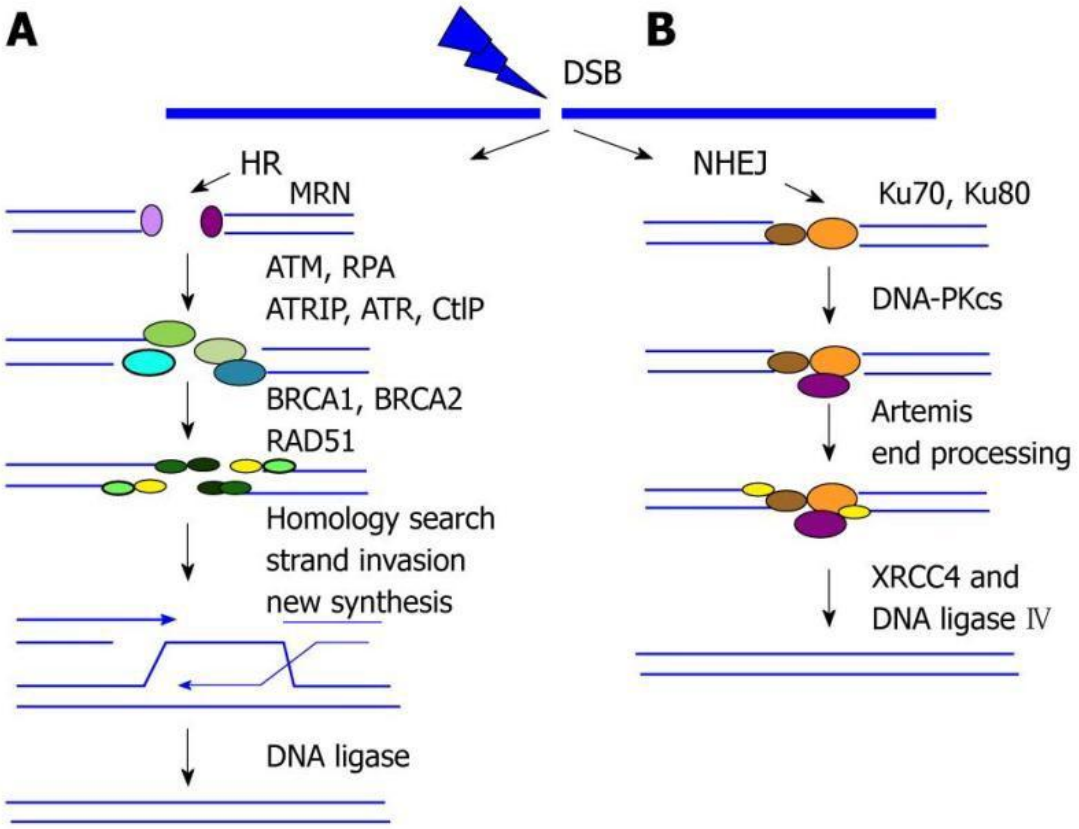

Figure 1:8 The major repair pathways of DSBs

(A) The HR pathway is triggered by the MRN complex which recognizes DSBs, followed by ATM kinase activation (DSB sensor proteins). Single-stranded DNA generated by CtIP is coated with RPA, which leads to ATR activation. RPA is then displaced by RAD51, which can subsequently perform a homology sequence search, creating a D-loop and a Holliday junction. (B) In the NHEJ pathway, the Ku70/80 heterodimer is a key player that directly processes the two broken end with participation of DNA-PKcs. Phosphorylation of the NHEJ-specific nuclease Artemis may also participate in end trimming via cleavage of 5' and 3' DNA overhangs. Following processing of the DNA termini, DNA ligation is performed by DNA ligase IV via direct interaction with XRCC4 (Peng and Lin, 2011).

1.6.5.1 **Recombination intermediate processing**

The Holliday junction is formed between sister chromatids during recombination or following replication fork demise (Wechsler et al., 2011). Crossover repair of damaged DNA leads to genome instability and chromosome rearrangements such as loss of heterozygosity (LOH). For this reason, DNA repair of somatic cells preferentially avoids crossover (CO) formation during mitotic division (Andersen et al., 2011). The first potential pathway that can prevent CO formation and dissociate the dHJ intermediate structure operates through the action of the Bloom protein (BLM) with RMI1, RMI2 and topoisomerase IIIa (BTR complex). This pathway reduces sister chromatid exchange events (SCEs), which are observed with elevated frequencies in Bloom syndrome. Bloom syndrome is an autosomal recessive disease characterized by immunodeficiency disorders, delayed growth, photosensitivity and high expectation of cancer occurrence (Xu et al., 2010) (Figure 1.9).

Two scenarios are proposed for CO suppression. The *Drosophila* orthologue of BLM (DmBlm) plays important role in the pathway of synthesis-dependent strand annealing (SDSA) see section 1.6.4.2.

Figure 1:9 Bloom syndrome symptoms

Due to genetic disorders at the molecular level, patients with Bloom syndrome show dermatological manifestations, including poikiloderma, which appears at different sites on the body (A) on the right cheek, (b) forehead (c) dorsum of the nose. (Arora et al., 2014)

Therefore, the proposed role of BLM in this mechanism is to dissociate D-loops generated by the invaded strand (McVey et al., 2004). A second proposal has suggested that BLM convergently promotes a migration step of two dHJ intermediates and the decatenation step is facilitated by TOP3α (Chen et al., 2014). These suggestions are confirmed by *in vitro* evidence such as the role of BLM in D-loop disruption and branch migration of the Holliday junction, together with TOP3α and other dHJ dissolvers.

In the absence of BLM, HJs can be processed by endonucleolytic cleavage by resolvases (dHJ resolution) including MUS81–EME1, SLX1–SLX4 and GEN1. MUS81 is binding protein for EME1 and together they are involved in CO formation in many organisms (Boddy et al., 2001). Human GEN1 and its yeast orthologue (Yen1) are also able to promote HJ resolution. They can cut static HJs symmetrically, resulting in non-CO outcomes (Ip et al., 2008). Several other observations have suggested that GEN1/Yen1 primarily compensates for the role of Mus81–Mms4/Eme. Recent work has also revealed a new meiosis HJ resolution activity of the MutLγ complex (Mlh1-Mlh3). This mechanism is postulated to cause CO formation in budding yeast and, by inference, in mammals (Zakharyevich et al., 2012).

1.6.5.2 **Synthesis-dependent strand annealing (SDSA) at two-ended DSBs**

Synthesis-dependent strand annealing (SDSA) is the second models of DSB repair by HR which initiated by a two-ended DNA DSB. It repair the DSBs by only a non-crossover manner throughout mitotic repair and during meiosis. In the same way as most homology directed repair pathways, SDSA performs the same initial steps including the resections and invasion steps. However, the elongated invading strand is disassembled from the D loop–recombination intermediates by RTEL1 and then reanneals to the other side on the other break end (Uringa et al., 2011). This is followed by trimming the sequence that is not involved in the annealing. When repair synthesis is complete, release of the newly synthesized strand may also be performed by several proteins such RAD54, WRN and BLM. The remaining gaps are filled and the nicks are ligated, thereby completing repair (Mazin et al., 2010) (Figure 1.10).

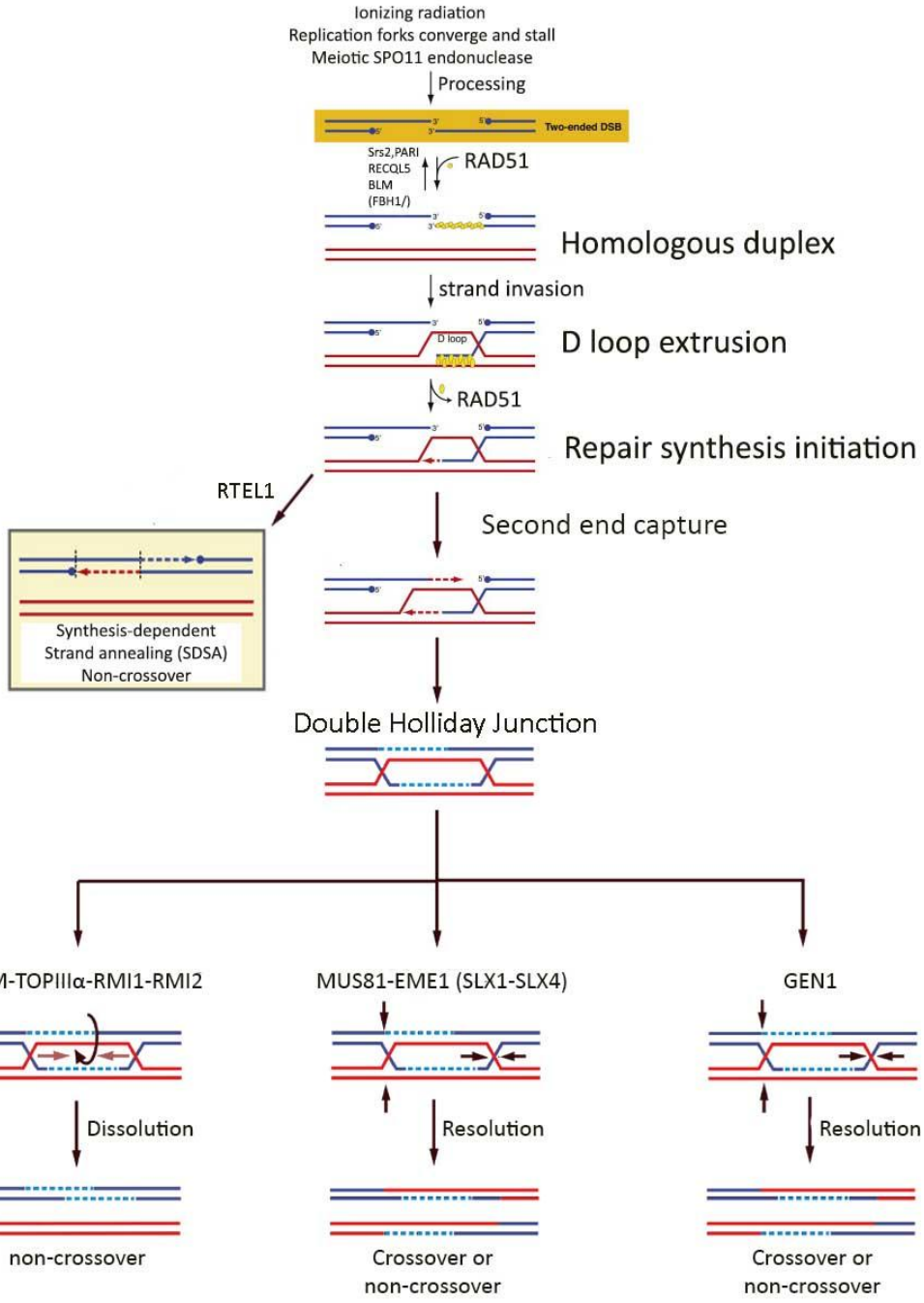

Figure 1:10 Pathway choices of double strand break (DSB) repair

Homologous recombination (HR) of two-ended DSBs is initiated by RAD51 loading onto single-strand DNA and catalysing the strand invasion. This step is regulated by several antirecombinases including Srs2/PARI, RECQL5, BLM, and perhaps FBH1.The extending D-loop may be disassembled by RTEL1 to promote synthesis-dependent strand annealing (SDSA) that guides the DSB toward non-crossover outcomes (yellow box). Alternatively, this second-end capture leads to Holliday junction (HJ) formation. HJs in mammalian cells can be removed with different pathways, depending on cleavage orientation. Helicase enzymes such as BLM dissolve HJs by migration followed by decatenation, in a process that forms non-crossover products. In contrast, the nuclease enzymes promote nucleolytic resolution, in a pathway that results in crossover or non-crossover outcomes depending on the position of the nucleolytic cutting. Adapted from (Chapman et al., 2012) (Wechsler et al., 2011).

1.6.5.3 **Deficiency in Holliday Junction Resolution**

Deficiency in HR processing leads to cellular problems even in the absence of DNA damaging agents. The budding yeast Mus81–Mms4 endonuclease complex has a vital role in cell cycle regulation and genome stability. Loss of Mus81–Mms4 function in cells lacking Sgs1 (an orthologue of BLM RecQ helicase) causes synthetic lethality, reduces cell viability and induces chromosomal rearrangements (Gallo-Fernandez et al., 2012). Another study on human cells has suggested that GEN1 activity has an important function in the presence of SLX4 deficiency, even in the presence of the BLM complex, due to the synthetic lethality between SLX4 and the absence of GEN1. It also shows that the loss of nucleolytic HJ processing threatens the cell viability (Garner et al., 2013). Moreover, depletion of MUS81 and EME2 resulted in a significant reduction of DSB formation after hydroxyurea treatment. It also had negative consequences on the cleavage and restart of stalled replication forks (Pepe and West, 2014).

Recent work on Bloom deficient cells derived from Bloom syndrome patients (BS cells) has shown the role of HJ resolvase/dissolvase in genome instability. Various chromosome aberrations were observed as a result of disturbing the Holliday junction processing pathways. Chromosomal condensation was hypothesised to be impaired, presumably due to failure of Holliday junction resolution/dissolution. Interestingly, MUS81 depletion in BS cells has led to a significant decrease in the elevated SCEs that are usually observed in these cells. The average number of SCE events within single chromosomes was also reduced, implying an effective biological role of MUS81 depletion for preserving genome stability. Accordingly, GEN1 has a redundant function with SLX4, MUS81 and BLM to suppress the high incidence of SCEs by resolving HJs in somatic BS cells (Wechsler et al., 2011) (Figure 1.11). Consistent with this study, GEN1 depletion causes a significant defect in HR repair of DSBs. Both GEN1 and SLX4 are postulated to work in an independent manner to resolve dHJs downstream of Rad51 (Gao et al., 2012).

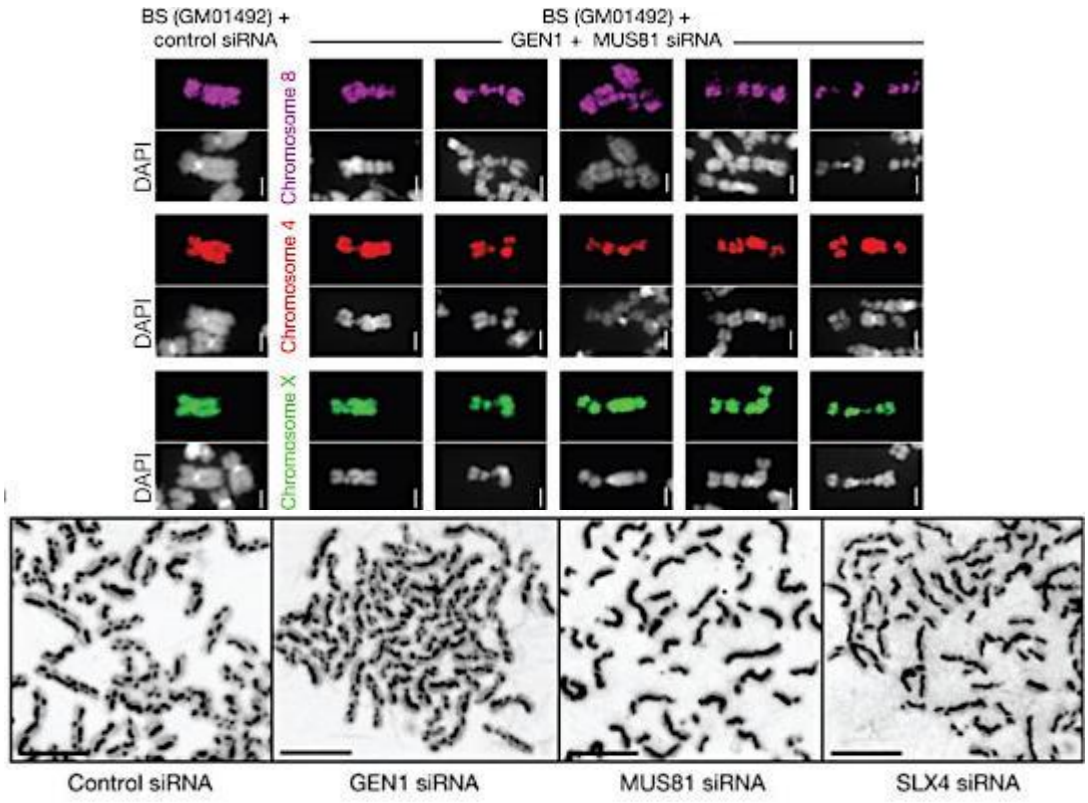

Figure 1:11: The impact of depletion GEN1, MUS81 and SLX4 on sister chromatid event (SCE) frequency and chromosomes morphology in Bloom (BS) cells.

The upper images show metaphase spreads of GM08505 (BS cells) hit with mock siRNA or siRNA of GEN1 and MUS81. They were stained with whole chromosome stains specific for chromosome 4, 8 or X, as indicated. In The lower images are Giemsa-stained metaphase spreads of GM08505 treated with the indicated siRNAs. They show the effects of each enzyme on SCE level. Notably, MUS81 depletion has reduced the elevated SCEs in the BS cell. Adapted from (Wechsler et al., 2011).

1.6.6 DNA damage response and in ESCs

ESCs are distinguished by their ability to form all embryonic tissues cells. This responsibility requires from the ESCs to have a powerful DNA repair mechanism to prevent any genome defects that may lead to detrimental consequences for the embryo as whole. This fact is supported by the ability of ESCs to reduce the mutation rate comparing to somatic cells (Cervantes et al., 2002). Therefore, one of the key defense mechanism against DNA damage in ESCs is their ability to keep genotoxic drugs out through ATP-binding cassette (ABC) transporters that are significantly expressed in ESCs (Padmanabhan et al., 2012). Also, higher activity of γH2AX are observed in ESCs supporting the greater levels of γH2AX are found in ESCs, demonstrating the existence of efficient DSB response pathway in ESCs compared to differentiated cells. Hence, the repair efficiency of IR-induced DSBs in ESCs seems to be more rapid than in somatic cells (Tichy and Stambrook, 2008).

Due to the high fidelity of HR repair, ESCs seem to repair DSBs mostly through HR and less frequently via NHEJ, this is opposite in somatic cells, a predominant role for HR in repairing DSB damage in ESCs (Middel and Blattner, 2011). Because of the important role of ESCs to create the whole embryo properly, it is only reasonable to propose that HR is more prevalent for ESCs due to its high fidelity for repairing DSBs rather than the error-prone NHEJ. This behavior is strengthening by the elevation level of HR regulators such as BRCA1 and Rad51 and the reduction of NHEJ proteins that correlate with the undifferentiation state. Moreover, most of the cell cycle of ESCs are spend on S and G2/M phases this where sister chromatids are available and increase the chance for HR repair (Maynard et al., 2008; Tichy et al., 2010).

Due to a short overall cell cycle of ESCs and the lack of a functional G1/S phase checkpoint, ESCs may facilitate the transition of damaged ESC through to the S phase where the damage is amplified and causing either the cell death via apoptosis or undergoing differentiation (Rocha et al., 2013). However, while the G1/S checkpoint is absence in ESCs, it has been shown a functional p21/WAF-independent G2 checkpoint through the ATM-dependent pathway (Filion et al., 2009).

1.6.7 Chromatin structure

DNA molecules within the cell nucleus are wrapped into string-like fibres called chromatin, which become tightly condensed into visible chromosomes during metaphase. Chromatin is comprised of a central unit of DNA and histones proteins called nucleosomes. The nucleosome core particle is the simplest packaging structure of chromatin, consisting of 147 bp wrapped around a cylindrical structure of histone protein. Typically, each nucleosome is a histone octamer made by two copies of four different highly conserved, basic histones, which are combined as a pair of histones H2A, H2B, H3 and H4. The nucleosomes are bridged together via another histone called the H1 linker histone (Luger et al., 2012).

The chromatin structure is divided to two major regions: heterochromatin and euchromatin. Euchromatin is relaxed chromatin and is rich in active genes. In contrast, heterochromatin is condensed and appears as a dark region of the stained nucleus; it is commonly associated with transcriptionally silent regions of the genomic DNA. Recent studies of gene mapping have challenged the dominant thought of heterochromatin being a "genetic junk yard" to promote it as the main player in genome stability and integrity (Rountree and Selker, 2010).

Histones are subjected to different post-translational modifications (PTMs) such as methylation, acetylation, ubiquitylation and phosphorylation. These modifications play important roles in genome packaging and contribute to the regulation of DNA-related activities such as gene expression and silencing (Lee et al., 2010). Histone acetylation is a well-studied modification that regulates chromatin condensation and commonly linked with active genes. Nucleosomes remodelling by acetylation can occur through neutralisation of the positive charge that drives interaction with DNA, thus weakening DNA histone interaction. It can also contribute to the transcription process by creating a docking site for bromodomain-containing proteins. Histone acetylation is a reversible reaction and is catalysed by histone acetyltransferases (HAT) that target lysine conserved residues. Histone deacetylation is used to control the balance of acetylation activity according to the physiological conditions of the cell through the enzymatic activity of histone deacetylases (HDACs) (Peserico and Simone, 2011). Numerous studies have identified several HDAC groups, such HDAC1, which promotes stem cell differentiation (Bannister and Kouzarides, 2011).

Histone methylation is another critical PTM that targets histone tails at lysine and arginine residues. It is a covalent modification and does not modify the charge of the histone (Crider et al., 2012). The most common histone methylations are found on histone H3 lysine 4 (H3K4). Methylation also has been identified recently at several lysine and arginine sites and in other histone proteins (H1, H2A, H2B, H3 and H4). The exact function of the recently reported methylation sites remains unclear (Stowell et al., 2013). Histone methylation is a reversible reaction as some H3K4 demethylases have been identified, such LSD1. The diverse array of methylation events has a dynamic function in cellular mechanisms such as in the self-renewal and differentiation of embryonic stem cells (Kidder et al., 2014). Therefore, reversible LSD1 inhibitors represent a potential target for chemotherapy, for example, for leukaemia stem cells (Stowell et al., 2013).

The combination of two different PTMs has unique consequences not seen individually. The same PTMs at different positions can also potentially lead to different activities. For instance, methylation of the lysine on the fourth residue of histone H3 (H3K4Me) is associated with active transcriptional states, whereas methylation of the lysine on the ninth residue of H3 (H3K9Me) is commonly recognised as a gene repression marker (Guillemette et al., 2011). Interaction and 'cross-talk' between these mechanisms make determining their specificity quite complex (Figure 1.12).

1.6.8 Centromeric Chromatin

Centromeric chromatin in many organisms, from yeasts to humans, is cytologically distinguished from the rest of the genome during the cell cycle. It is heterochromatic and transcriptionally inactive (Pidoux and Allshire, 2005). A centromere is recognized as a special region in the chromosome that links sister chromatids and separate each one into two arms. During metaphase, accurate chromosome segregation is directed by centromere through the kinetochore formation that is assembled around the centromere (McFarlane and Humphrey, 2010). The kinetochore proteins form a large

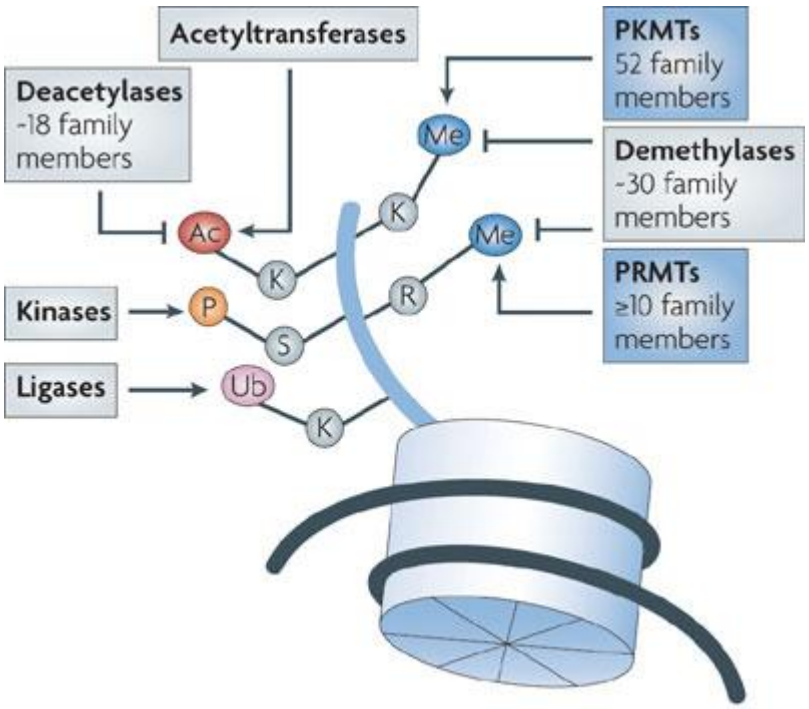

Figure 1:12 Examples of histone post-translational modifications that can regulate epigenetic processing.

Different modifications of histone tails are shown with their associated enzymes. Abbreviation AC: Acetylation, P: phosphorylation, Ub: ubiquitylation, Me: methylation, PKMT, protein lysine methyltransferase; PRMT, protein arginine methyltransferase (Chesworth et al., 2014)

centromere-associated complex with multiple roles to perform. The kinetochore acts as the interface to the microtubule fibres that point and guide the chromosomes to correct position within the cell. It also works as a checkpoint signal generator to ensure that everything is correctly attached and positioned and ready to undergo separation during anaphase (Cleveland et al., 2003).

Centromere dysfunction is associated with genome instability that causes genetic disorders, illness and cell lethality. Faithful centromere formation and maintenance contributes to germ cell formation, whereas its failure leads to abortion or developmental defects (Mehta et al., 2010). Furthermore, failure of the spindle assembly checkpoint (SAC) causes aneuploidy, which is a common feature of solid tumours (Kops et al., 2005).

1.6.9 Centromeric Sequence

The centromere structure in most organisms has common features that vary in their complexity, length and sequencing organization. The simplest "punctate" centromere is found in lower eukaryotes such as *Saccharomyces cerevisiae,* followed by plants and then the complex centromeres of higher eukaryotes such as mammals. Centromeric DNA of different sequence lengths can be observed within a single organism; for example, *Schizosaccharomyces pombe* shows variations in centromere sequences of their three chromosomes but each is organized in a similar pattern (Clarke, 1998). Although centromere structure has been intensively investigated in different cellular systems, a sequence that represents a centromere has never been fully identified, suggesting sequence specificity is not important.

The genome sequence of *S. pombe* revealed that the centromere consists of repetitive parts in sizes of 35, 65 and 110 kb and they are shared by three common regions. The central region (*cnt*) is the site of kinetochore formation and contains 4–7 kb of non-repetitive sequence rich in GC content. The *cnt* is flanked from the left and right by two inner-most repeats (*imr*1L, *imr*1R). The third region contains long tandem arrays of outer repeats (*otr*) and comprises variable numbers of *dg* and *dh* repeats, as shown in Figure 1.13 (Wood et al., 2002).

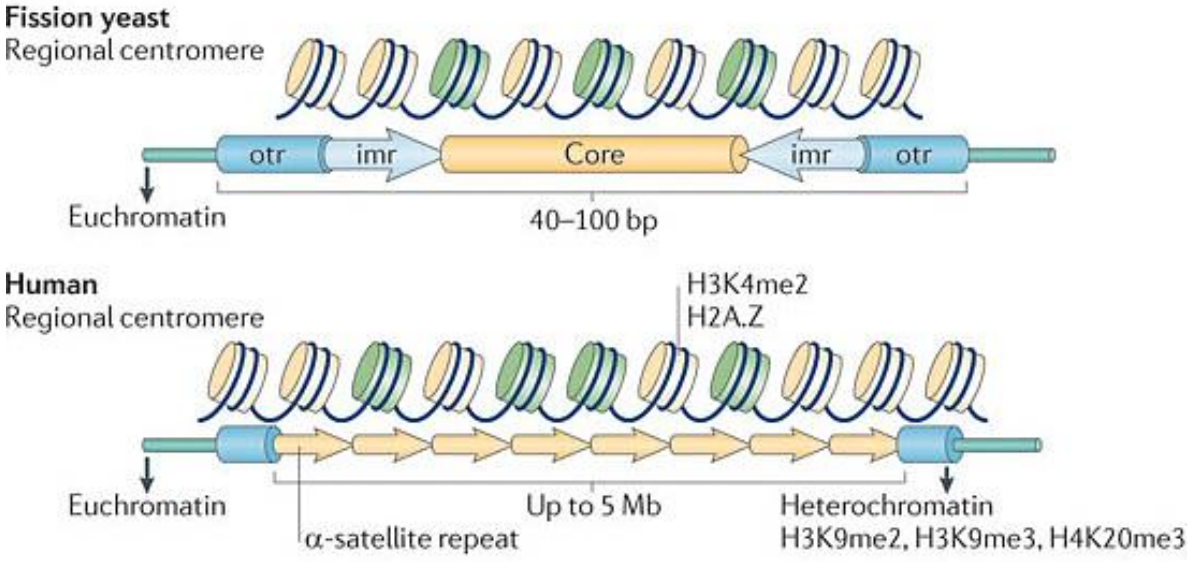

Figure 1:13: Centromere sequence organization in fission yeast and humans.

The upper schematic is a representation of the *Saccharomyces pombe* centromere. Blue arrows, outer repeats (*otr*); light blue arrows, inner repeats (*imr*); yellow cylinder, centre core (*cnt*). The lower schematic is a representation of the human centromere. The epigenetic markers are indicated in each nucleosome. The components of the heterochromatin are indicated above each arrow; yellow represents a CENP-A containing nucleosome while green shows an H3 containing nucleosome (Verdaasdonk and Bloom, 2011).

Human centromeres are more complex than those of yeasts and are distinguished by megabases of tandemly repeated alpha satellite DNA. Each chromosome is also characterized by a specific higher-order array of alphoid monomer units. This multimonomer unit is comprised of approximately 5 MB and is present within a single centromere thousands of times (Schueler and Sullivan, 2006). Sequencing analysis shows high homogeneity of about 99% of the sequences within each monomeric unit and about 70-80 % between individual monomers (Bayes and Malik, 2008).

1.6.10 The Centromeric Histone H3 Variant

Histone variants (paralogues of the conserved histones) differ in amino acid sequence, which denotes the diversity in their functions in a range of ways. Some have distinctive physical structures that may alter the nucleosome properties, whereas some variants localize to specific sites in the genome (Talbert and Henikoff, 2010). The centromeric chromatin contains a histone variant that is found uniquely in centromeric nucleosomes and replaces the typical histone H3. CenH3 is used to refer to all centromere-specific histones in different organisms such as CENP-A in mammals, CID in *Drosophila*, Cse4 in *S. cerevisiae* and Cnp1 in *S. pombe (Kamakaka and Biggins, 2005)*. It has, therefore, been suggested that centromeric identity is epigenetically identified by the presence of CenH3 (Bernad et al., 2009). Furthermore, PTMs on the N-terminal tail of CenH3 contain a specific sequence (that does not exist in the canonical H3) that serves as an extra sign for centromeric histones (Mariño-Ramírez et al., 2005).

1.6.10.1 Importance of CENP-A in Accurate Chromosome Segregation

The detailed characterisation of centromeric chromatin remains controversial, but CENP-A is recognised as a main unit in a vast majority of organisms. CENP-A itself has intensive epigenetic features; therefore, by replacing histone H3 it can serve as a primary marker for the formation of centromeres at a specific region on the genome (Allshire and Karpen, 2008). CENP-A containing chromatin plays a significant role in kinetochore protein assembly. It is also recruited in the chromosome cohesion maintenance, which is a vital player in chromosome segregation (Dai et al., 2006).

Deletion of CENP-A has been studied in a chicken DT40 cell line and led to mislocalisation of most kinetochore proteins in the CENP-A depleted cells. Its deletion

also caused a range of disruptions in cell cycle processes such as deficiency in kinetochore localization of the checkpoint protein BubR1 under conditions of spindle checkpoint activation by nocodazole, a microtubule-depolymerizing agent (Regnier et al., 2005). In contrast, overexpression of CID in *Drosophila* (*in vivo* and *in vitro*) increased the numbers of growth defects and generated mislocalisation of non-centromeric sites. It also resulted in the formation of ectopic centromeres and multicentric chromosomes (Heun et al., 2006).

1.6.10.2 Physical Features of CENP-A that Mark Centromeres

The determination of CENP-A crystal structures has revealed various features critical for centromere function and complex formation. Two CENP-A and two of each Histone H2A H2B H4 package DNA in a left-handed orientation similar to the H3 octamer structure. However, the major difference between H3 and CENP-A nucleosome structures is the presence of flexible regions of thirteen base pairs of the CENP-A nucleosome (invisible in the crystal structure), which possibly provide binding sites for other centromere proteins such as CENP-B and CENP-C (Tachiwana et al., 2011).

The rotation of the CENP-A–CENP-A interface also differs from that of the H3–H3 interface, probably as a result of non-conserved residues between CENP-A and H3. The (CENP-A/H4) tetramer crystal structure also shows an extended positive charge that protrudes from its surface and increases the hydrophobicity and rigidity of the CENP-A–H4, making it more compact and structurally stiffer than the H3-H4 tetramer. These structural features are regulated by the residues that contain the CENP-A targeting domain (CATD) (Sekulic et al., 2010) (Figure 1.14).

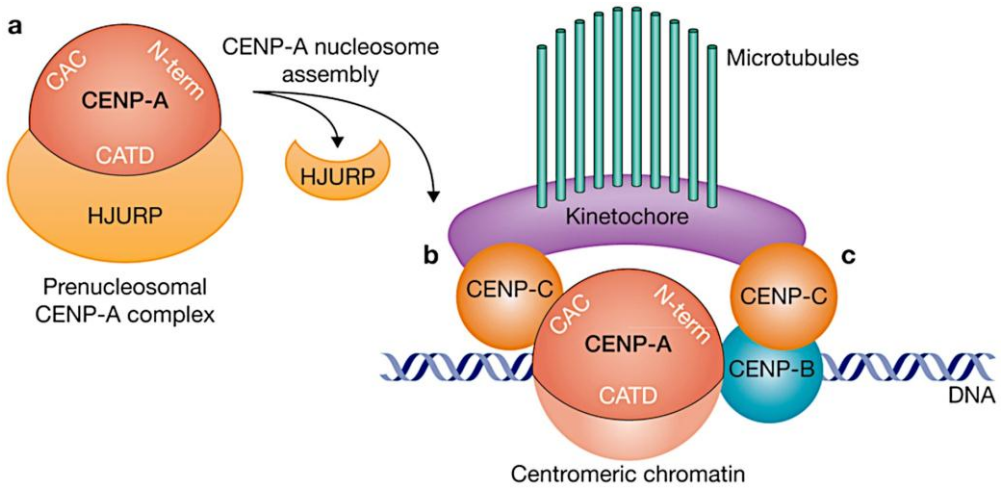

Figure 1:14 The functional domains that comprise the centromeric histone CENP-A

(a) The CENP-A targeting domain (CATD) is mediated by HJURP during CENP-A delivery. (b) Once CENP-A is deposited into the DNA at the centromeric nucleosome, the CENP-A C-terminus (CAC) directs kinetochore formation by binding CENP-C. (c) CENP-C is also assisted by the CENP-A N-terminus, possibly through CENP-B, contributing to kinetochore assembly (French and Straight, 2013)

1.6.10.3 Homologous Recombination in the Centromeric Region

Although centromeres are defined as silent regions, several studies have reported that recombination may occur between sister centromeres. The first observation of recombination events within a centromeric region was in budding yeast (Liebman et al., 1988). However, details of the mechanism of centromeric recombination, including its influence on centromere integrity, its frequency and nature, remain difficult to define.

Jaco et al. have uncovered more details about the frequency of centromeric recombination using mouse cells as a mammalian centromere model. They demonstrated that centromeres are highly recombinogenic and that recombination takes place at a higher frequency within the centromeres than in the chromosome arm regions. They also postulated that the major control of the epigenetic state of centromeric heterochromatin is by DNA methylation. The absence of DNA methyltransferases such DNMT1 and DNMT3 has elevated the centromere recombination up to double and caused alteration in the centromere length and sequence. These observations show that limitation of centromeric recombination is a vital mechanism to ensure the stability of binding sites for centromere proteins such as CENP-B and thereby faithful chromosome segregation (Jaco et al., 2008).

1.6.10.4 Centromeric Recombination in the Inverted Repeats of Fission Yeast

The centromeric DNA structure of the three *S. pombe* centromeres was already mentioned in Section 1.1.7; these centromeres vary in size but have similar organization. Remarkably, the inverted repeat sequence of each centromere has limited variation between repeats. This is strong evidence supporting the existence of genetic exchange (HR) between inverted repeat sequences, which supresses the genetic diversity potentially caused by mutations taking place on either repeat.

The transfer of genetic material has been reported to occur between transfer RNA (tRNA) genes of related sequences via mitosis in *S. pombe* (Munz et al., 1982). The extensive analysis of the *S. pombe* centromeric repeat sequences has revealed that tRNA genes exist within the inner most repeat (*imr*). Thus, the mechanism driving

inter-tRNA gene conversion has been postulated as the principal for inter-repeat recombination at the centromeric region.

The centromeric heterochromatin of *S. pombe* is replicated in the early S-phase (Kim et al., 2003). Conceivably, this replication event may be recruited within these tRNA genes to promote the formation of recombination-initiating lesions. Therefore, this model could improve our understanding about the maintenance of inverted-repeats in fission yeast centromeres. In addition, tRNA genes require RNA polymerase III transcription. It shows extra-transcriptional activities such as the suppression of the replication forks and neighbouring sequences. It also separates centromere chromatin into structurally distinct domains, thereby serving as a heterochromatin barrier. Loss of tRNA activity by mutation or deletion leads to the spread of pericentromeric heterochromatin and defects in chromosome segregation during meiosis (Gaither et al., 2014; Scott et al., 2007). These observations have led to the proposal of novel machinery based on the possibility of producing a covalent bond by recombination intermediates such as Holliday junctions. This bond would create a covalently closed loop (CCL) of centromeric DNA and CENP-A found within this region (McFarlane and Humphrey, 2010) (Figure 1.15).

1.6.10.5 CCL formation in Complex Centromeres

Higher eukaryotic centromere structures, such as those in humans, are much more complex than yeast centromeres. These centromeres are composed of a large array of direct repeat DNA elements, unlike the *S. pombe* centromere, which has inverted repeats. It is, however, still possible that the recombination process between repeated parts may form CCLs by co-alignment of two homologous directed repeats, consequently creating a loop structure of DNA. Furthermore, the development of non-covalently closed looping models for large centromeres has explained the colocalisation of CENP-A with centromeric nucleosome, as it is not present continuously on centromeres (McFarlane and Humphrey, 2010) (Figure 1.16).

Ultra-fine DNA bridges (UFBs) have been observed as mitotic structures that can only be visualized by immunostaining for proteins that bind to them, such as BLM. It localizes to anaphase bridges and cannot be stained with traditional nucleus staining.

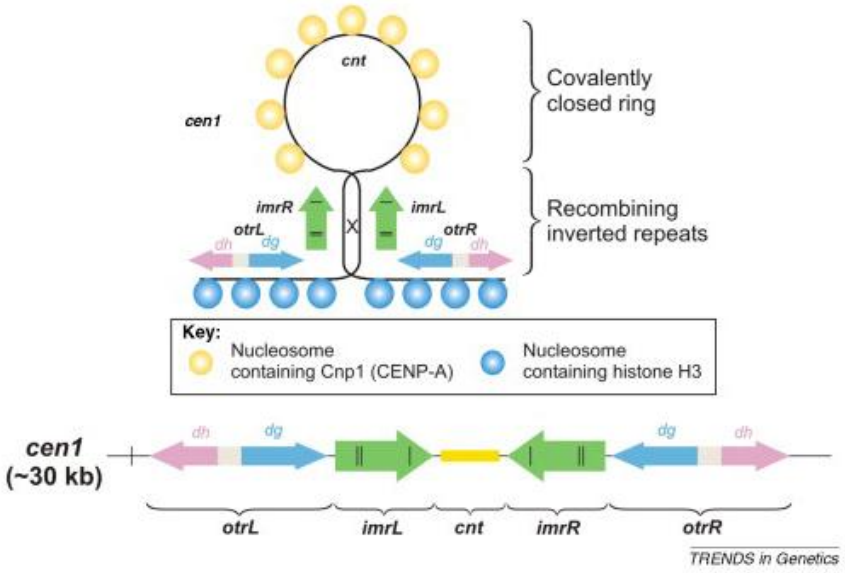

Figure 1:15: Inverted repeats of *Saccharomyces pombe* centromeres recombine to form a covalent ring structure

A schematic representation of the proposal model showing how inverted repeats within centromeres can connect by inter-repeat recombination, resulting in a covalently closed stem structure that creates a loop in the DNA region between two inverted repeats. This structure is elucidated by the *S. pombe* centromere 1.(McFarlane and Humphrey, 2010)

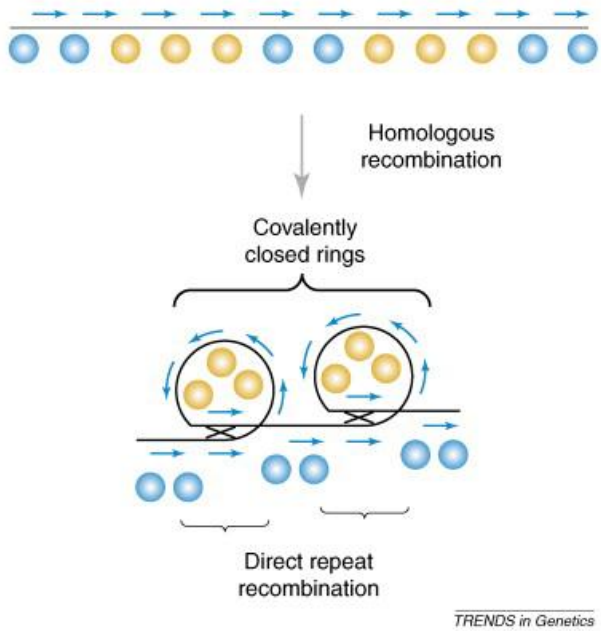

Figure 1:16 The possibility of generation covalently closed rings within large complex centromeres via recombination of directed repeats.

Regional complex centromeres may form loop structures by the homologous recombination between direct repeats. The pattern of distribution of CENP-A agrees with the recombination-mediated loop model (McFarlane and Humphrey, 2010).

Three different types of UFBs are recognised according to their location on the chromosomes. The common feature of the location of these structures is an association with a deficiency in DNA replication. C-UFBs are suggested to originate by centromeric cohesion after the suppression of the spindle assembly checkpoint (SAC) when anaphase is triggered. This linkage has been postulated to represent unresolved HJs that result because of the presence of looping DNA structures that can be created by recombination between homologous directed repeats (Liu et al., 2014b).

1.6.10.6 Chaperoning CENP-A at the Centromere

Nucleosomes serve as barriers for DNA-related activities. Chromatin is assembled with parental histones and newly synthesized histones during the S-phase when DNA replication is completed. Early studies suggested that this assembly takes place in a stepwise manner with the assistance of different histone chaperones (Burgess and Zhang, 2013). Chaperones act as histone binding proteins that ensure the deposition of histones to DNA without involvement in the final reaction product (Hamiche and Shuaib, 2012).

Consistent with the formation of recombination intermediates at the centromere, the Holliday junction recognizing protein (HJURP) has been reported as a CENP-A-specific histone chaperone (Kato et al., 2007). It has been examined *in vivo* using epitope-tagged human CENP-A proteins from new pre-nucleosome complexes. HJURP was absent from pre-nucleosomal H3, indicating its specificity for CENP-A. HJURP plays a vital role in the delivery of CENP-A to the centromere during the early G1 phase of the cell cycle. It appears gradually and is synchronized with the delivery of new CENP-A into the centromere (Dunleavy et al., 2009). The recent finding that HJURP has sequence homology with Scm3 of fission yeast suggests a similar function for the deposition of CenH3 in many eukaryotes (Sanchez-Pulido et al., 2009).

Analysis of the interaction of HJURP with CENP-A has indicated that the CENP-A targeting domain (CATD) is the key sequence determinant for HJURP recognition and maintenance of centromeric chromatin (Hill and Williams, 2009). It has been also identified several identified factors that are recruited in the CENP-A delivery including the Mis18 complex, which may function as the licensing factor (Barnhart-Dailey and Foltz, 2014). In addition, epigenetic study has identified that H3K4me2 is necessary for HJURP targeting and CENP-A assembly in the kinetochore region. HJURP also

shows clinical significance in breast cancer and is correlated with sensitivity to radiotherapy. Although the precise role of HJURP in genome stability remains unclear, the elucidation of its regulation may aid in finding and advancing therapeutic targets for anti-cancer drugs (Hu et al., 2010).

1.7 Project Aims

The conservation of repetitive DNA sequences within the centromere has led to the suggestion of a recombination mechanism at complex centromeres (McFarlane and Humphrey, 2010). A proposed functional role for homologous recombination within centromeric DNA has recently been proposed in which covalently closed DNA loops (CCLs) are formed. The aim of first part of this project is to examine this model through comprehensive analysis of abnormal structures found in cells with elevated numbers of Holliday junctions.

Recent work by the West group has demonstrated that disruption of the Holliday junction resolution/dissolution pathways in human cells resulted in some unusual chromosomal structures. They did not really account for what these might be, but they postulated that chromosomal condensation was impaired. This inference was due to Holliday junction resolution failure (Wechsler et al., 2011)

To test the proposal that HJURP requires a recombination intermediates to drive CENP-A deposition, we hypothesise that the residual Holliday junctions can become the site for another Holliday junction binding protein, HJURP. If HJURP can indeed recognise these Holliday junctions (which remain in the genome due to the reduction of the resolvases/dissolvases), then HJURP might have the ability to lay down CENP-A at these sites. This laying down of CENP-A could account for the failure of these chromosomes to condense correctly and could explain the observations of the West group. It would also provide direct supporting evidence for a role for Holliday junctions in targeting CENP-A to a genomic site.

In the second part of this work, we aim to investigate the genome stability pathways associated with the stem-like state in human cells. Andrews and co-workers recently demonstrated that human embryonic stem cell (ESCs) and embryonal carcinoma cells fail to activate the same checkpoint-dependent response to DNA replication inhibition (Desmarais et al., 2012). It appears that, rather than trying to cope with DNA replication-induced damage, these cells instead are directed down an apoptotic route (Desmarais et al., 2012).

In this study, we plan to use the colorectal cancer cell line HCT116 and SW480 as non-stem cell controls; these cells do activate a checkpoint and repair response to DNA replication-induced damage. We will derive so-called colonospheres from these cells

that take on a more stem-like state. We can use this cell system to address the question of whether cancer stem cell populations (the colonospheres) behave like ESCs and are stem-like in their response to DNA replicative stress induced by anti-cancer agents. Furthermore, in order to compare their behaviour with human stem cells, we will produce induced pluripotent stem cells using non-viral and non-integrated system from foreskins of human new-borns. The use of the colonospheres and iPS cells with their parental cells could represent an ideal isogenic control.

Chapter 2

Methods and materials

Chapter 2. Methods and Materials

2.1 Methods

2.1.1 Cell Culture Protocols

2.1.1.1 Cells lines

Cell culture refers to techniques for growing cells obtained from multicellular organisms, including humans, under controlled conditions. The present project took advantage of this technology and used several cell types, including non-cancerous primary cultured cells and cancer cell lines, which will be described in detail in the following sections.

132N1

The 132N1 cell line was purchased from the European Collection of Cell Cultures, (ECACC # 86030402). It is an astrocytoma cell line that was derived from a human brain tumour in 1972 as a subclone of the cell line 1181N1. Its morphology is classified as glial cells and it grows in adherent cultures. It was cultured in a humidified atmosphere of 5% CO_2 at 37°C in DMEM, High Glucose, GlutaMAX™, (Gibco® # 61965-026) supplemented with 10% foetal bovine serum (FBS). This medium contains a four-fold greater concentration of vitamins and amino acids than the original formula of Eagle's Minimal Essential medium.

BJ Fibroblasts

The BJ human fibroblasts were derived from the foreskin of a human newborn (ATTC #CRL-2522). These cells are distinguished from other fibroblasts by their capacity for dividing into as many as 85 doubling populations before the onset of senescence. These cells were cultured in modified MEM (ATCC® 30-2003™) containing non-essential amino acids, glutamine, sodium pyruvate, and sodium bicarbonate. The medium was supplemented with 10 % FBS (Atlas Biologicals F-0500-A) and Penicillin/Streptomycin (Gibco®, #15070-063). They were cultured in a 37 °C incubator in an atmosphere of 5% CO_2. Some of these cells have been reprogrammed successfully to pluripotency using modified mRNA (Mandal and Rossi, 2013).

HCT116

The HCT116 (ECACC # 91091005) is a line of malignant cells derived from a human male diagnosed with colon cancer. The cells were grown in McCoy's 5A (Modified), GlutaMAX™ (Gibco®, #36600-088) supplemented with 10% FBS at 37°C with 5% CO_2.

MEF cells

The CF-1 MEF 2M IRR (GlobalStem, #gsc-6201g) cells were embryonic fibroblasts derived from a mouse and mitotically arrested by irradiation. These cells were commonly used as a feeder layer for supporting undifferentiated human pluripotent stem cells in culture. The cells should be grown for 24 hours before plating the targeting cells and used within 10 days. The cells were grown in DMEM (Gibco®, #11960-044) supplemented with 10% of FBS, (Atlas Biologicals F-0500-A), GlutaMAX (Gibco®, #35050038) and Penicillin/Streptomycin (Gibco®, #15070-063).

NTERA2

The NTERA-2 (clone D1) line is a human embryonic carcinoma cell line that was kindly gifted by Professor Peter Andrews from the University of Sheffield. The cells have been established from a lung metastasis of a testicular germ cell tumour (Peter W. Andrews, 2006). It was cultured in DMEM, High Glucose, GlutaMAX™, (Gibco® # 61965-026) supplemented with 10% (FBS) in a 10% CO_2 atmosphere at 37°C.

NuFF cells

These cells are human fibroblasts obtained from the foreskin of a new-born human, Donor 11, (GlobalStem # GSC-3001G). They were growth-arrested by irradiation and are non-proliferative. The cells were used as a feeder layer for supporting and maintaining pluripotent stem cells, including support during reprogramming by modified mRNA.

Bloom's syndrome cell lines

All Bloom's syndrome cell lines used in this study were kindly supplied by Professor Ian Hickson from the University of Copenhagen. The GM08505 cell line is an SV40-transformed fibroblast cell line obtained from a human patient diagnosed with Bloom Syndrome, which is predicted to result in premature truncation of the BLM protein. A clone of GM08505 cells was stably transfected with pcDNA3/*BLM* and pcDNA3 to

produce, respectively, the PSNF5 and PSNG13 cell lines. This pair of isogenic controls differ only in the feature that the PSNF5 stably expresses a *BLM* gene with a C-terminal Flag epitope tag (Gaymes et al., 2002).

These cells were grown in α-MEM Nucleosides (Invitrogen, # 22571-038) supplemented with 10% GOLD FBS (PAA, #A11-251), 1x L-Glutamine (Gibco®, # 25030) and 1x Penicillin-Streptomycin (Gibco®, # 15070-063) in a 5% CO_2 atmosphere at 37°C. In addition, PSNF5 and PSNG13 need to be grown with 340 µg/ml G418 several days after the cells were nicely attached to flasks to maintain the plasmids that express or do not express *BLM*.

SW480

The SW480 (#87092801) line is an epithelial cell line isolated from a grade 3-4 human colorectal adenocarcinoma. Initially, the cells were derived from a mixture of epithelial and bipolar cells, but later most of the bipolar cells disappeared. It was cultured in DMEM, High Glucose, GlutaMAX™, (Gibco® # 61965-026) supplemented with 10% (FBS) in a 5% CO_2 atmosphere at 37°C.

Figure 2:1 Light microscope photograph of cell lines

2.1.1.2 **Thawing Frozen Cells**

Time is critical when cells are thawing and this procedure needs to be conducted in a short time. The vial of cells are removed from the liquid nitrogen tank and thawed in a water bath at 37ºC until only a small amount of ice remains (approximately 2 minutes). The vial is then decontaminated with 70% ethanol and the contents transferred to a sterile 15 ml conical tube with 5 ml of complete and warmed growth medium. The cells are then pelleted by centrifugation, the supernatant is replaced with fresh medium and this cell preparation is transferred to an appropriately sized vessel.

2.1.1.3 **Dissociation of Adherent Cells from Culture**

The following is a general protocol for detaching cells from a culture plate while maintaining cellular integrity. The optimal conditions used for individual cells lines should be determined practically. Firstly, the medium was removed and discarded. The attached cells were then washed with 1 x Dulbecco's phosphate-buffered saline (DPBS), (Gibco® #14190-250). An appropriate amount of trypsin (Gibco® #25300-054) was added to cover the cell layer surface and the plate was moved into the incubator. The cells were generally dissociated for 2 to 10 minutes but this varies according to the cell line. The plate was then gently rocked and placed in the upright position to allow the suspension to drain to the bottom. When the process was complete, medium containing serum was added to inhibit the trypsin activity. Trypsin Neutralizing Solution (ATCC, #PCS-999-004) can also be used at an equal volume to inhibit the trypsin when the culture protocol needs to be performed in serum-free conditions.

2.1.1.4 **Subculturing cell suspensions**

This protocol describes how colon cancer cells, such SW480 and HCT116, can be cultured as spheres in a non-adherent manner. The cells were grown to a density of 10,000 cells/ml in serum-free medium (SFM) on ultra-low attachment surface dishes (Corning®) containing a hydrogel layer that prevents cellular attachment (SGMA # CLS3262-20EA). The spheres should be grown in serum-free medium to prevent differentiation. The medium (SFM) should contain the following:

1. 49 ml DMEM/F-12, GlutaMAX™ (Gibco®, #31331-093)

2. 1 ml B-27® Serum-Free Supplement (50X) (Gibco®, # 17504-044)
3. 10 µl EGF Recombinant Human Protein (Conc. 20 mg/ml) (Gibco®, # PHG0314)
4. 5 µl FGF-Basic (AA 1-155) Recombinant Human Protein (Conc. 10 mg/ml) (Gibco®, # PHG0264)
5. 0.5 ml Penicillin-Streptomycin (10,000 U/mL) (Gibco®, # 15140-122)

The spheres were enzymatically treated in order to split them and generate a single-cell suspension. Suspended cells were then transferred to a 15 ml tube and the spheres were spun down in a centrifuge (500 × *g* for 1 minute). The spheres were washed with DPBS and resuspended in Accutase® Cell Dissociation Reagent (Gibco®, # A11105-01) for 10 minutes at room temperature. They were then washed with DPBS and diluted with an appropriate volume of SFM.

2.1.1.5 Trypan Blue Exclusion Test of Cell Viability:

Many techniques in this project involve the counting of cells. First, a Bright-Line™ Hemacytometer (Sigma-Aldrich, # Z169021-1EA) and its cover slip was gently wiped with ethanol. The cell suspension should be sufficiently diluted in DPBS and disrupted uniformly to get a reasonable estimation of the actual cell concentration. For accuracy, clumps of cells should be disrupted. The suspension was mixed and before cells settle, 10 µl of the suspension was removed and mixed with 10 µl of Trypan Blue (Gibco®.#15250-061) A 10 µl volume of this mixture was then used to fill the chamber through V-shaped wells using a 20P micropipette. A haemocytometer was then read using a Carl Zeiss Axiostar microscope and 10 × objectives. Live cells in the middle square (surrounded by 14 squares) were counted using a manual counter (from 50 to 200 cells maximum). Cells that touch the right and bottom borders of the square were excluded. Dead cells, which appear as dark cells (stained with Trypan Blue), can be counted individually to determine the percentage of living cells. Cell density per ml was equal to the total number of cells in the square × 10^4. This number was then multiplied by two to adjust for the dilution by Trypan blue.

2.1.1.6 Cryopreservation of cell lines:

The protection of the cells and repeatable results were ensured in this study by using scientific methods for cell storage. Many compounds have been used as cryoprotective

agents. Dimethyl sulfoxide (DMSO) is a commonly used and effective agent and was typically added at a concentration of 10% in combination with serum. Other commercial cryoprotectants were used occasionally, such as CryoStem Freezing Medium (Miltenyi Biotec, #130-095-851) for preserving iPS cells. CryoMaxx II (PAA, # J05-012) is a serum free cryoprotective medium also used in the process of colonosphere preservation.

Colonospheres were disrupted to single cells by Accutase before freezing them. The cells were mixed gently with 1 ml of the cryoprotective agent and moved to Nunc™ Cryogenic Tubes (Thermo, # 375353). They then undergo gradual cooling in order to avoid ice crystal formation during the freezing process. A constant cooling rate of 1°C per minute from room temperature is highly recommended for successful cell recovery. The cooling rate can be controlled by placing the vial in a Nalgene 'Mr Frosty' freezing container filled with isopropanol at -80°C. After 48 hours, the vials were moved to a liquid nitrogen tank for long-term storage.

2.1.1.7 **Mycoplasma detection**

All cell lines were checked regularly for the presence of mycoplasma. The LookOut® Mycoplasma PCR Detection Kit (Sigma-Aldrich, # MP0035-1KT) has been used to detect mycoplasma in cell culture media. The procedure utilised to detect possible mycoplasma contamination is Real Time PCR. The primers were designed to detect the conserved 16S rRNA coding region of the genome of most common mycoplasma species.

Cells were grown for several days in the absence of any mycoplasma antibiotic and then 100 µl of the medium is transferred to Eppendorf tubes. PCR tests were prepared in 25 µl volumes according to Table 2.1 (based on the manufacturer's guide).

Table 2.1 PCR preparation for a mycoplasma test

	Test Sample	**Positive control**	**Negative control**

DNA Polymerase / Rehydration Buffer	23 µl	25 µl	23 µl
Sample Volume	2 µl	-	-
DNA-free Water		-	2

The PCR procedure was conducted and the samples were run on 1.2 % agarose gel for 25 minutes at 100 V. Successful test performance (including the negative control) was confirmed by a distinct 481 bp band. The positive control sample generates a band at 259 bp. If the sample test was contaminated with mycoplasma, it will show a band between 260 ± 8 bp.

2.1.2 Western blotting protocols

2.1.2.1 Protein extraction

RIPA buffer (Radio Immuno Precipitation Assay buffer) was first used to extract the whole cell proteins, including those from the nucleus, cytoplasm and membranes. RIPA was prepared by the following recipe:

150 mM NaCl

1.0% Triton X-100

0.5% sodium deoxycholate

0.1% SDS (sodium dodecyl sulphate)

50 mM Tris, pH 8.0

A flask of cultured cells was washed with cool DPBS and the cells were then detached using trypsin. The resulting cell suspension is washed twice with DPBS. The total number of cells was counted and an appropriate volume of RIPA buffer was added (1 µl/3000 cells). A commercial cocktail of inhibitors was added to the RIPA such as Complete, Mini, EDTA-free (Roche, #11836170001) as well as 4-(2-Aminoethyl) benzenesulphonyl fluoride hydrochloride (Sigma-Aldrich, #A8456). Lysis buffer was added to the tube and it was placed in 95ºC heat block for 5 to 10 minutes until the cell pellet has dissolved. The extracted protein was stored at -20°C or colder.

Protein was extracted from adherent and suspension cells using M-PER® Mammalian Protein Extraction Reagent (Thermo, # 78501). A suspension of cells was washed and pelleted for 10 minutes by centrifugation at 2500 × *g*. The supernatant was removed and the wet pellet was weighed. A total of 10 µl of M-PER was added for each mg of cell pellet. This mixture was mixed gently by shaking and kept at room temperature for 10 minutes. Cell debris was removed by centrifuging the tube for 15 minute at 14000 × *g*. The supernatant was transferred to another tube and kept in freezer until it was required.

Phosphatase Inhibitor (Cell Signaling, #5872) was added to the lysis buffer at a final 1× concentration for an experiment to investigate the phosphorylation condition of a particular protein. This protects the phosphorylated residues from phosphatases within the whole cell extracts that might dephosphorylate the protein.

2.1.2.2 Protein concentration assay using BCA

Using an equal amount of protein was very important in western blot analysis. The Pierce™ BCA Protein Assay Kit (Thermo, #23225) was used to measure the protein concentration in order to determine the amount of protein extract to add to each well. The manufacturer's guide was followed with slight modifications. A set of protein standards was prepared from the bovine serum albumin provided with the kit. A working reagent was then prepared by combining 50 parts of Reagent A with one part of Reagent B. Standards and test samples were then added to the working reagent and incubated for 30 minutes at 37ºC in the dark. Analysis and standard curve measurements were carried out with 1 µl of each sample using a NanoDrop ND 2000c Spectrophotometer (Thermo, # WZ-83061-12).

2.1.2.3 Detection of target protein

Sodium dodecyl sulphate (SDS) sample buffer (Novex, # NP0004) was added to a protein sample containing Sample Reducing Agent (Novex, # NP0004) and then placed in a heating block for 10 minutes at 70ºC. Aliquots (20-30 µg) of cell protein were then separated on a commercially available (Invitrogen) denaturing gel with different concentrations of polyacrylamide. (See the list of gels with their appropriate running buffers, available from Invitrogen, in Table 2.2) MES Running Buffer was used for separating small-sized proteins because it allows proteins to run faster than

when separating them with MOPS buffer. All buffers were prepared as concentrated reagents (20×) and are diluted with distilled water before use.

Table 2.2 A list of protein gel electrophoresis and running buffers.

#	SDS Running Buffer	Cat No.	Gels	Cat No.
1	NuPAGE® MOPS	NP0001	Bolt™ 4-12% Bis-Tris Plus	BG04125BOX
2	NuPAGE® MES	NP0002		
3	Bolt™ MES	B0001	NuPAGE® Novex® 4-12% Bis-Tris	NP0322BOX
4	Bolt™ MES	B0002		

Precision Plus Protein Kaleidoscope standards (BIO-RAD, #161-0375) are a combination of pre-stained molecular weight markers. This standard was loaded in a lane next to the samples to facilitate estimation of protein sizes.

An electrotransfer technique is used to blot (transfer) the proteins onto a PVDF membrane. The membranes have different pore sizes, so each was used for different protein sizes. The Immobilon-P Membrane, PVDF, with pore size of 0.45 µm (Millipore, # IPVH00010) was used for most proteins but for targeted protein with sizes smaller than 20 KDa, a membrane with a smaller pore size (0.2 µm) was used (Millipore, # ISEQ07850).

The membrane was usually cut to match the gel size and activated with methanol before use. Proteins were transferred electrophoretically for 3.5 hours at a cold temperature at 400 mA using transfer buffer [30.3 g of Trizma® base (SIGMA, #T1503), 144 g of Glycine (SIGMA, #G8898) and distilled water to 1 litre].

The membrane was then washed with water several times, followed by a blocking step. The membrane was blocked either with non-fat dry milk or serum (such as BSA which prepared in .03-.05 % Tween20/PBS) for at least one hour. The membrane was then incubated with the primary antibody overnight at 4°C on a rocker plate (see list of antibodies in Table 2.5. After washing, the membrane was incubated with the

secondary antibodies were conjugated to the primary antibody (the secondary antibody was diluted 1:25,000 in blocking solution) for 1 hour at room temperature. Secondary antibodies conjugate to horseradish peroxidase (HRP) for chemiluminescence detection.

Signal-generating solution was applied to the membrane to amplify light that can be detected by X-ray film. Chemiluminescent Peroxidase Substrate-3 (Sigma, #CPS3100-1KT) or Super Signal West Pico Chemiluminescent Substrate (Thermo, #34080) were reacted with the membrane for 5 minutes and the membrane was then placed between two transparency films in X-Ray Cassettes and exposed to CL-XPosure film (Thermo, #34088) for a period of time that differs from one antibody to another. The film was developed in a dark room in an X-Ray Film Processor according to manufacturer's (MI-5) guide.

2.1.3 Immunostaining protocol

Cells were grown on sterile 13 mm circular cover glasses in 24-well plates at a density of 50,000 cells per well. Cells were grown for at least 24 hours to let them become well attached and so that they were sub-confluent when they were ready for staining. The medium is then removed and the cells were washed with DPBS. The cells were fixed with 4% paraformaldehyde for 25 minutes at room temperature. Fixation is an important step as it preserves the morphology and antigenicity of the cells. The cells were then incubated with 0.2% Triton X-100 to permeabilise them for detection of intracellular proteins. Unspecific antigen were blocked by incubating with 10% FBS/DPBS at 37°C for at least one hour.

After blocking, the cells were incubated with the primary antibody (see list of antibodies in Table 2.5) for one hour at 37°C. In some cases, incubation could be extended to overnight at 4°C. The cells were then washed three times with DPBS, followed by incubation with the appropriate secondary antibody for 30 minutes at 37°C. Secondary antibodies were labeled with one of the Alexa Fluor® fluorescent probes. All antibodies were prepared in 10% FBS/DPBS at different concentrations according to the manufacturer's guide. A mixture of nucleus stain with Vectashield® (Vector lab, # H-1000) was applied and the cover glass was sealed to the slide with nail polish. Images were acquired with an AxioCam HR microscope camera using

Zeiss Axioskop2 Microscope filters for DAPI, FITC and Rhodamine. The camera was controlled by Zeiss Axiovision software that facilitates image processing and analysis. Negative control samples were prepared by omitting the addition of the primary antibody to test the specificity of the immunostaining reactions.

2.1.4 siRNA gene silencing

Small interfering RNA (siRNA) is short double-stranded RNA consisting of 21 base pairs. The addition of siRNA to cells cultures has been shown to reduce protein production in a highly specific manner. FlexiTube GeneSolution is a predesigned siRNA from Qiagen for use with multiple siRNAs for each specific gene, and was chosen for use in this study. (see the list of siRNAs and their sequences in Table 2.6). The siRNAs were received in lyophilized form and were resuspended according to the Qiagen guide.

The siRNA transfections with HiPerFect (Qiagen, #301704) were conducted by seeding cells in 6-well plates the day before transfection (indirect transfection). The cell confluency was calculated for every cell line before the experiments to determine the seeding number. The siRNA was diluted in 100 µl of culture medium that does not contain serum, and then 0.6 µl of HiPerFect reagent was also added and mixed gently. The complex was incubated at room temperature for 20 minutes and then added to the well. The amount of siRNA and HiPerFect may vary from cell to cell and might need to be optimised. In some cases, the cells required multiple transfections with siRNA over several days. In some cases, transfection has been also conducted with 10 µl Lipofectamine® RNAiMAX (Invitrogen, # 13778-150).

AllStars Negative Control siRNA (Qiagen, # 97315239) was used as a negative control in addition to the transfection sample (mock knockdown). The efficiency of gene silencing was checked by western blotting or quantitative RT-PCR.

2.1.5 Metaphase chromosome spreading protocols

2.1.1.1. Metaphase chromosome preparation

Cells were grown for a few days and the medium was replaced with fresh medium prior to examination. Cells were arrested in metaphase by adding 10 ng/ml of KaryoMAX® Colcemid™ (Gibco®, # 15212-012) to the medium. Incubation

durations vary from one cell line to another, depending on the growth rate. If cells were transfected with siRNA, colcemid was added at the end of the treatment.

Mitotic cells were then harvested by a mitotic shake-off method. Cells usually round up during metaphase and become loosely attached. Flasks were therefore shaken several times and the medium containing mitotic cells was collected in a 15 ml conical tube. The cells were washed with DPBS and incubated with pre-warmed hypotonic 75 mM Potassium Chloride solution (Gibco®, # 10575-090) for 10 minutes. Fresh fixative is prepared from methanol and acetic acid (methanol: acetic acid 3:1). Slides were cleaned with alcohol and kept in the freezer until use. Fixatives were kept in a freezer and then added dropwise to the cells gradually against the tube wall (repeated twice). Slides were held vertically with forceps and 30 µl of cell suspension with fixative were dropped onto the middle of the slide from a distance. For better spreading, the slides were dried in a water bath for a few minutes and then kept in dry place until staining.

Slides were washed with DPBS for few minutes, followed by staining. Chromosomes were stained with any of the nucleus staining reagents such DAPI, PI, or Hoechst stains. Chromosomes were screened using a Zeiss Axioskop2 Microscope under a 100× objective and were photographed with an AxioCam HR microscope camera.

2.1.5.1 **Sister chromatid exchange assay**

The sister chromatid exchange (SCE) is one of the common techniques used to study genome instability and involves staining of the chromosomes with bromodeoxyuridine (5-bromo-2'-deoxyuridine, BrdU). BrdU (Sigma, # B9285) is a water-soluble compound and was prepared as a stock solution in DPBS by heating at 70°C (stable for few months). The reagent was filtered before use and added to the medium at concentration of 100 µM. Plates were kept in the dark and cells should complete a minimum of two cell cycles before harvesting. If the experiment was designed to study the effects of a specific siRNA on the SCE level, BrdU was added to the medium at the end of the transfection.

Colcemid was added to the medium and chromosome spreading was carried out as described in Section 2.1.5.1. The slides were then stained with Hoechst 33342 and placed in an Ultraviolet Crosslinker for 30 minutes at room temperature.

2.1.5.2 Immunofluorescent labelling of unfixed human metaphase chromosomes

Chromosomes are prepared for immunofluorescence staining to localize proteins of interest. Chromosomes were spread on a slide after hypotonic treatment using a cytocentrifuge (Hettich Rotofix 32A). A total of 200 µl of cell suspension at concentration of 200,000 cell/ml was added to the cytofunnel chamber and spun down for 10 minutes at 1800 rpm. The slide was then immediately immersed in potassium chromosome medium buffer (KCM), prepared from the following components: 120 mM KCl, 20 mM NaCl, 10 mM Tris-HCl, pH 8.0, 0.5 mM EDTA and 0.1% (v/v) Triton X-100. The primary antibody was diluted in 1% BSA/KCM and then applied to slide and incubated in a humidified chamber for one hour at 4°C. The slide was then washed twice in a Coplin jar and the secondary antibody (diluted in 1% BSA/KCM at the desired concentration) was applied to the slides. Following incubation, the slide was immersed in KCM buffer twice and then fixed with 4% (v/v) PFA/KCM. Slides finally were prepared and visualised as described previously in Section 2.1.3.

2.1.5.3 Chromosome Pan-Centromeric painting

Chromosomes spreads were prepared as described previously Section 2.1.5. The Star*FISH© paint system (CAMBIO, # 1695-F-01) was utilized to detect the centromeric DNA (Photoprobe biotin-labelling system). The kit is provided with DNA probes that detect the centromeric region of each chromatid.

Slides were pre-treated according to the manufacturer's guide. The slide was first immersed in a graded alcohol series then baked for 15 minutes. It was then transferred to acetone followed by incubation with 2×SSC+ RNase for 1 hour at 37°C. The slide was then washed with 2×SSC and PBS, followed by incubation with pepsin to remove excess protein. The slide was then washed and cellular DNA was denatured by passing the slide through 70% formamide.

Probes were prepared by warming up then and adding them to hybridisation buffer at a total of 12.5 µl per test. Chromosomes were denatured in formamide at 70°C, and then immersed in ice-cold 70% ethanol, followed by dehydration through an alcohol series. The probes were denatured for 10 minutes at 85°C, chilled instantly on ice and then applied to the slides. The hybridisation process for slides takes place overnight in a humidified chamber at 37°C.

On the second day, the slides were washed to remove unbound DNA, followed by a detection step using a Cambio Detection Kit (CAMBIO, #1089-KB-50). All washing reagents provided with the kit were prepared following the manufacturer's guide. Biotin Labelled Chromosomes were detected with FITC to facilitate visualizing them with the fluorescence microscope.

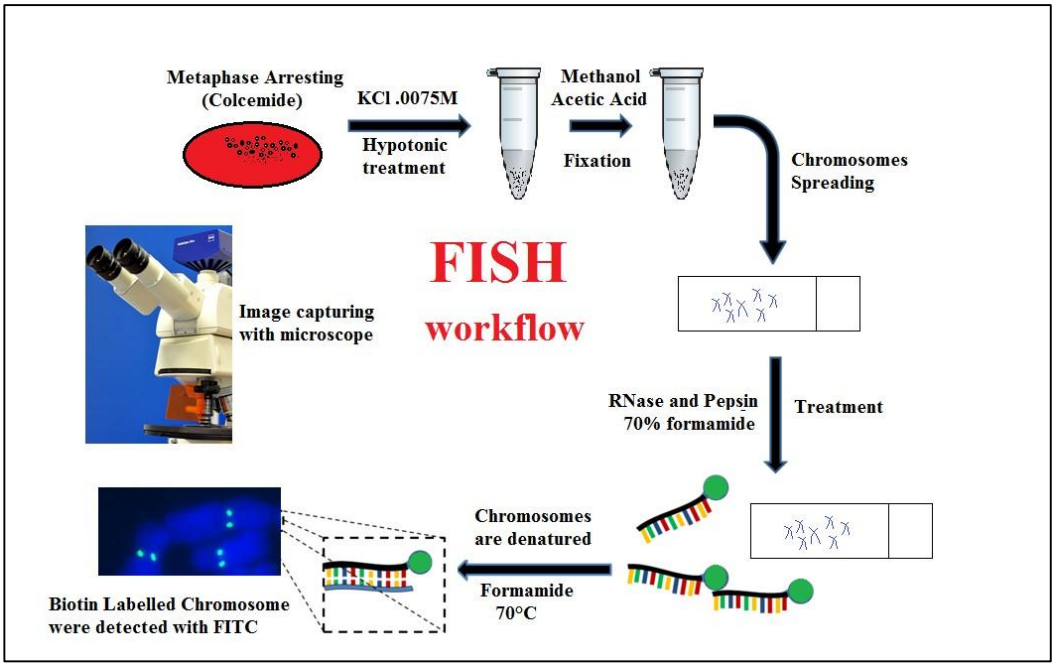

Figure 2:2 The workflow for performing FISH identification using the Star*FISH© paint system

2.1.6 Flow cytometry assays

Following the treatment, suspension cells (dissociated and washed with PBS) and attached cells (trypsinized and washed with DPBS) were pooled and spun down by centrifugation. The supernatants were discarded and the cell pellets were washed with PBS and then mixed gently with 90% ice-cold ethanol (in some cases, with 100% methanol). (Samples could be stored after fixation in -20°C for up to one month.) Cells were washed with DPBS followed by overnight incubation with 50 µg/ml of Propidium Iodide (PI) and Ribonuclease A from bovine pancreas. Cell cycle assays and nuclear DNA content were then quantitatively analyzed by flow cytometry using a Particle Analysing System (PAS III, Partec). This machine was operated with the Partec Robby® Partec FloMax® software on a Windows™ operating system.

2.1.7 PCR protocols

2.1.1.1. **RNA extraction**

RNA was isolated from cells using the RNeasy Plus Mini Kit (Qiagen, # 74134). Cells were first lysed and homogenised with Buffer RLT Plus, which contains guanidine isothiocyanate. Genomic DNA was then removed by passing the lysate through a gDNA Eliminator spin column. Ethanol was added and the sample was applied to an RNeasy MinElute spin column that specifically binds the RNA from the lysed cells. Buffer RW1 and Buffer RPE were applied to the sample and the flow-through was discarded. RNA was finally eluted in 20 to 30 µl with RNA-free water and collected in a fresh tube. RNA quality and concentration may be examined using a NanoDrop ND 2000c Spectrophotometer.

2.1.7.1 **RT-PCR and qRT-PCR**

RNA was reverse transcribed into complementary DNA (cDNA) from equal amount of RNA using the SuperScript III First Strand synthesis system (Invitrogen, # 18080051). Instructions in user manual has been followed. This cDNA was used in quantitative real-time PCR (qRT-PCR) reactions run in three replicates for each cDNA using CFX96 real-time PCR detection system. Reaction was performed using SYBR Green (Promega, #A6001) and commercial primers from Qiagen (Table 2.8). Analysing the results include the standard deviation between replicates and

normalizing the results was carried out using BioRad CFX Manager Software. Master mix were amplified with a pre-cycling hold at 95°C for 10 minutes, followed by 39 cycles of 95°C for 15 seconds and 60°C for 60 seconds. Melt curve analysis was taken place after completion the 39 cycles. cDNA is also used for reverse transcription (RT-) PCR. Primers of each genes were designed to span introns where possible. A total volume of 2 µl diluted cDNA was used in the PCR with a final volume of 50 µl. BioMixTM Red (Bioline; BIO-25006) was used for the PCR amplification as per the manufacturer's instructions.RT-PCR for *β*-Actin and was carried out for all cDNA samples as controls. PCR products were separated on 1.5 % agarose gels stained with peqGREEN the non-toxic RNA dye (PEQLAB, # 37-5010).

2.1.8 Induced pluripotent stem cells protocol methods

2.1.8.1 Overview

The Stemgent mRNA Reprogramming Kit (Miltenyi Biotec, #130-097-19) was used in this project to produce induced pluripotent stem cells (iPSCs) from human fibroblasts through direct delivery of modified mRNA, which increased the expression of transcription factors. This system is a non-integrated and virus-free method, which makes it safer and less risky in terms of genome integrity (see Table 2.3 for the components of the kit). The User Manual provided with kit is described here briefly.

Table 2.3 The components of Stemgent mRNA Reprogramming Kit

#	Product	Description	Catalog No.
1	Oct4 mRNA	transcription factors	05-0014
2	Klf4 mRNA	transcription factors	05-0015
3	Sox2 mRNA	transcription factors	05-0016
4	c-Myc mRNA	transcription factors	05-0018
5	Lin-28 mRNA	transcription factors	05-0017
6	nGFP mRNA	transcription factors	05-0019
7	B18R	Recombinant Protein Carrier-Free	34-8185-85
8	Pluriton™	Reprogramming Medium	00-0070

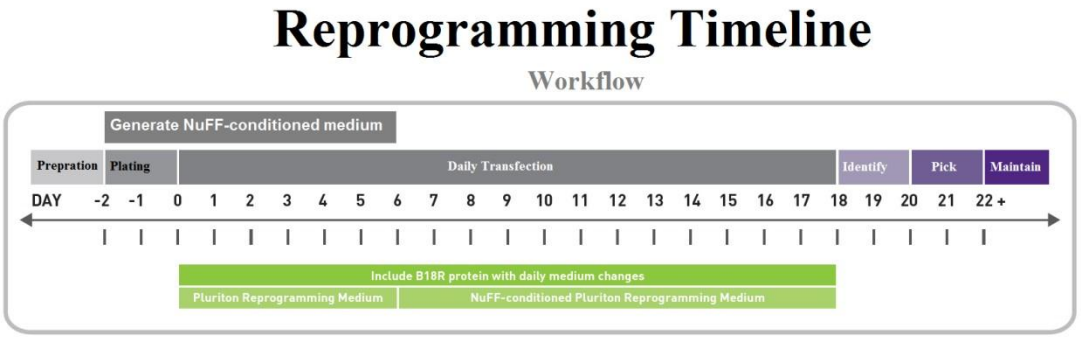

Figure 2:3 This timeline shows the stages required for mRNA reprogramming as described in the Stemgent mRNA Reprogramming Kit User Manual.

2.1.8.2 Cell preparation and plating

On day 2, human NuFF feeder cells were seeded in a gelatin coated plate at the density of 2.5x 10^6 cells per well in a 6-well plate. Cells were incubated overnight at 37°C in a 5% CO_2 atmosphere. NuFF cells were also plated in T75 flasks to generate NuFF-conditioned Pluriton™ Medium. On the following day, the culture medium was removed and BJ fibroblasts (human foreskin) were plated in individual wells at densities of 5000, 10000 and 25000 cells per well in BJ culture medium.

2.1.8.3 mRNA transfection

All materials were prepared and aliquoted as described in the manufacturer's manual, include master mRNA cocktail, Pluriton™ supplement and B18R Recombinant Protein Carrier-Free medium, and then stored at -80°C. On day 0, the culture medium is removed and the B18R medium was added to Pluriton™ Reprogramming Medium after equilibration. B18R should be applied to the cells prior to each transfection to reduce the interferon response of the cells.

On day 1, a single aliquot of mRNA cocktail was thawed and transferred immediately to Opti-MEM® reduced serum medium (Invitrogen, # 31985-062). In a separate tube, mRNA transfection complex was generated by adding Lipofectamine™ RNAiMAX to Opti-MEM® medium. Both tubes were combined, mixed gently, and then incubated at room temperature for 15 minutes. The transfection complex was then added dropwise to the cells and distributed uniformly across the well. The culture medium

was replaced with fresh equilibrated Pluriton reprogramming medium (with B18R protein) after 4 hours of incubation.

From day 1 to day 21, the cells undergo daily transfection at the same time as the first transfection was performed. The cells are observed regularly and the expression of nGFP was monitored using a Nikon TE2000-U microscope. Beginning from day 6, Pluriton™ medium was replaced with NuFF-conditioned Pluriton™ Reprogramming Medium.

2.1.8.4 **Identifying iPS Cells**

Following the completion of mRNA transfection series, iPSC colonies were observed with distinguished morphological change. The colonies were then allowed to expand for a few days in NuFF-conditioned Pluriton™ Reprogramming Medium with B18R.

Priority was given to the colonies that express the pluripotency marker. The expression of TRA-1-60 on live iPSC is examined using StainAlive™ TRA-1-60 antibody (Stemgent, #09-0068).

In addition, cells were stained with Alkaline Phosphatase Live Stain (Molecular Probes®, #A14353) that stains only undifferentiated iPSCs. Phenotypic assessment of iPSCs was performed using the AP staining kit (Stemgent, #00-0009). Cells were fixed and then incubated with 0.05% Tween 20/DPBS at room temperature. The stained cells appear red or pink, whereas the surrounding cells are colourless. The colour can be visualized by eye or with a light microscope.

2.1.8.5 **Picking and Passaging iPSCs Colonies**

The procedure of picking and transferring was done in aseptic condition. The priority was given to the cells that showed the proper ES cell morphology with distinguished colony edges. Each colony was divided into four parts and each part was transferred into an individual well of a 24-wells plate using an insulin syringe. Syringes were changed for each colony to avoid contamination with other colony. The plate was plated with an irradiated MEF feeder layer one day before picking the colony, at a density of 50,000 cells per well.

The cells were expanded in Pluriton™ Reprogramming Medium for 3 passages without B18R. The iPSC medium was changed every day to provide essential growth

factors and nutrients for the cells. For a few passages, the iPSCs were passaged manually without enzyme. For optimum passaging, the StemPro® EZPassage™ tool (Invitrogen, # 23181010) was utilized to cut the colony into uniform sized pieces. Pluriton™ Reprogramming Medium was replaced with human iPSC medium, as described in the guide (see Table 2.4). The medium was then filtered using a Stericup-GP filter unit with a 0.22 µm pore size (Millipore, #SCGPU01RE) and then stored at 4°C for no more than two weeks.

Table 2.4 Components of Human iPSC culture medium

#	Product	Catalogue	Origin
1	400 ml of DMEM/F-12, HEPES	11330-032	Gibco
2	100 ml of Knockout™ Serum Replacement	10828-028	Invitrogen
3	5 ml of Non-Essential Amino Acids (100X)	11140-050	Gibco
4	5 ml of L-glutamine (200 mM)	25030-081	Gibco
5	1 ml of bFGF (at 10 µg/ml; 20 ng/ml final concentration)	03-0002	Stemgent
6	500 µl of β-mercaptoethanol (1000X)	21985-023	Gibco
7	5 ml Penicillin/Streptomycin (100X) (optional)	15070-063	Gibco

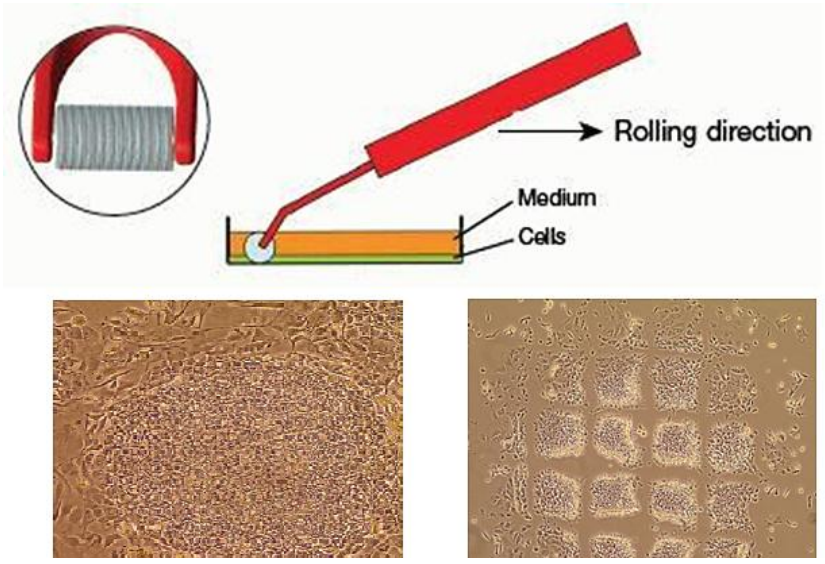

Figure 2:4 Manual passaging of iPSCs using the STEMPRO® EZPassage™ tool.

2.2 Materials:

2.2.1 List of Antibodies

Table 2.5 list of antibodies

#	Antibody	Catalogue No.	Origin
1	Rabbit polyclonal to Ki67	ab15580	ABCAM
2	Rabbit polyclonal to GEN1	ab102836	ABCAM
3	Rabbit polyclonal to Bloom Protein BLM	ab2179	ABCAM
4	Mouse monoclonal (3-19) to CENP-A	AB13939	ABCAM
5	Mouse monoclonal to Mus81	Ab14387	ABCAM
6	Rabbit polyclonal to PCNA	ab15497	ABCAM
7	Mouse monoclonal to SSEA4	ab16287	ABCAM
8	Mouse monoclonal to TRA-1-60 [R]	ab16288	ABCAM
9	Rabbit polyclonal to Oct4 - ChIP Grade	ab19857	ABCAM
10	Rabbit polyclonal to Nanog	ab21624	ABCAM
11	Rabbit polyclonal to Rad51	ab63801	ABCAM
12	Rabbit polyclonal to FANCM	ab95014	ABCAM
13	Rabbit polyclonal to SOX2	ab97959	ABCAM
14	Rabbit polyclonal to CENP-A	2186s	Cell Signalling
15	Rabbit polyclonal to Phospho-Chk1 (Ser345)	2341S	Cell Signalling
16	Mouse to total Chk1	2345s	Cell Signalling
17	Rabbit monoclonal to Phospho-Histone H2A.X	#9718P	Cell Signalling
18	Rabbit monoclonal to Phospho-Chk1 (Ser345)	#2348P	Cell Signalling
19	Mouse monoclonal to total-chk1 (2G1D5)	#2360S	Cell Signalling
20	Rabbit monoclonal to cleaved Caspase-3 (Asp175)	9664s	Cell Signalling
21	Alexa Fluor® 568 Goat Anti-Rabbit IgG (H+L)	A-11011	Invitrogen
22	Alexa Fluor® 488 Goat Anti-Rabbit IgG (H+L)	A-11008	Invitrogen
23	Peroxidase- Donkey Anti-Rabbit IgG (H+L)	711-035-152	Jackson immuno
24	Peroxidase- Donkey Anti-Mouse IgG (H+L)	715-035-150	Jackson immuno
25	Anti SSEA-4	130-098-369	Miltenyi Biotec
26	Rabbit polyclonal to Mus81	NBP1-32054	Novus

27	Mouse polyclonal to Brachyury	AF2085	R&D
28	Rabbit polyclonal to HJURP (H-277)	sc-134696	Santa Cruz
29	Goat polyclonal to HJURP HJURP (S-14)	sc-168091	Santa Cruz
30	Mouse anti-goat IgG-TR	sc-3916	Santa Cruz
31	StainAlive™ TRA-1-60 Antibody	09-0068	Miltenyi Biotec
32	Mouse monoclonal to Tra-1-60	130-095-624	Miltenyi Biotec
33	Mouse monoclonal to Tra-1-81	130095627	Miltenyi Biotec
34	Monoclonal Anti-α-Tubulin antibody produced in mouse	T6199	SIGMA

2.2.2 siRNA reagents

Table 2.6 List of siRNA and their target sequences

Gene	Product name	Cat. No	Target sequence	Gene ID
BLM	Hs_BLM_4	SI00000959	GACGCTAGACAGATAAGTTTA	GS641
	Hs_BLM_5	SI03033387	AAGCGACATCAGGAGCCAATA	GS641
	Hs_BLM_1	SI00000938	CCGAATCTCAATGTACATAGA	GS641
	Hs_BLM_2	SI00000945	CTGACCATCTGTGACTATAAA	GS641
GEN1	Hs_FLJ40869_6	SI04174604	CACCTAAGGATCATGAACGTA	GS348654
	Hs_FLJ40869_8	SI04284007	TTCGAATTGTTAAGACTCGAA	GS348654
	Hs_FLJ40869_4	SI00414757	ATGGAGAATTTGCTTTATTAA	GS348654
	Hs_FLJ40869_5	SI04153870	CTGGTTGGATTAGCAATACTT	GS348654
MUS81	Hs_MUS81_6	SI04300877	ACCATTAAGTGTGGGCGTCTA	GS80198
	Hs_MUS81_7	SI04342968	CCGGGTATACCTGGTGGAAGA	GS80198
	Hs_MUS81_4	SI00652036	CACGCGCTTCGTATTTCAGAA	GS80198
	Hs_MUS81_5	SI04222428	CGGGAGCACCTGAATCCTAAT	GS80198

2.2.3 Chemical reagents

Table 2.7 list of chemical reagents

#	Product	Solvent	Classification	catalogue	Origin
1	Thymidine	Water	Chemotherapeutic	T9250	Sigma
2	Cisplatin	Water	Chemotherapeutic	P4394	Sigma
3	Aphidicolin	DMSO	Chemotherapeutic	A0781	Sigma
4	Camptothecin	DMSO	Chemotherapeutic	C9911	Sigma
5	Bromodeoxyurdine	Water	Thymidine analogue	B9285	Sigma
6	Formaldehyde	DPBS	Fixative	28906	Thermo

2.2.4 RT-PCR primers

Table 2.8 RT-PCR Primers and their expected product size

Gene	Primer sequence	Product size (bp)
OCT4/3	F CTGGAGAAGGAGAAGCTGGA	509
	R GCATAGTCGCTGCTTGATCG	
Nanog	F CTGCTGAGATGCCTCACACG	497
	R GCTCCAGGTTGAATTGTTCC	
SOX2	F GCAACCAGAAAAACAGCCCG	590
	R CGAGTAGGACATGCTGTAGG	
Bloom	F GACCAGCGATCGCTTATGTG	680
	R GCTATTGGCTCCTGATGTCG	
β-Actin	F AGAAAATCTGGCACCACACC	553
	R AGGAAGGAAGGCTGGAAGAG	

2.2.5 qRT-PCR primers

Table 2.9 list of qPCR primers

#	Assay name	Catalogue	Origin	Comments
1	Hs_RECQL4	QT00201740	Qiagen	RecQ protein-like 4
2	Hs_RECQL	QT01007363	Qiagen	DNA helicase Q1-like
3	Hs_RECQL5	QT00084973	Qiagen	RecQ protein-like 5
4	Hs_WRN	QT00074809	Qiagen	Werner syndrome, RecQ helicase-like
5	Hs_BLM	QT00027671	Qiagen	Bloom syndrome, RecQ helicase-like
6	Hs_NTF3	QT00204218	Qiagen	Neurotrophin 3
7	Hs_RTEL1	QT00053095	Qiagen	Regulator of telomere elongation helicase 1
8	Hs_BRIP1	QT00086548	Qiagen	BRCA1 interacting protein C-terminal helicase1
9	Hs_CDKN2A	QT00998459	Qiagen	Cyclin-dependent kinase inhibitor 2A
10	Hs_PRM2	QT01173830	Qiagen	Protamine 2
11	Oct-3/4	GSR-1001	Globalstem	Undifferentiated pluripotent marker
12	Nanog	GSR-1001	Globalstem	Undifferentiated pluripotent marker
13	Rex1	GSR-1001	Globalstem	Undifferentiated pluripotent marker
14	Dppa4	GSR-1001	Globalstem	Undifferentiated pluripotent marker
15	DNMT3b	GSR-1001	Globalstem	Undifferentiated pluripotent marker
16	GAPD	GSR-1001	Globalstem	Housekeeping gene
17	GUSB	GSR-1001	Globalstem	Housekeeping gene
18	YWHAZ	GSR-1001	Globalstem	Housekeeping gene

2.2.6 Tools and Equipment

Table 2.10 list of tools and equipment

#	Item	Code or model	Origin
1	Centrifuge Hettich Rotofix 32A	GB-C1206	WOLF LAB
2	Centrifuge	C3 series	JOUAN
3	Rotor for cytology work 6 place swing out	GB-A1626	WOLF LAB
4	Bucket CYTO-suspension with lid	GB-A1680	WOLF LAB
5	One chamber cyto slide carrier	GB-A1662	WOLF LAB
6	Cyto angle chamber with sealing	GB-A1671-C	WOLF LAB
7	Pack of filter cards for angle cyto chamber	GB-A1696	WOLF LAB
8	NanoDrop - Spectrophotometer	ND 2000c	THERMO
9	Bright-Line™ Haemocytometer	Z359629-1EA	SIGMA
10	Filter unit	10626921	FISHER
11	Carl Zeiss Microscope	Axioskop 2 Plus	ZEISS
12	ECLIPSE- inverted microscope	TE2000-U	NIKON
13	Corning® Ultra-low attachment culture dishes	CLS3262	SIGMA
14	Partec Flow Cytometry	PAS-III	PARTEC
15	Imaging System	Evos™ XL Core	FISHE
16	Inverted Research Phase Microscope	TMS-F	NIKON
17	Circular cover glass 13 mm	1200851/1	LAB LTD
18	Immobilon-P Membrane, PVDF, 0.45 µm	IPVH00010	MILLIPORE
19	Slides	S9400	SIGMA
20	The Bioer GenePro - thermal cycler	TC1120	Alpha Labs
21	CFX96 real-time PCR detection system	C1000	Bio-Rad
22	CyFlow®	Cube 8	Partec

Chapter 3

Results

Chapter 3. The role of homologous recombination in CENP-A depositioning in human centromere

3.1 Introduction

Centromeres are critical sites within a chromosome that are recognized by microtubules for spindle attachments. Centromeric DNA is not conserved in sequence and remains ill-defined, although large centromeres share similar features such as repetitive DNA elements (Pauleau and Erhardt, 2011; Pidoux and Allshire, 2005). Centromere function appears to be defined epigenetically as all characterized centromeres contain the histone H3 variant CENP-A. Plasticity in centromere locations is apparent, as illustrated by induced and naturally occurring neocentromeres which strongly supports the notion that centromere are defined by epigenetic factors (Stellfox et al., 2013). In rare but naturally occurring cancer patient cases, centromeres appear at other locations within the chromosome and without any obvious DNA rearrangements (Jansen et al., 2007).

CENP-A is distinguished from typical histones in the mechanism and timing of its loading in centromeric nucleosome. Histones H2A, H2B, H3 and H4 were identified to be inserted during DNA synthesis but CENP-A insertion in most cases take place outside S-phase with different timing in every organism. Loss of CENP-A from centromeres causes chromosomes miss-segregation that can result in cell cycle disruption. Additionally, overexpression of CENP-A has been demonstrated in some cancers including breast cancer, bowel cancer and malignant hepatoma (Doherty et al., 2014).

Existing CENP-A is quantitatively preserved at centromeres in late G1 and redistributed to sister centromeres after chromosomes duplication. Therefore, constant inheritance of the centromere locus needs CENP-A delivery for every cell cycle and such processes depend on the CENP-A-specific chaperone HJURP, that directs the loading of CENP-A into chromatin with the collaboration of the Mis18 complex. Yet, the mechanism by which Mis18 assists HJURP at centromeres remains poorly understood to date (Zasadzińska et al., 2013).

The current model of centromere structure and integrity has not yet fully explained the existence of repetitive DNA sequences at centromeres. However, a recent model has

addressed the importance of repeated DNA elements (McFarlane and Humphrey, 2010). This model proposes a role of centromeric recombination through the formation of covalently closed DNA loops (CCLs) in both inverted and direct repeat containing centromeres (McFarlane and Humphrey, 2010). It also postulates the need for recombination intermediates (possibly HJs) to drive HJURP CENP-A loading.

Independent of this model, a recent study has showed that disrupting the Holliday junction dissolution/resolution pathways in Bloom syndrome cells resulted in abnormal morphological changes. MUS81 and GEN1 depletion has led to chromosomes breakage and noticeable reduction in cells viability. They suggested that this might be because of losing HJ processing which led to sister chromatid entanglements and impairing chromosome condensation (Wechsler et al., 2011).

This work in this chapter aims to utilize observed chromosome aberrations to examine the current model of centromere structure and function. We hypothesize that unresolved HJs caused by loss of HJ dissolution/resolution activity may employ HJURP to load new CENP-A at sites of unresolved HJs. The possibility of CENP-A deposition will provide strong supporting evidence for a role of HJs in targeting CENP-A to genomic sites.

3.2 Results

3.1.1 Localization of CENP-A and HJURP in Human Cells

To address the core hypothesis, a first step was to demonstrate CENP-A could be accurately localized in cells. Commercial antibody to CENP-A were tested for the correct staining pattern. CENP-A protein was visualized in human cells NT2, HCT116, GM08505 and 132N1. Cells were grown in culture then fixed and permeabilized for standard immunustaining procedure (as described in Chapter 2). CENP-A was labelled with a commercial antibody (ABCAM, 2186s) followed by fluorescence-labelled secondary antibody. CENP-A is observed exclusively in the nucleus as multiple foci. Immuno staining of α-tubulin was used for specifying the cytoplasm region (Figure 3.1). The specificity of this antibody was confirmed by immunostaining of NT2 cells with secondary antibody without the addition of anti-CENP-A as shown in appendix (8.1) Similar CENP-A staining was observed in HCT116, GM08505 and 132N1 (data not shown).

To localize the CENP-A on metaphase chromosomes, NT2 cells were arrested by Colcemid then collected by the mitotic shake-off technique. The advantage of this procedure is that it increased the number of cells in metaphase and gave a chance to assess CENP-A localization on condensed chromosomes (Figure 3.2.). As expected, immunolocalization of CENP-A on human metaphase chromosomes demonstrated characteristic foci at the expected centromeric region within every chromatid as shown in Figure 3.2.

Considering the role of HJURP in depositing new CENP-A at centromeres, the co-localization of HJURP in metaphase cells relative to CENP-A was examined (Figure 3.3). Their locations were consistent with previous work (Dunleavy et al., 2009), showing a discrete foci pattern in the nucleus and specificity not similar to CENP-A within the centromere region. Cells demonstrated varying levels of HJURP intensity and some of them did not exhibit any fluorescence. Co-localization of HJURP and CENP-A was not observed to any high degree, however a low percentage of cells did exhibit co-association of HJURP to CENP-A signals as shown in Figure 3.3b. Notably, in some cells that are presumably at the stage of cytokinesis, HJURP localized in the nucleus in a specific spotted pattern as shown in Figure 3.3a.

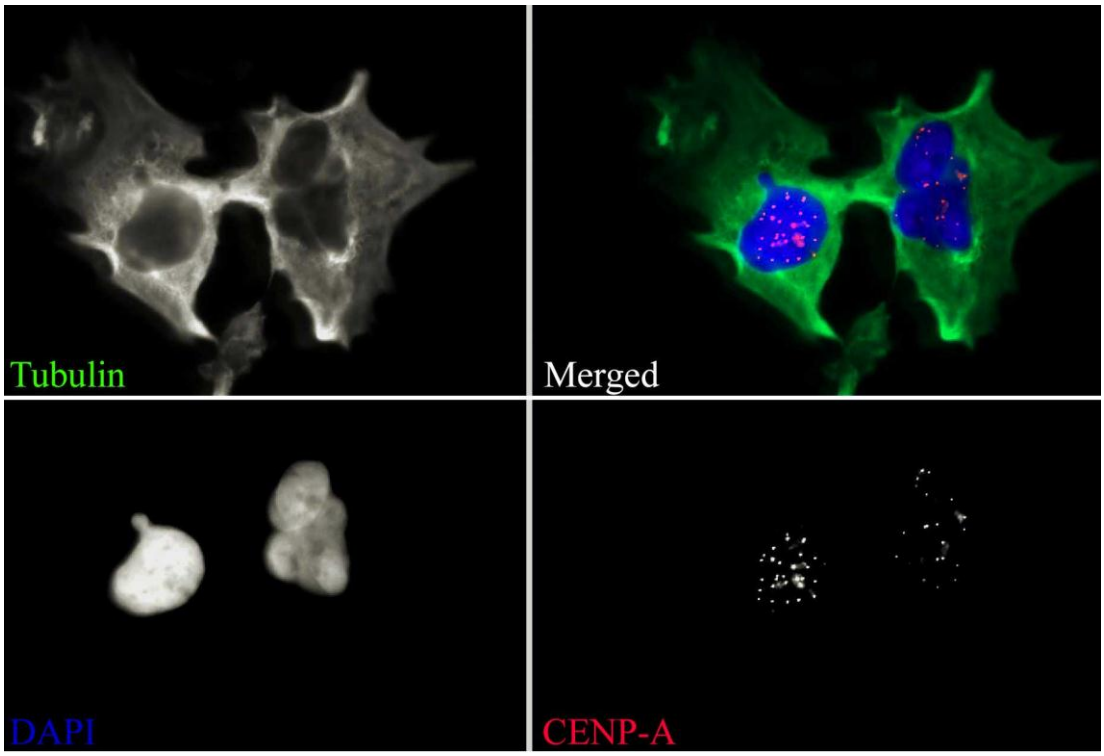

Figure 3:1: Fluorescence image showing the localization of CENP-A in human cells

Immunofluorescent staining of NT2 cells with anti-CENP-A (Red) and anti-Tubulin (Green). Nuclei were visualized with DAPI staining (blue). The photographs were taken under a Zeiss Axioskop 2 fluorescent microscope (100 x objective).

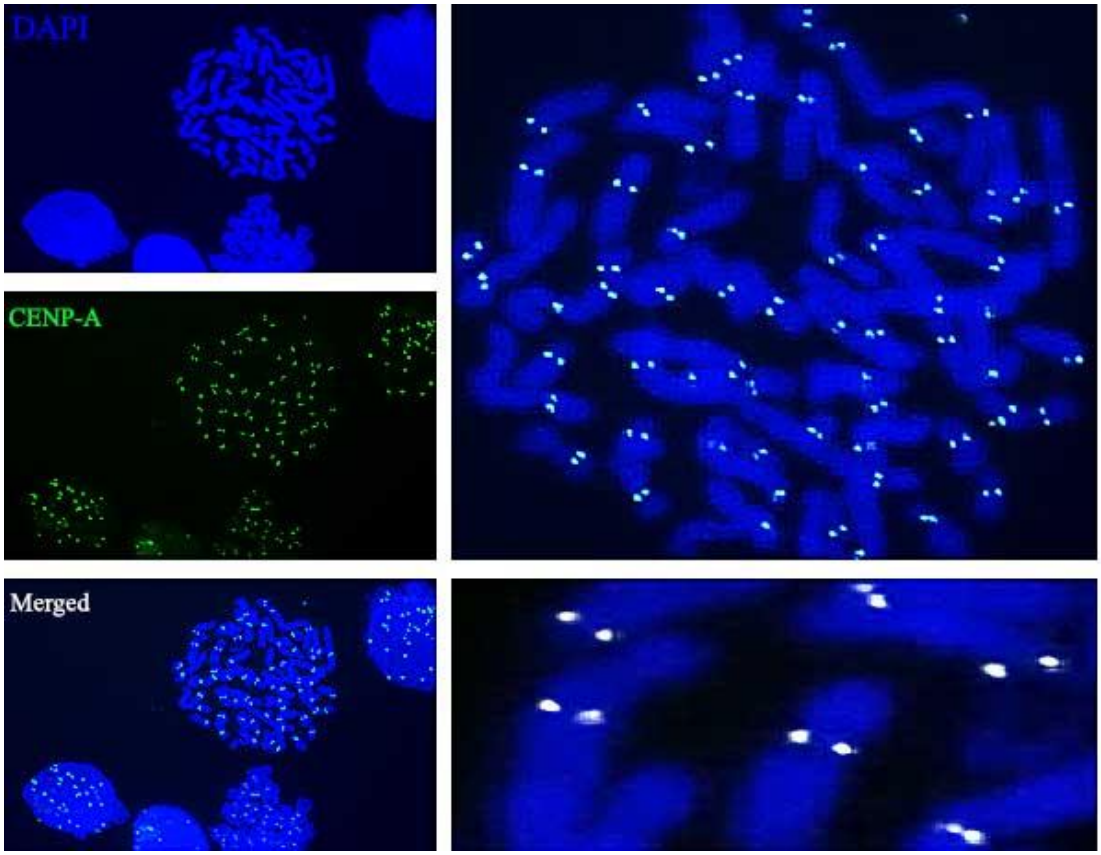

Figure 3:2 Visualizing CENP-A on metaphase chromosomes.

This shows human metaphase chromosomes of NT2 stained with anti-CENP-A antibody (green). This antibody localizes to centromeres. Chromosome spreads were prepared using "mitotic shake-off" procedure. Nuclei were visualized with DAPI staining (blue). The photographs were taken under a Zeiss Axioskop 2 fluorescent microscope (100 x objective). A right panel shows the selected sections at higher magnification.

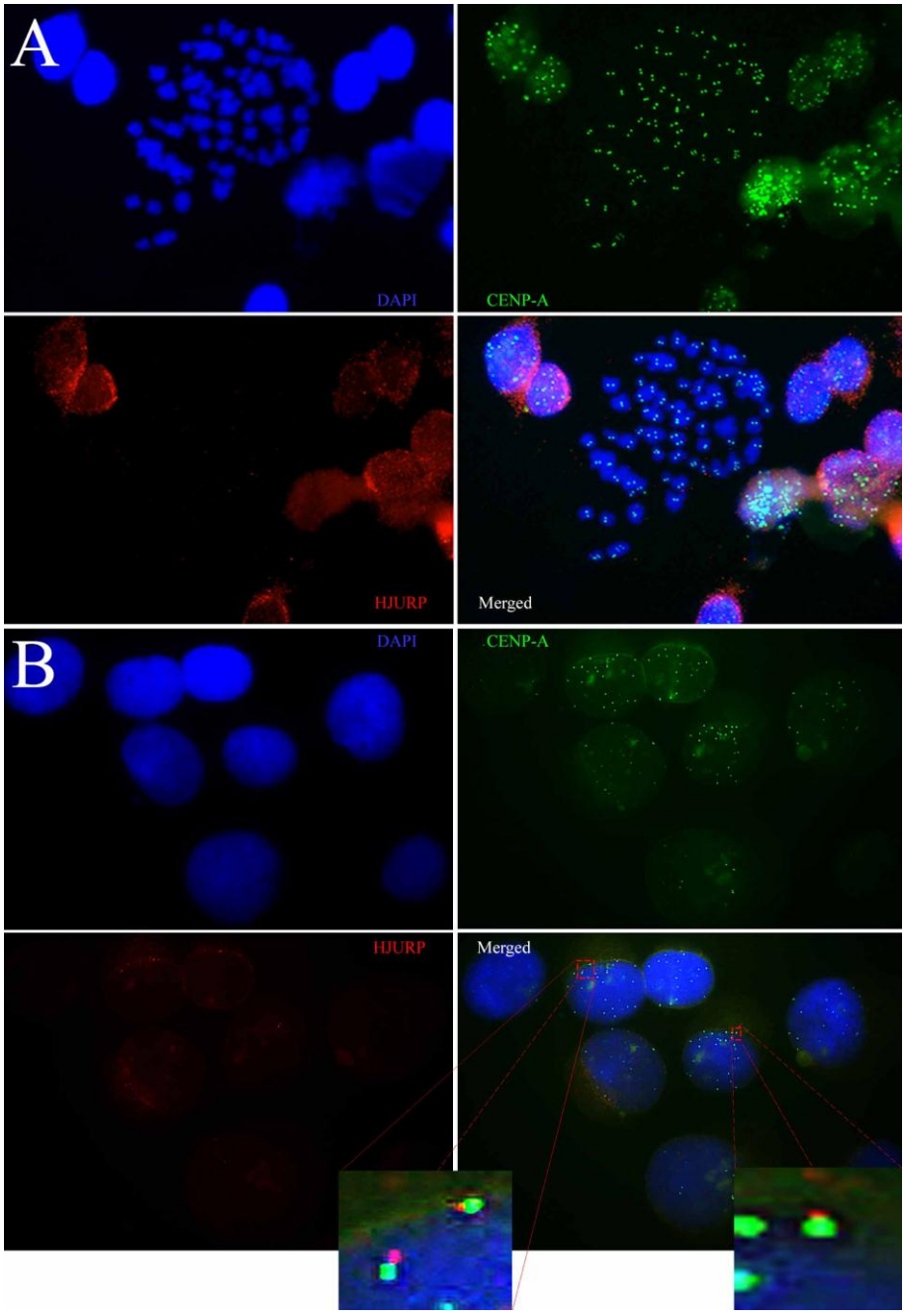

Figure 3:3 Centromeric localization of HJURP in Bloom Syndrome cells

Co-staining reveals HJURP (red) and CENP-A (green) in metaphase chromosomes (A) and non-metaphase cells (B). Both images show variation in the level of HJURP intensity. It is showing a discrete foci pattern in the nucleus and specificity not similar to that obseved by CENP-A signals within the centromere region. Bottom boxes show the selected sections of signal co-association at higher magnification. The photographs were taken under a Zeiss Axioskop 2 fluorescent microscope (100 x objective).

3.1.2 Depletion of BLM, GEN1and MUS81

The key goal is to reduce the levels of the HJ resolvases/disolvases in cells to determine the effect on the deposition of CENP-A. Work from the West group has indicated that disrupting the Holliday junction dissolution/resolution pathways was mediated by MUS81 and GEN1 depletion in Bloom Syndrome (BS) cells. Therefore we set out to perform triple depletion of BLM, MUS81 and GEN1 to generate cells with unresolved HJs to address whether these now provide CENP-A loading target sites.

Firstly, the process of depleting these proteins was conducted individually in cells that express the genes. For instance, NT2 cells were transfected indirectly with siRNA of Hs_BLM_4 against *BLM* using HiPerfect transfection reagent that was prepared with serum-free medium. The procedure details of knockdown were described in Chapter 2. siRNA concentration was 6 pmol/well of a 6 well-plate and was doubled with a second treatment "hit". The preference was given to siRNA number 4 because it is existed in the middle of *BLM* cDNA and its target sequence covers more than one exon (appendix 8.2). Considering the half-life of BLM protein (appendix 8.3), BLM depletion has only been successful with the second treatment of siRNA after 24 hrs. Protein was extracted after 24 hrs of the second transfection and the reduction was verified by a western blot (Figure 3.4B).

Following the same conditions resulted in an inefficient depletion of MUS81 and GEN1. Successful knockdowns occurred only by transfecting the cells with mixes of Hs_FLJ40869 (number 4, 5, 6 and 8) for GEN1 and mixed of Hs_MUS81 (number 4, 5, 6 and 7) for targeting MUS81. An untreated sample was included for each assay and cells were treated with non-interfering siRNA as negative control sample (Figure 3.4).

The same timing and conditions that were used in previous attempts were combined and siRNA were applied together, except that one more hit for BLM was added on the third day. siRNA transfection caused some cell death as observed by floating cells. Extracted protein was analysed by western blot showing that the protein level was reduced for MUS81 and partially in BLM. Surprisingly, GEN1 levels slightly increased (more intense band) (Figure 3.5). For further investigation, we conducted a western blot on dead floating cells to determine whether the loss of these protein caused cell death under these conditions. The results showed that the presence of BLM and GEN1 band is obviously lower than the correct size, potentially indicating protein

degradation (Figure 3.5). Several conditions, including an increase in the siRNA concentration growing, the cells at different densities and growing the cells without serum led to similar outcomes and showed no significant change.

Furthermore, we conducted another attempt of triple knockdown by switching to HCT116 and 132N1 cells. The cells were transfected with 1.2 pmole/well of combined siRNA for three times, at daily intervals, over 72 hrs. Protein was extracted after 24 hrs following the third treatment for western blot analysis. Reduction in protein was only observed for MUS81. Consistent attempted knockdown in NT2 cells, relative GEN1 levels of transfected cells were observed to increase compared to the untreated and negative control cells. A similar outcome has also been observed when siRNA concentration was doubled in HCT116. 132N1 cells showed no change in their protein levels following this treatment as shown in Figures 3.6.

The examination of siRNA transfection effect on chromosomes morphology has been performed. Aberrations in chromosomes morphology has been seen in those cells. Transfected HCT116 showed breakage in some chromatids following the transfection. However, chromosomes morphology of 132N1 cells showed no change corresponding to the western blot analysis results (Figure 3.7).

As NT2 has shown significant reduction in BLM levels, we checked SCEs in those cells. NT2 Cells were incubated with BrDU when the transfection course was completed for 48 hrs. Later, chromosomes were prepared for SCE analysis (see Chapter 2). There was an elevation in the frequency sister chromatid exchange events in depleted cells of about 50 % as compared to untreated sample. NT2 depleted for BLM also appeared to show evidence of some chromosomes fusion (Figure 3.8).

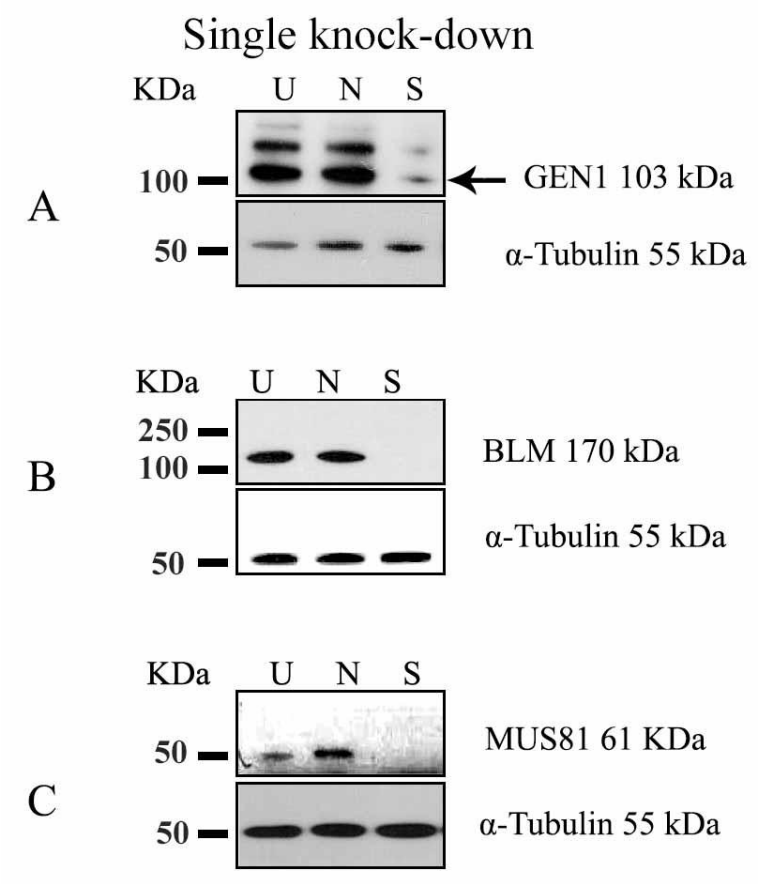

Figure 3:4 Successful knockdown of BLM, GEN1 and MUS81 in NT2

Images show western blot analysis of the whole cell extract from NT2 that transfected individually by siRNA of GEN1, BLM and MUS81. α-Tubulin levels were used to monitor equal protein loading. Approximate predicted size are given. U: untreated smaple, N: sample treatetd with non-interferance siRNA and S: smaple treated with indicated siRNA.

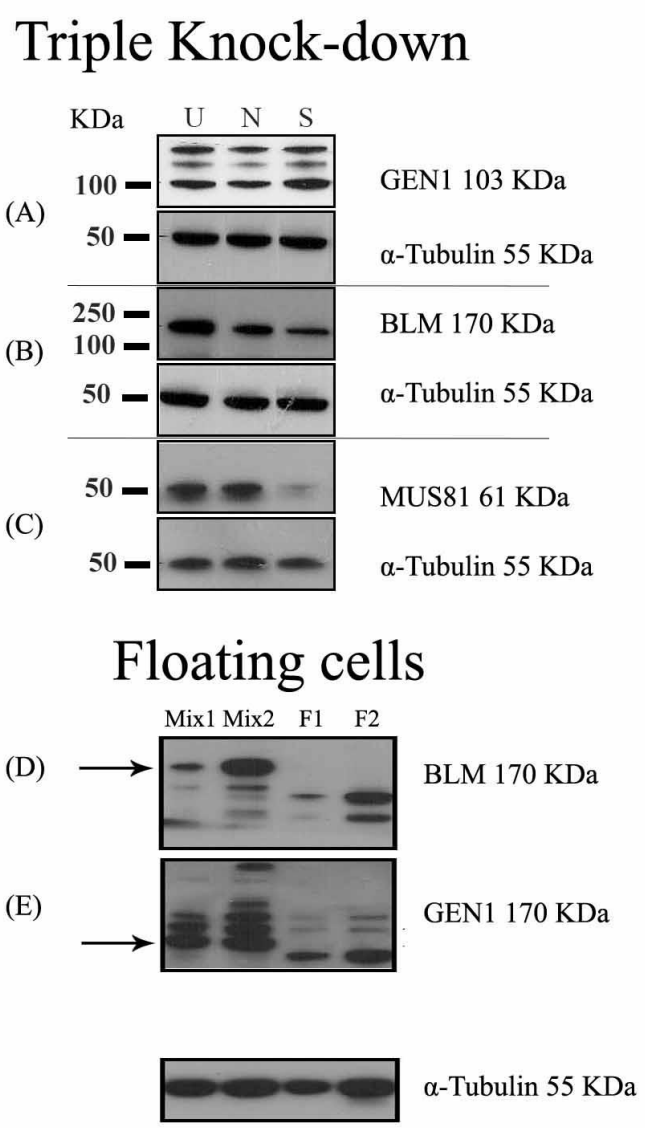

Figure 3:5 Attempt to triple depletion of BLM, GEN1and MUS81

Images show protein level of GEN1, BLM and MUS81 of transfected NT2 with combined siRNA that targeted all of them. Slight increase of GEN1 observed in this case and other two genes show decreased in their expression level. Bottom panel show two attempt of triple knockdown (mix1 and mix2) for NT2. It is compared to the protein that collected from the floating cells (F1 and F2). α-Tubulin were tested for checking loading equality in each sample. Arrow indicates the band of predicted size.

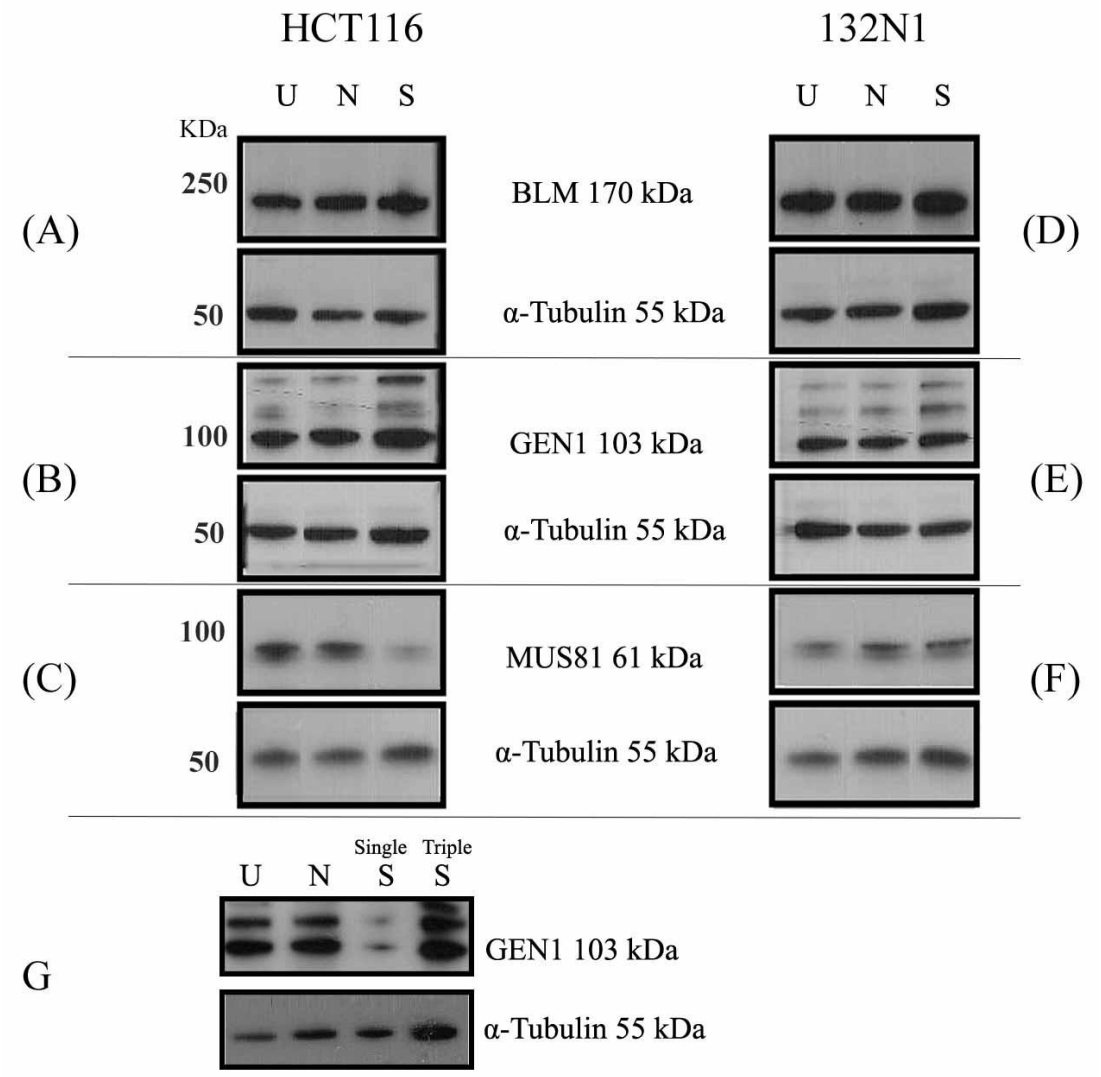

Figure 3:6 Attempt of triple knockdown of BLM, GEN1 and MUS81 in HCT116 and 132N1 cells

Left image shows the protein expression of the attempt of triple knockdown for HCT116 cells. Cells were transfected with combined siRNA of BLM, GEN1 and MUS81 Reduction only observed for MUS81. Right image shows unsuccessful triple knockdown of 132N1cells. (G) Shows another attempt of triple knockdown of HCT116 cells with double concentration of siRNA. Tubulin levels were used to monitor equal protein loading.

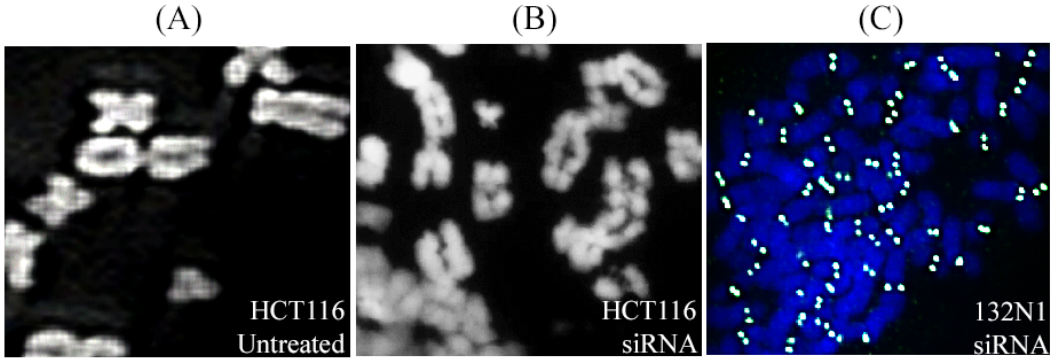

Figure 3:7 Aberration in chromosome that observed following the depletion

(A) Representive images of chromosomes prepared from HCT116 untreated cells (negative control). (B) Shows chromosomes breakage observed in HCT116 cells after triple knockdown attempts. (C) Shows chromosome spreads of 132N1 cells after transfection with CENP-localization. There is no effect seen on their morphology. Chromosomes images were taken using Zeiss Axioskop 2 fluorescence microscope (100 x objective).

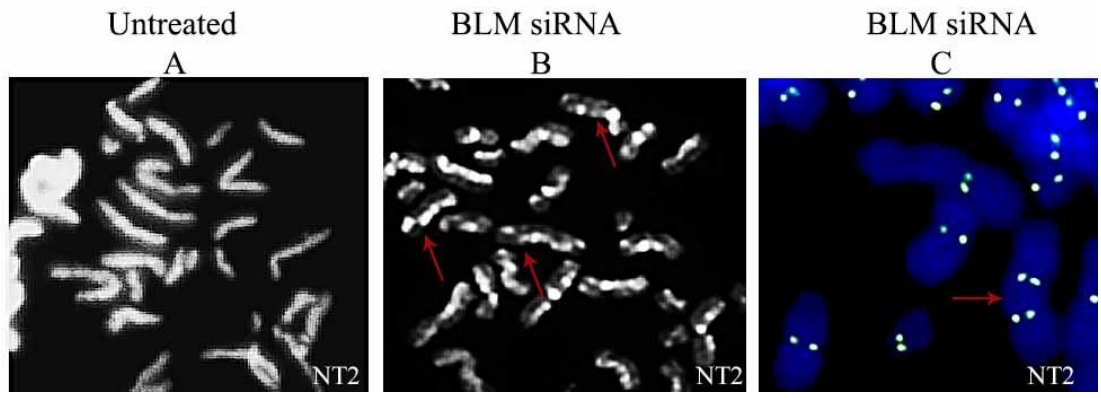

Figure 3:8 BLM depleted NT2 cells exhibit elevated SCEs

NT2 cells were analysed by sister chromatid exchange assay using BrDU staining for untreated cells (A) and following siRNA triple knockdown (B). Chromosomes were stained with Hoechst 33342 and visualized with ×100 objective lens after spreading. Arrows indicates several SCE observed in transfected cells. (C) Shows chromosome fusion that is observed in transfected NT2. Arrow indicates one of them. Cell were labelled with CENP-A. DAPI represents nucleus staining (blue). Chromosomes images were taken using Zeiss Axioskop 2 fluorescence microscope (100 x objective).

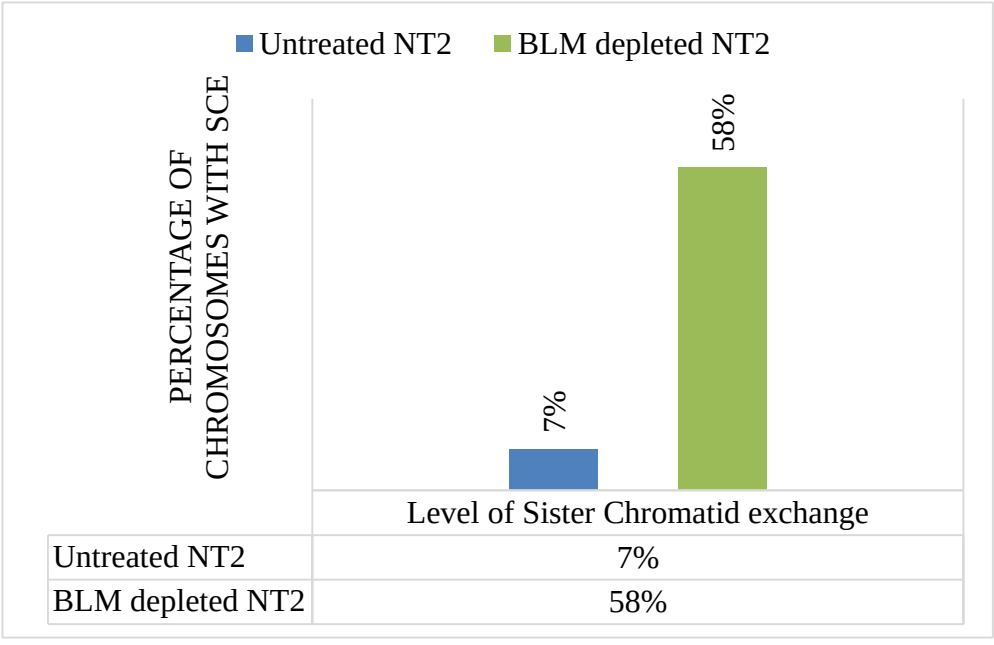

Figure 3:9 Quantification of SCE frequency on BLM-depleted cells for NT2 cells

Each bar represents the ratio of chromosomes that exhibit SCEs to normal chromosome. For each condition more than 250 chromosomes were analysed.

3.1.3 Double Knockdown of MUS81 and GEN1 in BS Cells

Attempts for triple knockdown of BLM, GEN1 and MUS81 have been unsuccessful as shown in the previous section. We decided to carry out double knockdowns in Bloom Syndrome cell lines, which were kindly supplied by Professor Ian Hickson from the University of Copenhagen. The GM08505 cell line was obtained from Bloom Syndrome patient. A clone of GM08505 cells was stably transfected with pcDNA3/BLM and pcDNA3 to produce (control), respectively, the PSNF5 and PSNG13 cell lines. This pair of isogenic controls lines differ only in the fact that the PSNF5 stably expresses a functional *BLM* gene (Gaymes et al., 2002).

The mammalian vector pcDNA3 confers cellular resistance to the antibiotic Geneticin (G418). Therefore GM08505, PSNF5 and PSNG13 were grown in 340 µg/ml G418. PSNF5 and PSNG13 were only able to grow in the presence of G418 confirming the existence of inserted plasmid (Figure 3.10). RT-PCR has been also performed on RNA extracted from those cells to examine *BLM* expression. *BLM* band was observed in PSNF5 confirming that *BLM* is stably express in these cells. However, a faint band was also observed on GM08505 and PSNG13 at 40 PCR cycles (Figure 3.11).

SCE analysis samples have been prepared from those cells. As expected, SCE events have been observed with high frequency in both GM08505 and PSNG13 as result of *BLM* mutation. In contrast, the presence of *BLM* expression in PSNF5 has reduced SCE events as shown in Figure 3.12.

For double targeting gene knockdown of MUS81 and GEN1, 300,000 cells of PSNG13 were seeded in 6 cm culture dish. After 8 hrs of seeding, cells were transfected with 800 pmol of combined siRNA against *GEN1* (No.5) and *MUS81* (No.5) using Lipofectamine RNAiMAX. The efficiency of transfection was checked by western blotting on protein extracted 60 hrs after second treatment. Levels of both GEN1 and MUS81 were successfully reduced down as shown in Figure 3.13.

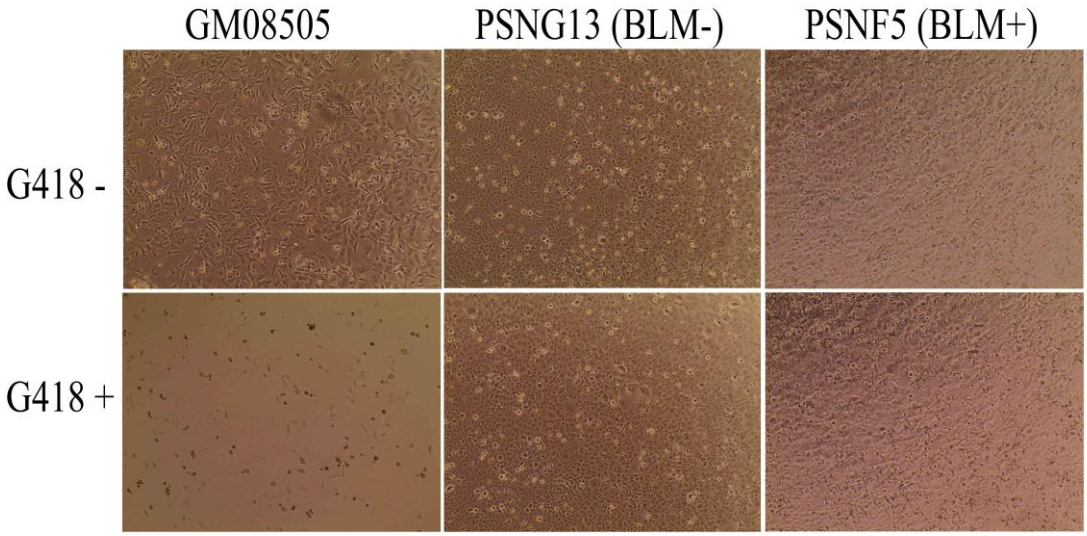

Figure 3:10 Growing the Bloom syndrome cell lines in the presence G418

Images show a comparison of the three cells line GM08505, PSNG13 and PSNF5 in the presence of G418. The upper row shows untreated cells and the bottom shows the same cells incubated with G418 for several days. Only PSNG13 and PSNF5 were able to continue growing in the presence of G418 indicating the functionality of the BLM expression plasmid in this cell line. Images have been taken using ECLIPSE- inverted microscope (5 X lens).

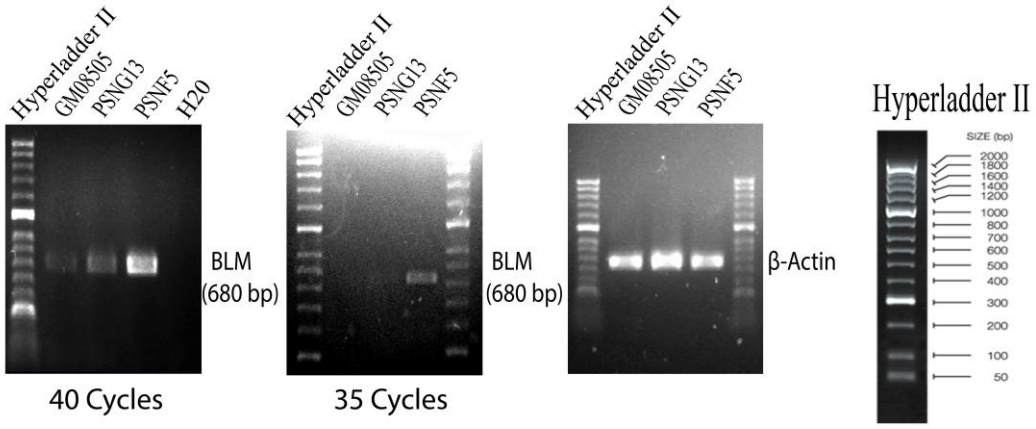

Figure 3:11 *BLM* expression in Bloom Syndrome cells lines

Agarose gel images demonstrate RT-PCR results of three cells line GM08505, PSNG13 and PSNF5. *BLM* band is observed for PSNF5 cells at the expected product size. However, faint bands are observed at 40 PCR cycles. The expression for β-Actin is displayed as a positive control for the cDNA samples. Hyper ladder II has been used as molecular weight markers. GM08505 has not incubated with G418.

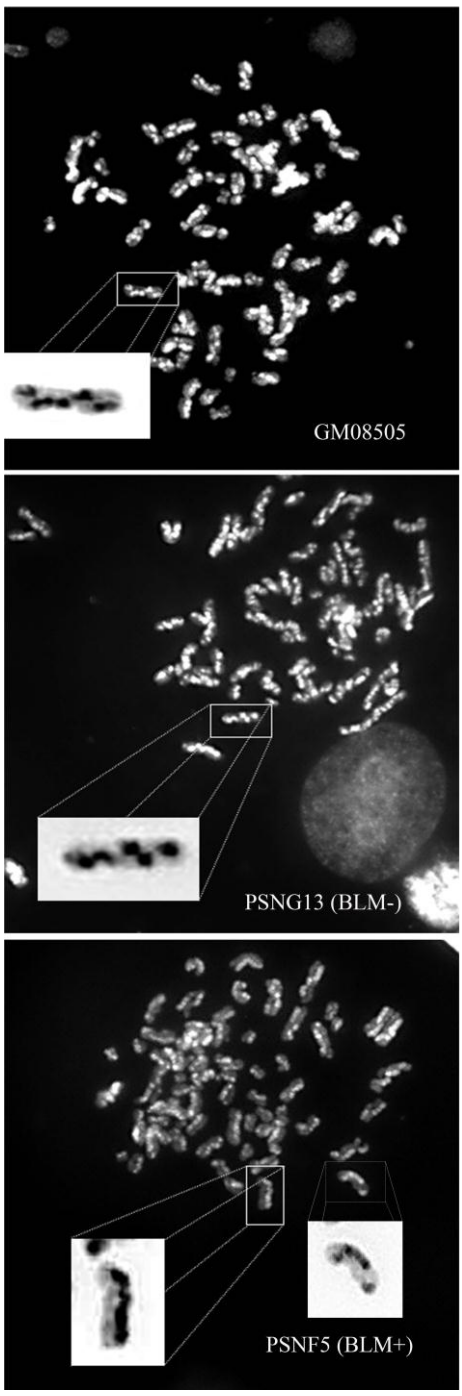

Figure 3:12 Examination of SCEs in Bloom Syndrome cells lines

Images shows SCE assay of Bloom cells. GM08505 and PSNG13 demonstrate high frequency of SCE events while it is significantly decreased in PSNF5. Higher magnification of the selected chromosomes was shown in inverted colour (corner). Chromosomes images were taken using Zeiss Axioskop 2 fluorescence microscope (100 x objective).

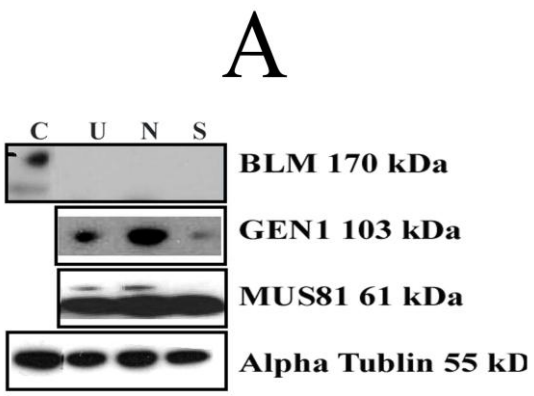

Figure 3:13 The efficiency of siRNA-mediated depletion of GEN1 and MUS81

The PSNG13 cell line has been treated with non-interference siRNA (N) or siRNA against GEN1 and MUS81(S). Protein level were analysed in whole cell extract by western blotting. As expected BLM band is not detected. Efficient depletion was observed in GEN1 and MUS81. NT2 has been used as positive control for BLM expression. α-Tubulin provided a loading control. Reduction in GEN1 expression level of untreated sample is explained by the amount of protein loading as seen in α-Tubulin. U: untreated smaple, N: sample treatetd with non-interferance siRNA and S: smaple treated with indicated siRNA.

3.1.4 Aberrant chromosome morphology in BS cells following the depletion of GEN1 and MUS81

Metaphase spreads were prepared from cells that were treated by non-interference siRNA or siRNA against *GEN1* and *MUS81*. Many metaphases of depleted cells exhibited aberration such as elongated and segmented chromosomes and 'beads-on-a-string' morphology as shown in Figure 3.14. These unusual structures have been observed in four individual attempts. Beads-on-a-string morphology has been explained previously as results of condensation defect within single chromosome and not because of translocation events between multiple chromosomes (Wechsler et al., 2011). West and co-workers postulated that this defect is caused by the failure in HJ processing.

To test the possibility of loading new CENP-A at unresolved HJs, we conducted anti-CENP-A immunostaining on chromosomes prepared form the depleted cells. Analysis of segmented chromosomes did not show CENP-A fluorescence loaded at the unusual structures. Notably, some chromosomes exhibited extra foci of CENP-A within some chromosomes. However, analysing CENP-A localization on untreated cells revealed that dicentric chromosomes are also found in Bloom deficient cells (Figure 3.15).

In order to assess the functionality of the extra foci of CENP-A that are observed in depleted cells whether they are new regions of CENP-A loading or whether they represented sites for real centromere of attached chromosomes (fusion), co-localization with an active kinetochore factor was carried out. ZW10 is one of the main elements of kinetochore of the human centromere (Larissa et al., 2011). Chromosomes were immnustained using anti-ZW10 antibodies. ZW10 signal were observed in both untreated and depleted chromosomes as double and quadruple foci within individual chromosomes suggesting these are *bona fide* dicentric chromosomes in BLM-deficient cells (Figure 3.16).

In the above analysis, CENP-A localization of BLM-deficient cells indicated that some chromosomes contain extra centromeres with active kinetochore marker. To further determine whether these sites were centromeric, we performed FISH analysis on metaphase chromosomes prepared from GM08505 and PSNG13 cells lines. Cells were grown in culture then chromosomes were labelled with DNA probes to identify the centromeric region of each chromosome "pan-centromeric". FISH-chromosome

painting results revealed the abnormal centromeres were due to dicentric chromosomes (Figure 3.17).

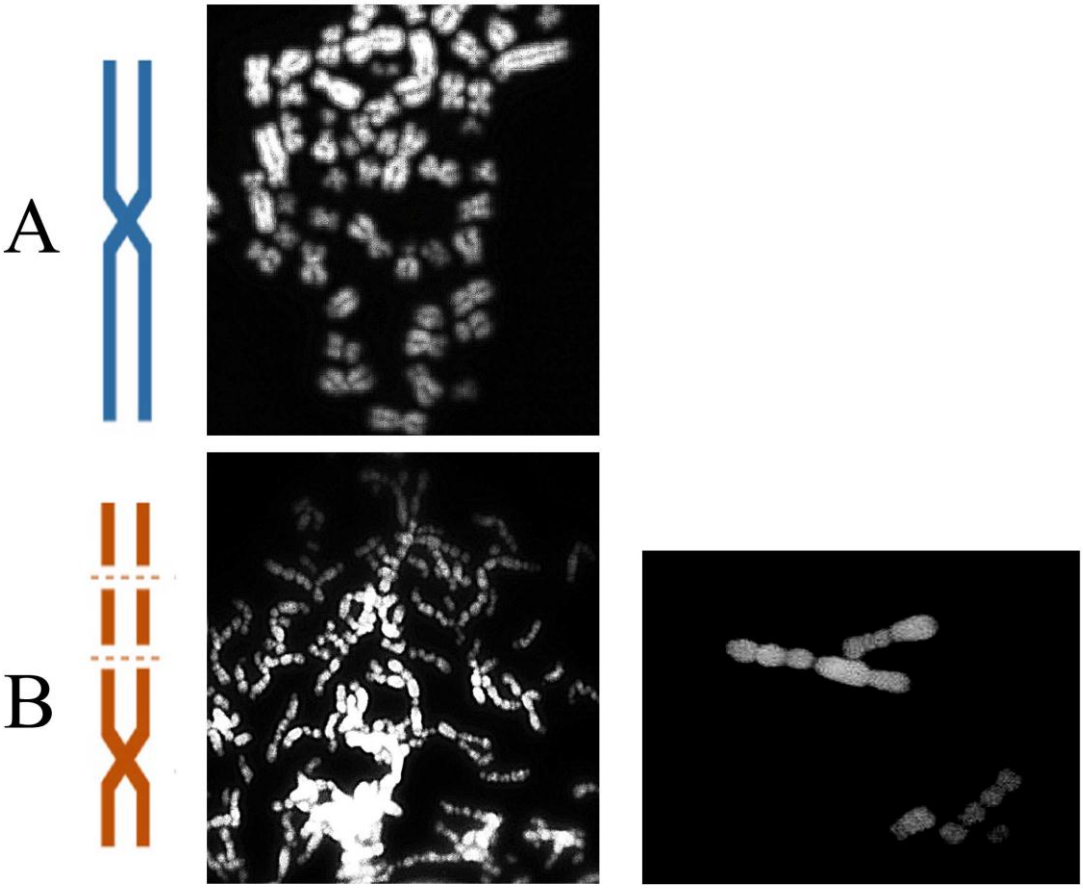

Figure 3:14 Chromosome abnormalities for PSNG13 cells following siRNA-mediated depletion of GEN1 and MUS81

(A) Image shows DAPI-stained chromosomes spread of PSNG13 treated with non-interference siRNA. Staining was performed after sample fixation with Methanol: Acetic Acid. (B) Metaphase spread was prepared form depleted cells. Schematic illustration (left). A right panel shows the selected sections of abnormal metaphases at higher magnification.

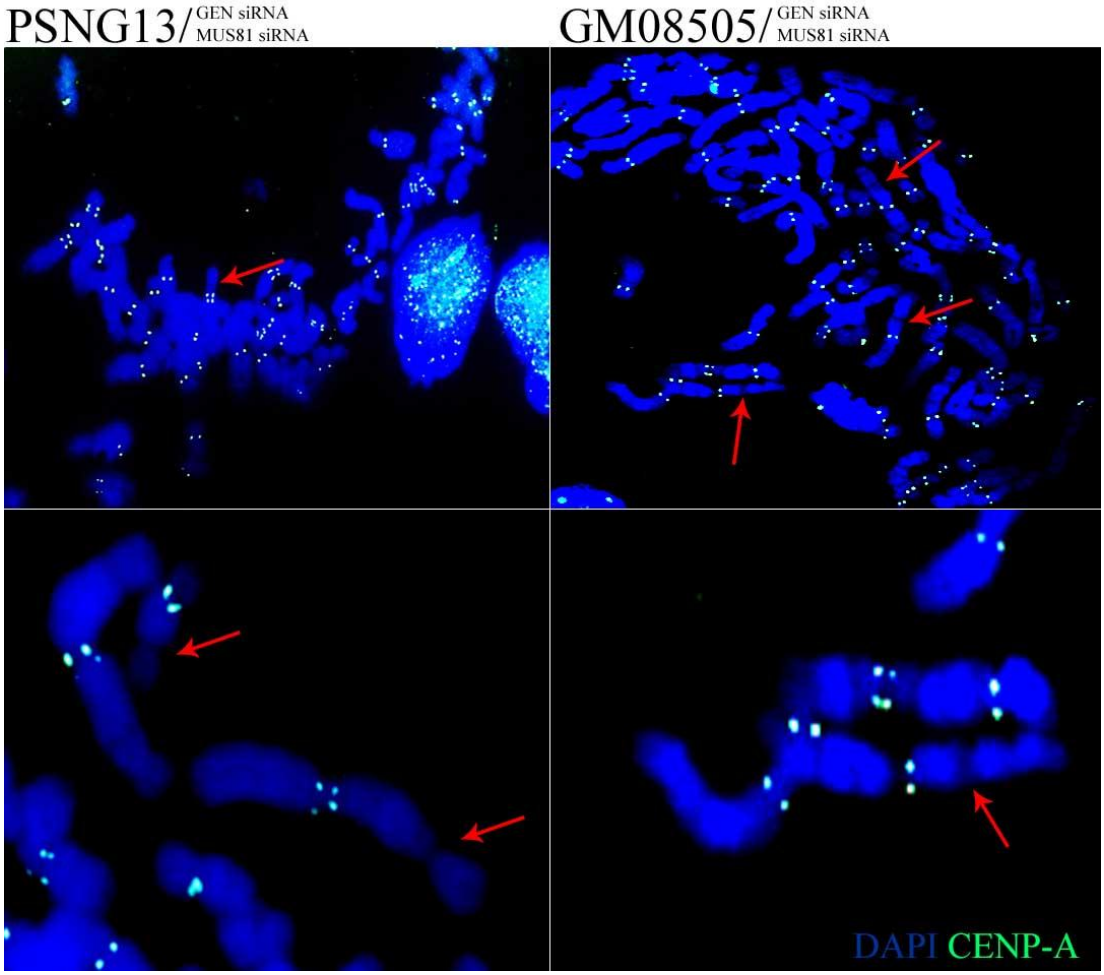

Figure 3:15 Localization of CENP-A in HJ processing defective cells

The representative images show metaphase spreads for PSNG13 and GM08505 depleted cells lablled with anti-CENP-A. Chromosomes are counterstained with DAPI (blue). Lower panels show selected chromosomes that exhibit extra foci of CENP-A at higher magnification. Cells were blocked in metaphase with colcemid and collected by mitotic shake-off. Red arrows indicate the examples of defective chromosomes. Chromosomes images were taken using Zeiss Axioskop 2 fluorescence microscope (100 x objective).

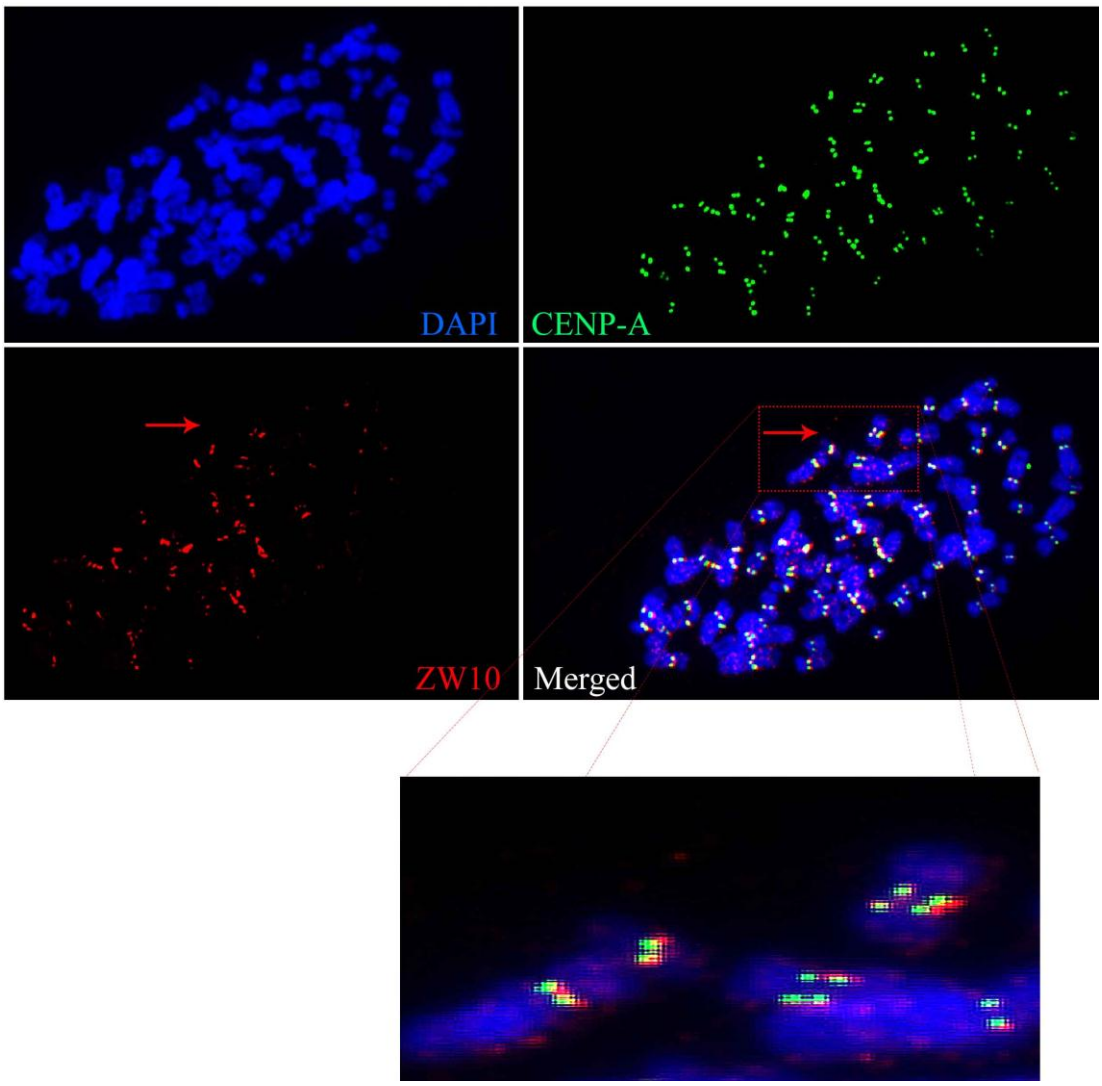

Figure 3:16 Co-localization of CENP-A with ZW10 in BLM-deficient cell line.

This image show co-immunostaining of ZW10 (red) and CENP-A green for chromosomes prepared from GM08505 cell line. Both markers are co-targeted on dicentric chromosomes (red arrows). Chromosomes are stained with DAPI (blue). Cells were blocked in metaphase with colcemid and collected by mitotic shake-off. Chromosomes images were taken using Zeiss Axioskop 2 fluorescence microscope (100 x objective).

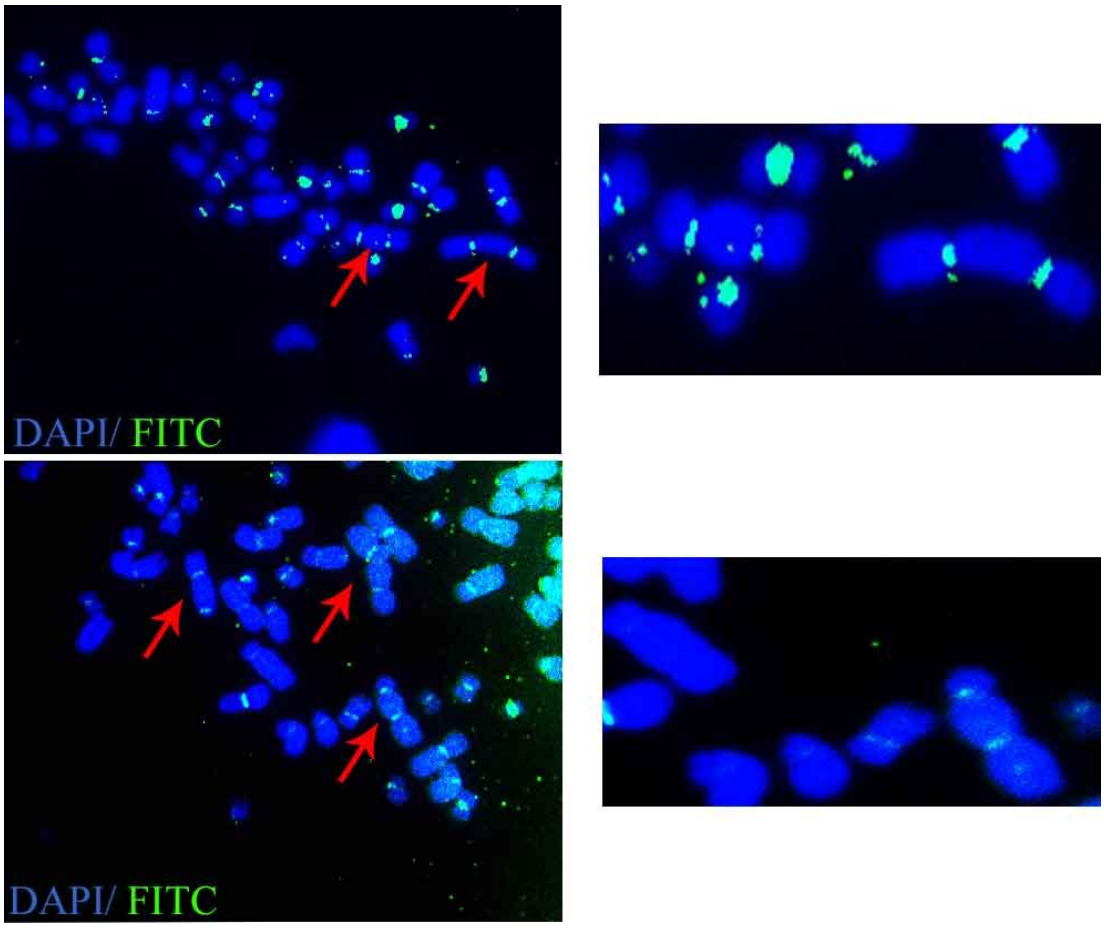

Figure 3:17 A FISH examination of chromosome fusion.

Images show chromosomes prepared from PSNG13 (top) and GM08505 (bottom) cells lines labelled with human Pan-Centromeric probes. Metaphase chromosomes were DAPI stained following the denaturation and hybridization procedure used for FISH. Red arrows are indicating regions of chromosomal fusion. Probes were labelled with Biotin and detected with FITC filter. Images were taken using Zeiss Axioskop 2 fluorescence microscope (100 x objective). A right panel shows the selected sections of dicentric chromosomes at higher magnification.

3.2 Discussion

3.2.1 Cellular co-localization of CENP-A and HJURP

CENP-A has been used for determination the site of centromere assembly since 1985. Earnshaw and co-workers have identified the centromere protein family using sera of patients with scleroderma that contained several autoantibodies that detect centromere region in the nucleus (Earnshaw and Rothfield, 1985). The main aim of this chapter was to assess the role of recombination in CENP-A deposition to the centromeres region via HJURP. Here commercial antibodies to CENP-A give the correct staining pattern. Staining was observed exclusively in the nucleus as multiple foci (Figure 3.1). CENP-A localises to the centromeres of each chromatid in different human cell lines in metaphase chromosomes (Figure 3.2).

HJURP antibodies have been tested as well, examining its co-localization with CENP-A. However, it showed a discrete foci pattern in the nucleus and did not fully co-localize with CENP-A within the centromere region. Cells demonstrated varying levels of HJURP intensity and some of them did not exhibit any fluorescence. Furthermore, HJURP did not co-localize with CENP-A signal in the nucleus in all cells (Figure 3.3). However a low percentage of cells did exhibit co-association of HJURP to CENP-A signals as shown in Figure 3.3b. This can be explained by the transient appearance of HJURP. Recent studies have revealed that the recruitment of HJURP in CENP-A loading takes place at late telophase/early G1. They found that the phosphorylation status of the HJURP C-terminal domains; HCTD together with cyclin-dependent kinase (CDK) activity determines the period of HJURP recruitment to centromeres specifically (Müller et al. 2014) (Figure 3.18). This is consistent with another study that demonstrated that HJURP localizes transiently to the centromere at a certain time during the cell cycle (2 to 3 hrs) (Dunleavy et al., 2009), corresponding specifically to the time when CENP-A is most active (Hemmerich et al., 2008).

Moreover, correct physiological protein localization and function is important for the biological activities in normal cells. Some diseased cells show aberrant protein localisation such as cancer cells, which are the result of mutations which alter the protein expression (Hung and Link, 2011). Therefore the localisation of HJURP in the BS cells might be similar to that observed in cancer cells because Bloom Syndrome

arises from mutations in *BLM* resulting in a highly increased risk of cancer (German, 1993).

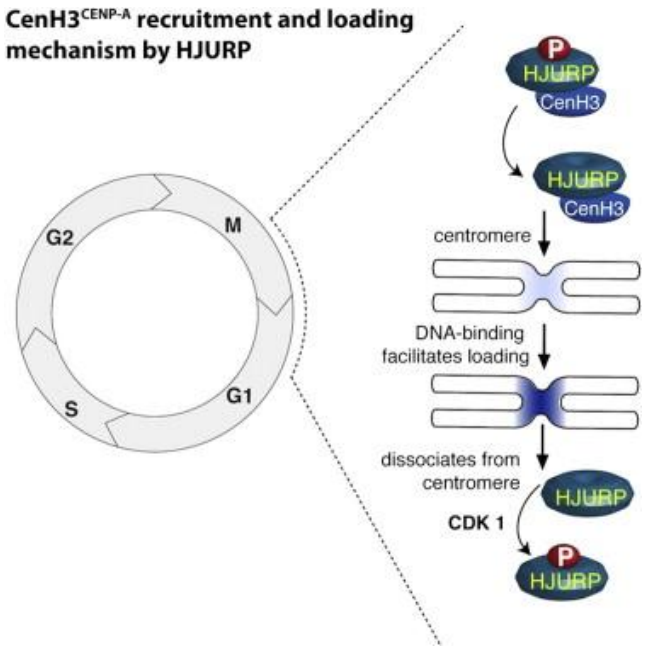

Figure 3:18 The recent model of CENP-A deposetioning by HJURP

This model summarizes how HJURP lays down CENP-A at centromeres. It starts with dephosphorylation of HJURP at the HCTD1 which is results in its loading to centromeres in telophase/early G1. Secondly, HJURP drives CENP-A to the centromeres. Finally, HJURP is phosphorylated again in the HCTD1, causing its detachment from centromeres, concomitant with raising the activity of CDK (Müller et al. 2014).

3.2.2 siRNA knockdown of BLM, GEN1and MUS81

The main aim was to perform a triple depletion of BLM, GEN1 and MUS81 in order to block Holliday junction dissolution/resolution. Firstly, short interfering RNA (siRNA)-mediated depletion of BLM in NT2 was achieved here by transfection of cells twice within 48 hrs. Significant reduction was detected in BLM levels by western blot analysis, using commercial siRNAs. BLM depletion was detected previously in normal fibroblast (Hemphill et al., 2009) and here we report it in cancer cells (Figure 3.4 B).

Choosing the right sequence of siRNA represented a major challenge for gene knockdown because its efficiency varies from one sequence to another. Here, four siRNA sequences per target gene demonstrated more efficiency. We reported successful knockdowns for GEN1 and MUS81 individually by adding an additional hit (three hits in total) using a conjunction of siRNAs for each target (Figure3.4 A,C).

An antibody's reliability depends on its ability to recognize a specific protein target. The evaluation of some commercial antibodies has been reported to be not specific for their target using siRNA-mediated protein knockdown (Sullivan et al., 2008). siRNA validation of BLM, GEN1 and MUS81 antibodies for Western blotting and other protein detection applications has been demonstrated in this study (Figure 3.4).

3.2.3 Depletion of BLM, GEN1 and MUS81 show mechanisms of compensation in human cells

Triple knockdown of (BLM, GEN1 and MUS81) in NT2 was unsuccessful whilst targeting all three genes. A reduction was only observed in MUS81 levels, although the same conditions were followed as for the successful, individual knockdowns were followed. Similar results were obtained in the attempt of the triple knockdown for HCT116. Also, in both cases relative GEN1 levels of transfected cells were observed to increase compared to the untreated and negative control cells (Figure 3.5 and 3.6). Likewise, previous work in *Drosophila* revealed overlapping or compensatory interaction between *GEN* and *MUS81*. Mutants in the *GEN1* ortholog in *Drosophila* show more sensitivity to genotoxic agents than *MUS81* mutants, suggesting that *GEN* plays a more significant role in the processing of HJ (Andersen et al., 2011).

This conclusion is also supported by other evidence in mammalian cells. Double knockdown of MUS81 and GEN1, or SLX4 and GEN1 in BS cells demonstrated severe chromosome abnormalities. In contrast, when MUS81 and SLX4 were depleted without GEN1, less chromosomal abnormalities were observed, suggesting the compensatory role of GEN1 (Wechsler et al., 2011).

BLM promotes dHJ dissolution actions and has essential role in preventing cross over (CO). BLM-depleted cells show an elevation in SCEs and genome rearrangements comparing to untreated cells (Figure 3.7 and 3.8). Moreover, HJs can be cut by several enzymes such as *MUS81* and *GEN1* that are found in human cells. In yeast, loss of *SGS1*, the *BLM* ortholog, wih *MUS81-EME1* demonstrates lethal interactions (Fabre et al., 2002). In this work a high amount of cell death was observed following attempts at depleting those genes (*BLM*, *GEN1* and *MUS81*). We conclude that the inviability of depleted cells due to loss of these genes means they have an essential role in the biological activity.

3.2.4 Double Knockdown of MUS81 and GEN1 in BS Cells

As an alternative approach to the previous attempt for triple knockdown, double knockdowns of GEN1 and MUS81 were performed in *BLM*-deficient cells. The efficiency of knockdown was measured by Western blotting. Levels of both GEN1 and MUS81 were successfully reduced down as shown in Figure 3.13. In addition, BLM was not detected in these cells as expected. However, GEN1 compensation has not seen in this case. This could be explained by frameshift mutation that exists on bloom syndrome cells. The faulty BLM protein that produced by these cells may partially function to dissolve the Holliday junction.

As expected, depleted cells exhibited aberrations such as elongated and segmented chromosomes and a ‘beads-on-a-string’ morphology as shown in Figure 3.14. West and co-workers made similar observations following the depletion. As they postulated that this defect resulted in disruption of HJ processing, we attempted to test our main hypothesis by labelling those chromosomes with CENP-A. Unresolved HJ might employ HJURP to lay down CENP-A at sites of unresolved HJs. CENP-A deposition at unresolved HJs will provide supporting evidence for its role in HJs, recombination in the centromere and hence centromere function.

Remarkably, some chromosomes exhibited extra foci of CENP-A within some chromosomes of depleted *MUS81* and *GEN1* Bloom deficient cells. However, those extra foci were also found in the untransfected BLM-deficient cells (Figure 3.15). Furthermore, co-localization of CENP-A with an active kinetochore factor was carried out. A ZW10 signal was observed as double and quadruple foci within individual chromosomes which suggested that these were *bona fide* dicentric chromosomes in BLM-deficient cells (Figure 3.16). This was also consistent with a doubling of centromeres that we observed in BLM-depleted cells for NT2. Further analysis of these centromeres using FISH confirmed that the abnormal centromeres were probably a result of chromosome fusion (dicentric and acentric chromosomes). Chromosome fusion has been reviewed earlier as a result of deletions, insertions or translocations (Kasparek and Humphrey, 2011). Therefore it is unsurprising to see chromosome rearrangements in Bloom Syndrome cells. Nevertheless, the lack of CENP-A detection is could be due to the low amount of CENP-A that is loaded on the unresolved sites, consequently it is hard to detect under the microscope. Neocentromeres are rare cases in humans where chromosome contains functional centromere in non-centromeric region, which can provide the platform to form functional kinetochores. Interestingly, these neocentromeres appear to bind less number of CENP-A comparing to normal centromeres(Marshall et al., 2008).

To conclude, detecting CENP-A on unresolved sites was not possible, thereby a potential_ functional role for HJ in CENP-A deposition of human metaphase chromosomes could not be established in present study. More efficient means of depleting BLM, GEN1 and MUS81 on normal cells may be required to establish the effect that disruption of HJ processing may have on the CENP-A loading such as using a TALEN-based approach (Cermak et al., 2011) or a small hairpin RNA (shRNA) (Xiang et al., 2006).

Chapter 4

Results

Chapter 4. Analysis of recombination regulation factors in cancer stem-like cells

4.1 Introduction

4.1.1 Cancer stem-like cells

Sub-populations of cells within tumour have distinct genetic and epigenetic features, thus generating intra tumour heterogeneity. The hierarchy model of cancer identifies a rare population of cancer cells that carry stem cell characteristics responsible for initiating a heterogeneous tumour and cancer recurrence following chemotherapy. Those cells are called tumour-initiating cells (TICs), cancer stem-like cells or cancer stem cells (CSCs). Several studies have reported the presence of CSCs in solid tumours of the breast, colon, brain, pancreas, bladder, head/neck, liver, lung, ovary, pancreas, prostate and skin (Mathews et al., 2013; Sarvi et al., 2014). Despite some intense debates about the existence of CSCs, the CSCs theory has gained wide acceptance in the scientific community (Hardin et al., 2013).

4.1.2 Colon cancer stem cells

Colorectal neoplasm is one of the main types of cancer that causes death and illness. Most colorectal cancer patients are diagnosed after the age of 50, which supports the sequential theory of colorectal carcinogenesis elucidated by an age-related accumulation of genetic mutations. Intestinal epithelial cells require a long time to develop malignant phenotypes. Therefore, stem cells that exist normally in the colon crypt represent potential targets for tumorigenic mutations, owing to both their long life and self-renewing capability compared to their cellular progeny. They may also give rise to CSCs with tumour-initiating and sustaining capability (Chen et al., 2011; Fanali et al., 2014). The “bottom-up” model of colorectal histogenesis also provides supporting evidence for stem cell-driven intestinal tumorigenesis. The “bottom up” model is based on the findings that transformation originates from the stem cell that occupies the bottom of the crypt, which may give rise to crypt-restricted lesions. Recent studies have also demonstrated that tumour-initiating mutations can arise in either crypt stem cells or following its differentiation, as long as these cells dedifferentiate and re-express pluripotency markers (Figure 4.1). Therefore, increased

understanding of the complexity of CSCs is helping to develop the optimisation of novel anti-cancer treatments (Puglisi et al., 2013).

4.1.3 Non-adherent sphere culture

CSCs can be isolated by flow cytometry using several approaches such as Hoechst side population (SP) and based on the cell surface marker expression (e.g., CD133) (Cabarcas et al., 2011). One of the main advances in CSCs research is the ability to form spheroids and grow under non-attached conditions in a defined serum-free medium (SFM) supplemented with cell growth factors. Sphere formation, initially reported in normal human stem cells, extended to cancerous cells where more studies have shown that spheroids can be formed by tumours including breast, pancreatic, prostate, ovarian and colon cancer. The non-adherent sphere culturing method has several advantages; most importantly, it can enrich the population of cells that are enriched in CSC-like traits. In addition, cancer cells show more tumorigenicity in a spheroid state (Mathews et al., 2013). Compared to the two-dimensional cell culture systems, this method allows researchers to grow the cells within a microenvironment that mimics real tissues (Pampaloni et al., 2009).

4.1.4 DNA replication inhibitors

DNA replication can be inhibited by several chemical agents, which are commonly used as cancer treatment and antiviral agents. DNA replication inhibitors can act on two mechanisms: (1) interference with DNA synthesis by inhibiting DNA polymerization and/or initiation of replication; and (2) cell cycle and checkpoint control (Fischer and Gianella-Borradori, 2005; Helleday et al., 2008).

Camptothecin (CPT) is a chemotherapeutic poison that targets DNA topoisomerase I (Top 1) enzyme. The CPT mechanism is based on reversible inhibitory action to re-ligate the activity of Top 1 by creating a ternary complex with the enzyme and DNA. This leads to a collision between moving replication forks and CPT-stabilised cleavable DNA-top I. Subsequently, the replication fork will be arrested and lethal DSBs are formed (Tesauro et al., 2013).

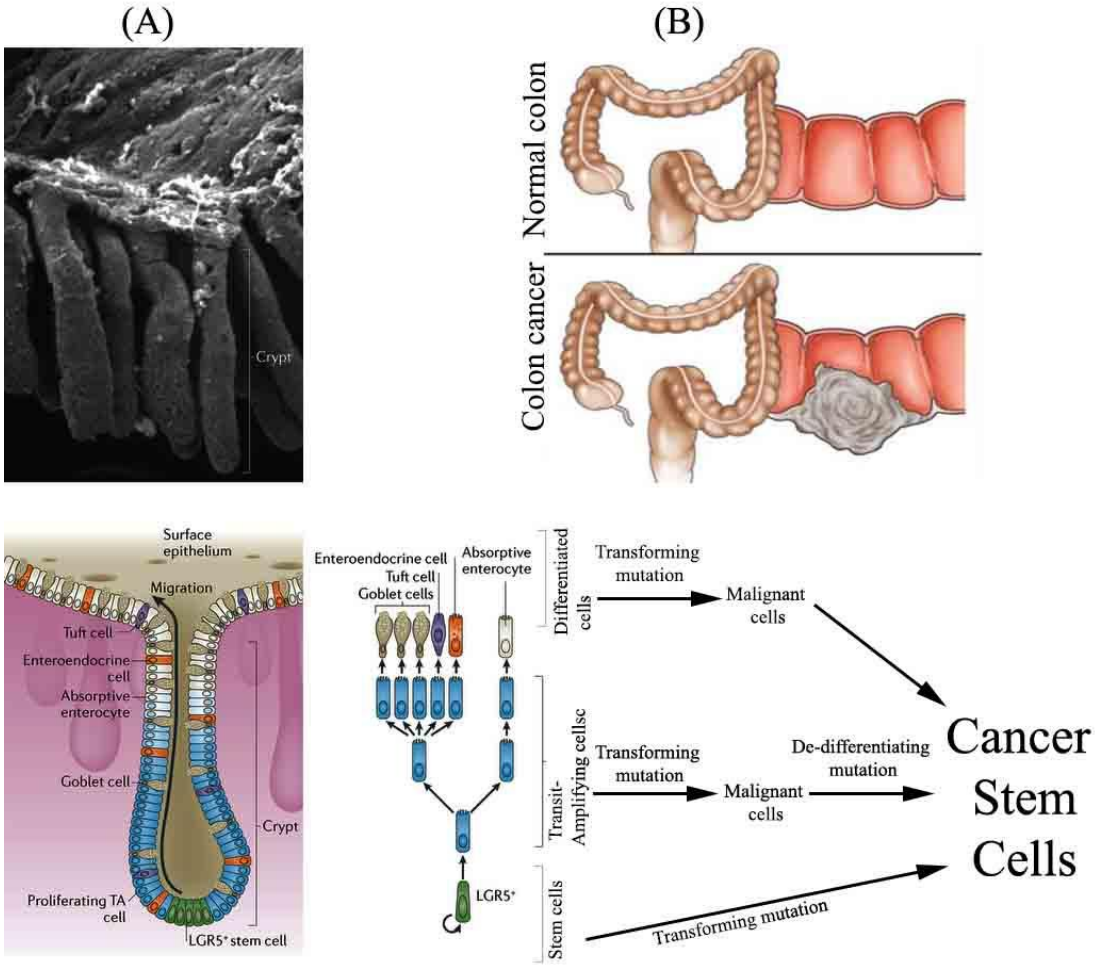

Figure 4:1 The origin of colon CSCs

The upper panel shows the human colon crypt as visualised under an electron micrograph. The lower diagram shows the cell organisation of the crypt. LGR5+ stem cells are located at the bottom of the crypt and are responsible for generation of Transient Amplifying (TA) cells. TA cells have the potential to undergo differentiation into the functional crypt cells, as indicated in the branched tree next to it. Colon CSCs may arise because of a mutation to stem cells. In addition, differentiated cells include TA cells that might gain mutations that transfer them back to a stem-like state. The crypt scan and diagram are adapted from (Barker, 2014). (B) The comparison between the normal and colon cancer is adapted from (Todaro et al., 2010).

Aphidicolin (APH) is also a replication inhibitor that inhibits eukaryotic DNA polymerase α activity by competing with the four deoxynucleoside triphosphates (dNTPs). During APH binding, it uses activated DNA as a template-primer, which leads to replication fork stalling and eventually DSB formation (Hofstetrova et al., 2010; OGURO et al., 1979).

Cis-diamminedichloroplatinum II (Cisplatin) is a synthesised platinum complex commonly drug used against different type of cancer (Werengowska-Ciećwierz et al., 2014). Cisplatin binds to DNA by creating intra and interstrand adducts, particularly between a djacent guanines. Consequently, DNA adducts induce significant distortions of the helical structure of the DNA and causes arrest in the replication (Dhar and Lippard, 2011; Wang and Lippard, 2005).

Excess thymidine (more than 2 mM) inhibits DNA replication progress by blocking the cell cycle at the G1/S border. This is caused as negative feedback on nucleotide production due to nucleotide pool imbalances. Thymidine, as a reagent, is used to obtain populations of synchronised cells. However, its activity can be applied and reversed consistently (Alfred and DiPaolo, 1968; Darzynkiewicz et al., 2011; Harper, 2005).

4.1.5 DNA repair and SCE

Genomic instability is a main feature of most cancer cells, which is caused by the failure of individual DNA repair pathways or a wide range of other damaging events. It is believed that genomic destabilisation occurs in early tumour progression driving genomic heterogeneity and conferring a selective property to a given cell, which controls cell proliferation. Instability may or may not progress tumour formation. One cause that drives genomic destabilisation is dysregulation or dysfunction of DNA damage repair by homologous recombination (HR) (Stults et al., 2011). HR is an essential mechanism required for repairing many forms of DNA lesions including DSBs, interstrand cross-linking and collapsed replication forks. The biological function of HR for influencing overall genomic integrity in human diseases such as cancer has been described in Chapter 1 (Mehta and Haber, 2014).

One of the most common methods utilised to detect dysregulation levels of HR, whether in cells with defective/deficient HR capacity or in response to DNA replication stress, is the sister chromatid exchange (SCE) assay. This assay involves

the differential staining of sister chromatids of each chromosome using bromodeoxyuridine (BrdU) and Hoechst 33258 dye. It enables microscopic visualisation of the physical exchange for DNA generated by crossover-associated HR (Stults et al., 2014). The SCE assay is used as an assessment system for chromosomal mutagenicity of chemical agents. Clinically, it is also used for diagnosis purposes of some diseases associated with chromosome aberration. (Rimoin et al., 2013). Chemical agents that form DNA inter-strand crosslinking, such as cisplatin, cause the induction of SCE, since HR is required to repair the lesions caused by replication blockage. Depletion or deficiency of the BLM protein function, the genetic determinant of Bloom Syndrome (BS), which is required to supress SCEs by dissolution of HJs, causes a significant elevation in SCE events (Killen et al., 2009).

Mammalian stem cells are known for their low frequency of mutations compared to differentiated cells. In the differentiated cells, inter homologue mitotic recombination was reported to be the main inducer for mutations that related to loss of heterozygosity (LOH) (Cervantes et al., 2002). This suggests that pluripotency is associated with alteration in recombination regulation, especially for inter homologue events. CSCs are protected against conventional chemotherapy using several mechanisms and abnormal activation of DNA damage repair pathways (Maugeri-Sacca et al., 2012). Therefore, colonospheres offer the opportunity to provide a model for studying the relationship between DNA repair and stemness in cancer cells.

During studies into the cell cycle regulation of cells transforming from attached cultures to spheres, it was noted that BLM protein levels became significantly reduced (McFarlane/ Wakeman groups, unpublished data). Here we set out to further confirm and characterise this observation and address whether it has a biological role in differentially controlling genome stability in these cells.

4.2 Results

4.2.1 Generation and characterisation of colonospheres

To obtain CSCs, two different human colon cancer cell lines (HCT116 and SW480) were suspended in SFM medium containing DMEM/F12 and supplemented with B27, epidermal growth factor (EGF) and fibroblast growth factor (FGF). The cells were then cultured in ultra-low-attachment dishes. In agreement with previous observations (Kanwar et al., 2010), incubating the cells in SFM resulted in large round, unattached floating spheroid colonies (termed colonospheres) over a period of 5 days and 7 days for HCT116 and SW480, respectively. Colonospheres were collected after that and dissociated into single cells with Accutase®. Then, they were re-cultured back into serum-containing medium in adherent plates. The floating spheroid cells re-attached, converted gradually to adherent cells and returned to the epithelial morphology (post-sphere)**.** These two cell lines were used in multiple experiments in the three states (pre-sphere, sphere, post-sphere) throughout the project (Figure 4.2).

To elucidate whether the colonospheres could enrich cells expressing putative stem cell markers, total protein was isolated from parental cells and spheres and was examined by western blotting. In HCT116, the levels of the stem marker Oct4/3 significantly increased from the second day of the sphere formation compared with parental and post sphere cells. In SW480, the western blotting data showed that the expression of Oct4 was also up-regulated in spheres compared with the parental cells, but on the seventh day after the sphere was formed. However, the reduction in Oct4/3 levels of post-sphere of SW480 cells was not observed. SW480 sphere also showed higher levels of CD44vs than the corresponding parental and post-sphere cells. These observations indicate the presence of CSCs population within the colonospheres (Figure 4.3).

Previously, $p16^{ink4}$ has been observed significantly reduced in iPS/ES cells compared to MEFs (parental of iPS), indicating its role for efficient re-programing (Li et al., 2009; Price et al., 2014). However, we also measured the expression levels of $p16^{ink4}$, which was significantly repressed in the spheroids of SW480 compared to their parental cells. All tests were normalised to α-Tubulin expression. The test was performed using the Bio-RAD CFX Manager. (Figure 4.4)

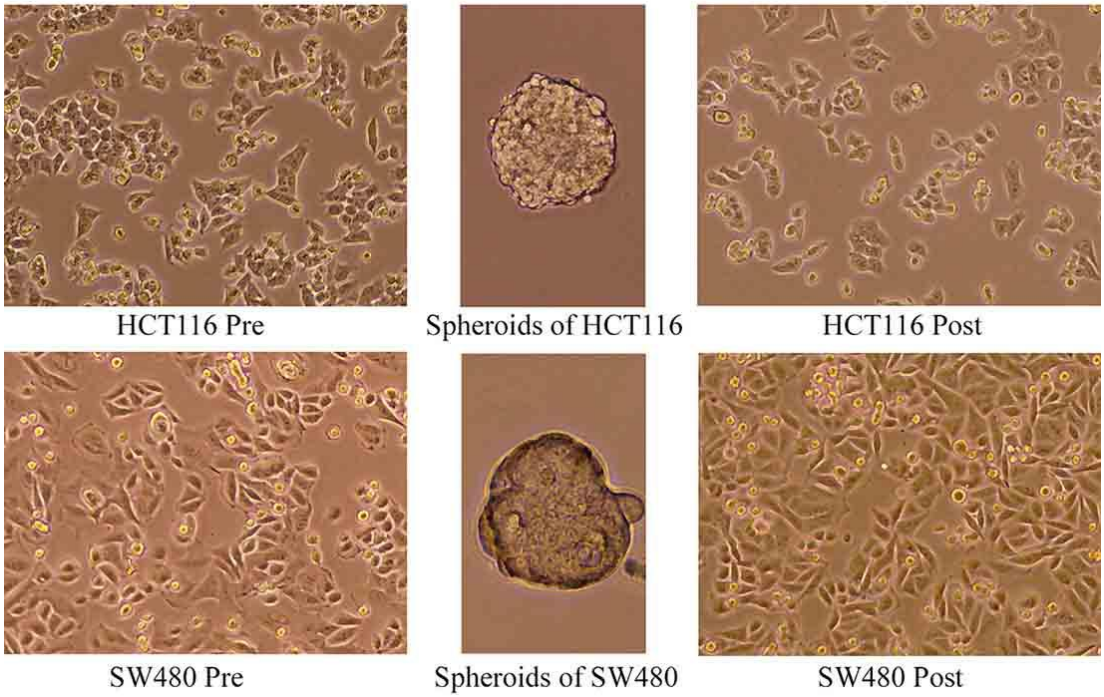

Figure 4:2 The formation of colonospheres/spheroids from colon cancer cells

The left panel shows representative images of colon cancer cells (HCT116 and SW480) in the attached condition (Pre). Both HCT116 and SW480 can form large round, floating spheroids cells when grown with SFM. These grow in ultra-low attachment dishes under specific conditions (middle panel). When spheroid cells were grown back in serum-containing medium in attached plates, the floating spheroid cells re-attached and converted gradually to adherent cell morphology (left panel). Images were captured by Evos™ XL Core using a 10x objective lens.

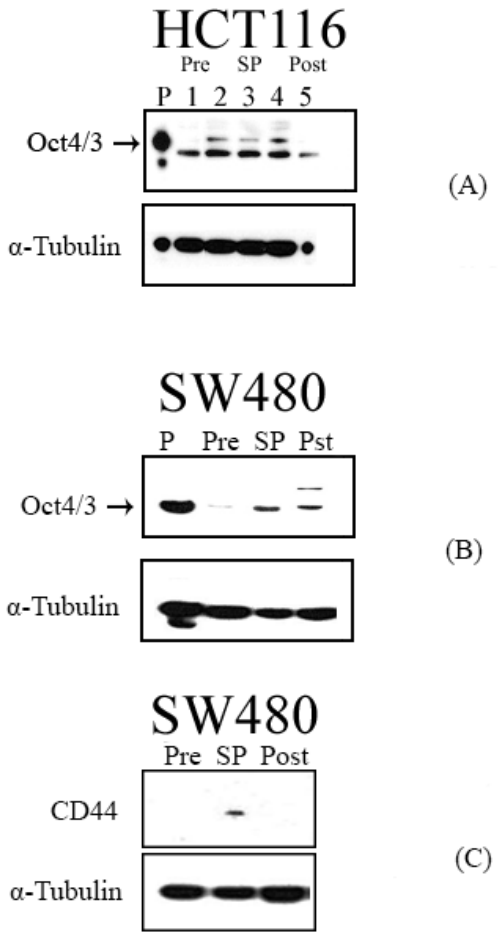

Figure 4:3 The expression of stem cells marker on colonospheres

(A) Western blot analysis of protein lysate isolated from HCT116 colon cancer cells (Pre) was compared to spheroid cells (SP) and post sphere cells (Post). NT2 lysate was loaded as a positive control for Oct4/3 (P). Oct4/3 appeared on the third day of sphere formation, which is indicate by the number (2). It was also expressed on the fourth and fifth days (3, 4). (B) In the SW480 spheroid cells, Oct4/3 appeared only on the seventh day. Oct4/3 has level did not reduce after being grown back in the attached condition (post). α-Tubulin levels are given as a loading control. (C) CD44vs levels in the spheroids of SW480 loaded and compared to their parental.

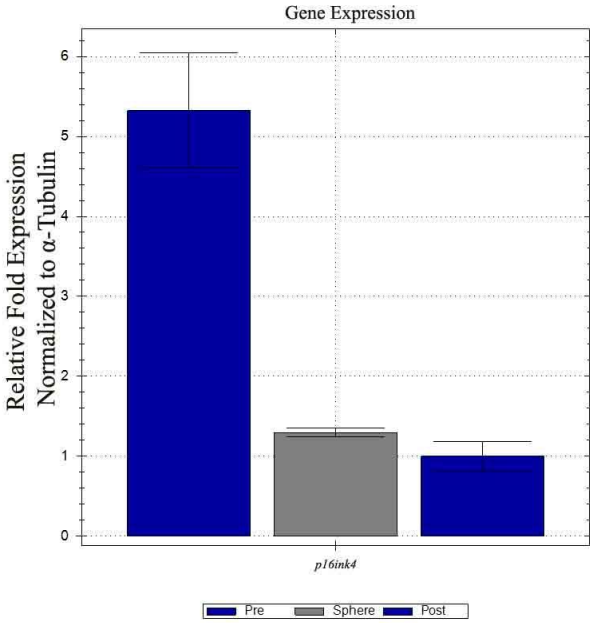

Target	Sample	Expression	Expression SEM	Corrected Expression SEM	Mean Cq	Cq SD	Cq SEM
p16^{ink4}	Post	1.00000	0.18543	0.18543	38.44	0.45978	0.26545
p16^{ink4}	Pre	5.32524	0.71878	0.71878	39.09	0.32120	0.18545
p16^{ink4}	Sphere	1.29302	0.05486	0.05486	39.25	0.00000	0.00000
Tubulin	Post				16.76	0.05757	0.03324
Tubulin	Pre				19.82	0.10289	0.05940
Tubulin	Sphere				17.95	0.06121	0.03534

Figure 4:4 SYBR® Green-based real time RT-PCR of *p16^{ink4}* in the spheroids of SW480 cells compared to their parental and post-sphere cells

The bar chart shows the gene expression results for *p16^{ink4}* normalised to α-Tubulin expression. The test was performed using the Bio-RAD CFX Manager. The error bars indicate the standard error for three repeats. The table shows the readings summary of the tests. Abbreviations: Cq: quantification cycle, SD: standard deviation, SEM: calculation of standard error of the mean. NRT and NTC were included as negative controls.

4.2.2 Down-regulation of Bloom levels in the colonospheres

BLM is a key player required for many cellular repair mechanisms. To examine the BLM protein levels in on the CSCs, total protein was isolated from parental cells, spheres and post-spheres, and was then examined by western blotting. The levels of BLM were significantly reduced in the sphere compared with parental and post sphere cells in both HCT116 and SW480 (Figure 4.5). *BLM* gene expression was also assessed in spheres and compared to attached cells. RT-PCR were performed on cDNA made from those cells to examine BLM expression. BLM was stably expressed in these cells without significant change (Figure 4.6).

For further analysis, SYBR® Green-based real time qRT-PCR was performed for human RecQ DNA helicase family genes in the spheroids of SW480 cells compared with their parental and post-sphere cells. In agreement with RT-PCR, *BLM* expression showed no significant change. Similar results were observed on the expression of *RECQL4* (RecQ protein-like) and *WRN* (Werner) (Figure 4.6 and 4.7).

4.2.3 Down-regulation of GEN1 levels in the colonospheres

In mitotic cells, the second major mechanisms of removing the Holliday junction (HJ) is mediated by structure-selective endonucleases, which resolve joint molecules to form either crossover or non-crossover products. These include MUS81-EME1, SLX1-SLX4 and GEN1 (Chan and West, 2014). To determine whether GEN1 is also affected in the stem-like state and by replication inhibitors, we checked the protein level GEN1 on the sphere of SW480. Colonospheres were made from SW480 cells then treated with CIS and TDR, as described earlier in this chapter. Remarkably, we also found significant decreases in GEN1 levels in sphere cells compared to their attached cells. We also examined MUS81 levels. Slight reductions of MUS81 were only observed on the CIS treated cells on the sphere and post-sphere cells. (Figure 4.8)

Proliferating cell nuclear antigen (PCNA) is involved in several cellular mechanisms including DNA replication, DNA repair and proliferation in several cancers. It was also suggested that PCNA may serves as CSC markers (Horton and Mathew, 2013). However, western blot analysis shows a stable expression of PCNA in both attached and sphere cells without variables observed, as seen Figure 4.8

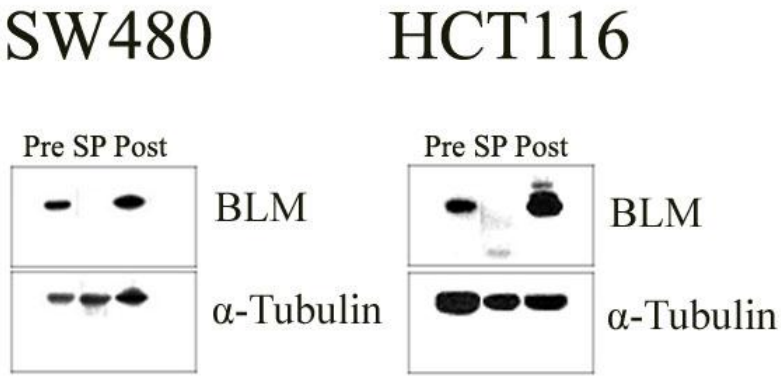

Figure 4:5 Western blot analyses of BLM in the spheroids of SW480 and HCT116 cells compared to their parental and post-sphere cells

Western blot analyses were carried out to test the BLM levels on spheroids of HCT116 (right) and SW480 (left). The levels of BLM were significantly reduced in the sphere compared with parental and post sphere cells in both cell lines. The estimated predicted size of BLM is 170 KDa. Anti-α-tubulin was used as a loading control.

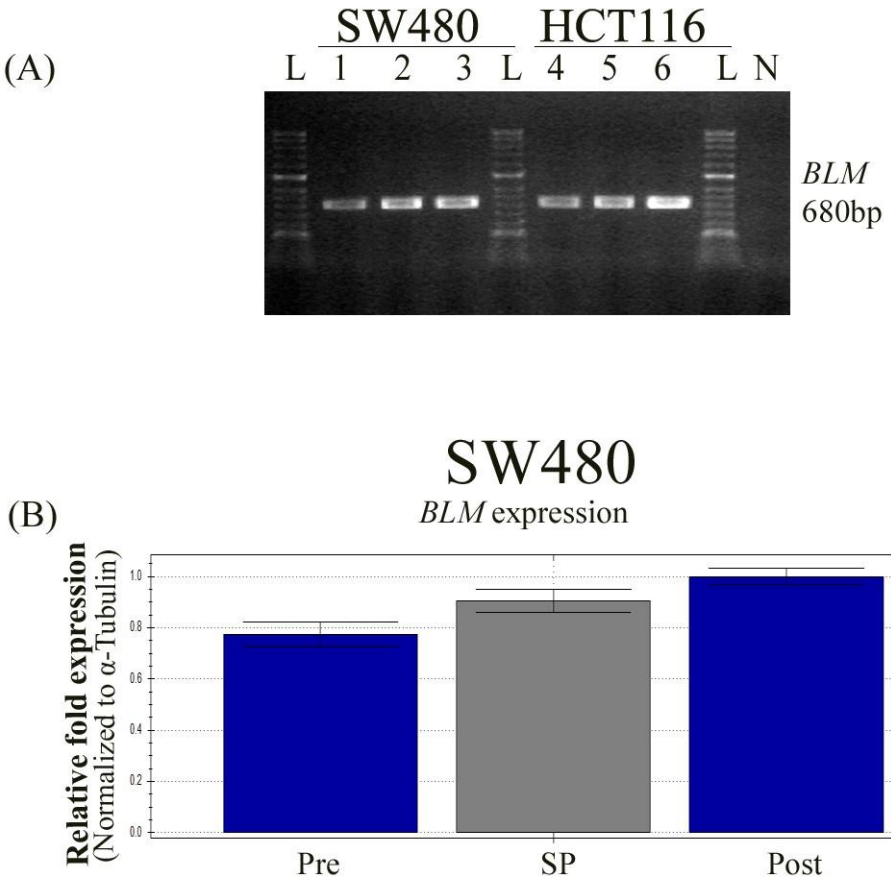

Target	Sample	Expression	Expression SEM	Corrected Expression SEM	Mean Cq	Cq SD	Cq SEM
BLM	Post	1.00000	0.03130	0.03130	25.91	0.05296	0.03058
BLM	Pre	0.77194	0.04849	0.04849	29.34	0.11853	0.06843
BLM	Sphere	0.90521	0.04397	0.04397	27.24	0.10481	0.06051
Tubulin	Post				16.76	0.05757	0.03324
Tubulin	Pre				19.82	0.10289	0.05940
Tubulin	Sphere				17.95	0.06121	0.03534

Figure 4:6 RT-PCR and SYBR® Green-based real time RT-PCR analysis For *BLM*

(A) Agarose gels showing the expression of *BLM* in the spheroids cells compared to their parental and post-sphere cells. (B) The bar chart shows the gene expression results for *BLM* normalised to α-Tubulin expression. The test was performed using the Bio-RAD CFX Manager. The error bars indicate the standard error for three repeats. The table shows the readings summary of the tests. Abbreviations: Cq: quantification cycle, SD: standard deviation, SEM: calculation of standard error of the mean. NRT and NTC were included as negative controls.

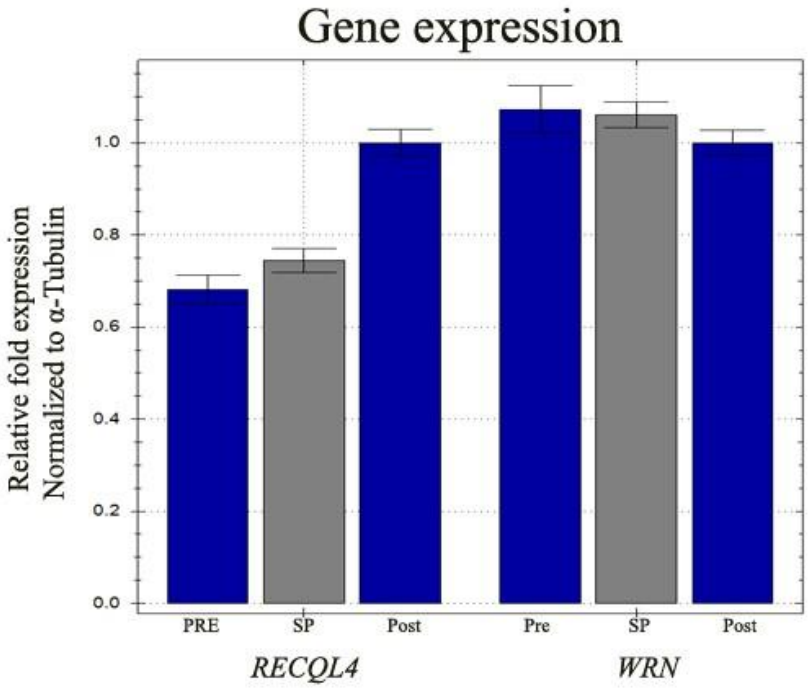

Target	Sample	Expression	Expression SEM	Corrected Expression SEM	Mean Cq	Cq SD	Cq SEM
REQ4	Post	1.00000	0.02907	0.02907	24.70	0.04429	0.02557
REQ4	Pre	0.68130	0.03102	0.03102	28.31	0.04856	0.02804
REQ4	Sphere	0.74497	0.02610	0.02610	26.31	0.06259	0.03613
WRN	Post	1.00000	0.02725	0.02725	26.44	0.03638	0.02100
WRN	Pre	1.07308	0.05057	0.05057	29.40	0.05727	0.03307
WRN	Sphere	1.06138	0.02803	0.02803	27.54	0.02467	0.01424
Tubulin	Post				16.76	0.05757	0.03324
Tubulin	Pre				19.82	0.10289	0.05940
Tubulin	Sphere				17.95	0.06121	0.03534

Figure 4:7 SYBR® Green-based real time RT-PCR for some of human RecQ DNA helicase family in the spheroids of SW480 cells compared to their parental and post-sphere cells

The bar chart shows the gene expression results for *RECQL4* (RecQ protein-like) and *WRN* (Werner) normalised to α-Tubulin expression. The test was performed using the Bio-RAD CFX Manager. The error bars indicate the standard error for three repeats. The table shows the readings summary of the tests. Abbreviations: Cq: quantification cycle, SD: standard deviation, SEM: calculation of standard error of the mean. NRT and NTC were included as negative controls.

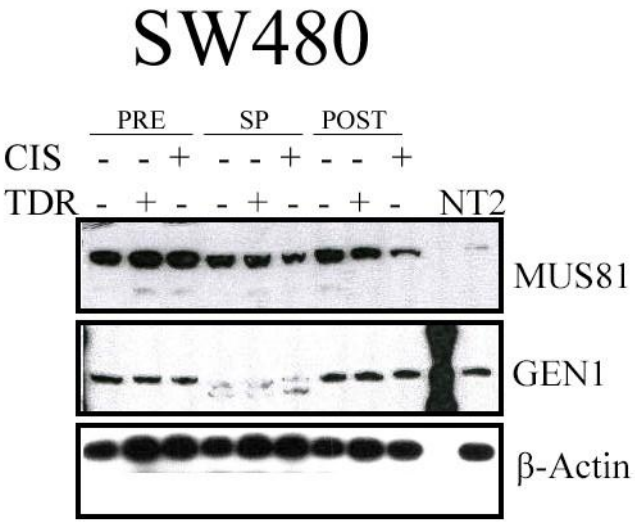

Figure 4:8 Reduction of GEN1 levels in spheroids of SW480

Western blotting analysis of MUS81 and GEN1 levels in the whole lysate extracted from the spheroids of SW480 cells compared to their parental (Pre) and post-spheroid (post) cells. Cells have been treated with indicated agent. NT2 were included as positive control. β-Actin was checked as a loading control test.

4.2.4 The effects of drugs that disrupt DNA replication on the recombination intermediates in colonospheres

To improve our understanding of the repair mechanisms used by colonospheres in response to DNA replication stress during a stem-like state, four drugs have been selected to study their response via different mechanisms: Thymidine (TDR), Cisplatin (CIS), Aphidicolin (APH) and Camptothecin (CPT).

SW480 cells were seeded in 10 cm dishes at a density of 2.5×10^6 cells/dish. The cells were grown for 48 hours then treated for 24 hours with 200 μM/ml of TDR, 15μl/ml of CIS, 1 μM/ml of APH and 1 μM/ml of CPT. For CIS and CPT, cells were incubated for three hours with the treatment and fresh media were replaced until the end of the treatment. For TDR treatment, foetal bovine serum (FBS) was replaced by dialyzed FBS. The same conditions were followed with HCT116 cells except that the seeding number was 1.8×10^6 cells/dish and they were grown for 24 hours because of their high dividing rate compared to SW480. For sphere experiments, 1×10^5 cells were cultured for four and six days for HCT116 and SW480, respectively, in a 10/cm ultra-low attachment dish. Then drugs were added as described above. Concentrations were chosen based on previous studies (Desmarais et al., 2012). Untreated cells and DMSO-treated cells were also included.

After the treatment was completed, the cells were harvested for western blot analysis. Consistent with previous observations (Figure 4.5), the overall reduction of BLM levels were seen on both spheres of SW480 and HCT116 compared to the attached cells. However, the pre-sphere cells of HCT116 show BLM reduced in response to TDR treatment and increasing in CPT treatment. Increasing BLM levels were observed in post-sphere cells of HCT116 when treated with CIS and TDR (Figure 4.9).

Fanconi anaemia (FA) genes were shown to have an important role in DNA repair in collaboration with BLM (Deans and West, 2009). Therefore, we examined the FANCM (FA gene) levels on the same lysate used above. No change of FANCM level is apparent from the western blot analysis, as shown in Figure 4.10.

We further analysed the proteins that play central roles in the accurate repair of DNA DSBs and in protection of stressed replication forks. In HR repair at damaged forks, RAD51 recombinase mediates the homology-dependent strand invasion step with the interaction of BLM (Ouyang et al., 2013). It has been also postulated that Sgs1, BLM,

and RECQL5 work as anti-recombination factors as they can cause disruption to HR-mediated DSB repair by inhibiting the RAD51 nucleoprotein filament (Croteau et al., 2014). We examined the RAD51 level on SW480 and HCT116 cells compared to their spheroids cells. RAD51 level were relatively reduced on the sphere of SW480 compared to their parental cells. In the sphere of HCT116, the reduction of RAD51 were more obvious compared to SW480. However, RAD51 levels were slightly increased following TDR and CIS induction (Figure 4.10).

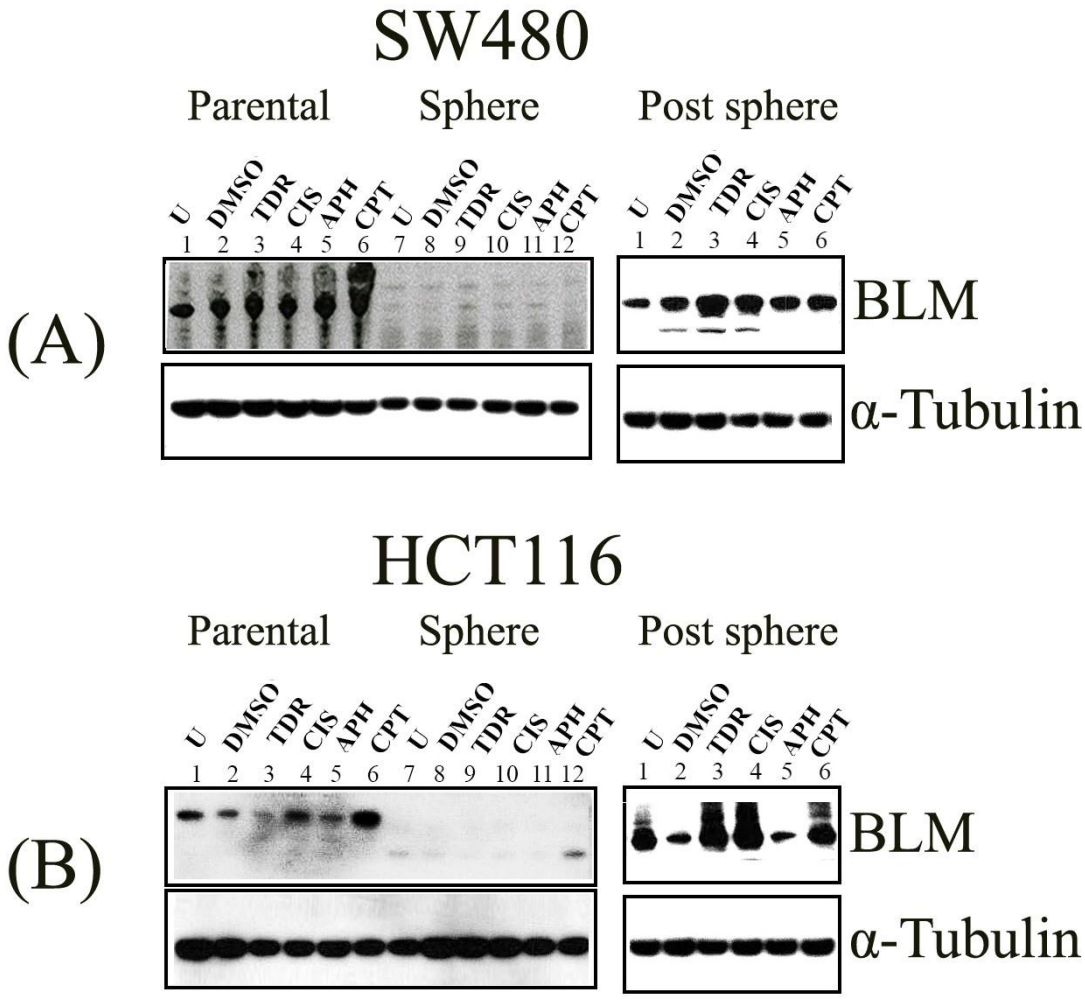

Figure 4:9 Reduction of the Bloom expression level in spheroids formed by colon cancer cell lines

(A) Western blotting analysis of BLM levels on the whole lysate extracted from the spheroids of SW480 cells compared to their parental cells. Cells have been treated with indicating agent. (B) Western blotting analysis of BLM levels on the whole lysate extracted from the spheroids of HCT116 cells compared to their parental cells. Recovery of BLM levels for post-sphere of SW480 and HCT116 is observed. Anti-α-tubulin was given as a loading control. Abbreviations: U: untreated, TDR: Thymidine, CIS: Cisplatin, APH: Aphidicolin, CPT: Camptothecin.

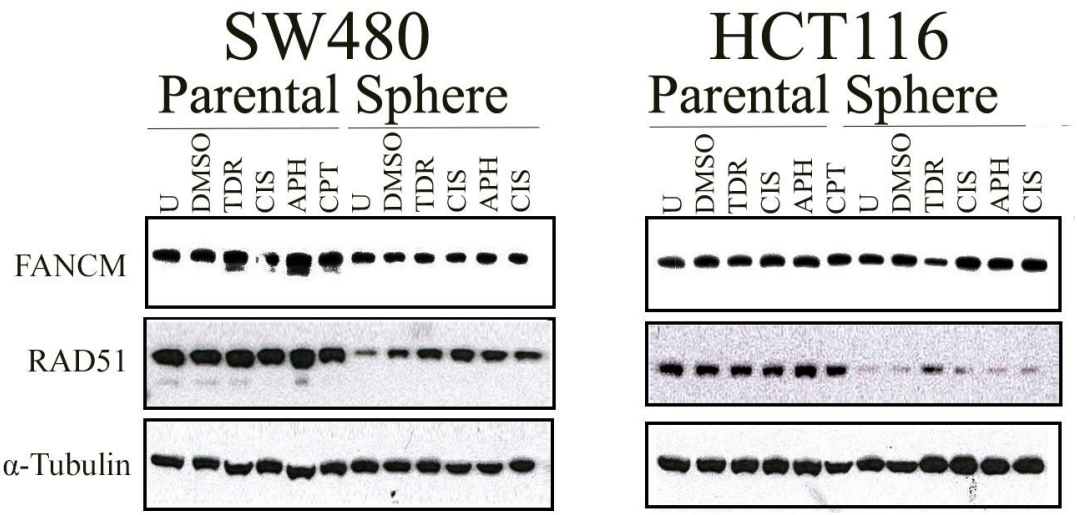

Figure 4:10 Western blot analysis for FANCM and RAD51 in SW480 and HCT116 cell lines compared to their spheroids cells

Western blotting analysis of BLM levels on the whole lysate extracted from the spheroids of SW480 (left) and HCT116 (right) compared to their parental cells. Cells have been treated with indicated agent. Anti-α-tubulin was given as a loading control.

4.2.5 SCE and chromosome aberration analysis in colonospheres exposed to DNA replication stress

SCE frequency has direct proportionality with genomic instability. BLM has an important function in preventing SCE events. Therefore, here, we aimed to investigate the effect of BLM reduction observed on colonospheres using the SCE assay. Following the treatment described in Section 4.2.3, cells were incubated with BrdU for 48 hours in the dark for the SCE assay. Metaphase spreads were prepared on the slide and stained with Hoechst dye, resulting in sister chromatid differentiation.

For APH treatment, metaphase of attached HCT116 cells displays a low number of mitotic cells but differentiated BrdU staining is not evident, where SW480 cells display apparent fragmented chromosomes. For TDR treatment, metaphase spread of both SW480 and HCT116 cells shows abnormal patterns of chromatid BrdU staining. In CPT treatment, mitotic cells (in metaphase) were rarely found. However, some metaphase exhibited a high frequency of SCE events, as seen on HCT116 cells (Figure 4.11). Therefore, metaphase spread prepared for cells treated by TDR, APH and CPT were excluded from SCE analysis.

To measure the SCE frequency, 10 images of metaphase spread for each condition were captured under an immunofluorescence microscope. Control samples (untreated) of both SW480 and HCT116 exhibited normal average levels of SCE, which is less than three events per cell/metaphase. In the colonospheres that already show reduced BLM levels, no change was observed, and the average number of SCEs remained at normal level. However, an apparent elevation to the SCE levels were observed in colonospheres after CIS induction. Elevation was also observed on the Post-sphere of HCT116 cells following CIS treatment (Figure 4.12 and 4.13). The calculations of the SCE events are summarised in Figure 4.14. Each bar represents the average number of SCE events for 10 cell/metaphase that were scored blindly for each condition.

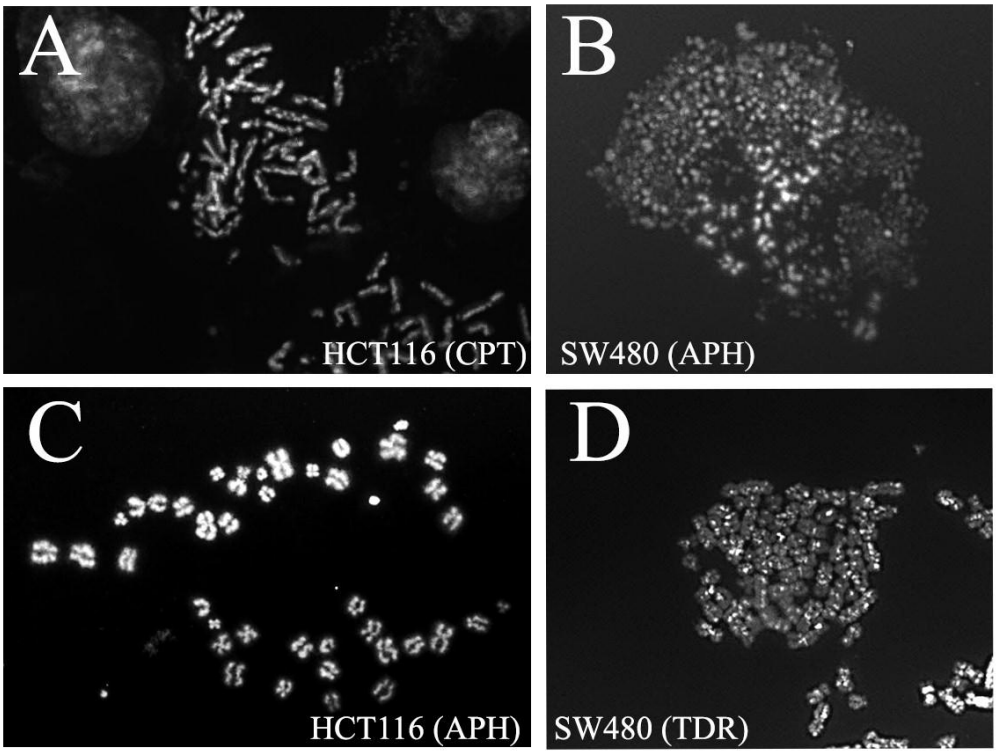

Figure 4:11 SCE analysis following treatment with DNA damaging agents

Cells were incubated with BrdU for two cell cycles. Chromosomes were then exposed to UV light. (A) Represented image of HCT116 cells metaphases stained to visualise SCEs following treatment with 1 µM of CPT for three hours. (B) SW480 cells treated with 1µM APH for 24 hours displays apparent fragmented chromosomes. (C) HCT116 cells treated with 1 µM APH for 24 hrs displays few mitotic cells but does not show differentiated BrdU staining. (D) SW480 cells treated with 200 µM of TDR for 24 hrs show an abnormal pattern of chromatid BrdU staining. Cells were collected using the shake-off method and fixed. Chromosome images were taken using Zeiss Axioskop 2 fluorescence microscope (100 x objective).

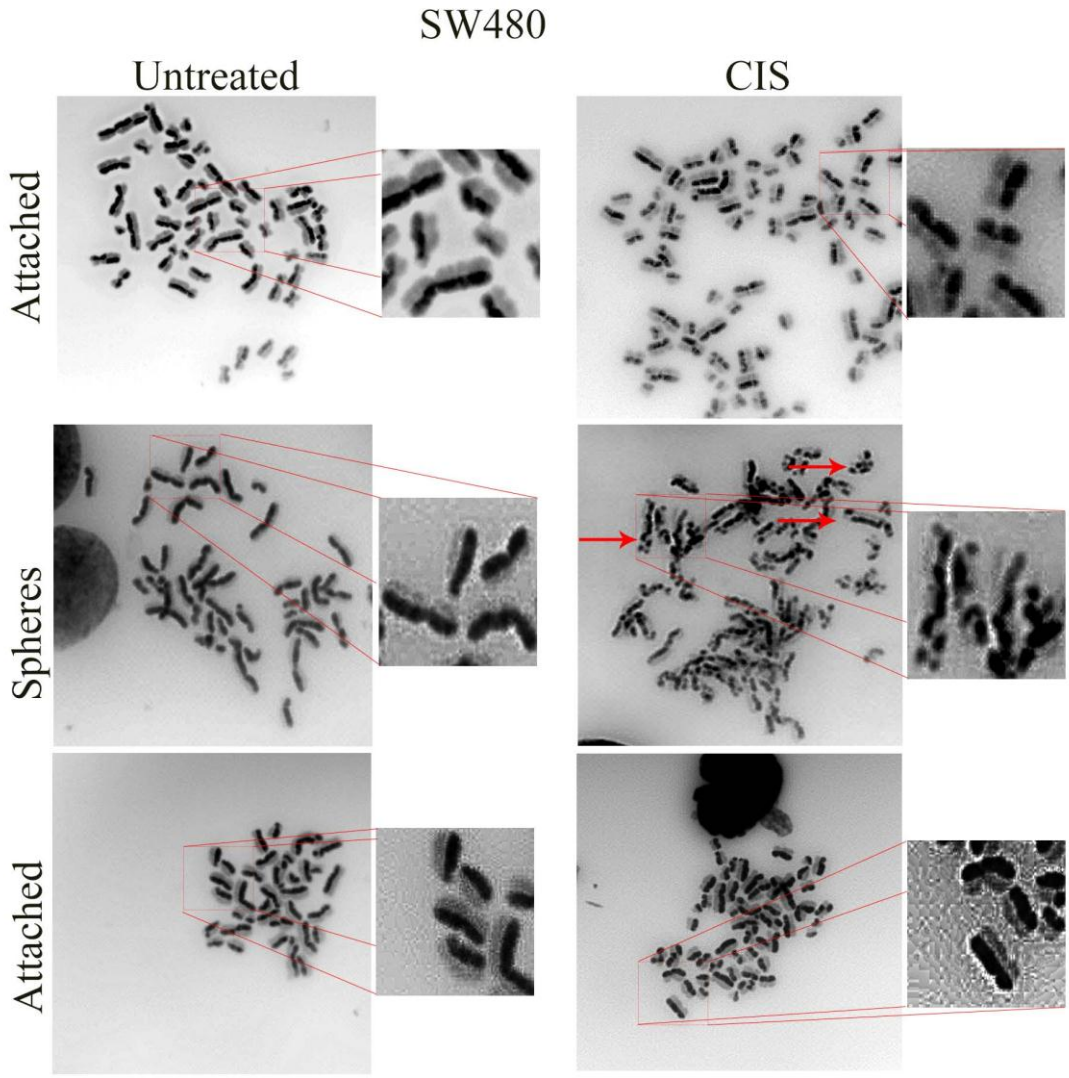

Figure 4:12 Representative images of metaphase spreads prepared from SW480 and their spheroids treated with cisplatin

Parental cells (attached) were treated with 15 µM of cisplatin (CIS) for 24 hours then analysed for SCE. Spheres were disrupted with Accutase® and prepared on slides. Following the treatment, the cells show several SCEs, some of which are indicated by red arrows. The chromosomes were stained by Hoechst 33342. The photographs were taken under a Zeiss Axioskop 2 fluorescent microscope (100 x objective). Higher magnification of the selected chromosomes is shown on the right side of each image.

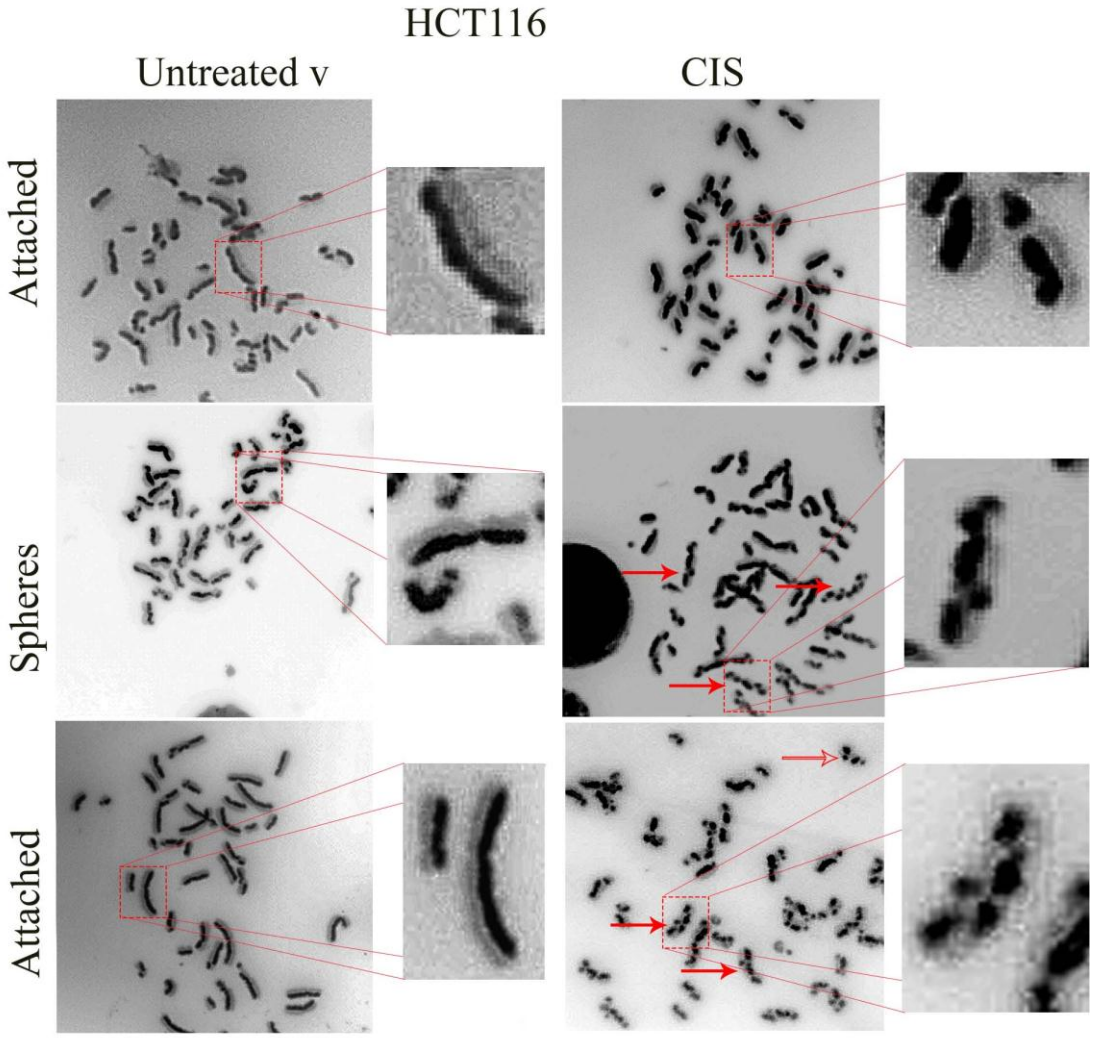

Figure 4:13 Representative images of metaphase spreads prepared from HCT116 and their spheroids treated with Cisplatin

Parental cells (attached) were treated with 15 µM of cisplatin (CIS) for 24 hours then analysed for SCE. Spheres were disrupted with Accutase® and prepared on slides. Following the treatment, the cells show several SCEs, some of which are indicated by red arrows. Chromosomes were stained by Hoechst 33342. The photographs were taken under a Zeiss Axioskop 2 fluorescent microscope (100 x objective). Higher magnification of the selected chromosomes is shown in the right of each image.

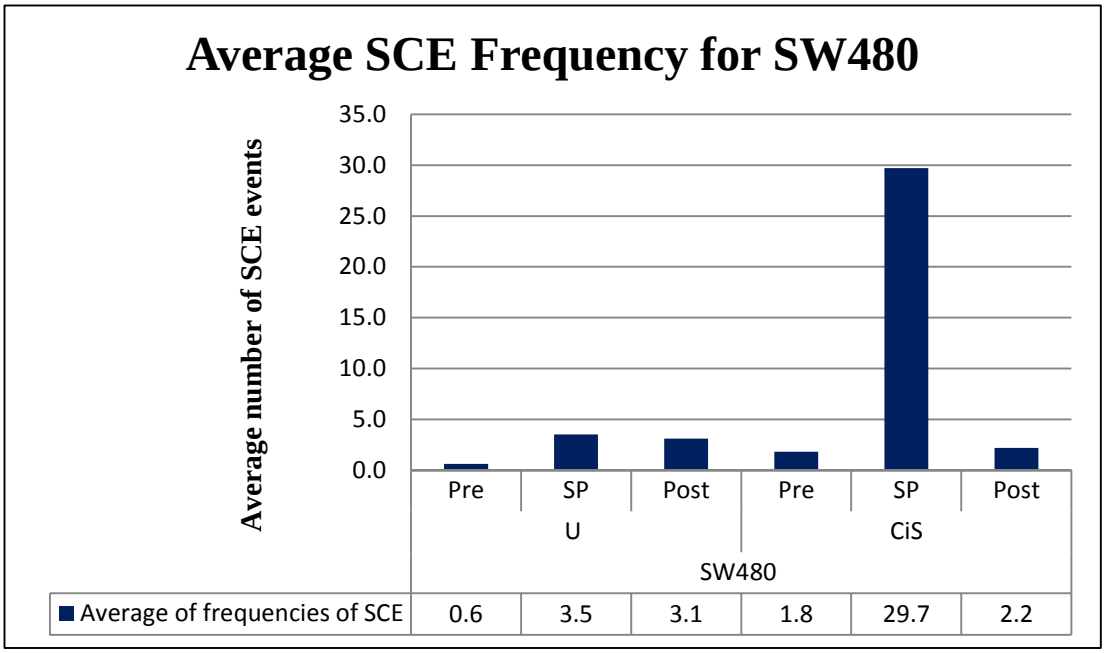

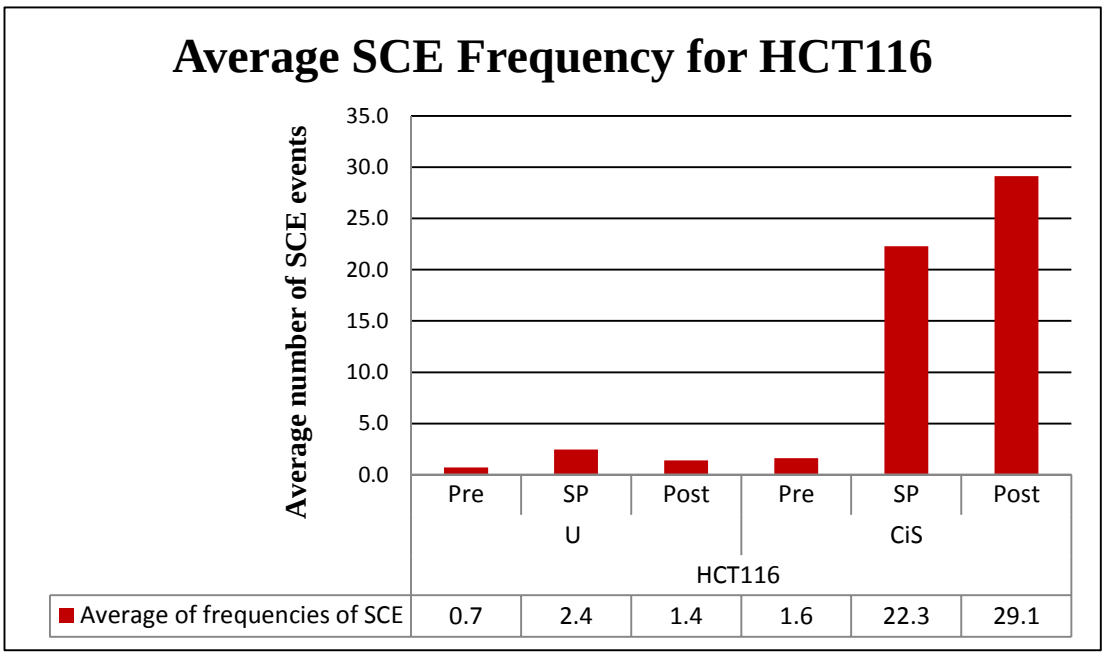

Figure 4:14 Quantification of SCE frequency following Cisplatin induction on SW480 and HCT116 cells compared to their spheres

The bar charts show quantification of SCE frequency after Cisplatin induction. Each bar represents the average number of SCEs for 10 cell/metaphase that was scored blindly for each condition.

4.3 Discussion

4.3.1 CSCs formation

In the present study, we generated colonospheres from two colorectal cancer cell lines, SW480 and HCT116, which possess the characteristics of CSCs. We found that the stemness gene Oct4/3 is expressed in both sphere cells but it is absent in their parental cells and post-spheres for HCT116. However, Oct4/3 was expressed the post-sphere of SW480 cells. This might be explained by the presence of a subpopulation of CSCs remaining within the cells, which need longer to differentiate or return to their original state. As a key regulator of pluripotency that promotes lineage commitment during early development, Oct4/3 alone is sufficient to transform cells directly into induced pluripotent stem cells (Kim et al., 2009). Oct3/4 has also been reported as an important factor required for an anti-apoptotic behaviour of chemo-resistant colorectal cancer cells. Secondly, we found that the spheroids of SW480 are CD44 positive. CD44 is one of the common surface markers for CSCs in several solid tumours and many haematological malignancies (Wen et al., 2013).

Li et al found that the *Ink4a/Arf* locus, which encodes tumour suppressors ($p16^{Ink4a}$) and p53 activator ($p19^{Arf}$), is inhibited during iPS reprogramming. They postulated that this repression occurs early in reprogramming, indicating a regulatory function of the reprogramming factors on this locus. $p16^{Ink4a}$ also has a positive influence on the direct neuronal transdifferentiation (Li et al., 2009; Price et al., 2014). We reported down-regulation of $p16^{Ink4a}$ following sphere formation, as shown in Figure 4.4. Accordingly, CSCs, as result of a re-programming-like mechanism, may also exhibit similar behaviour during their transformation to a stem-like state. Together these observations demonstrate the enrichment of cells that are re-programmed to CSCs within the colonospheres.

One of the controversial issues about CSCs is their capability to divide and renew themselves for a long time. In this study, cells were grown and formed spheres continuously for several passages, but we did not test this phenotype in our study. However, recent work addressed this issue and found that CSCs undergo symmetric and asymmetric division by using an Oct4/3 promoter driven GFP system. They demonstrated that the majority of Oct4/3-positive cells were divided symmetrically,

while the minority were divided asymmetrically and produced Oct4/3-positive and Oct4/3-negative cells (Wen et al., 2013).

4.3.2 Down-regulation of BLM and GEN1 in CSCs

One of the key observations that we found in this study is the dramatic reduction of BLM and GEN1 levels in correlation to stem cell markers and sphere formation (Figures 4.5, 4.8 and 4.9). This behaviour was observed by individual members of our lab making preliminary observations and revealing novel phenomena about CSCs. When this aggregate and spheroid structure forms, it leads to change genome stability regulated pathways. BLM and GEN1 are the two key processors of the HJ. If the cells switch off BLM and GEN 1, it means they become more susceptible to genetic change and possibly drive selection pressure in that population of cells, which is supported by the model for tumour cell heterogeneity. The more cell heterogeneity a tumour has, the more cells change genetically, and the greater ability they have to become resistant to chemotherapy. It also poses a challenge to personalised cancer medicine (Burrell et al., 2013). If that occurs in the CSC population, it will likely lead to poorer progresses.

MUS81 is another key processor that mediates the restart of stalled replication forks and the resolution of the HJ. We presented in this chapter that MUS81 levels were stably expressed in the CSCs (Figure 4.8). MUS81 belongs to the XPF (xeroderma pigmentation group F) family of structure-specific DAN endonucleases. MUS81 and its partner Eme1 (the Mms4 ortholog) play essential roles in cleaving a range of branched DNA structures, including HJs. Biochemical analysis of Mus81–Eme1 complex in a fission yeast study has found that it is the main promoter HJ resolves. It also demonstrated a significant reduction in spore viability (an indicator of meiotic failure) in mutants of Mus81–Eme1. However, further kinetic and enzymatic analysis of the substrate specificity of Mus81–Eme1/Mms4 from different organisms indicated that this enzyme actually has a cleavage preference for structures such as nicked HJs, partial HJs and D-loops. MUS81 substrate specificity suggests that Mus81–Eme1/Mms4 might cleave D-loops before they develop into fully formed X-structures, instead of resolving dHJs (Mukherjee et al., 2014; Whitby, 2005). Therefore, that may suggest that when cancer cells become sphere, either they modulate their standard pathway or follow a unique pathway of repair that does not involve forming or resolving dHJs.

4.3.3 Do CSCs activate a meiosis-specific pathway?

The reduction of BLM and GEN1 during sphere formation may also be explained by a special mechanism in meiosis in yeast when the cells induce another pathway that dissolves HJ, involving something called the HJ MutLγ complex (Mlh1-Mlh3). Recent work has revealed a new meiosis HJ resolution activity of the MutLγ complex. This mechanism is postulated to cause CO formation in budding yeast and, by inference, in mammals (Zakharyevich et al., 2012).

This also supported by the down-regulation of RAD51 that we observed in CSCs, as seen in Figure 4.10. While Rad51 is required for HR during both meiotic and mitotic recombination, Dmc1 (meiosis-specific paralogue of Rad51) is only needed in meiosis (Da Ines et al., 2012). Nevertheless, a number of studies have found that the up-regulation of key meiotic genes including DMC1 was linked with reversible polyploidy and induced meiosis-like programmes in multiple cancer types (Erenpreisa and Cragg, 2013).

A recent study has shown that down-regulation of the Rad51 function is required during meiosis to prevent Rad51 from competing with Dmc1 for repair of meiotic DSBs in yeast (Liu et al., 2014a). In humans, down-regulation of RAD51 is associated with dysregulation of critical DNA repair pathways in hypoxic cancer cells (Bindra et al., 2004). Interestingly, recent experimental evidence indicates that hypoxia provided by microenvironments of tumours can cause a reversible phenotype that is required in maintaining a stem-like state to ensure survival of the tumour (Grosse-Gehling et al., 2013; Heddleston et al., 2010).

Another speculation that might be added to this scenario is that, during sphere formation, cells may activate a meiosis-specific pathway. Because morphological changes occur in spheres, the way of sticking to each other and activating Oct4/3, allows the cells to exhibit more germline behaviour and switch off the standard pathway during sphere formation. The possibility of activating a meiosis-specific pathway is supported by several evidences. Previous studies of humans have reported the expression of a number of germline genes (meiosis-specific genes) in non-testis tissues. For example, the expression of *REC8* and *STAG3* were present in normal tissues including the colon. In addition, some testis-restricted meiosis Cancer Testis (meiCT) genes such as *RAD21L*, *PRDM9*, *C1orf65* and testis selective meiCT gene

like *TEX19* were found expressed in colon cancer tissue (Feichtinger et al., 2012; Sammut et al., 2013).

Down-regulation of meiosis-specific genes is explained by mitotic cells of yeast, where post-transcriptional mRNA degradation supress the production of Rec8 protein (Harigaya et al., 2006; Hiriart et al., 2012). This is also supported by recent work that linked the expression of germ line genes to advanced and aggressive lung tumours. The data also shows a correlation of activation of the gremlin gene with the acquisition of embryonic stem cell phenotypes (Rousseaux et al., 2013).

4.3.4 Possible post-transcriptional regulation of BLM in CSCs

When we looked at the gene regulation level with RT-PCR and qRT-PCR, *BLM* expression did not go down and the mRNA levels were similar in both the sphere and attached cells. This shows the possible post-transcriptional regulation mechanism of that gene. The microRNAs (miRNAs), or short non-coding RNAs, control the gene expression post-transcriptionally by binding it to the target mRNA resulting in its degradation or translation repression (Li and Zhang, 2014). Though cancer cells have an abnormal expression of miRNAs, evidence supports the functional properties of miRNAs in CSC phenotype including self-renewal (Li and Zhang, 2014). For example, specific miRNAs were found to play an important role in suppressing tumour formation generated by human breast CSCs (Shimono et al., 2009).

4.3.5 Chromosomal instability in CSCs

Chromosomal instability is a common feature of human cancers driven by genetic aberrations and is proposed to be involved in the initiation of tumorigenesis. However, the exact mechanism of how chromosomal instability may contribute to the initiation of CSCs remains unclear (McGranahan et al., 2012; Rao et al., 2013). Thus, we were intent on investigating the genomic integrity of CSCs compared to their parental cells and following DNA replication stress by SCE assay. SCE frequency is a common method used for assessing the level of chromosomal stability in response to endogenous and exogenous DNA damage and mutagenesis (Rimoin et al., 2013; Sonoda et al., 1999).

In normal mitotic dividing cells, HJ dissolution is mediated by BTR (BLM–topoisomerase IIIα–RMI1–RMI2) complex in a process that limits SCE formation by

minimising crossover events. In addition, this pathway can reduce the risk of (LOH) that can lead to development of cancer (Sarbajna and West, 2014). However, colonospheres of SW480 and HCT116 cells that lack BLM exhibited low levels of SCEs, indicating that HJs are removed by alternative pathways. Perhaps, HJs are processed by a third pathway of the HJ resolution mediated by MUS81, which provides backup for the BTR complex function. In contrast, colonospheres displayed elevation in SCE frequency compared with their parental cells in response to DNA damage, such as that induced by CIS, as shown in Figure 4.12 and 4.13. This suggests that MUS81 pathway of colonospheres were unable to cope with a high amount of HJs.

Consistent with this, resolution pathways of SCE formation have been studied in BS cells and normal human fibroblast cells. This study has shown that the absence of the SLX-MUS pathways (MUS81 and SLX work in the same way) or GEN1 led to a significant reduction of SCEs in BS cells. This indicates the primary role of each pathway for HJ resolution. It also demonstrates that SCE formation in normal cells is dependent upon the HJ resolvases following CIS treatment (Wyatt et al., 2013).

In summary, the presence of stem-like cells within different colon cancer cell lines has been reported. The cellular mechanisms by which CSCs arise from different types of tumours and how these cells acquire their features require further investigations in the future. We also found some genes involved in the standard repair pathway to be down-regulated, suggesting a different repair mechanism in this population of cells. Further analysis of enzymes required for the HJ processing and their alternatives and the pathways that they act in holds promise for a comprehensive understanding of the biology of the CSC. Nevertheless, the possibility of activating a specific-meiosis pathway in CSCs may also offer scope for the development of new therapeutic approaches to treat these highly aggressive tumours.

Chapter 5

Results

Chapter 5. Cell cycle regulation in cancer stem-like cells following DNA replication stress

5.1 Introduction:

DNA can be damaged in different ways by chemical and physical factors such UV radiation, viruses and reactive oxygen species (ROS) (Chapter 1). When replicative cells suffer irreparable DNA damage, they may either enter senescence or undergo programmed cell death (apoptosis) for elimination from the cell population. DNA damage that induces apoptosis includes O6-methylguanine formation, base N-alkylations, bulky DNA adduct formation, DNA double-strand breaks (DSBs) and DNA cross-links. Thus, specialised mechanisms for the repair of these lesions are essential for avoiding apoptosis (Rodriguez-Rocha et al., 2011).

The efficiency of DNA damage repair is ensured in cancer stem cells (CSCs) by activation of a number of DNA repair mechanisms that require a wide variety of factors and proteins (Mathews et al., 2011). Cancer cells, as well as CSCs, can evade cell cycle checkpoints and enter into a stage of uncontrolled DNA replication and cell growth. This suggests a high capacity for efficient DNA repair in CSCs for preservation of genome integrity commensurate with proliferation. Therefore, better understanding of DNA repair may provide a clearer explanation of cancer development and responses to therapy through the mechanism based on the suitable DNA damaging approaches (Figure5.1) (Clevers, 2011).

Embryonic stem cells (ESCs) are characterised by a high rate of proliferation and a short G1 phase, but they maintain DNA stability and genome integrity exceeding DNA damage will drive apoptosis as a primarily pathway. This maintenance is important in ensuring that the correct information is transmitted to differentiated cells and cell lineages derived from ESCs including the germ line cells (Neganova et al., 2011). Genome integrity of ESCs, together with environmental factors, contributes to control of the balance of cell-fate decisions (self-renewal, differentiation, senescence or death) (Blanpain et al., 2011). However, DNA repair remains poorly understood in the context of CSCs.

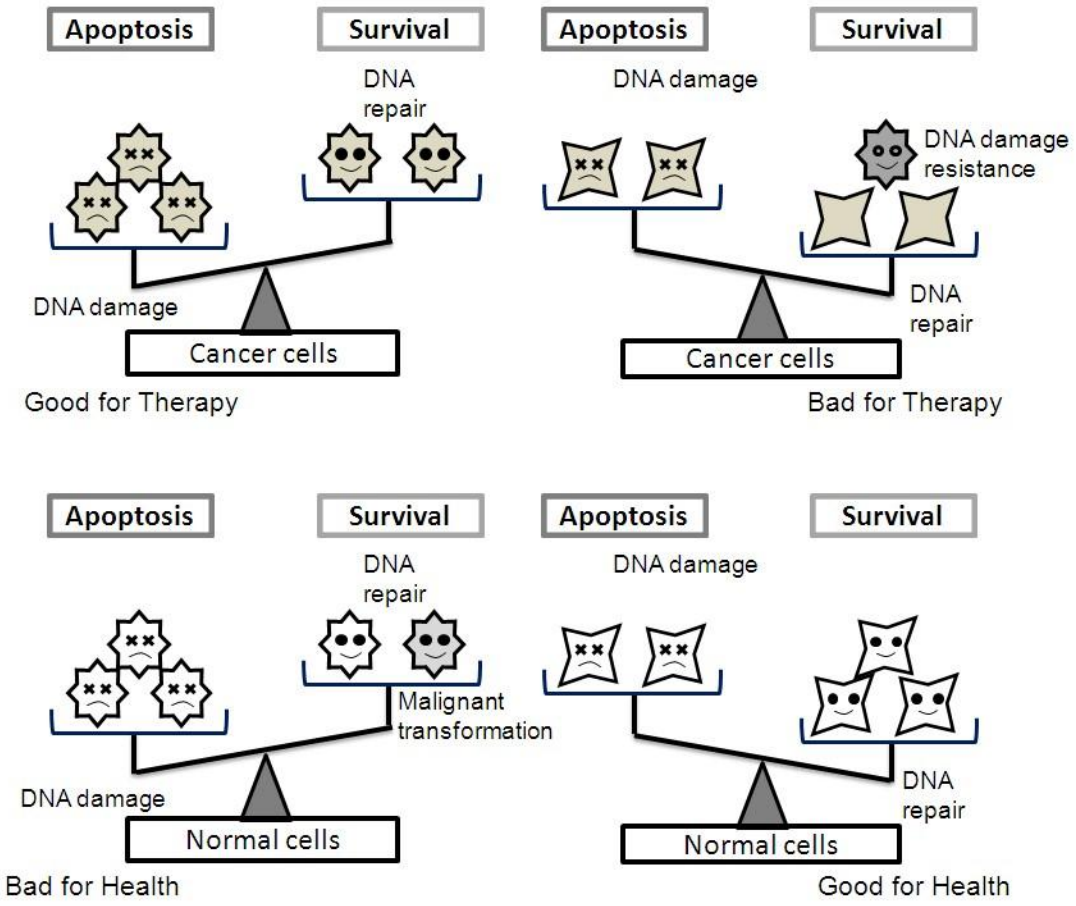

Figure 5:1 Balancing of resistance and sensitivity to DNA damage in normal and cancer cells.

Chemotherapy resistance is the main challenge in cancer therapy. The apoptotic stimulus represents cells of healthy individuals. The diagram summarises how the survival or apoptosis is bifacial or represents a risk for the normal and cancer cells. The determination of cell fate (either survival or apoptosis) depends on the balancing between DNA damage and the amount of DNA repair.(Kitagishi et al., 2013)

The efficient repair mechanism operating in stem cells to protect their genome poses a threat in CSCs, where it works to reverse the DNA lesions caused by therapeutic agents.

Damaged DNA is detected by specific "sensor" proteins that exist in normal cells and scan across the DNA. When one of these proteins finds damaged DNA, it is activated and initiates a signalling cascade, causing cell cycle arrest, DNA repair or apoptosis. These "sensor" proteins include Ataxia telangiectasia mutated (ATM), ataxia telangiectasia and Rad3-related protein (ATR) and DNA-dependent protein kinase (DNA-PK). Their activation leads to phosphorylation of several proteins including p53, CHK2, CHK1 and H2AX.

One of the earliest responses to DSBs that plays an important role in the recognition and triggering of DSB repair is the phosphorylation of histone variant protein H2AX at serine 139 generating γ-H2AX (Podhorecka et al., 2010). This phosphorylation results in the formation of "nuclear foci", which can be detected by immunofluorescence microscopy and used as consistent and quantitative markers of DSBs (Rogakou et al., 1999; Wu et al., 2013).

ESCs and mESCs employ similar factors to those used by somatic cells in response to DSBs (Momcilovic et al., 2009). High basal levels of γ-H2AX have been reported in mouse ESCs (mESCs) and induced pluripotent stem cells (iPSCs), even in the absence genotoxic agents (Turinetto et al., 2012). Similar findings have been reported in human ESCs and iPSCs (Momcilovic et al., 2010). In contrast, several studies have shown that ESCs fail to activate γ-H2AX in response to replication stress when compared to their parental cells and differentiated cells (Fan et al., 2011; Saretzki et al., 2008). Andrews and co-workers demonstrated that human ESCs and embryonal carcinoma cells failed to activate cell cycle checkpoint factors CHK1, RAD51 and γ-H2AX in response to DNA replication inhibition (Desmarais et al., 2012). It appears that, rather than trying to deal with DNA replication-induced damage, these cells instead are directed down an apoptotic pathway (Lundholm et al., 2013). A study of cancer stem cells of lung exposed to genotoxic agents showed that CHK1 was activated more efficiently, and that fewer γ-H2AX foci were observed in the CSCs compared to differentiated cells (Lundholm et al., 2013).

Based on these findings, we used the colorectal cancer cell lines HCT116 and SW480 as non-stem cell controls, as these cells activate a checkpoint in response to DNA replication-induced damage. We aimed to address whether checkpoint response look more stem-like when cells change context to give a more stem-like phenotype (colonospheres) and to address whether there is a plasticity to this biological response.

Results

5.1.1 Failure of DNA replication inhibitors to activate CHK1 in CSCs

The CHK1 kinase is required for highly conserved DNA-repair and functioning of the cell-cycle checkpoint pathways induced by genotoxic stress. Activation of CHK1 following DNA insult involves phosphorylation at two C-terminal residues of serine (S317 and S345) (Rawlinson and Massey, 2014). The possible activation of this protein in CSCs was examined by exposing the HCT116 and SW480 cancer cells and corresponding colonosphere cells (spheroids) to the following replication inhibitors; thymidine, cisplatin, aphidicolin and camptothecin. Drug concentrations and timing of addtion were as described earlier in Chapter 4. Cells were then harvested for Western blot analysis and evaluation of activation of the CHK1 (P-CHK1) checkpoint protein using phospho-specific antibodies. The levels of CHK1 phosphorylated at ser345 were elevated in the parental cell line of SW480 after treatment. In contrast, no phosphorylation of CHK1 was detected in their spheroids following treatment (Figure 5.2 A).

TDR treatment of HCT116 cells induced P-CHK1 in the parental cells but not in their spheroids. DMSO treated cells were included as controls and showed no change in the P-CHK1 level. Tests of total CHK protein (T-CHK1) levels did not show significant changes in the parental cells. However, a slight reduction in T-CHK1 was observed on the spheroids, particularly following TDR treatment (Figure 5.2 B).

5.1.2 Enhancing apoptosis after replication stress

Apoptosis is a critical pathway that is targeted by chemo and radiotherapy to kill cancer cells. Activation of caspase is a characteristic of cells committed to apoptosis, so this was examined in spheroids and parental cells for both SW480 and HCT116 cell lines. Caspase cleavage was strongly triggered following APH treatment in the parental SW480 cells but not in their spheroids. The other DNA damaging agents also did not induce caspase cleavage in spheroids. DNA damaging agents were also not efficient inducers of apoptosis in parental cells or in the spheroids of the HCT116 cell line (Figure 5.3). However, caspase was activated by CIS in spheroids derived from late passage SW480 cells and but failed to activate in the parental cells (Figure 5.4).

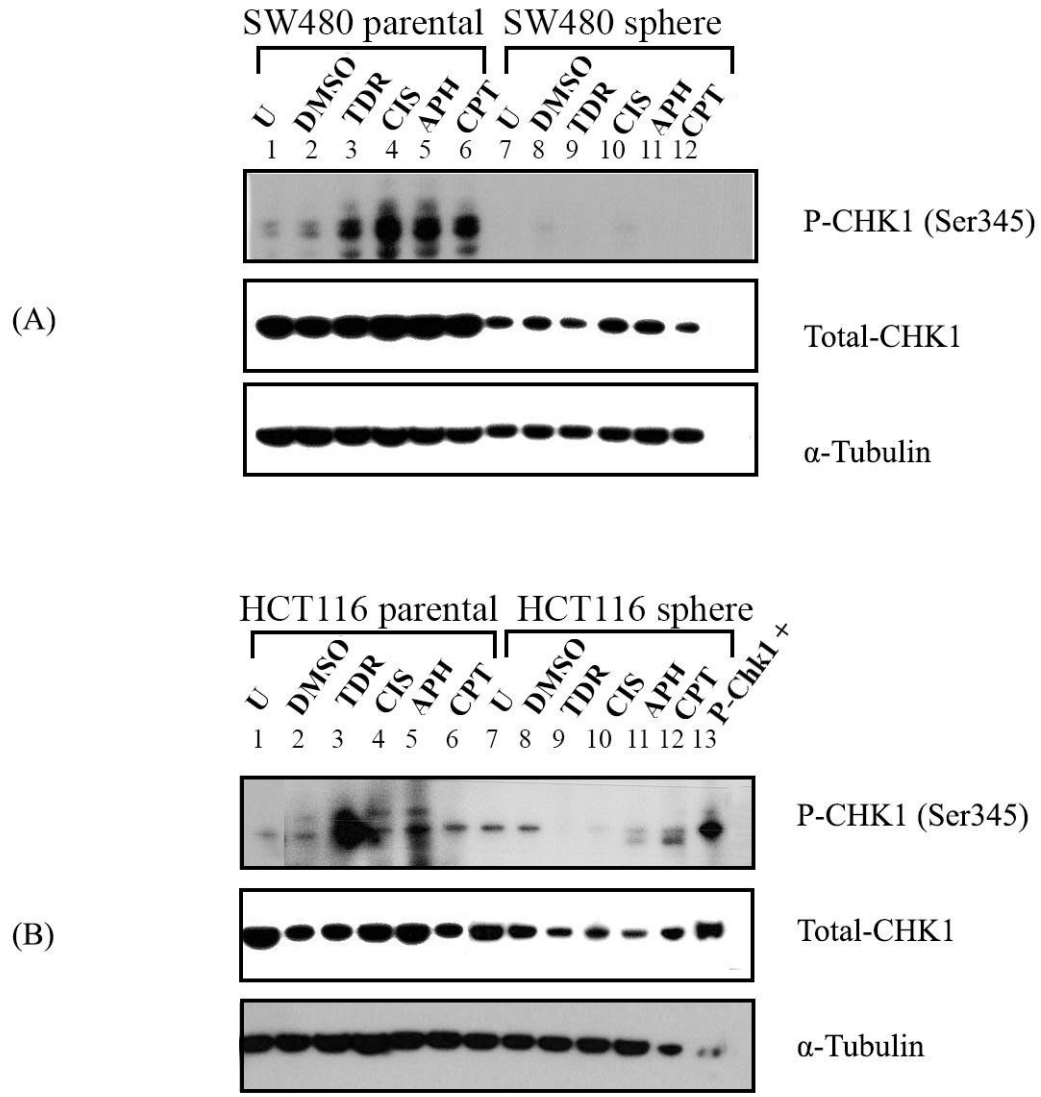

Figure 5:2 Defective activation of P-CHK1 in response to replication stress in CSCs

(A) Western blot analysis of parental SW480 (lanes 1 to 6) and their spheroids (lane 7 to 12). (B) Western blot analysis of HCT116 (lanes 1 to 6) and their spheroids (7 to12). Lane 13: total cell extracts from 293 cells, treated with UV light, serve as a positive control for P-CHK1. α-Tubulin samples are included as loading controls. Abbreviations: CHK1, checkpoint kinase 1; P-CHK1 (Ser345), phosphorylated CHK1 at serine 345; U, untreated cells; DMSO, dimethyl sulfoxide; TDR, Thymidine; CIS, Cisplatin; APH, Aphidicolin; CPT, Camptothecin.

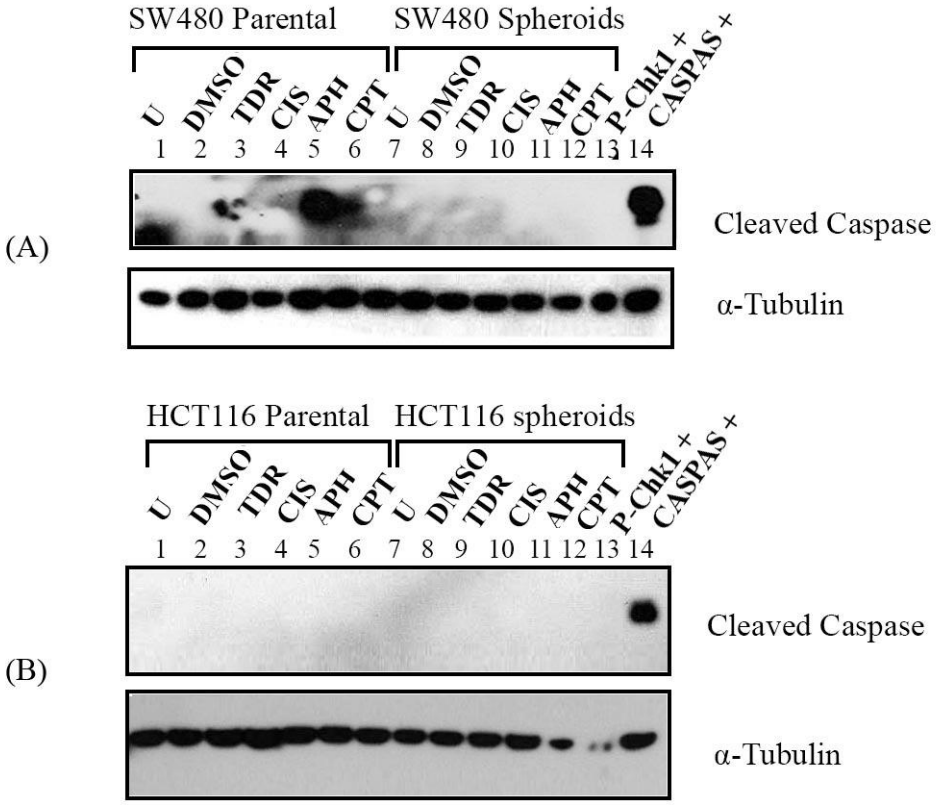

Figure 5:3 Induction of apoptosis by replication inhibitors in CSCs

Western blot analysis of caspase cleavage in the spheroids from (A) SW480 and (B) HCT116 cell lines following treatment, compared to their parental cells. Cytochrome c treated Jurkat cell extracts serve as a positive control for caspase cleavage (Caspase+). Total cell extracts from 293 cells, treated with UV light, serve as a positive control for P-CHK1 (P-CHK1+). α-Tubulin was used as a loading control.

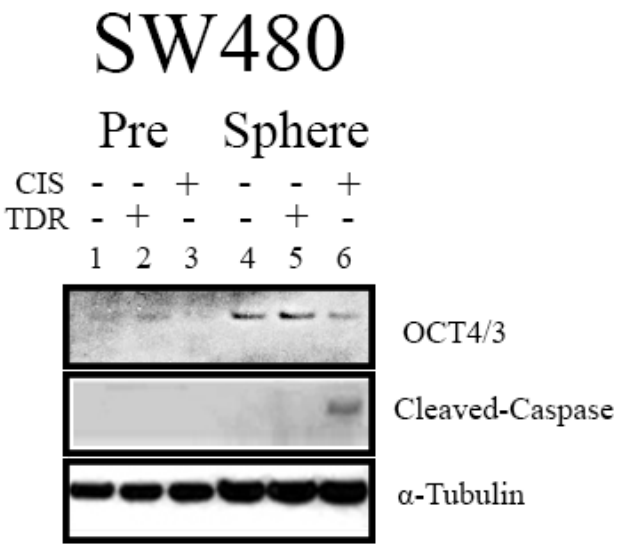

Figure 5:4 Induction of apoptosis by replication inhibitors in sphere made from late passage SW480 cells

Western blot analysis showing activation of caspase in SW480 spheroids following treatment with cisplatin compared to their parental cells. Caspase activation was correlated with a slight reduction in the intensity of the stem cell marker (OCT4/3). α-Tubulin was used as a loading control. Abbreviations: TDR, Thymidine; CIS, Cisplatin.

5.1.3 Comparison of γ-H2AX activity levels between CSCs exposed to replication inhibitors and parental controls

The previous observation that CHK1 was not activated following replication stress suggested that CSCs may not respond to DNA replication inhibitors in the same way that most cancer cells do. γ-H2AX is an established marker for DSBs and is used for assessing cancer therapy effects. γ-H2AX foci can be used to measure the response of cells and the efficiency of their DNA repair processes (Kuo and Yang, 2008). We next investigated whether decreased levels of CHK1 activity might translate into decreased levels of DNA damage by measuring γ-H2AX foci.

SW480 and HCT116 cells were seeded on circular cover slips, placed in 24 well-plate and grown for 24 hours. Cells were then treated for 24 hours with the same drugs and in the same manner described earlier in this Chapter. Spheroid experiments were run by first dissociating of the spheroids with Accutase to enable counting of the foci-positive cells. Cells were then cytospun onto circular cover slips, transferred into 24 well-plates, and then fixed and prepared for immunostaining. Untreated cells and DMSO-treated cells were also included as controls. We used a monoclonal antibody that detects Phospho-Histone H2AX (Ser139) at the C-terminal region of H2AX (Cell Signaling # 9718p).

Immunofluorescent images of the cells were obtained and the cells were then counted for quantitative analysis. The cells exhibited different staining patterns, so we sorted them into three categories: (1) Bright for the cells that showed a bright pan-nuclear γ-H2AX staining; (2) Med for the cells that showed high numbers of γ-H2AX foci; and (3) Weak for the cells that showed a small number of dim nuclear γ-H2AX foci or no staining at all. The percentages for each category were then calculated from at least 50 cells per experiment. Representative images and quantitation of the γ-H2AX staining patterns are shown in Figures 5.5 and 5.6.

The vast majority of both cell lines and their spheroids showed very weak signals or no signal in untreated samples. No significant effect of DMSO was observed in the cells. The HCT116 spheroids showed no induction of γ-H2AX foci in response to TDR treatment. In contrast, a high proportion (80%) of the parental cells formed γ-H2AX foci (bright and med) after TDR treatment, comparable to that of untreated cells. The high induction of γ-H2AX was also observed in post-sphere cells. Similar observations

were made in SW480 cells, except that their spheroids showed a small proportion of cells with induced foci (med). A decreased level of γ-H2AX foci was also seen in the HCT116 spheroids compared to their parental cells following the treatment with CIS and CPT. A decrease in the formation of γ-H2AX foci was only seen in the SW480 spheroids following APH induction. However, treatment with CPT resulted in a distinct pan-nuclear staining of γ-H2AX indicating a further accumulation of these foci.

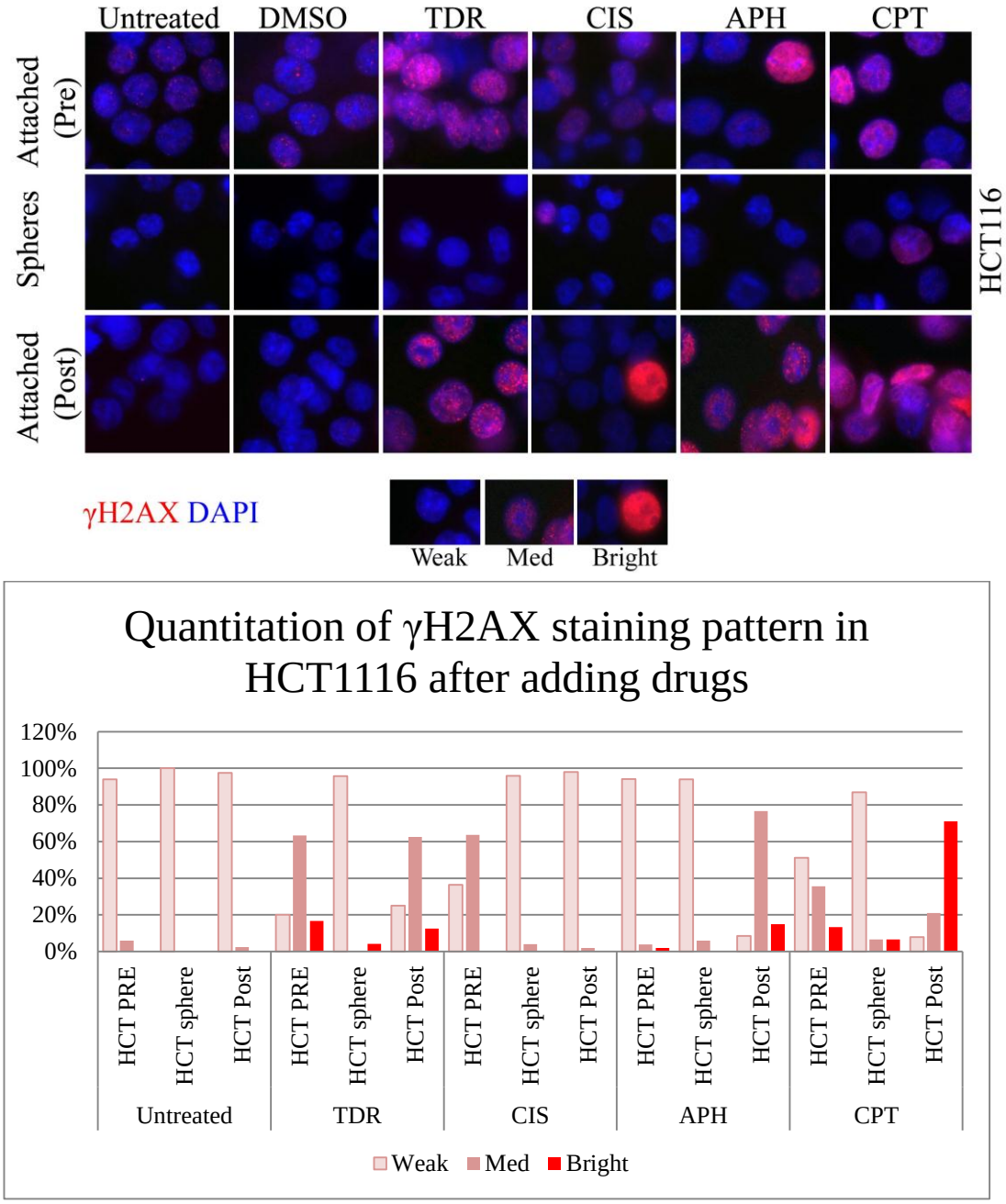

Figure 5:5. γ-H2AX foci are not induced in the spheroids of HCT116 in response to replication stress.

(Upper) Representative images showing nuclear morphology and γ-H2AX staining of HCT116 cells and their spheroids following treatment with the indicated chemotherapeutic agents for 24 hours. (Lower) Quantitation of H2AX staining patterns in HCT1116 cells following treatment. Percentages are calculated from 50 cells per experiment. The staining pattern is classified into three categories; Bright: Cells that show a bright pan-nuclear of γ-H2AX staining; Med: Cells that show high numbers of γ-H2AX foci; and Weak: Cells that show small numbers of dim nuclear γ-H2AX foci or no staining at all. Nuclei were stained with DAPI dye. (blue fluorescence). Images were taken using a Zeiss Axioskop 2 fluorescence microscope (65 x objective).

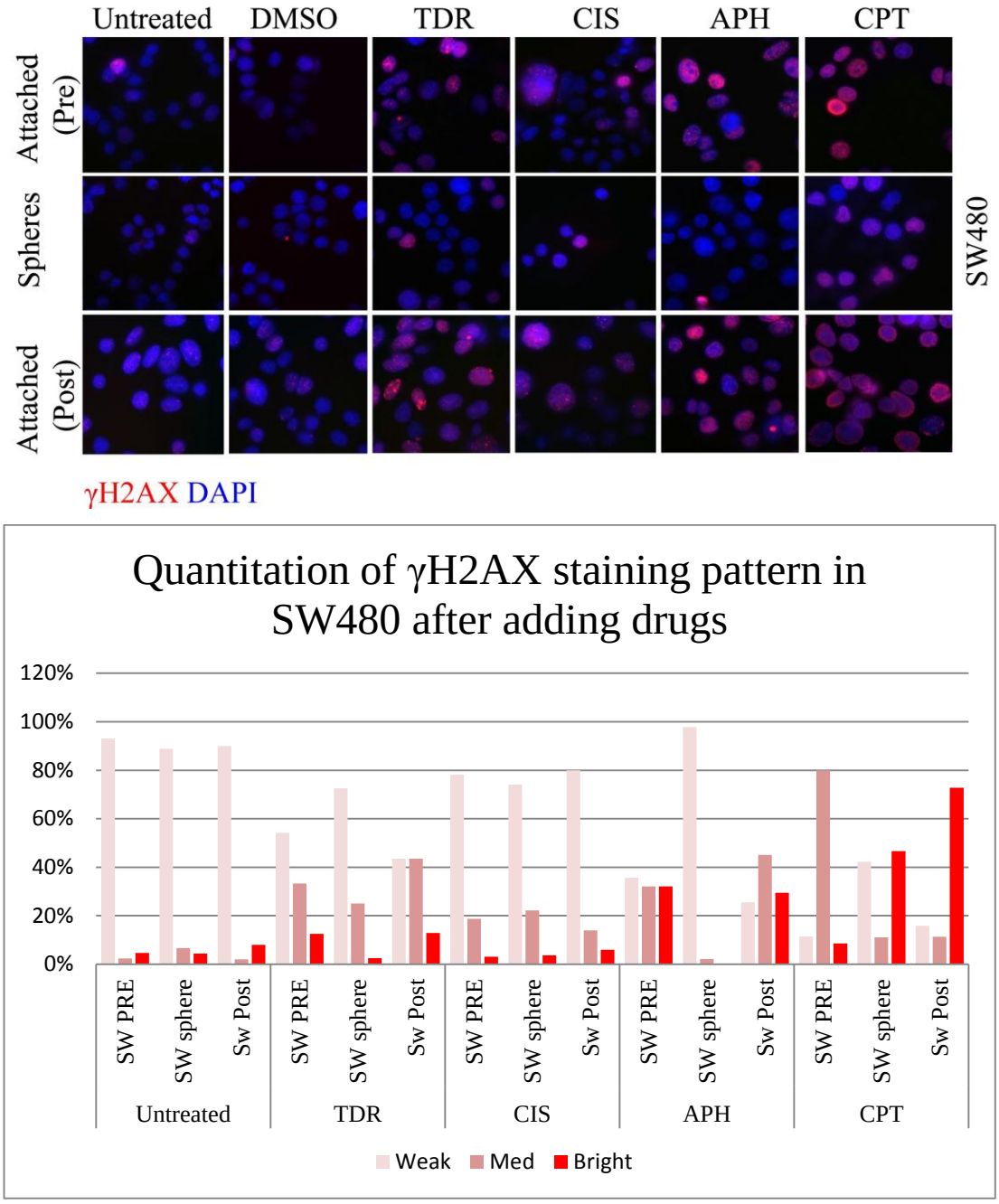

Figure 5:6. γ-H2AX foci are not induced in the spheroids of SW480 in response to replication stress

(Top) Representative images showing nuclear morphology and γ-H2AX staining of SW480 cells and their spheroids following treatment with the indicated chemotherapeutic agents for 24 hours. (Bottom) Quantitation of H2AX staining pattern in SW480 cells following treatment. Percentages are calculated from 50 cells per experiment. The staining pattern is classified into three categories—Bright: Cells that showed a bright pan-nuclear γ-H2AX staining; Med: Cells that showed high numbers of γ-H2AX foci; and Weak: Cells that showed small numbers of dim nuclear γ-H2AX foci or no staining at all. Nuclei were stained with DAPI dye (blue fluorescence). Images were taken using a Zeiss Axioskop 2 fluorescence microscope (65 x objective).

5.1.4 Cell cycle regulation in CSCs following DNA insults

The cellular DNA content of a cell and cell cycle distribution can be obtained rapidly by flow cytometry. We investigated the status of the cell cycle following DNA replication stress in the CSCs and compared their response to their attached cells using a Particle Analysing System (PAS III, Partec).

The fluorescent molecule propidium iodide (PI), which binds to DNA, was added to a suspension of single cells following fixation and RNase treatment. A total of 15000 cells was used for each test. Method details were described earlier in Section 2.1.6. This technique gives the distribution of cells in three clustered phases of the cycle (G1, S and G2). It also allows determination of apoptotic cells, which are characterised by fractional DNA content and defined as sub-G1 populations. Typically, G2 cells show twice the DNA fluorescence intensity when compared to the G1 cell population, while S-phase cells exhibit a range of fluorescence, as they are synthesising DNA (Henderson et al., 2013).

The cell cycle of untreated HCT116 and SW480 cells was initially examined and served as a control sample. Generally, a classical distribution was observed for each phase in both colon cancer cell lines and their spheroids. Treatment of cells with DMSO did not cause any significant cell cycle redistribution, apart from a slight shift toward the right in the parental SW480 cells.

We first examined the effect of TDR on the cell cycle status. Cells were incubated with the drug for 24 hours before collection for analysis of cellular DNA content. TDR slows DNA replication through negative feedback on nucleotide production due to nucleotide pool imbalances. Consistent with this fact, TDR treatment resulted in the accumulation of SW480 cells (attached and spheroids) with a G1/S DNA content characteristic of cells delayed in the S-phase. Treatment of attached HCT116 cells resulted in S phase accumulation as well shifting of some cells to the G2 phase. By contrast, HCT116 spheroid cells appeared to accumulate in the G1 phase (Figure 5.7 and 5.8).

The effect of CIS on the cell cycle status of these cells was also studied, given the importance of this drug in the treatment of CSCs. Cells were subjected to CIS induction for 3 hours, fresh media were then added and the cells were harvested after 21 hours. CIS induced G1/S accumulation in parental SW480 cells and post spheroid

cells, whereas the cell cycle was shifted slightly toward the S phase in spheroid cells. Treatment of attached HCT116 cells (pre and post) with CIS arrested the cell cycle and most cells accumulated in the G2 phase. The HCT116 spheroid cells failed to undergo cell cycle arrest in response to CIS induction, indicating that, rather than trying to deal with DNA damage, these cells instead exhibited a classical distribution of each phase (Figure 5.8).

Cell cycle progression of these cells was also examined following APH treatment. The parental SW480 cells showed a significant decrease in S-phase and G2 phase cells as a major effect, and an enhanced level of cells with a sub-G1 DNA content (characteristic of apoptotic cells) after treatment, when compared to untreated cells, while the cell cycle was shifted toward the S phase in the SW480 spheroid cells. APH treatment also caused accumulation of cells with a G1/S DNA content in the attached HCT116 cells (pre and post) and their spheroids (Figure 5.8).

These paradoxical effects between the parental and spheroid cells in response to replication inhibition were also observed after CPT induction. Treatment of attached SW480 cells (sphere and post) with CPT resulted in arrest of most cells in the G2 phase, whilst the number of cells in the G1 phase was significantly decreased. The definitive cell cycle of the SW480 spheroid cells was lost after treatment. The HCT116 cell cycle histograms showed that the cytotoxicity of CPT arrested the cells mainly in the G2 phase for attached cells and in the S phase in spheroid cells.

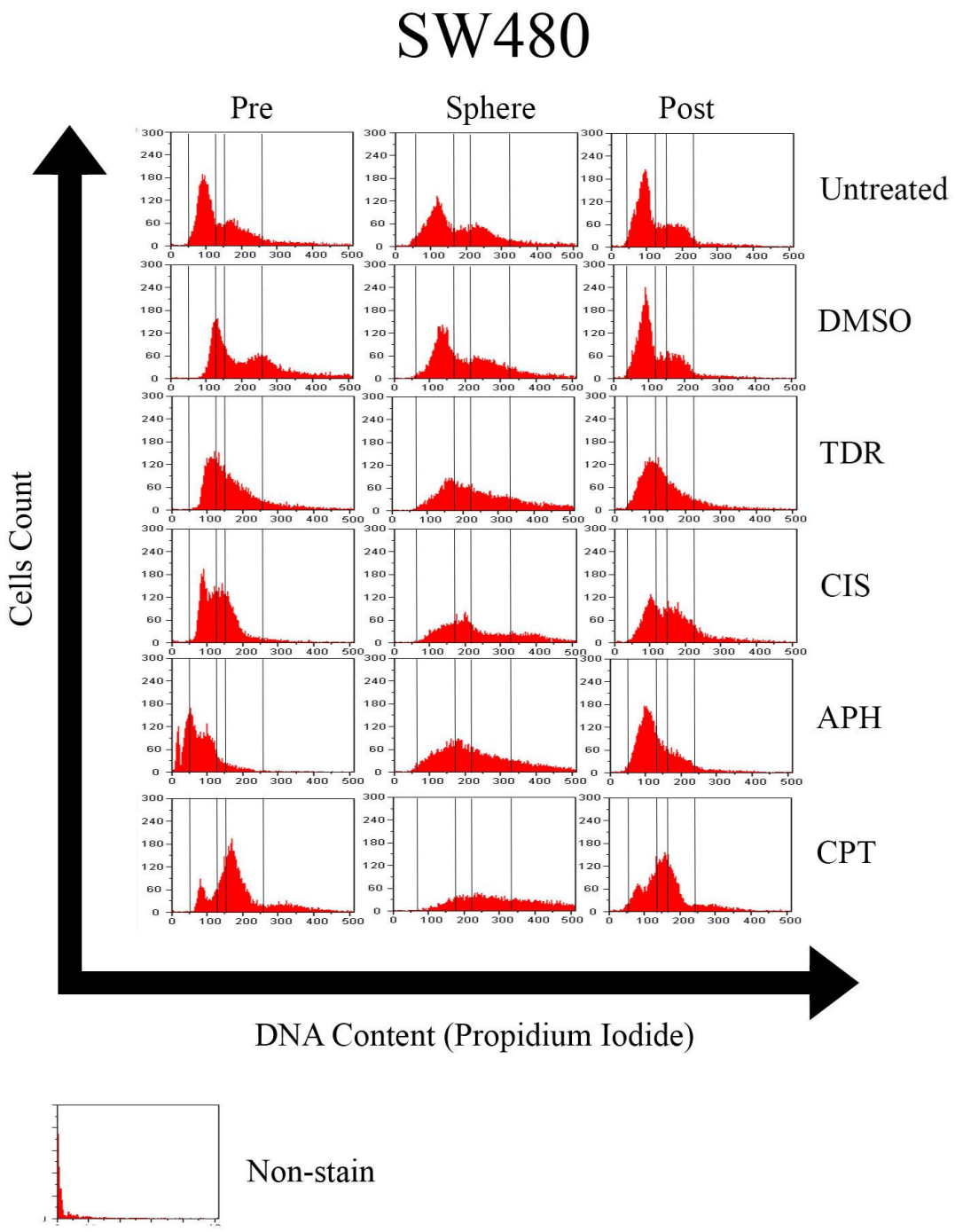

Figure 5:7 DNA content analysis of SW480 sphere cells by flow cytometry and comparison to their parental (Pre) and Post-sphere (post) cells following treatment

Cell cycle profiles for propidium iodide-stained untreated cells and cells treated with indicated agents. Adherent cells were trypsinised, fixed and stained, while spheroids were disrupted with Accutase to obtain single cells, followed by fixation and staining. DNA content histograms were analysed with a Partec PAS-III Flow Cytometer as described in the methods section. The figure also show unstained and untreated (non-stained) cells.

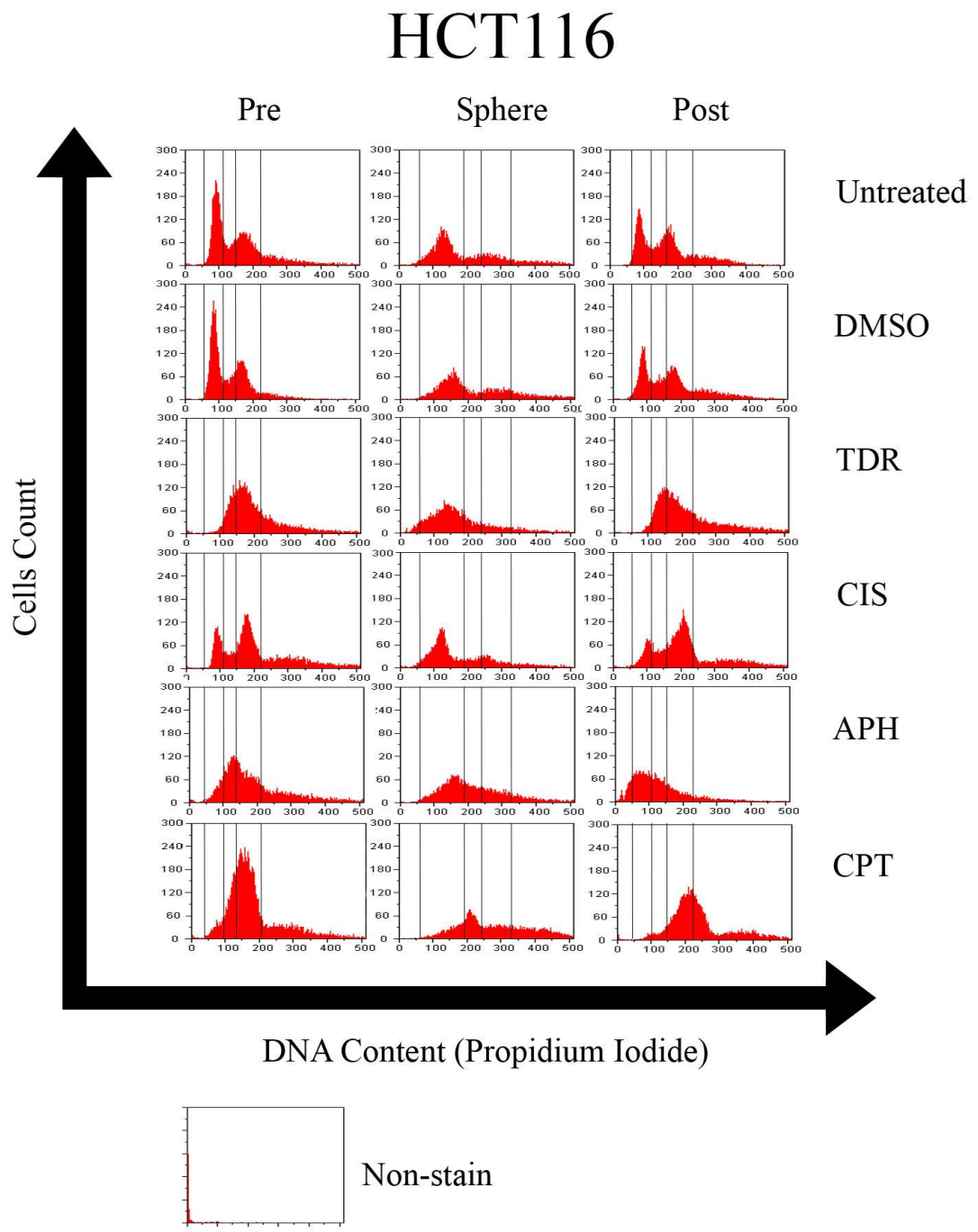

Figure 5:8 DNA content analysis of HCT116 sphere cells by flow cytometry and comparison to their parental (Pre) and Post-sphere (post) cells following treatment

Cell cycle profiles for propidium iodide-stained untreated cells and cells treated with the indicated agents. Adherent cells were trypsinised, fixed and stained, while spheroids were disrupted with Accutase to obtain single cells, followed by fixation and staining. DNA content histograms were analysed with a Partec PAS-III Flow Cytometer as described in the methods section. The figure also shows unstained and untreated (non-stained) cells.

5.2 Discussion

Deregulation of the cell cycle is one of the main hallmarks of cancer and enhances malignant transformation (Diaz-Moralli et al., 2013). The maintenance of genomic stability in normal stem cells has a fundamental role in preserving entire cell lineages. However, this efficient repair mechanism poses a threat when it works to maintain CSCs after oncogenic transformation.

The contribution of CHK1 in radioresistance of CSCs and in tumour recurrence through preferential checkpoint responses and DNA repair has been reported *in vitro* and *in vivo*. An association was reported between chemoresistance of CSCs from non-small-cell lung cancer (NSCLC) and rapid and sustained CHK1 activation, suggesting CHK1 as a therapeutic target (Bartucci et al., 2011). A brain tumour study also showed that brain cancer stem cells activate the DNA damage checkpoint in response to radiotherapy, indicating a higher DNA repair capacity of these cells (Bao et al., 2006).

In contrast to these previous observations, our results showed a failure in the induction of CHK1 phosphorylation in response to replication stress. This failure was correlated with spheroid formation in the colon cancer cell lines. CSCs appear to behave like ESCs and embryonal carcinoma cells, as demonstrated by the results of Andrews and co-workers (Desmarais et al., 2012). Our findings are also consistent with a recent paper that proposed an innovative strategy for suppression of tumour growth through activation, but not inhibition, of CHK1 under normal growth conditions (Zhang and Hunter, 2014). CHK1 is not the only cell cycle regulator; therefore, DNA replication stress may activate other cell cycle checkpoints in CSCs, such CHK2 and the CDK inhibitor p21, as these are well known to have important complementary roles in the cell cycle machinery (Lossaint et al., 2011). Consequently, no definitive conclusion could be drawn due to lack of comprehensive data regarding the activity of other cell cycle regulators.

The spheroids from SW480 and HCT116 cell lines were examined for their sensitivity to genotoxic stress in order to study the relationship between cell cycle progression and apoptosis. We found no apoptotic response in HCT116 cells and following spheroid formation, whereas treatment with APH (a well-known DNA polymerase α inhibitor) rapidly induced caspase cleavage in the parental SW480 cells. Caspase

activation was consistent with the accumulation of cells with Sub-G1 DNA content, suggesting a resistance mechanism used by CSCs in response to this agent.

Apoptosis and differentiation are required and highly regulated pathways in both ESC and primordial germ cells. A correlation between differentiation and resistance to apoptosis was reported in non-malignant ESC and primordial germ cells and appeared to be maintained when these cells become cancerous, though this relation is not found in all other types of cancers. The caspases, p53 and other cell cycle mediators are suggested to play important roles in the differentiation of ESCs and testicular germ cell tumours (GCTs). This balancing in all likelihood protects the integrity of the genome during development and germ cell formation.

Our results also showed that SW480 spheroids (at late passage) showed an enhanced apoptotic response to CIS in addition to the failure of activation critical S-phase checkpoints. Caspase activation was correlated with reduced intensity of a stem cell marker (OCT4/3). This observation is supported by the fact that DNA lesions caused CIS induce both differentiation and apoptotic programs in embryonal GCTs. The cell fate decision is then regulated by the balance of these mechanisms and the relative robustness of the cells (Abada and Howell, 2014). This also suggests that CSCs are possibly not completely resistant to all drugs and this resistance could be overcome by efficient induction of cell death downstream in the apoptosis pathway. Activation of apoptosis at a higher passage may explain why tumours become difficult to treat at advanced stages. Therefore, further investigations using alternative genotoxic substances at different concentrations and durations could be very informative for studying resistance in CSCs.

We also examined the levels of DSBs as reflected by γ-H2AX nuclear foci following treatment. We again observed significantly lower levels of DNA damage in spheroid cells than in attached cells. Previous studies have shown reductions in γ-H2AX foci in breast cancer stem cells isolated from mice ($Thy1^+$ $CD24^+$ Lin2 cells) when compared to non-tumorigenic cells (NTCs) (Diehn et al., 2009). The authors of this previous study suggested that the lower level of DSBs observed in this phenotype was linked to the decreased level of reactive oxygen species (ROS), which is also a characteristic of normal tissue stem cells. A lower rate of γ-H2AX induction was also reported in human CSCs from breast and pancreatic cancers (Al-Assar et al., 2009; Brunner et al., 2012).

The analysis of cell cycle distribution was performed by a classical method using flow cytometry. Sphere formation was associated with different cell cycle distributions in response to DNA damaging agents. Compared to the untreated control cells, CIS treatment increased the numbers of HCT116 cells in the G2 phase, consistent with the findings of a previous study (Desmarais et al., 2012). In contrast, spheroid cells treated with CIS showed a typical cell cycle distribution. This may suggest that CSCs escape G2 arrest and cell cycle checkpoint through a specific mechanism or they have a greater capacity to recover from the damage because the treatments were present in the culture for 3 hours. A similar effect was observed after treatment with CPT, which is a powerful inhibitor of topoisomerase I. Both cell lines were arrested in the G2 phase, but their spheroids were not.

In conclusion, we analysed cell cycle regulation of CSCs following DNA replication stress. We demonstrated that transformation of colorectal cancer cells from attached cultures to spheroids changed their response to DNA damage, suggesting a biological role for differential control of genome stability in these cells. Given these findings, CSCs exposed to genotoxic stress would be expected to show greater survival compared to the other cancer cells within the tumour. The fact that this is reversible indicate that CSCs could be modulated in situ to revert to non-stem-like state, thus opening up a therapeutic opportunity.

Chapter 6

Results

Chapter 6. DNA Damage Responses in Human induced pluripotent stem cells

6.1 Introduction

6.1.1 Pluripotent Stem cells

Stem cells have a remarkable potential to give rise to different types of cells with a wide range of functional capacities. According to their level of developmental versatility, they are classified into different types of stem cells: multipotent, totipotent and pluripotent. A pluripotent stem cell is one that can develop into a complete organism, producing every cell type within that organism (Robinton and Daley, 2012). The concept of cell pluripotency was first described by Eduard Driesch in 1891, when he succeeded in separating two cells of a sea urchin blastocyst demonstrating their ability to independently form identical twins. Embryonic stem cells (ESCs), which are derived from the inner mass of the early blastocysts, are naturally pluripotent. The first successful derivation of ESCs from human blastocysts, performed by Thomson and his colleagues in 1998, has sparked a moral debate in the scientific community and beyond. Although ESCs have short lives in the embryo *in vivo*, these cells can be grown indefinitely in culture and maintained in an undifferentiated state in the presence of specialised inhibitory factors such as leukaemia inhibitory factor (LIF)(Tamm et al., 2011).

ESCs have played a vital role in many fields of clinical and biological research over the last two decades. Mouse knockout technology has provided an effective tool for the investigation of gene function and regulation *in vivo*. Currently, more than 17,400 mutant mouse ESC clones have been generated utilising gene targeting and high-throughput gene trapping tools (Bradley et al., 2012). ESCs can also be used to study embryo development *in vitro*, without the need to harvest peri-implantation embryos, and are useful for the study of basic events that regulate the earliest stages of lineage specification such as cardiogenesis in ESCs (Van Vliet et al., 2012). The ability to generate heart cells *in vitro* and transplant them into a patient may offer a novel treatment for heart failure (Mignone et al., 2010). The same principle may provide therapeutic strategies for other diseases such as Parkinson's disease, spinal cord injuries and cancer (Takahashi and Yamanaka, 2013).

6.1.2 Reprogramming somatic cells into induced pluripotent stem cells (iPSCs)

The study and isolation of ESCs have presented many challenges, but great advances are being made in understanding the regulation and the maintenance of pluripotency for ESCs. One breakthrough discovery was that of Takahashi and Yamanaka, who demonstrated the successful derivation of induced pluripotent stem cells (iPSCs) from somatic cells of a mouse by using retroviral vectors to enforce expression of four embryonic transcription factors. These factors are OCT4, SOX2, KLF4 and c-MYC, which are also called Yamanaka factors (Robinton and Daley, 2012; Takahashi and Yamanaka, 2006). This discovery inspired scientists and was followed by several successful reprogramming attempts with cells of other organisms, including human fibroblasts, and then with a wide range of other human cell types. The pioneering technology of iPS made reprogramming much easier than it had been with early reprogramming technologies such as somatic cell nuclear transfer (SCNT). This technology also avoided the ethical issues such as the foetus' destruction that was necessary for harvesting ESCs. Importantly, the generation of patient-specific iPSCs could be used to improve and test new drugs *in vitro* (Bellin et al., 2012).

6.1.3 Generation of non-integration iPSCs

This original iPSC induction system used viral vectors, including retroviruses and lentiviruses, which provided high reprogramming efficiency. However, the genome may be mutated by integrating the transcription factors (extra copy), thereby raising concerns about safety (Zhou and Zeng, 2013). Additionally, the insertion of tumorigenic genes like c-Myc has a high risk of tumour formation, which hinders the therapeutic usefulness of the iPSC system (Lin and Ying, 2013). Consequently, reprogramming systems that use viral vectors are considered too risky to be utilised in clinical research and regenerative medicine.

Several subsequent studies introduced different successful and safer approaches for generating transgene-free iPSCs, which include the use of *piggyback* (PB) transposition, plasmids, episomal vectors, non-integrating adenoviruses and Sendai virus (Malik and Rao, 2013) (Table 6.1). However, the overall reprogramming efficiency is decreased and a longer activation of transcriptional factors is required to

achieve full reprogramming. Hence, efficient production of non-integrated iPSCs by new methods may promote their clinical use.

Recent studies have identified several reprogramming approaches using proteins, RNAs and small-molecule compounds to generate safe iPSCs. For example, Zhou et al reported the production of protein-iPSCs using recombinant cell-penetrating reprogramming proteins by fusing the C-terminus of the proteins with poly-arginine (Peitz et al., 2014; Zhou et al., 2009). One recent study showed that mouse and human iPSCs can be efficiently produced by microRNA (miRNA) mediated reprogramming, as iPSCs were effectively derived by direct transfection of somatic cells using mature miRNA, without a need for exogenous transcription factors (Anokye-Danso et al., 2011). Hou et al (2013) have also developed an iPS induction method that is performed by a combination of seven small-molecule compounds. Other studies also have reported pluripotency reprogramming using synthetic modified RNAs, which overcome the innate response of viruses (Warren et al., 2010). Unlike methods that use viral systems, these new methods can be utilised to produce safe iPSCs without transgene integration (Feng et al., 2013) (Table 6.1).

Several reports show that ensuring genetic stability plays an important role in maintaining the ESCs and iPSCs. DNA repair pathways also appear to be essential for the reprogramming of human cells when iPSCs are produced. Therefore, the understanding of how cultured pluripotent stem cells maintain the genome stability are highly relevant for their safe clinical applications, at the same time that cellular therapy is a potential for DNA repair deficient patients (Rocha et al., 2013).

Previous work found that human ESCs (hESCs) behave in a unique way that differs from the somatic cell in response to DNA damage due to their remarkable capability of self-renewal and differentiation into different lineages. Therefore, we aimed in this chapter to generate iPSCs from human fibroblast using a non-viral and non-integrating system. We used those cells and their isogenic parental cells to examine their sensitivity and their response to DNA replicative stress induced by replication inhibitors to determine whether these response differ from those observed in isogenic somatic tissues and/or embryonic stem cells.

Table 6.1 Summary of reprogramming approaches for iPSCs production (Feng et al., 2013)

Vector	Genomic integration	Advantages	Disadvantages	year
Retrovirus	Yes	Stability and high efficiency	Mutation and cancer formation	2006
Lentivirus	Yes	Low risk of transgene and high efficiency	High risk of insertional tendencies	2009
Adenovirus	No	Virus-free and efficient	Tend to carry the virus genome	2008
Sendai virus	No	Virus-free and efficient	Tend to carry the virus genome	2009
***piggyback* transposon**	No	Virus-free	A labour-intensive process	2009
Plasmid	No*	Virus-free; non-integrated	Lower efficiency; four rounds of transfection	2010
Episomal vector	No	Virus-free; a single transfection	Lower efficiency	2009
Minicircle vector	No	Virus-free; higher transfection efficiency	Longer ectopic expression	2010
Recombinant Protein	No	Virus-free	Lower efficiency	2009
mRNA	No	Virus-free; high efficiency- non-integrated	Labour-intensive procedures	2011
Small molecule	No	Virus-free	Lower efficiency	2013

6.2 Results

6.2.1 Generation of human iPSCs using non-integrating and virus-free system

In this study, we used modified mRNA (Miltenyi Biotec, #130-097-19) to reprogram human fibroblast to iPSCs. As discussed above, this is the most effective and safest available method despite it being more costly and labour intensive. Human primary newborn foreskin (BJ) fibroblasts were placed on the feeder into a 6-wells plate and these BJ cells served as target cells. The cells were then cultured in Pluriton™ medium and subjected to daily transfection with a master mRNA cocktail, using lipofectamine RNAiMax. B18R recombinant protein carrier-free medium was applied to the cells prior to each transfection to reduce the interferon response of the cells. The mRNA cocktail contained five mRNA reprogramming factors (OCT4, SOX2, KLF4, C-MYC and LIN28). We also included a modified mRNA that encodes the green fluorescent protein (GFP) for monitoring the reprogramming process and ensuring transfection efficiency. The timeline of the experiment is outlined in Figure 6.1. A negative control sample (non-transfected cells) was also included while performing reprogramming experiments.

From day 1 to day 21, the cells underwent daily transfection at the same time that the first transfection was performed. From day 6, Pluriton™ medium was replaced with NuFF-conditioned Pluriton™ Reprogramming Medium. The cellular morphology was monitored regularly and the expression of GFP was assessed. The GFP fluorescence was examined on day 8. Treated cells expressed GFP fluorescence, while the negative control BJ cells exhibited no GFP fluorescence, indicating transfection efficiency. The transfected cells also began to appear in small clusters with a more compacted morphology compared to the morphology before starting transfection, as shown in Figure 6.2.

The colonies were then allowed to expand for a few days in NuFF-conditioned Pluriton™ Reprogramming Medium with B18R. The expression of cell surface pluripotency marker TRA-1-60 on live transfected cells was examined using Stain Alive™ TRA-1-60 antibody (Stemgent, #09-0068). Cells were expressing TRA-1-60 on day 17, indicating the pluripotency transformation (Figure 6.3).

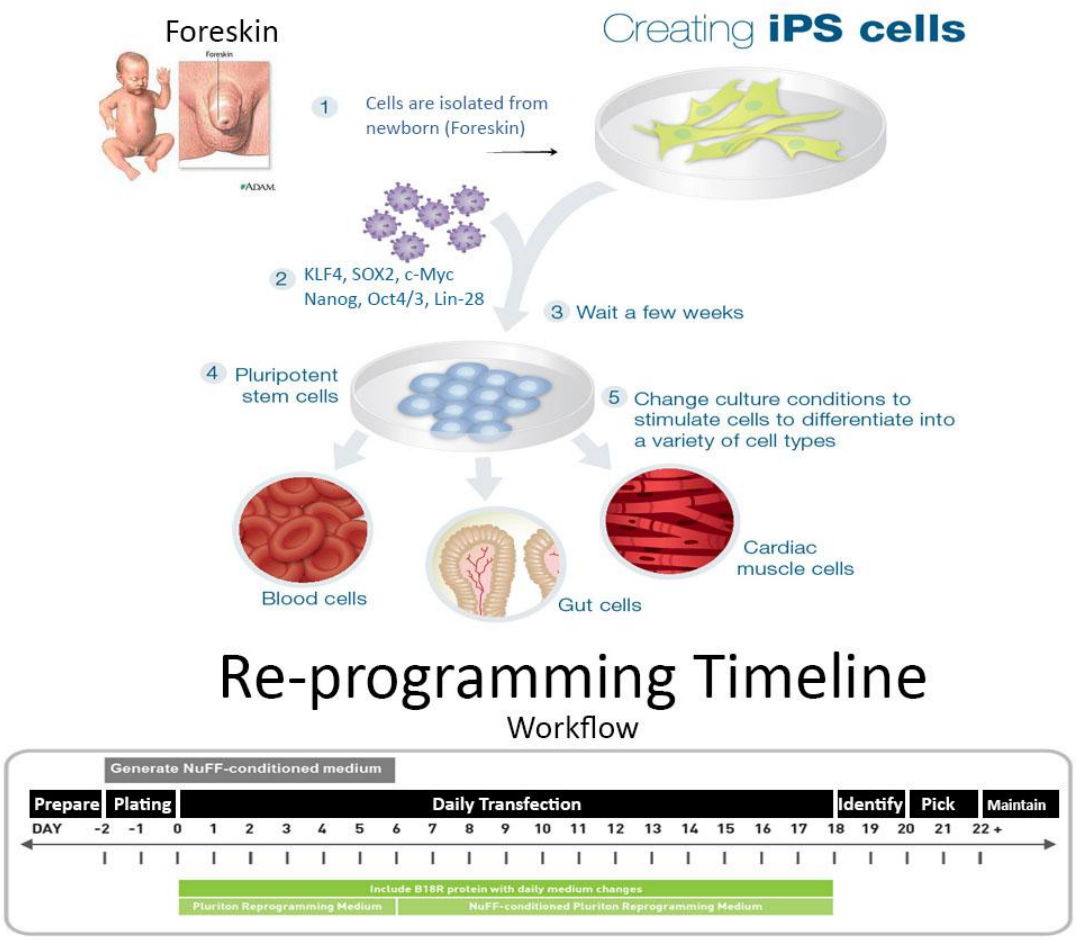

Figure 6:1 Production of iPSCs using modified mRNA factors

This diagram summarises the method of production of iPSCs. They were generated from foreskin cells of a newborn (BJ cells). Following isolation, BJ cells were plated *in vitro* and transfected with an mRNA cocktail, which is designed by Stemgent. It contains mRNA encoding OCT4, KLF4, SOX2, c-MYC and LIN-28, which is associated with pluripotency. As pluripotent cells, iPSCs have the potential to differentiate into all cell types such as adipocytes, cardiomyocytes, hematopoietic and neuronal cells. The image is adapted from 'The Genetic Science Learning Centre at The University of Utah' with some modifications. The bottom box is the timeline showing the main six steps for the mRNA reprogramming system and indicating the timing of essential events. The protocol was described in detail in the methods section 2.1.8.

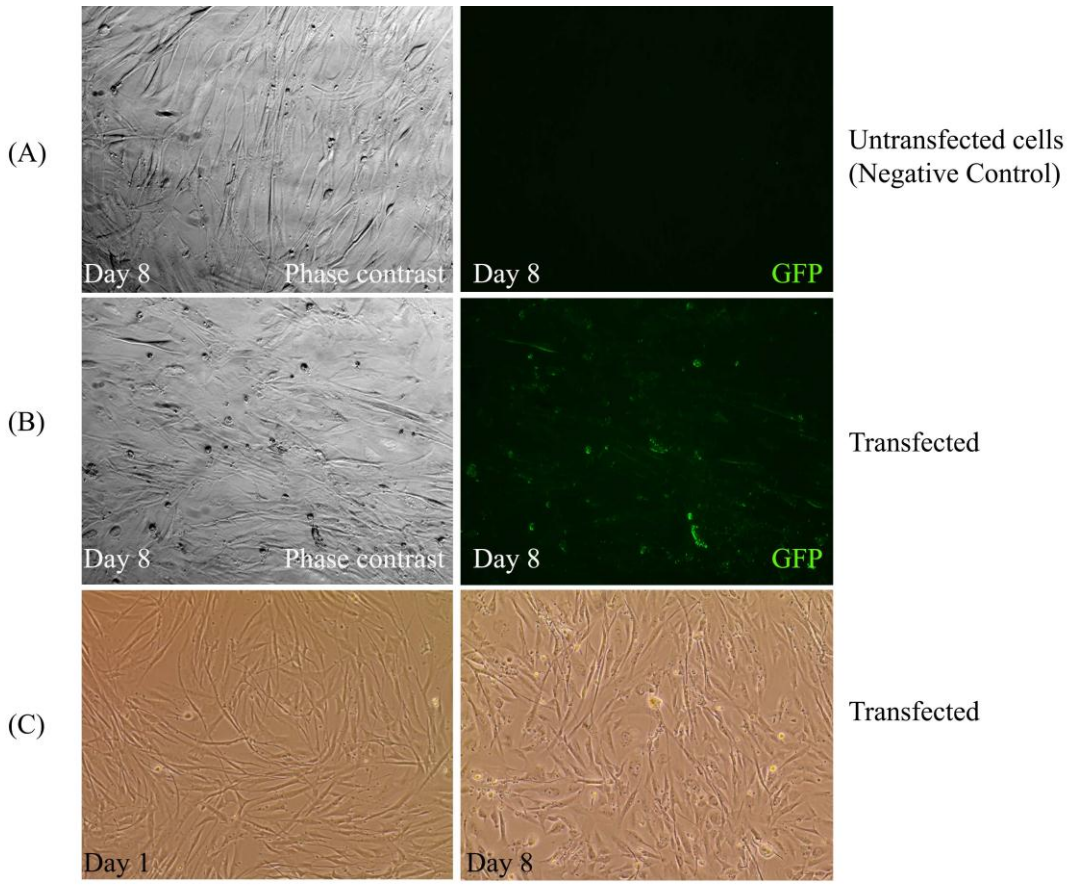

Figure 6:2 Monitoring GFP expression and morphology changes

The GFP fluorescence was observed on day 8 of daily transfection, while the negative control (untransfected) BJ cells exhibited no GFP fluorescence. A nuclear GFP marker was used to monitor transfection efficiency. Images were taken using an Eclipse inverted microscope (20x objective). (C) Transfected cells began to appear in small clusters with a more compacted morphology relative to the morphology of the first day. Images were captured by Evos™ XL Core using a 20x objective lens.

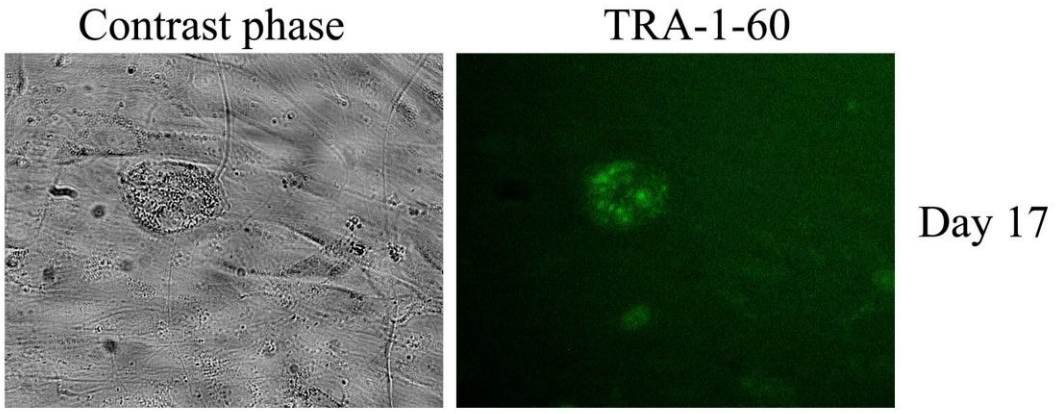

Figure 6:3 Immunofluorescence analysis of TRA-1-60 on live reprogrammed cells

The phase contrast shows the live transfected cells in culture and the same field of cells that were stained with StainAlive TRA-1-60 Antibody (DyLight 488). Images were taken using Eclipse inverted microscope (20x objective).

6.2.2 Transformation of reprogrammed iPSCs

Following the completion of mRNA transfection series, several distinct colonies appeared with distinguished morphological change (Figure 6.4). These colonies displayed a flat and tightly packed morphology, and the cells had a high nucleus/cytoplasm ratio and prominent nucleoli. Subsequently, other new colonies started appearing periodically over the next four days. To pick reprogrammed cells, priority was given to the colonies that express the pluripotency marker. Colonies that expressed TRA-1-60 and displayed ESCs morphology and distinguished edges were divided into four parts. Each part was transferred into an individual well of a 24-wells plate, which was plated with Mouse embryo fibroblast (MEF) feeder layer one day before picking the colony. Furthermore, these cells were passaged every 4 to 7 days in culture. The iPSCs used in this study were obtained from colony number 7, which we thus refer to as Bi7ZH.

Cells were expanded in Pluriton™ Reprogramming Medium for three passages without B18R. Next, cells were stained with Alkaline Phosphatase Live Stain (Molecular Probes®, #A14353), which stains only undifferentiated iPSCs. Cells expressed TRA-1-60, as shown in Figure 6.5, indicating successful reprogramming. Phenotypic assessment was also performed using the Alkaline Phosphatase (AP) staining kit (Stemgent, #00-0009). Cells were fixed and then incubated with 0.05% Tween 20/DPBS at room temperature. The stained cells appeared red or pink, whereas the surrounding cells were colourless (Figure 6.6).

6.2.3 Characterization of iPSCs after extended culture

iPSCs were then expanded and switched to a feeder-free system using Nutristem™ XF/FF culture medium. Culture plates were coated with Matrigel™ hESC-Qualified matrix (BD, # 354277) according to the manufacturer's instructions. Afterward, further characterisation for pluripotency marker was performed. iPSCs were grown in a 24-wells plate for immunostaining experiments. Cells were then fixed in 4% PFA and immunostained, as described early in Section 2.1.3. Immunostaining analyses of typical ESCs markers demonstrate they are positive for OCT4, and for ESC-specific surface markers TRA-1–60 and SSEA-4 (Figure 6.7).

RT-PCR analysis was performed to validate the expression of several pluripotency genes. The iPSCs expressed *OCT4*, *SOX2* and *NANOG*, while the parental fibroblast showed no bands of these genes. Similarly, analysis of qRT-PCR for *OCT4* expression showed a significant increase in iPSCs cells. For both experiments, commercial RNA were used as a positive and negative control for the expression of stem cells markers (Figure 6.8). We further characterised OCT4 protein levels of iPSCs that grew on the feeder-free system for several passages, as shown by Western blot analysis (Figure 6.8). Human embryonal carcinoma cell line NTera2 (NT2) was used as positive control.

(A)

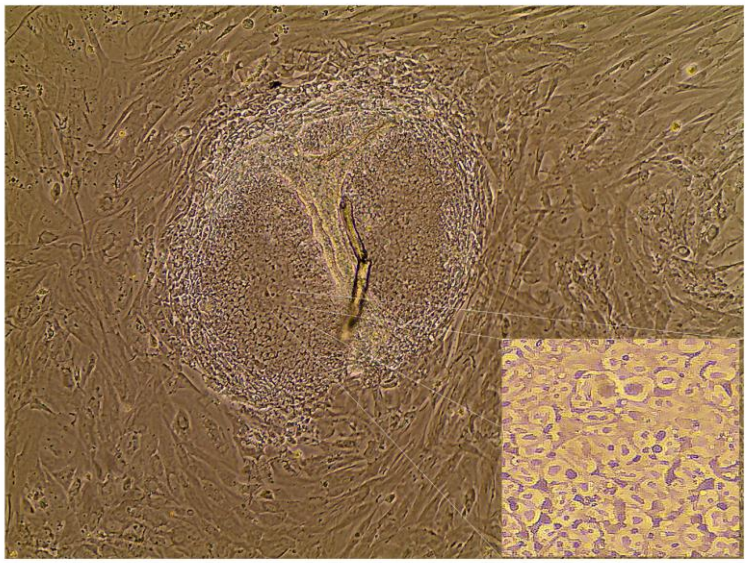

(B)

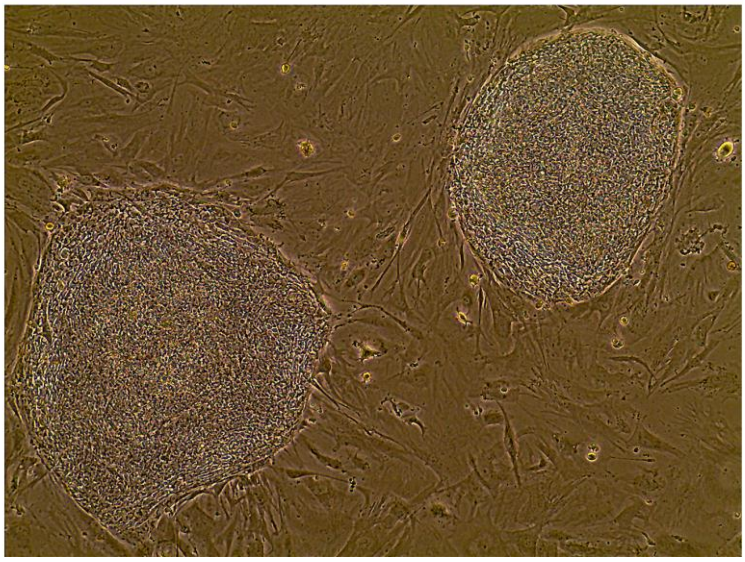

Figure 6:4 Colony formation of human iPSCs

ES-like colonies were observed 20 days after daily transfection of mRAN cocktail (A). A high-magnification image of reprogrammed BJ cells shows a high nucleus/cytoplasm ratio and prominent nucleoli (corner). Cells also maintained similar morphology after several passages (B). Images were captured by Evos™ XL Core using a 5x objective lens.

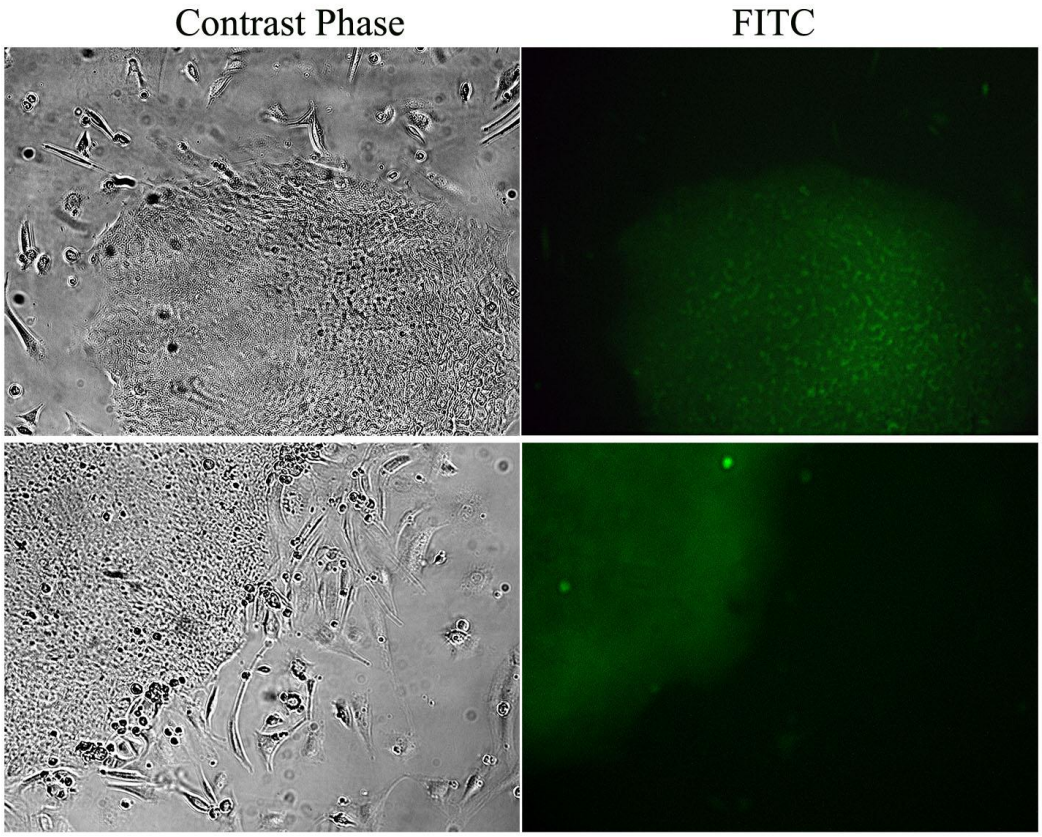

Figure 6:5 Analysis of Alkaline Phosphatase (AP) live staining of iPSCs

The images show that the iPSCs cells were stained with AP live stain for pluripotency evaluation. The phase contrast shows the live iPSCs and the same field of cells that were stained with (AP) Live Staining. The images were taken using Eclipse inverted microscope (20x objective).

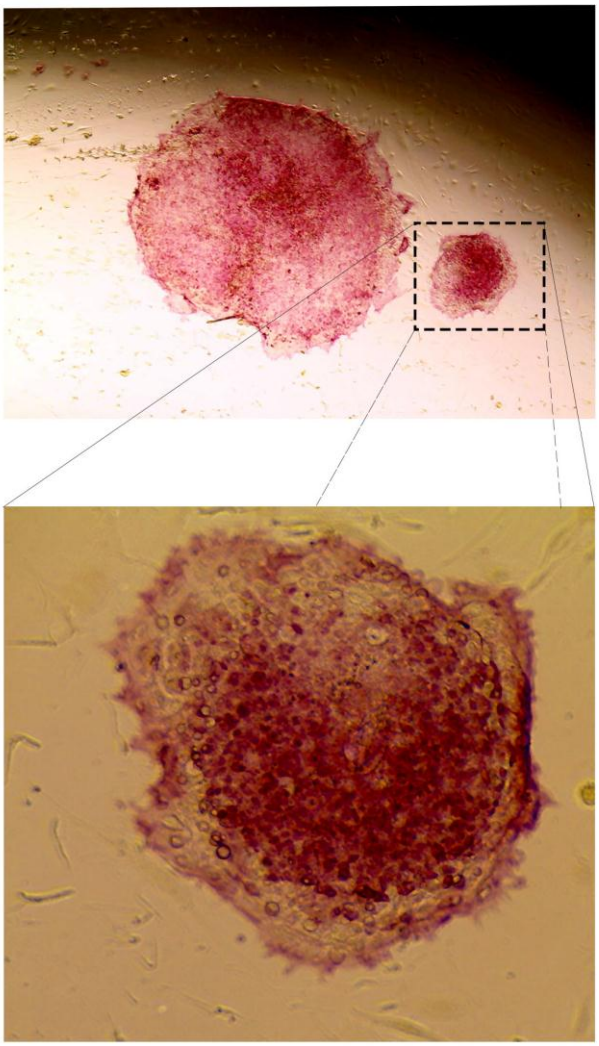

Figure 6:6 Alkaline phosphatase staining of fixed iPSCs colony

The images show that the iPSCs colony were fixed then stained with AP staining using the Stemgent kit. The stained cells appeared red or pink, whereas the surrounding cells (feeder cells) were colourless, indicating an undifferentiated state of these cells. The image was taken under a phase contrast microscope (5x and 10x objective).

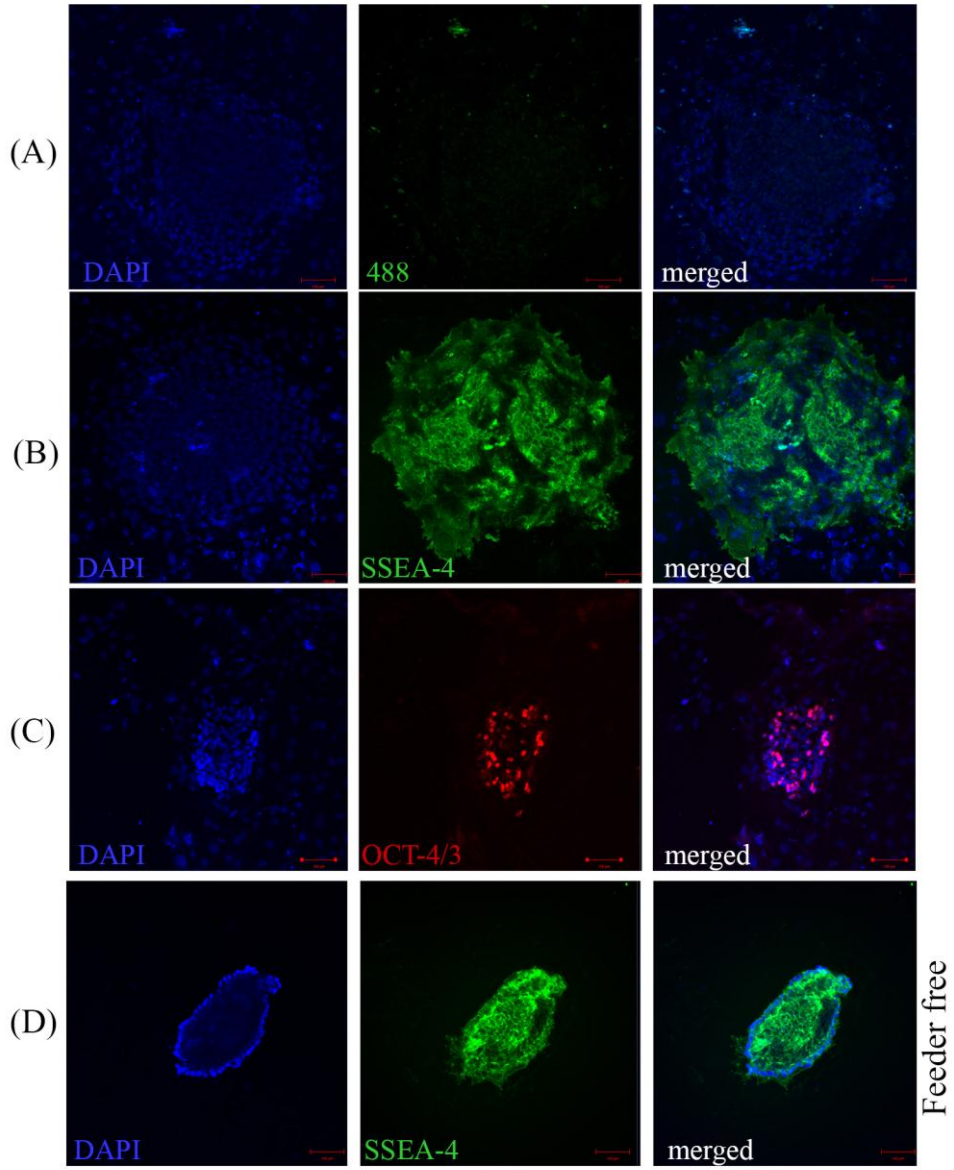

Figure 6:7. Immunostaining analysis of pluripotency and surface markers for iPSCs

(A) iPSCs incubated with Alexa Fluor® 488 Conjugate in the absence of primary antibody incubation, which served as the negative control. (B) SSEA-4 is strongly detected on iPSCs, localising mostly on the cell membrane and cytoplasm (not in the nucleus). (C) OCT4 stained cells were labelled with Alexa Fluor® 568 (red). OCT4 localise to the nucleus. Staining is not observed on the feeder cells indicating specificity for iPSCs. (D) SSEA-4 stained iPSCs after transferring them onto a feeder-free system with NutriStem medium. Nuclei stained with DAPI dye (blue fluorescence). The images were produced using a confocal microscope. Scale bars, 100 μm.

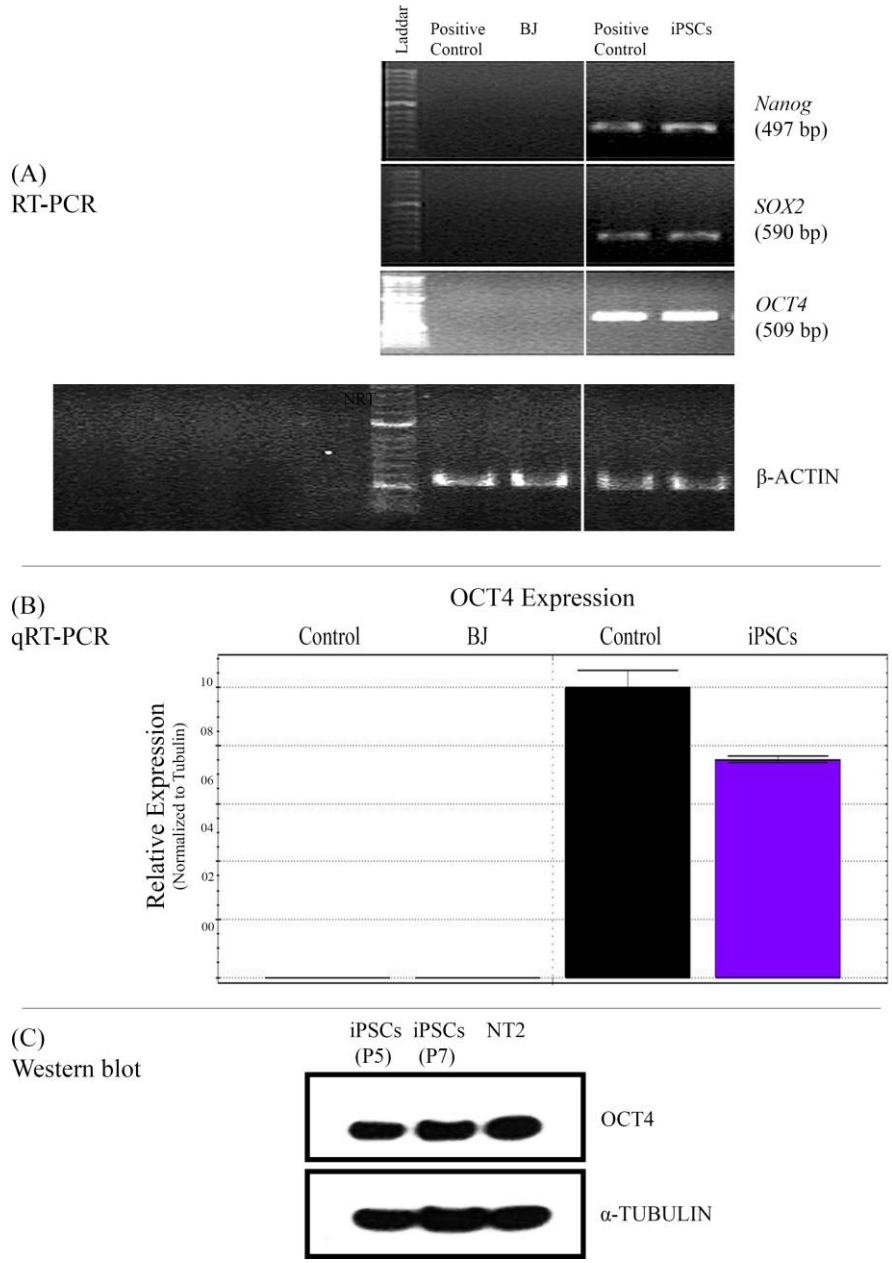

Figure 6:8 Expression of pluripotency markers (protein and mRNA levels) in iPSCs

(A) Agarose gels showing the expression of *OCT4*, *SOX2* and *NANOG* in iPSCs compared to their parental BJ cells. cDNA was made from the total RNA extracted from the BJ and iPSCs. Commercial RNA was used as a reference (positive control). iPSCs show the bands of *OCT4*, *SOX2* and *NANOG* expression, which was not observed on the BJ cells. β-Actine was used as a positive control for the cDNA, as shown in the bottom panel. (B) SYBR® Green-based real time RT-PCR for OCT4 in iPSCs compared to BJ cells. The bar chart shows the gene expression level normalised to α-Tubulin expression. Tests were performed using the Bio-RAD CFX Manager. The error bars indicate standard error for three repeats. (C) Western blot analysis showing OCT4 levels in the whole protein lysates isolated from iPSCs at passages 5 and 7. Human embryonal carcinoma cell line NTera2 (NT2) was used as positive control. Cells were grown in Matrigel (feeder-free system). Antibodies against α-Tubulin were tested to check the equality of protein amount in each well.

6.2.4 DNA Damage Responses in Human iPSCs

During studies into the cell cycle regulation of SW480/HCT116 in a stem-like state (Chapter 4 and 5), it was noted that these cells behave differentially in response to DNA replication stress compared to their parental cells. Here, we extend our investigation to study iPSCs sensitivity to genotoxic agents compared to their isogenic parental BJ cells. We also intended to test whether the induction of iPSCs differentiation would affect the sensitivity of these cells. Therefore, iPSCs cells were first differentiated using 10 mM of Retinoic Acid (RA) for 7 days. The qRT-PCR results showed a significant level of reduction in *OCT4* in RA treated cells indicating the differentiation efficiency, as shown in Figure 6.9. The experiments of this chapter have not yet been completed due to time limitations; thus, we will present below our progress to date.

We compared the effect of DNA replication stress on parental BJ cells, iPSCs and differentiated iPSCs cells through the evaluation of caspase activity following treatment. Cells in three states were grown in 6-well plates for Western blot analysis and in 24-well plates for immunofluorescent staining. Cells were exposed to 200 μM of TDR and 15 μM of CIS. Following three hours of treatment, a flask of CIS treatment was replaced with fresh media, and 24 hours later, the cells were harvested for analysis. The Western blot results show that caspase induction was triggered following iPSCs treatment, whilst it was not induced in the BJ and differentiated cells (Figure 6.10). In addition, detachment of iPSCs from the surface was observed in a cell culture dish following treatment. Caspase induction was also confirmed by immunostaining results, as demonstrated in Figure 6.10. Taken together, these data indicate that DNA damage response of iPSCs differs from responses in somatic cells.

We also examined the activation of other cell cycle regulators by Western blot following treatment. Phosphorylation of CHK1 at ser345 (P-Ckh1) was detected following TDR treatment, while it was not detected in cells treated with CIS. Proliferation marker PCNA was stably expressed without detectable change. Activity of Cdk2 is suppressed in response to DNA damage in somatic cells by increased inhibitory phosphorylation at Thr14/Tyr15. The study of mouse ESCs has shown that the activity of Cdk2 was not affected by DNA damage (Koledova et al., 2010). Here Cdk2 phosphorylation at Tyr15 remained unchanged following treatment in iPSCs.

Phosphorylation of histone H3 on Ser-10 has an important role during apoptosis and is linked with mitotic chromatin condensation (Park and Kim, 2012). Our results demonstrated that histone H3 Phosphorylation is induced after treatment with TDR and the phosphorylation level was more intense when treated with CIS (Figure 6.11).

To determine whether the treatment triggered differentiation, the expression of *OCT4* was assessed by qRT-PCR. As shown in Figure 6.12, DNA damage decreased the expression of *OCT4* indicating the possibility of differentiation activity and iPSCs possible loss of stem cell features.

We next investigated γ-H2AX activation on iPSCs and BJ cells. iPSCs failed to induce γH2AX foci in response to TDR and CIS treatment. In contrast, a number of BJ cells formed γH2AX foci after treatment comparable to that of the untreated cells (Figure 6.13).

During studies of CSCs, it was noted that BLM protein levels became significantly reduced. We thus investigated whether iPSCs share a similar reduction behaviour compared to their parental BJ cells. Noticeably, iPSCs exhibited significant elevation on BLM protein levels. *BLM* expression also increased, as observed in the qRT-PCR results. However, DNA damaging of iPSCs resulted in decreased BLM levels and expression, more clearly following CIS induction (Figure 6.14). We next analysed the cell cycle profile of BJ and iPSCs. DNA content histograms showed a shortened G1 cell cycle phase for iPSCs, which is the phenomenon of mammalian ESCs. The experiments were performed using CyFlow® Cube 8 flow cytometry (Figure 6.15).

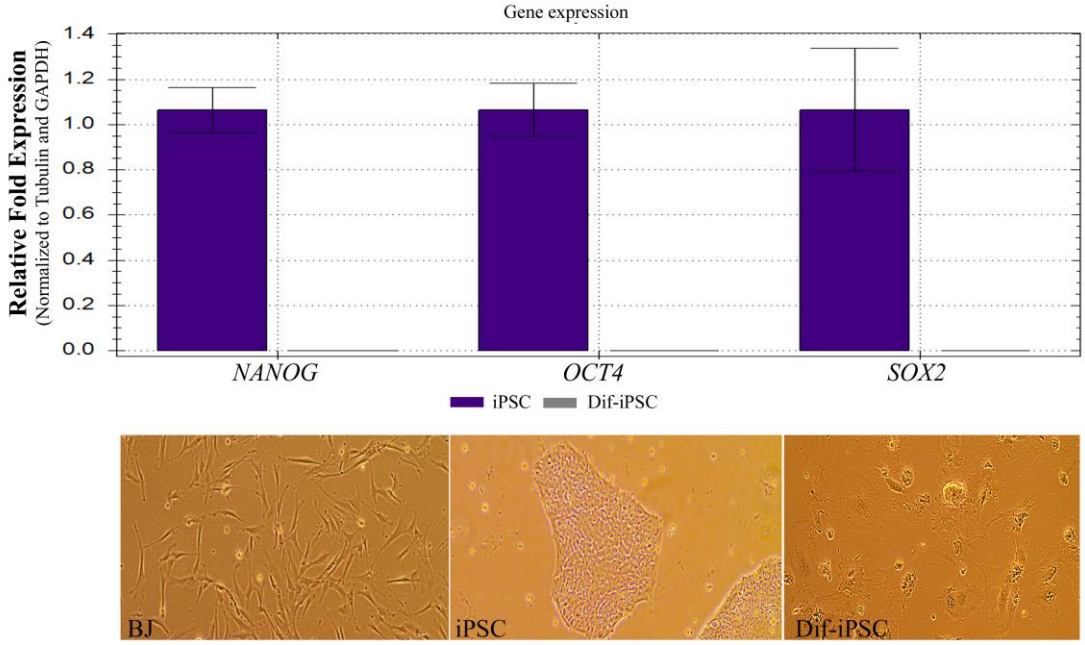

Figure 6:9 Direct differentiation of iPSCs using Retinoic Acid

(Top) SYBR® Green-based real time RT-PCR for pluripotency marker in differentiated iPSCs compared to undifferentiated iPSCs. The bar chart shows the gene expression level that normalised to α-Tubulin and GAPDH expression. Tests were performed using the Bio-RAD CFX Manager. The error bars indicate standard error for three repeats. Photos show the cell morphology of iPSCs before their re-programming and after the differentiation (Dif). Photographs were taken using an Eclipse inverted microscope with a 5x objective lens.

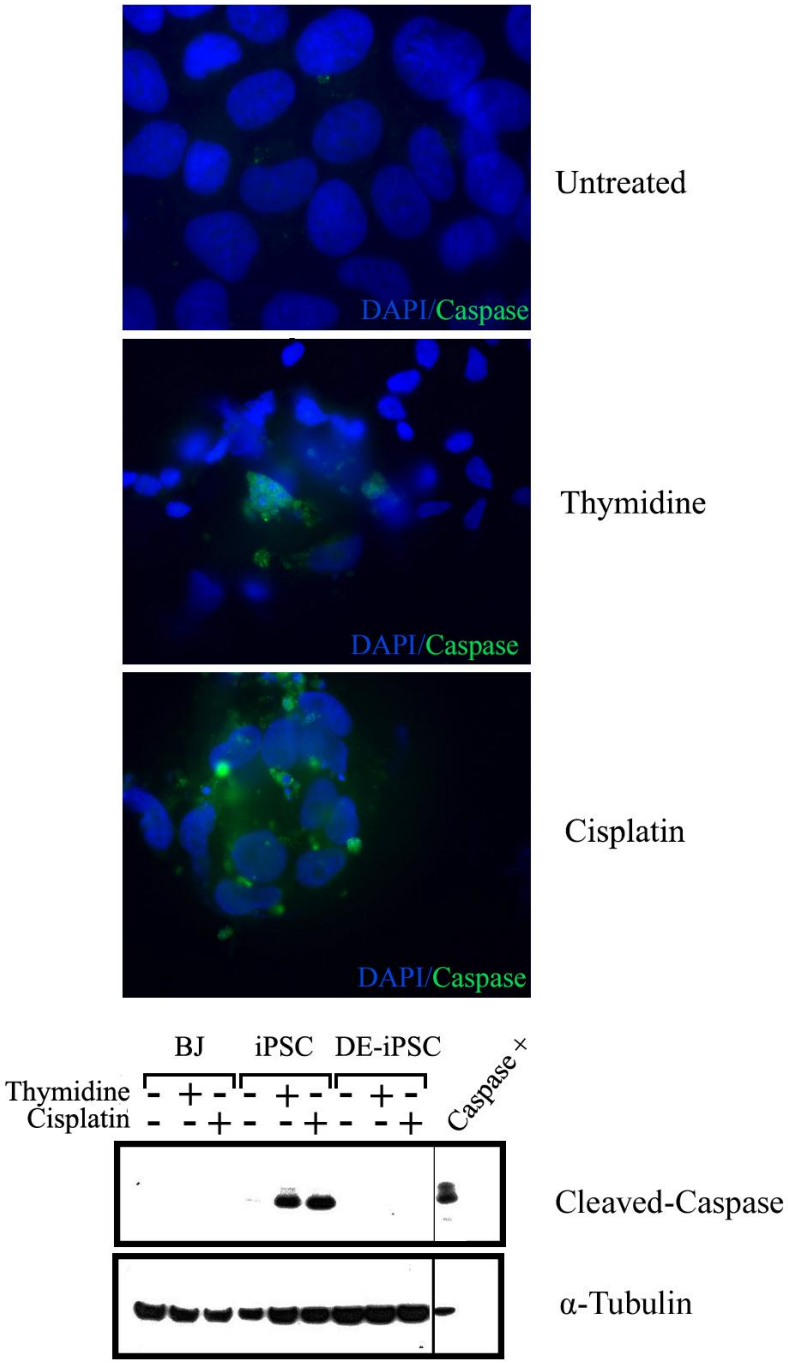

Figure 6:10 iPSCs commit to apoptosis in response to DNA Replication Stress

iPSCs were stained with active caspase-3 then labelled with Alexa Fluor® 488 as a secondary antibody (green) and counterstained with DAPI (blue). Western blot analysis shows activation of caspase in iPSCs following treatment. α-Tubulin is tested for loading control. Cytochrome c treated Jurkat cells extracts serve as a positive control for caspase cleavage (Caspase+). Abbreviations: TDR, Thymidine; CIS, Cisplatin

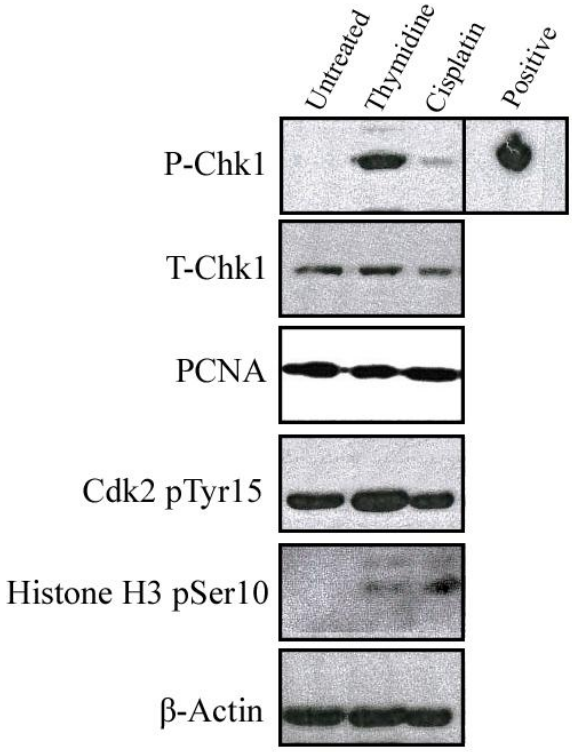

Figure 6:11 Western blot analysis of cell cycle regulation proteins in iPSCs cells following treatment

iPSCs cells were treated with 2 mM thymidine and 15 μM of cisplatin for 24 h. Total cell extracts from 293 cells, treated with UV light, serve as a positive control for P-CHK1. β-Actine is tested for loading control. Abbreviations: CHK1, checkpoint kinase 1; P-CHK1 (Ser345), phosphorylated CHK1 at serine 345; PCNA, Proliferating cell nuclear antigen; cdk2 pTyr15, Phosphorylation of Cyclin-dependent kinase 2 at Tyr15.

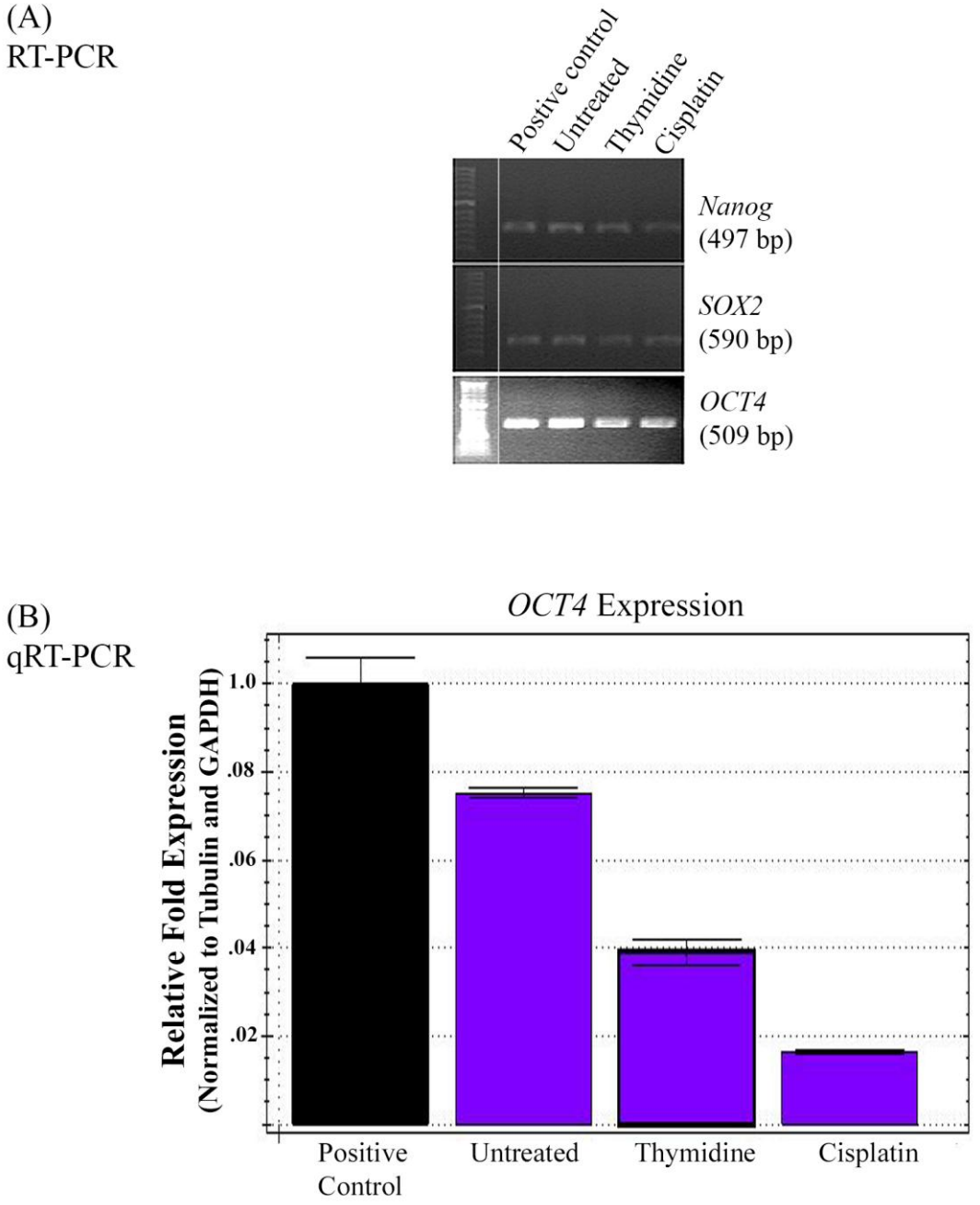

Figure 6:12 RT-PCR and qRT-PCR analysis of stem cells marker in iPSCs following treatment

(A) Agarose gels showing the expression of OCT4, SOX2 and NANOG in iPSCs following treatment with indicated drugs. Commercial RNA used as a reference (positive control) for stem cells marker. (B) SYBR® Green-based real time RT-PCR for OCT4 in treated iPSCs compared to untreated cells. The bar chart shows the gene expression level that normalised to α-Tubulin and GAPDH expression. Tests were performed using the Bio-RAD CFX Manager. The error bars indicate standard error for three repeats. Commercial RNA was used as a reference (positive control) for OCT4.

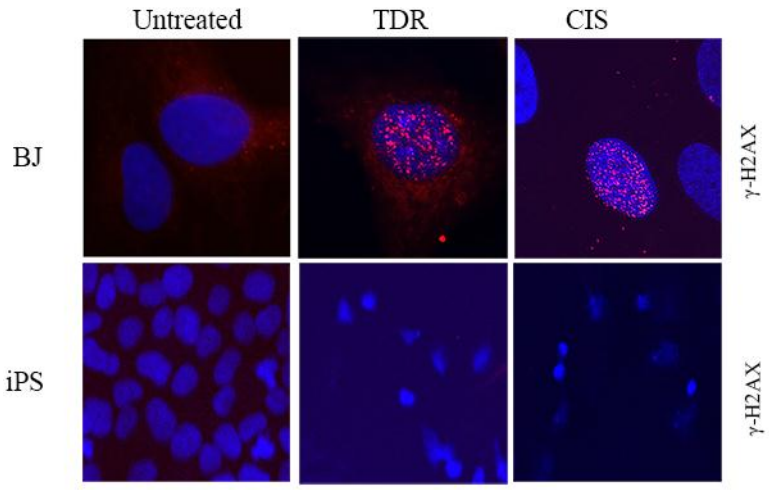

Figure 6:13 γH2AX foci are not induced in human iPSCs in response to replication stress

Representative images of γH2AX foci induced in BJ (65x objective) in iPSCs (20x objective) treated with 200 µlM TDR for 24 hours or 15 µlM with CIS for 24 hours. Nuclei were stained with DAPI dye (blue fluorescence). Images were produced using a confocal microscope.

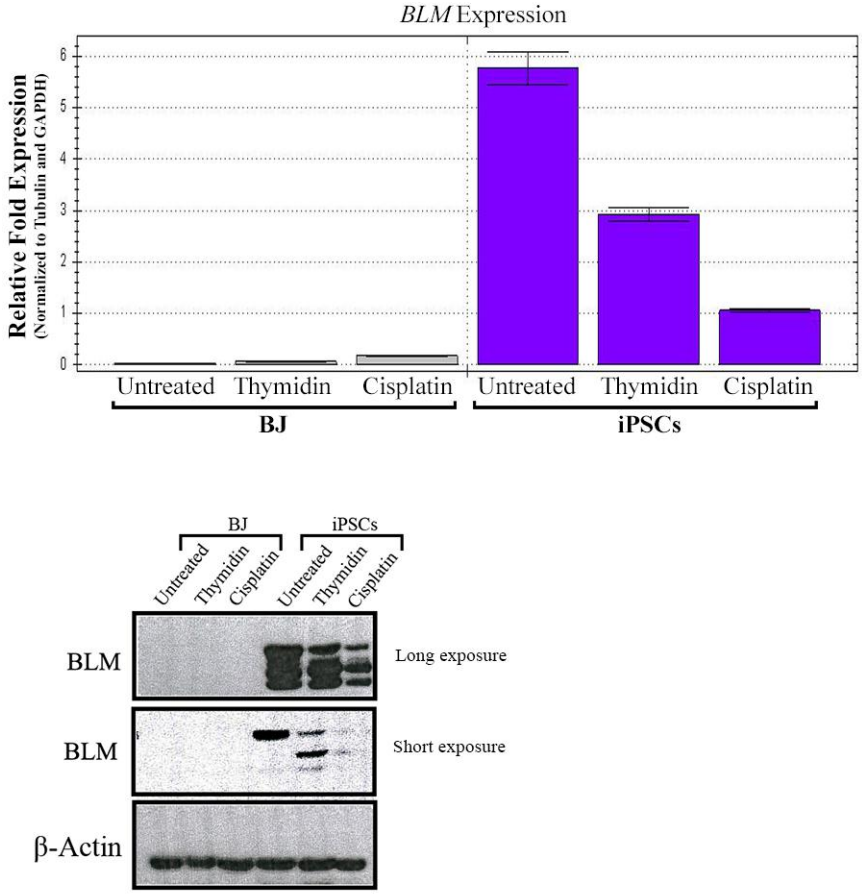

Figure 6:14 qRT-PCR and Western blot analysis BLM in BJ cells and iPSCs following treatment

SYBR® Green-based real time qRT-PCR for BLM in BJ and treated iPSCs compared to untreated cells. The bar chart shows the gene expression level that normalised to α-Tubulin and GAPDH expression. Tests were performed using the Bio-RAD CFX Manager. The error bars indicate standard error for three repeats. The Western blot results show the BLM proteins levels for same samples. β-Actine were tested for checking the loading control.

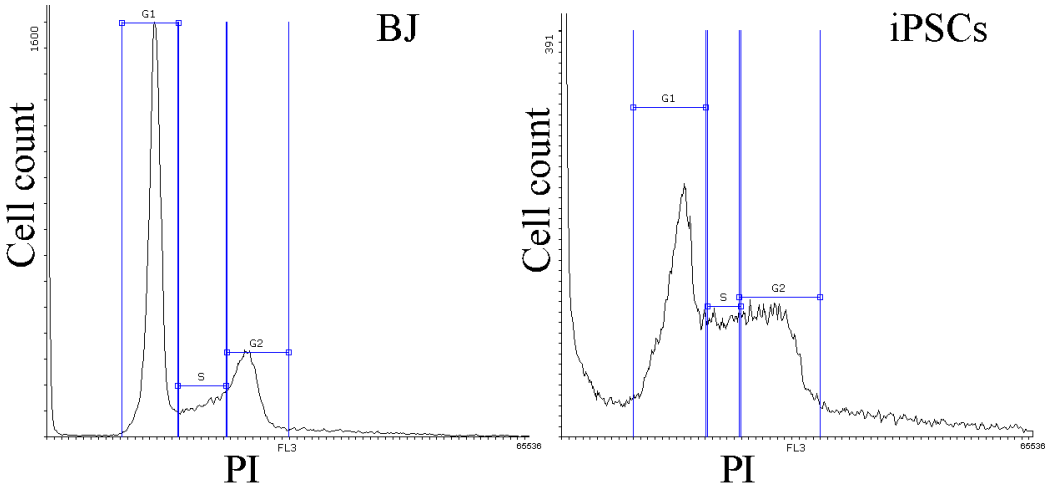

Figure 6:15 DNA content analysis of iPSCs and BJ cells by flow cytometry

Cell cycle profiles for propidium iodide-stained (PI) untreated cells. Experiments were performed using CyFlow® Cube 8low cytometry. DNA content histograms display a decline in the G1 phase on iPSCs. Data were analysed using Flowing Software 2.5.1.

6.3 Discussion

Induced transcriptional cell reprogramming to pluripotency has been successfully reported here. iPSCs generation was achieved by transient ectopic expression of the four reprogramming factors that were first discovered by Yamanaka and colleagues and used for the derivation of iPS in mouse. Initially this technology was achieved by utilising retroviral vectors to deliver reprogramming factors to cells, which has been widely used because it is a reliable, direct and economical method. Despite these advantages, the integration of viral sequences into the host genome carry a critical safety concern for the potential use of these cells in clinical applications (Mandal and Rossi, 2013).

Here, we report the use of modified mRNA to generate viral-free non-integral iPSCs from the foreskin of a newborn. As this method eliminates the risks associated with genome alteration, it will broaden the potential for regenerative medicine. The efficiency of iPSCs formation was evidenced in several ways, including ES-like morphology, AP activity and expression of pluripotency markers OCT4, NANG and SOX2. Cells also expressed the marker that not among reprogramming factors such SSEA-4 and TRA-1-60. However, other iPSCs validation methods have not been performed due to time limitations. These methods include karyotyping, teratoma formation assay and differentiation to three germ layers.

Despite several methods being available to generate iPSCs, the differentiation of pluripotent cells to their defined fates and the derivation of many cell types, the main challenge remains with cell-based therapies (Tabar and Studer, 2014). However, the power of modified-mRNA tools has some features that allow it to be applied to directing cell fate. These features include the ability of modified mRNA to mediate the expression of virtually any protein in many cell types. Moreover, it could also be used in the process of transforming a somatic cell into a different type of cell without undergoing an intermediate pluripotent state or progenitor cell type (transdifferentiation) (Warren et al., 2010). Consistent with this anticipation, a recent paper showed that modified mRNA of vascular endothelial growth factor-A (VEGF-A) has the ability to mediate the differentiation of heart progenitor cells and regenerate the vascular for infracted myocardium *in vivo* (Zangi et al., 2013).

Beyond the uses of modified mRNA for cell fate specification, it can be delivered to certain tissues to express therapeutic protein *in vivo*. Rudolph and co-workers were able to prolong the life of a mouse model of congenital lung disease that was characterised by the deficiency of surfactant protein B. They show the recovery of the wild-type SP-B expression on a treated mouse through the delivery of modified mRNA encoding surfactant protein B (Kormann et al., 2011).

Pluripotent stem cells are found to behave in a distinct manner that differs from the somatic cell in response to DNA damage due to their remarkable capability of self-renewal and differentiation into different lineages. Therefore, genomic integrity and the sensitivity to DNA damage of iPSCs need to be addressed before use in clinical applications. It also has important implications for cancer treatment, as CSCs share stem cells differentiation potential and capability to respond to genotoxic stress. It has been indicated that iPSCs are more likely to have genomic aberration as consequences of the reprogramming process (Pasi et al., 2011).

Here, we examined the behaviour of somatic cells BJ, the iPSCs line derived from these BJ and differentiated iPSCs in response to two replication inhibitors thymidine and CIS. Previously, hESCs and iPSCs were found to rapidly undergo apoptotic cell death following exposure to radiation (Hyka-Nouspikel et al., 2012; Momcilovic et al., 2010) A similar effect was also observed in hESCs in response to replication inhibitors, ionising radiation and other genotoxic agents (Desmarais et al., 2012; Momcilovic et al., 2009). Consistent with these findings, we found that both replication inhibitors induced a strong apoptotic response, resulting in cleavage of caspase-3. Remarkably, these cells also fail to activate critical checkpoints CHK1 when exposed to CIS, an effective treatment used against germ cell tumours (GCT) (Voss et al., 2011). Thus, it is likely that a high tendency to apoptosis is a common characteristic of pluripotency state, possibly a strategy to protect their genome from the lethal effects of this agent by favouring apoptosis rather than coping with DNA damage. This idea is also supported by observation of massive apoptosis reported in the inner cell mass of the embryo, following the activation of zygotic genome (Byrne et al., 1999) and the essential role of apoptosis during embryogenesis to eliminate abnormal cells in preimplantation embryos (Li et al., 2010).

We further characterised treated cells that showed apoptotic activity and found they still expressed pluripotency markers *OCT4*, *NANOG* and *SOX2*. However, the qRT-

PCR results displayed decreased *OCT4* expression, which was more significant in CIS treated cells, indicating that these cells might be differentiated. In agreement with this finding, downregulation of OCT4 and differentiation induction of human embryonal carcinoma cell line NTera2 following treatment with CIS has been reported recently (Abada and Howell, 2014). The higher level of damage caused by CIS could also explain the increase of phosphorylation of Histone H3 on Ser-10, an important inducer of apoptosis by Apoptotic Phosphorylation of Histone H3 on Ser-10 by Protein Kinase Cδ (PKCδ) following DNA damage (Park and Kim, 2012).

This could be explained by the fact that p53 in hESCs fails to activate the transcription of its target genes following DNA replication stress. Consequently, growing hESCs under genotoxic stress causes an accumulation of p53, which promotes spontaneous apoptosis of hESCs via the intrinsic (mitochondrial) apoptotic pathway. The accumulated p53 can also repress the expression of OCT4 and NANOG well-established pluripotency regulators and triggers the spontaneous differentiation of hESCs. However, the regulation details and balancing of apoptosis activity in pluripotent stem cells remains incompletely understood (Liu et al., 2014c; Qin et al., 2007).

We also examined the activation DNA repair marker γH2AX by immunofluorescence. We found iPSCs treated cells exhibit a very low number of γH2AX foci compared to BJ treated cells. Unfortunately, the foci number could not be counted. Previously, the low level of γH2AX activity in hESCs compared to their differentiated cells has been reported (Saretzki et al., 2008). In addition, the failure of hESCs to activate of γH2AX following exposure to replication inhibitors was reported and reasoned by a lack of phosphorylation of ATM and ATR pathways, the main activators of γH2AX (Desmarais et al., 2012). Furthermore, a time-course immunofluorescence for iPSCs exposed to ionising irradiation revealed that these cells were activating γH2AX for up to 6 hours, suggesting that the DNA repair occurs during this time frame before its disappearance (Momcilovic et al., 2010).

We presented here an elevation of BLM protein levels and expression of iPSCs, while it was significantly reduced on their parental BJ cells. Similarly, in a study of mESCs, BLM levels of undifferentiated mESCs were higher than their differentiated cells. Cell cycle distribution of iPSCs showed a reduction on G1 phase, which is characteristic of stem cells (Sela et al., 2012). During the cell cycle, TopBP1 protects BLM from the

degradation during S, G2/M phases, while it is degraded during the G1 phase (Wang et al., 2013). Therefore, the increase of BLM in iPSCs is probably due to the decline of G1 phase. Moreover, the reduction of BLM following the DNA damage accompanied by OCT4 reduction could support the suggested collaboration between the function of BLM and OCT4 (Campbell et al., 2007). Our data suggest a unique regulation of BLM during the differentiation pluripotency state. This regulation may also have an important role in genome integrity by reducing SCE events in the pluripotent stem cells. Finally, we may conclude that iPSCs generated by modified mRNA show high degrees of similarity in DNA damage response to both the hESCs and the classical iPSCs.

Chapter 7

General discussion

Chapter 7. General discussion

7.1 The centromere recombination model

Centromeres are critical sites within eukaryotic chromosomes to ensure proper chromosome segregation during cell division. Centromeric DNA is not conserved in sequence and remains ill-defined, although large centromeres share similar features such as repetitive DNA elements (Pauleau and Erhardt, 2011; Pidoux and Allshire, 2005). Centromere-specialized chromatin regions are characterized by the presence of the histone H3 variant CENP-A. Our initial aim was to examine a recent centromere model, which postulated that a recombination-based mechanism has an important role in the maintenance of centromere integrity and structure. We hypothesized that the Holliday junction recognition protein HJURP might load new CENP-A at sites of unresolved Holliday junctions (HJs) on aberrant chromosomes arising from failed HJ resolution/dissolution. However, the available results did not allow us to conclude a direct role of recombination events in centromere function. Nevertheless, establishing a role for recombination in centromere function would improve our understanding of centromere assembly and function during the cell cycle, in addition to elucidating the role of repetitive DNA in centromere determination and dynamics.

Two main findings in this study revealed the challenge of addressing our hypothesis. First, the compensatory relationship between BLM, MUS81 and GEN1 led to the failure of triple knockdown of all of three genes. This finding is supported by recent studies indicating that a degree of functional redundancy exists between these genes (Kim et al., 2013). Second, in BLM-deficient cells a CENP-A signal was observed as double and quadruple foci within individual chromosomes, suggesting that these were bona fide dicentric chromosomes in BLM-deficient cells. This unforeseen finding confounded our study, as the influence of the dicentric chromosome on normal segregation is unclear.

Further investigations are required to fully understand the cause of unusual structures in cells defective for HJ resolution. Characterization of some cytogenetically distinct but unresolved mitotic DNA structures has been reported; for example, anaphase DNA bridges appear as thread-like DNA structures when visualized by nuclear stains such DAPI. These bridges are phenomena of BLM-deficient cell and are likely to be

potential sources of aberrant chromosome morphology. More recent reports have newly identified a much more prevalent type of mitotic bridge structure called the ultrafine DNA bridge (UFB). These UFBs only can be detected by antibodies of proteins that bind to them, such BLM, PICH and FANCM helicases (Biebricher et al., 2013; Germann et al., 2014) . BLM is known to process DNA recombination structures, so these UFBs may represent recombination intermediates such as HJs. Hickson and co-workers have suggested these might be formed by unresolved centromere recombination intermediates (Mankouri et al., 2013).

In general, unusual chromosomal structures observed in eukaryotic cells (include that we observed in cells defective for HJ resolution) seem to reflect their specific utilization of the non-homologous end joining (NHEJ) and homologous recombination (HR) pathways, but a variety of other pathways can arise due to the failure of NHEJ or HR and lead to chromosomal aberration. Persistent or aberrantly processed DNA damage can be generated by modular processes includes annealing, end processing, strand invasion, replication, DNA synthesis, ligation and telomere addition. The final outcome appears to be affected by competition between the available molecular processes for which the lesion serves as a substrate, and some of these pathways might be inhibited in normal cells. In addition, the interrelationship of multiple DSB repair pathways and a number of reported modular combinations makes chromosomal aberration appear complex and heterogeneous and required further investigation (Kasparek and Humphrey, 2011).

7.2 An alternative approach

Human artificial chromosomes (HACs) are mini-chromosomes that contain functional human centromeric DNA and represent a potential approach for studying the structure and function of the higher eukaryote centromere. HACs are also used as an alternative safe methodology for the expression of integrated exogenous genomic DNA and overcome some of the disadvantages of conventional viral-based delivery systems. HACs can be maintained in a stable form independently of the chromosomes of host cells; thus, this approach differs from the classical approach where an extra gene is introduced, often randomly, into the genome (Ikeno and Suzuki, 2011). HACs also

exhibit a similar chromatin organisation and bind centromeric proteins such as CENP-A (Moralli et al., 2013).

The bottom-up HAC is one of the recent strategies utilized to construct HACs through the transfection of cloned or synthetic centromeric alphoid DNA precursors in human and other mammalian cells (Kouprina et al., 2013). Kouprina and her colleagues have recently used a synthetic alphoid DNA array to generate a bottom-up HAC carrying tetracycline operator (tetO) sequences and were able to insert this HAC *de novo* into HT1080 human cells (Kouprina et al., 2012). The unique feature of this HAC is its ability for reversible control (on/off) of the centromere activity by expression of tet-repressor (tetR) fusion proteins. Thus, construction of an alphoid^{tetO}-HAC with conditional centromeres provides a valuable approach for improving our understanding of centromere function and complexity. For example, assessing the efficiency of centromere activation on this system following the reduction of homologous recombination factors such as RAD51 (which promotes DNA strand invasion the key step in HR) may suggest indirect role of the recombination in the centromere function.

7.3 The role of BLM in the pluripotency state of human cells

The essential role of BLM helicase in HR, particularly in dissolving dHJs, underscored the importance of investigating its relationship with the potency state of cancer stem-like cells and human stem cells, and with DNA damage repair induced by replication inhibitors. One of the key findings in the present work is the significantly reduced levels of BLM and GEN1 that correlated with the appearance of stem cell markers and sphere formation. When cells switch off BLM and GEN1, they become more susceptible to genetic change and this could possibly drive selection pressure in that population of cells. Unlike BLM-deficient cells, the CSCs that lacked BLM exhibited low levels of sister chromatid exchange (SCE), indicating that the cells in this state may prefer alternative pathways for removal of HJs. The HJs might be processed by the third pathway for HJ resolution mediated by MUS81, which provides backup for the BTR complex function. However, colonospheres displayed elevations in SCE frequency in response to DNA damage when compared with their parental cells. This suggests that the MUS81 pathway of the CSCs were unable to cope with a higher

number of HJs and could offer insight into a potential therapeutic window. Another explanation may be that BLM is not completely switched off in those cells but it is maintained at a low level that allows the cells to cope with a low amount of DNA damage in the absence of exogenous DNA damage.

In contrast, the BLM levels in iPSCs were higher than those of the isogenic parental and differentiated cells. Several observations suggest possible explanations, and the answer may lie in a combination of these. First, the correct physiological protein function is important for the biological activities in normal cells. Cancer cells show aberrant protein function as a result of mutations that alter the protein expression of some genes (Hung and Link, 2011). For example, a key DNA repair regulator the p53 gene in SW480 cells has been reported to carry mutations in its three copies (Rochette et al., 2005). Second, up-regulation of BLM in iPSCs probably occurs due to the decline in the G1 phase, and BLM is protected against degradation during G1 via TopBP1 activity (Biebricher et al., 2013; Wang et al., 2013). Several epigenetics alterations have shown to profoundly influence the regulation of gene expression and protein function in CSCs and human stem cells which considered to lie behind the on/off switches of gene expression patterns in those cells (Munoz et al., 2012; Wang et al., 2014). Therefore, the reduction of BLM and GEN1 in CSCs suggests distinctive regulation at the level of translation and protein degradation for those protein within this population of cells. For example, the protein abundances is affected by MicroRNAs (miRNAs) which are a class of endogenous non-coding RNAs that regulate the protein synthesis of their target messenger RNAs (Ha and Kim, 2014). Remarkably, several studies have reported a number of miRNAs that play a significant role in various aspects of CSC properties including colon cancer stem cells (Bu et al., 2013; Takahashi et al., 2014). Moreover, recent reports have revealed that RNA-binding proteins (RBPs) act as key players in the genome instability and integrity. RBPs can protect the cellular system from RNA/DNA lesions and are required in the DNA damage response (DDR). Indeed, DNA repair involves selective regulation of DDR genes which can be regulated at post-transcriptional levels via specific RBPs (Dutertre et al., 2014). Deregulation of RBP can prohibit miRNAs from associating with their target sites and that reported in several malignancies. For instance, the role of RBPs DND1, DAZL and PUM2 has been proposed in the development of germline

and involve in the post-transcriptional regulation of stem cells maintenance (van Kouwenhove et al., 2011).

The lack of HJ regulators (BLM or GEN1) in CSCs could be not necessarily correlated with stemness rather than to associate with certain cellular mechanism in parallel with the sphere formation. All together this findings suggests that although CSCs share some essential features of human pluripotent stem cells include self-renewal and differentiation, CSCs may employ distinct DNA repairing mechanism in response to replication stress.

7.4 Apoptosis as a therapeutic target in cancer and cancer stem cells

Aberrant regulation of apoptosis is a common hallmark of cancer development and progression. Considering the plasticity of CSCs, the question arises whether strategies that induce apoptosis would be more effective at eradicating these cells, also taking into account their exposure to variable microenvironments. In the present study, we showed that the spheroids of HCT116 cells demonstrated resistance to replication inhibitors by evading cell cycle arrest and by failure to activate P-CHK, H2AX and caspase 3 in response replication inhibitors. However, a limited activation of caspase-3 was observed in the SW480 spheroid in response to cisplatin induction.

This observation is supported by a report demonstrating that cisplatin triggered apoptosis in the outer cell layers of spheroid sections. Staining with Ki-67, which identifies proliferating cells, was also evident at the surface of the spheroid sections (Fayad et al., 2009). This spatially limited apoptosis may reflect incomplete penetration of the anticancer drug (Liu et al., 2013; Tannock et al., 2002). This might also have occurred as consequence of a low sensitivity of cisplatin against quiescent cells in the deeper spheroid layers. However, a screening study has revealed that NSC647889 can act as a potent apoptotic drug. Spheroids of HCT116 treated with NSC647889 demonstrated significant increases in apoptosis in response to cisplatin induction (Mohanty et al., 2013).

It is worth mentioning that a strategy to improve the efficiency of chemotherapy drugs that target CSCs should consider the safety concerns and the protection of adult stem cells. Thus, further characterization of adult stem cells and CSCs is required in order

to minimize alterations of the critical mechanisms for stem cells that exist normally in the human body, and especially when treating of paediatric and young adult patients.

Finally, this study addressed genome stability maintenance mechanisms in human cancer cells and stem cells. Collectively, the results show that chemotherapy resistance is a complex process with a mechanism that seems to require multiple genes that regulate the response to drugs through a wide range of processes. Although the results presented here, together with other findings, could generate improvements in effective diagnostic and therapeutic strategies, the intra-tumour heterogeneity that leads to treatment resistance and failure should be considered in the future. Furthermore, several studies on DNA replication stress in different types of cancer have indicated that replication stress fosters intra-tumour heterogeneity and could lead to the acquisition of multidrug resistance (Lee and Swanton, 2012). Thus, targeting cancer chromosomal instability represents an effective methodology for limiting cancer cell proliferation, but might help drive unwanted genome evolution and adaptation.

References

Abada, P.B. & Howell, S.B. 2014, "Cisplatin Induces Resistance by Triggering Differentiation of Testicular Embryonal Carcinoma Cells", *PloS one,* vol. 9, no. 1, pp. e87444.

Al-Assar, O., Muschel, R.J., Mantoni, T.S., McKenna, W.G. & Brunner, T.B. 2009, "Radiation response of cancer stem-like cells from established human cell lines after sorting for surface markers", *International Journal of Radiation Oncology* Biology* Physics,* vol. 75, no. 4, pp. 1216-1225.

Alfred, L.J. & DiPaolo, J.A. 1968, "Reversible inhibition of DNA synthesis in hamster embryo cells in culture: action of 1,2-benzanthracene and 7,12-dimethylbenz(a)anthracene", *Cancer research,* vol. 28, no. 1, pp. 60-65.

Allshire, R.C. & Karpen, G.H. 2008, "Epigenetic regulation of centromeric chromatin: old dogs, new tricks?", *Nature reviews.Genetics,* vol. 9, no. 12, pp. 923.

Andersen, S.L., Kuo, H.K., Savukoski, D., Brodsky, M.H. & Sekelsky, J. 2011, "Three structure-selective endonucleases are essential in the absence of BLM helicase in Drosophila", *PLoS genetics,* vol. 7, no. 10, pp. e1002315.

Anokye-Danso, F., Trivedi, C.M., Juhr, D., Gupta, M., Cui, Z., Tian, Y., Zhang, Y., Yang, W., Gruber, P.J. & Epstein, J.A. 2011, "Highly efficient miRNA-mediated reprogramming of mouse and human somatic cells to pluripotency", *Cell stem cell,* vol. 8, no. 4, pp. 376-388.

Arora, H., Chacon, A.H., Choudhary, S., McLeod, M.P., Meshkov, L., Nouri, K. & Izakovic, J. 2014, "Bloom syndrome", *International journal of dermatology,* .

Badura, M., Braunstein, S., Zavadil, J. & Schneider, R.J. 2012, "DNA damage and eIF4G1 in breast cancer cells reprogram translation for survival and DNA repair mRNAs", *Proceedings of the National Academy of Sciences of the United States of America,* vol. 109, no. 46, pp. 18767-18772.

Bannister, A.J. & Kouzarides, T. 2011, "Regulation of chromatin by histone modifications", *Cell research,* vol. 21, no. 3, pp. 381-395.

Bao, S., Wu, Q., McLendon, R.E., Hao, Y., Shi, Q., Hjelmeland, A.B., Dewhirst, M.W., Bigner, D.D. & Rich, J.N. 2006, "Glioma stem cells promote radioresistance by preferential activation of the DNA damage response", *Nature,* vol. 444, no. 7120, pp. 756-760.

Barker, N. 2014, "Adult intestinal stem cells: critical drivers of epithelial homeostasis and regeneration", *Nature Reviews Molecular Cell Biology,* vol. 15, no. 1, pp. 19-33.

Barnhart-Dailey, M.C. & Foltz, D.R. 2014, "Centromere licensing: Mis18 is required to Polo-ver", *Current biology : CB*, vol. 24, no. 17, pp. R808-10.

Bartucci, M., Svensson, S., Romania, P., Dattilo, R., Patrizii, M., Signore, M., Navarra, S., Lotti, F., Biffoni, M. & Pilozzi, E. 2011, "Therapeutic targeting of Chk1 in NSCLC stem cells during chemotherapy", *Cell Death & Differentiation*, vol. 19, no. 5, pp. 768-778.

Bayes, J.J. & Malik, H.S. 2008, "The evolution of centromeric DNA sequences", *eLS*, .

Bee, L., Fabris, S., Cherubini, R., Mognato, M. & Celotti, L. 2013, "The efficiency of homologous recombination and non-homologous end joining systems in repairing double-strand breaks during cell cycle progression", *PloS one*, vol. 8, no. 7, pp. e69061.

Bellin, M., Marchetto, M.C., Gage, F.H. & Mummery, C.L. 2012, "Induced pluripotent stem cells: the new patient?", *Nature Reviews Molecular Cell Biology*, vol. 13, no. 11, pp. 713-726.

Bernad, R., Sánchez, P. & Losada, A. 2009, "Epigenetic specification of centromeres by CENP-A", *Experimental cell research*, vol. 315, no. 19, pp. 3233-3241.

Biebricher, A., Hirano, S., Enzlin, J.H., Wiechens, N., Streicher, W.W., Huttner, D., Wang, L.H., Nigg, E.A., Owen-Hughes, T. & Liu, Y. 2013, "PICH: a DNA translocase specially adapted for processing anaphase bridge DNA", *Molecular cell*, vol. 51, no. 5, pp. 691-701.

Bindra, R.S., Schaffer, P.J., Meng, A., Woo, J., Maseide, K., Roth, M.E., Lizardi, P., Hedley, D.W., Bristow, R.G. & Glazer, P.M. 2004, "Down-regulation of Rad51 and decreased homologous recombination in hypoxic cancer cells", *Molecular and cellular biology*, vol. 24, no. 19, pp. 8504-8518.

Blanpain, C., Mohrin, M., Sotiropoulou, P.A. & Passegué, E. 2011, "DNA-damage response in tissue-specific and cancer stem cells", *Cell Stem Cell*, vol. 8, no. 1, pp. 16-29.

Boddy, M.N., Gaillard, P.L., McDonald, W.H., Shanahan, P. & Russell, P. 2001, "Mus81-Eme1 are essential components of a Holliday junction resolvase", *Cell*, vol. 107, no. 4, pp. 537-548.

Brabletz, T. 2012, "EMT and MET in metastasis: where are the cancer stem cells?", *Cancer cell*, vol. 22, no. 6, pp. 699-701.

Bradley, A., Anastassiadis, K., Ayadi, A., Battey, J.F., Bell, C., Birling, M., Bottomley, J., Brown, S.D., Bürger, A. & Bult, C.J. 2012, "The mammalian gene function resource: the international knockout mouse consortium", *Mammalian genome*, vol. 23, no. 9-10, pp. 580-586.

Brady, C.A. & Attardi, L.D. 2010, "P53 at a Glance", *Journal of cell science,* vol. 123, no. Pt 15, pp. 2527-2532.

Brevini, T.A. & Pennarossa, G. 2013, "Gametogenesis" in *Gametogenesis, Early Embryo Development and Stem Cell Derivation* Springer, , pp. 1-25.

Brunner, T.B., Kunz-Schughart, L.A., Grosse-Gehling, P. & Baumann, M. 2012, "Cancer stem cells as a predictive factor in radiotherapy", *Seminars in radiation oncology*Elsevier, , pp. 151.

Bu, P., Chen, K., Chen, J.H., Wang, L., Walters, J., Shin, Y.J., Goerger, J.P., Sun, J., Witherspoon, M. & Rakhilin, N. 2013, "A microRNA miR-34a-regulated bimodal switch targets notch in colon cancer stem cells", *Cell stem cell,* vol. 12, no. 5, pp. 602-615.

Burgess, R.J. & Zhang, Z. 2013, "Histone chaperones in nucleosome assembly and human disease", *nature structural & molecular biology,* vol. 20, no. 1, pp. 14-22.

Burrell, R.A., McGranahan, N., Bartek, J. & Swanton, C. 2013, "The causes and consequences of genetic heterogeneity in cancer evolution", *Nature,* vol. 501, no. 7467, pp. 338-345.

Byrne, A.T., Southgate, J., Brison, D.R. & Leese, H.J. 1999, "Analysis of apoptosis in the preimplantation bovine embryo using TUNEL", *Journal of reproduction and fertility,* vol. 117, no. 1, pp. 97-105.

Cabarcas, S.M., Mathews, L.A. & Farrar, W.L. 2011, "The cancer stem cell niche—there goes the neighborhood?", *International Journal of Cancer,* vol. 129, no. 10, pp. 2315-2327.

Campbell, P.A., Perez-Iratxeta, C., Andrade-Navarro, M.A. & Rudnicki, M.A. 2007, "Oct4 targets regulatory nodes to modulate stem cell function", *PLoS One,* vol. 2, no. 6, pp. e553.

Cermak, T., Doyle, E.L., Christian, M., Wang, L., Zhang, Y., Schmidt, C., Baller, J.A., Somia, N.V., Bogdanove, A.J. & Voytas, D.F. 2011, "Efficient design and assembly of custom TALEN and other TAL effector-based constructs for DNA targeting", *Nucleic acids research,* vol. 39, no. 12, pp. e82.

Cervantes, R.B., Stringer, J.R., Shao, C., Tischfield, J.A. & Stambrook, P.J. 2002, "Embryonic stem cells and somatic cells differ in mutation frequency and type", *Proceedings of the National Academy of Sciences of the United States of America,* vol. 99, no. 6, pp. 3586-3590.

Chan, Y.W. & West, S.C. 2014, "Spatial control of the GEN1 Holliday junction resolvase ensures genome stability", *Nature communications,* vol. 5.

Chapman, J.R., Taylor, M.R. & Boulton, S.J. 2012, "Playing the end game: DNA double-strand break repair pathway choice", *Molecular cell,* vol. 47, no. 4, pp. 497-510.

Chen, K., Pan, F., Jiang, H., Chen, J., Pei, L., Xie, F. & Liang, H. 2011, "Highly enriched CD133 CD44 stem-like cells with CD133 CD44high metastatic subset in HCT116 colon cancer cells", *Clinical & experimental metastasis,* vol. 28, no. 8, pp. 751-763.

Chen, S.H., Plank, J.L., Willcox, S., Griffith, J.D. & Hsieh, T. 2014, "Top3α Is Required during the Convergent Migration Step of Double Holliday Junction Dissolution", *PloS one,* vol. 9, no. 1, pp. e83582.

Chesworth, R., Wigle, T.J., Kuntz, K.W., Smith, J.J. & Richon, V.M. 2014, "Histone Methyltransferases: Opportunities in Cancer Drug Discovery" in *Epigenetic Therapy of Cancer* Springer, , pp. 189-226.

Choudhuri, S. 2014, *Bioinformatics for Beginners: Genes, Genomes, Molecular Evolution, Databases and Analytical Tools,* Elsevier.

Chow, A.Y. 2010, *Cell Cycle Control by Oncogenes and Tumor Suppressors: Driving the Transformation of Normal Cells into Cancerous Cells*, Nature Education.

Clarke, L. 1998, "Centromeres: proteins, protein complexes, and repeated domains at centromeres of simple eukaryotes", *Current opinion in genetics & development,* vol. 8, no. 2, pp. 212-218.

Cleveland, D.W., Mao, Y. & Sullivan, K.F. 2003, "Centromeres and kinetochores: from epigenetics to mitotic checkpoint signaling", *Cell,* vol. 112, no. 4, pp. 407-421.

Clevers, H. 2011, "The cancer stem cell: premises, promises and challenges", *Nature medicine,* , pp. 313-319.

Crider, K.S., Yang, T.P., Berry, R.J. & Bailey, L.B. 2012, "Folate and DNA methylation: a review of molecular mechanisms and the evidence for folate's role", *Advances in nutrition (Bethesda, Md.),* vol. 3, no. 1, pp. 21-38.

Croteau, D.L., Popuri, V., Opresko, P.L. & Bohr, V.A. 2014, "Human RecQ helicases in DNA repair, recombination, and replication", *Annual Review of Biochemistry,* vol. 83, pp. 519-552.

Da Ines, O., Abe, K., Goubely, C., Gallego, M.E. & White, C.I. 2012, "Differing requirements for RAD51 and DMC1 in meiotic pairing of centromeres and chromosome arms in Arabidopsis thaliana", *PLoS genetics,* vol. 8, no. 4, pp. e1002636.

Dahm-Daphi, J., Hubbe, P., Horvath, F., El-Awady, R.A., Bouffard, K.E., Powell, S.N. & Willers, H. 2005, "Nonhomologous end-joining of site-specific but not

of radiation-induced DNA double-strand breaks is reduced in the presence of wild-type p53", *Oncogene,* vol. 24, no. 10, pp. 1663-1672.

Dai, J., Sullivan, B.A. & Higgins, J.M. 2006, "Regulation of mitotic chromosome cohesion by Haspin and Aurora B", *Developmental cell,* vol. 11, no. 5, pp. 741-750.

Darzynkiewicz, Z., Halicka, H.D., Zhao, H. & Podhorecka, M. 2011, "Cell synchronization by inhibitors of DNA replication induces replication stress and DNA damage response: analysis by flow cytometry" in *Cell Cycle Synchronization* Springer, , pp. 85-96.

Davis, A.J. & Chen, D.J. 2013, "DNA double strand break repair via non-homologous end-joining", *Translational cancer research,* vol. 2, no. 3, pp. 130.

Deans, A.J. & West, S.C. 2009, "FANCM connects the genome instability disorders Bloom's Syndrome and Fanconi Anemia", *Molecular cell,* vol. 36, no. 6, pp. 943-953.

Delia, D., Fontanella, E., Ferrario, C., Chessa, L. & Mizutani, S. 2003, "DNA damage-induced cell-cycle phase regulation of p53 and p21waf1 in normal and ATM-defective cells", *Oncogene,* vol. 22, no. 49, pp. 7866-7869.

Desmarais, J.A., Hoffmann, M.J., Bingham, G., Gagou, M.E., Meuth, M. & Andrews, P.W. 2012, "Human Embryonic Stem Cells Fail to Activate CHK1 and Commit to Apoptosis in Response to DNA Replication Stress", *Stem cells,* vol. 30, no. 7, pp. 1385-1393.

Dhar, S. & Lippard, S.J. 2011, "Current Status and Mechanism of Action of Platinum-Based Anticancer Drugs", *Bioinorganic medicinal chemistry,* , pp. 79-95.

Di Leonardo, A., Linke, S.P., Clarkin, K. & Wahl, G.M. 1994, "DNA damage triggers a prolonged p53-dependent G1 arrest and long-term induction of Cip1 in normal human fibroblasts", *Genes & development,* vol. 8, no. 21, pp. 2540-2551.

Diaz-Moralli, S., Tarrado-Castellarnau, M., Miranda, A. & Cascante, M. 2013, "Targeting cell cycle regulation in cancer therapy", *Pharmacology & therapeutics,* vol. 138, no. 2, pp. 255-271.

Diehn, M., Cho, R.W., Lobo, N.A., Kalisky, T., Dorie, M.J., Kulp, A.N., Qian, D., Lam, J.S., Ailles, L.E. & Wong, M. 2009, "Association of reactive oxygen species levels and radioresistance in cancer stem cells", *Nature,* vol. 458, no. 7239, pp. 780-783.

Doherty, K., Meere, M. & Piiroinen, P.T. 2014, "A Mathematical Model of CENP-A Incorporation in Mammalian Centromeres", *Mathematical biosciences,* .

Dunleavy, E.M., Roche, D., Tagami, H., Lacoste, N., Ray-Gallet, D., Nakamura, Y., Daigo, Y., Nakatani, Y. & Almouzni-Pettinotti, G. 2009, "HJURP is a cell-cycle-dependent maintenance and deposition factor of CENP-A at centromeres", *Cell,* vol. 137, no. 3, pp. 485-497.

Dutertre, M., Lambert, S., Carreira, A., Amor-Guéret, M. & Vagner, S. 2014, "DNA damage: RNA-binding proteins protect from near and far", *Trends in biochemical sciences,* vol. 39, no. 3, pp. 141-149.

Earnshaw, W.C. & Rothfield, N. 1985, "Identification of a family of human centromere proteins using autoimmune sera from patients with scleroderma", *Chromosoma,* vol. 91, no. 3-4, pp. 313-321.

Elliott, A., Adams, J. & Al-Hajj, M. 2010, "The ABCs of cancer stem cell drug resistance", *IDrugs : the investigational drugs journal,* vol. 13, no. 9, pp. 632-635.

Erenpreisa, J. & Cragg, M.S. 2013, "Three steps to the immortality of cancer cells: senescence, polyploidy and self-renewal", *Cancer cell international,* vol. 13, no. 1, pp. 92-2867-13-92.

Fabre, F., Chan, A., Heyer, W.D. & Gangloff, S. 2002, "Alternate pathways involving Sgs1/Top3, Mus81/ Mms4, and Srs2 prevent formation of toxic recombination intermediates from single-stranded gaps created by DNA replication", *Proceedings of the National Academy of Sciences of the United States of America,* vol. 99, no. 26, pp. 16887-16892.

Fan, J., Robert, C., Jang, Y., Liu, H., Sharkis, S., Baylin, S.B. & Rassool, F.V. 2011, "Human induced pluripotent cells resemble embryonic stem cells demonstrating enhanced levels of DNA repair and efficacy of nonhomologous end-joining", *Mutation Research/Fundamental and Molecular Mechanisms of Mutagenesis,* vol. 713, no. 1, pp. 8-17.

Fanali, C., Lucchetti, D., Farina, M., Corbi, M., Cufino, V., Cittadini, A. & Sgambato, A. 2014, "Cancer stem cells in colorectal cancer from pathogenesis to therapy: Controversies and perspectives", *World journal of gastroenterology: WJG,* vol. 20, no. 4, pp. 923.

Fayad, W., Brnjic, S., Berglind, D., Blixt, S., Shoshan, M.C., Berndtsson, M., Olofsson, M.H. & Linder, S. 2009, "Restriction of cisplatin induction of acute apoptosis to a subpopulation of cells in a three-dimensional carcinoma culture model", *International journal of cancer.Journal international du cancer,* vol. 125, no. 10, pp. 2450-2455.

Feichtinger, J., Aldeailej, I., Anderson, R., Almutairi, M., Almatrafi, A., Alsiwiehri, N., Griffiths, K., Stuart, N., Wakeman, J.A., Larcombe, L. & McFarlane, R.J. 2012, "Meta-analysis of clinical data using human meiotic genes identifies a novel cohort of highly restricted cancer-specific marker genes", *Oncotarget,* vol. 3, no. 8, pp. 843-853.

Feng, C., Jia, Y. & Zhao, X. 2013, "Pluripotency of Induced Pluripotent Stem Cells", *Genomics, proteomics & bioinformatics,* vol. 11, no. 5, pp. 299-303.

Filion, T.M., Qiao, M., Ghule, P.N., Mandeville, M., Van Wijnen, A.J., Stein, J.L., Lian, J.B., Altieri, D.C. & Stein, G.S. 2009, "Survival responses of human embryonic stem cells to DNA damage", *Journal of cellular physiology,* vol. 220, no. 3, pp. 586-592.

Fischer, P.M. & Gianella-Borradori, A. 2005, "Recent progress in the discovery and development of cyclin-dependent kinase inhibitors", *Expert opinion on investigational drugs,* vol. 14, no. 4, pp. 457-477.

Fisher, R., Pusztai, L. & Swanton, C. 2013, "Cancer heterogeneity: implications for targeted therapeutics", *British journal of cancer,* vol. 108, no. 3, pp. 479-485.

Forget, A.L. & Kowalczykowski, S.C. 2010, "Single-molecule imaging brings Rad51 nucleoprotein filaments into focus", *Trends in cell biology,* vol. 20, no. 5, pp. 269-276.

Frank, N.Y., Schatton, T. & Frank, M.H. 2010, "The therapeutic promise of the cancer stem cell concept", *The Journal of clinical investigation,* vol. 120, no. 1, pp. 41-50.

French, B.T. & Straight, A.F. 2013, "Swapping CENP-A at the centromere", *Nature cell biology,* vol. 15, no. 9, pp. 1028-1030.

Friedmann-Morvinski, D. & Verma, I.M. 2014, "Dedifferentiation and reprogramming: origins of cancer stem cells", *EMBO reports,* vol. 15, no. 3, pp. 244-253.

Fu, D., Calvo, J.A. & Samson, L.D. 2012, "Balancing repair and tolerance of DNA damage caused by alkylating agents", *Nature Reviews Cancer,* vol. 12, no. 2, pp. 104-120.

Fukui, K. 2010, "DNA mismatch repair in eukaryotes and bacteria", *Journal of nucleic acids,* vol. 2010, pp. 10.4061/2010/260512.

Gaither, T.L., Merrett, S.L., Pun, M.J. & Scott, K.C. 2014, "Centromeric barrier disruption leads to mitotic defects in Schizosaccharomyces pombe", *G3 (Bethesda, Md.),* vol. 4, no. 4, pp. 633-642.

Gallo-Fernandez, M., Saugar, I., Ortiz-Bazan, M.A., Vazquez, M.V. & Tercero, J.A. 2012, "Cell cycle-dependent regulation of the nuclease activity of Mus81-Eme1/Mms4", *Nucleic acids research,* vol. 40, no. 17, pp. 8325-8335.

Gao, M., Danielsen, J.R., Wei, L., Zhou, D., Xu, Q., Li, M., Wang, Z., Tong, W. & Yang, Y. 2012, "A novel role of human Holliday junction resolvase GEN1 in the maintenance of centrosome integrity", *PloS one,* vol. 7, no. 11, pp. e49687.

Garner, E., Kim, Y., Lach, F.P., Kottemann, M.C. & Smogorzewska, A. 2013, "Human GEN1 and the SLX4-associated nucleases MUS81 and SLX1 are essential for the resolution of replication-induced Holliday junctions", *Cell reports*, vol. 5, no. 1, pp. 207-215.

Gaymes, T.J., North, P.S., Brady, N., Hickson, I.D., Mufti, G.J. & Rassool, F.V. 2002, "Increased error-prone non homologous DNA end-joining--a proposed mechanism of chromosomal instability in Bloom's syndrome.", *Oncogene*, vol. 21, no. 16, pp. 2525-2533.

German, J. 1993, "Bloom syndrome: a mendelian prototype of somatic mutational disease", *Medicine*, vol. 72, no. 6, pp. 393-406.

Germann, S.M., Schramke, V., Pedersen, R.T., Gallina, I., Eckert-Boulet, N., Oestergaard, V.H. & Lisby, M. 2014, "TopBP1/Dpb11 binds DNA anaphase bridges to prevent genome instability", *The Journal of cell biology*, vol. 204, no. 1, pp. 45-59.

Ghosh, S., Feingold, E. & Dey, S.K. 2009, "Etiology of Down syndrome: evidence for consistent association among altered meiotic recombination, nondisjunction, and maternal age across populations", *American Journal of Medical Genetics Part A*, vol. 149, no. 7, pp. 1415-1420.

Gil, J., Stembalska, A., Pesz, K.A. & Sąsiadek, M.M. 2008, "Cancer stem cells: the theory and perspectives in cancer therapy", *Journal of Applied Genetics*, vol. 49, no. 2, pp. 193-199.

Grosse-Gehling, P., Fargeas, C.A., Dittfeld, C., Garbe, Y., Alison, M.R., Corbeil, D. & Kunz-Schughart, L.A. 2013, "CD133 as a biomarker for putative cancer stem cells in solid tumours: limitations, problems and challenges", *The Journal of pathology*, vol. 229, no. 3, pp. 355-378.

Guillemette, B., Drogaris, P., Lin, H.S., Armstrong, H., Hiragami-Hamada, K., Imhof, A., Bonneil, E., Thibault, P., Verreault, A. & Festenstein, R.J. 2011, "H3 lysine 4 is acetylated at active gene promoters and is regulated by H3 lysine 4 methylation", *PLoS genetics*, vol. 7, no. 3, pp. e1001354.

Ha, M. & Kim, V.N. 2014, "Regulation of microRNA biogenesis", *Nature Reviews Molecular Cell Biology*, vol. 15, no. 8, pp. 509-524.

Halacli, S.O., Canpinar, H., Cimen, E. & Sunguroglu, A. 2013, "Effects of gamma irradiation on cell cycle, apoptosis and telomerase activity in p53 wild-type and deficient HCT116 colon cancer cell lines", *Oncology letters*, vol. 6, no. 3, pp. 807-810.

Hamiche, A. & Shuaib, M. 2012, "Chaperoning the histone H3 family", *Biochimica et Biophysica Acta (BBA)-Gene Regulatory Mechanisms*, vol. 1819, no. 3, pp. 230-237.

Hanahan, D. & Weinberg, R.A. 2011, "Hallmarks of cancer: the next generation", *Cell*, vol. 144, no. 5, pp. 646-674.

Hanahan, D. & Weinberg, R.A. 2000, "The hallmarks of cancer", *Cell*, vol. 100, no. 1, pp. 57-70.

Hardin, H., Montemayor-Garcia, C. & Lloyd, R.V. 2013, "Thyroid cancer stem-like cells and epithelial-mesenchymal transition in thyroid cancers", *Human pathology*, vol. 44, no. 9, pp. 1707-1713.

Harigaya, Y., Tanaka, H., Yamanaka, S., Tanaka, K., Watanabe, Y., Tsutsumi, C., Chikashige, Y., Hiraoka, Y., Yamashita, A. & Yamamoto, M. 2006, "Selective elimination of messenger RNA prevents an incidence of untimely meiosis", *Nature*, vol. 442, no. 7098, pp. 45-50.

Harper, J.V. 2005, "Synchronization of cell populations in G1/S and G2/M phases of the cell cycle" in *Cell Cycle Control* Springer, , pp. 157-166.

Heddleston, J., Li, Z., Lathia, J., Bao, S., Hjelmeland, A. & Rich, J. 2010, "Hypoxia inducible factors in cancer stem cells", *British journal of cancer*, vol. 102, no. 5, pp. 789-795.

Hejmadi, M. 2010, *Introduction to cancer biology*, Bookboon.

Helleday, T., Petermann, E., Lundin, C., Hodgson, B. & Sharma, R.A. 2008, "DNA repair pathways as targets for cancer therapy", *Nature Reviews Cancer*, vol. 8, no. 3, pp. 193-204.

Hemmerich, P., Weidtkamp-Peters, S., Hoischen, C., Schmiedeberg, L., Erliandri, I. & Diekmann, S. 2008, "Dynamics of inner kinetochore assembly and maintenance in living cells", *The Journal of cell biology*, vol. 180, no. 6, pp. 1101-1114.

Hemphill, A.W., Akkari, Y., Newell, A.H., Schultz, R.A., Grompe, M., North, P.S., Hickson, I.D., Jakobs, P.M., Rennie, S., Pauw, D., Hejna, J., Olson, S.B. & Moses, R.E. 2009, "Topo IIIalpha and BLM act within the Fanconi anemia pathway in response to DNA-crosslinking agents", *Cytogenetic and genome research*, vol. 125, no. 3, pp. 165-175.

Henderson, L., Bortone, D.S., Lim, C. & Zambon, A.C. 2013, "Classic "broken cell" techniques and newer live cell methods for cell cycle assessment", *American journal of physiology.Cell physiology*, vol. 304, no. 10, pp. C927-38.

Heun, P., Erhardt, S., Blower, M.D., Weiss, S., Skora, A.D. & Karpen, G.H. 2006, "Mislocalization of the Drosophila centromere-specific histone CID promotes formation of functional ectopic kinetochores", *Developmental cell*, vol. 10, no. 3, pp. 303-315.

Hill, E. & Williams, R. 2009, "Super-coil me: Sizing up centromeric nucleosomes", *The Journal of cell biology*, vol. 186, no. 4, pp. 453.

Hiriart, E., Vavasseur, A., Touat-Todeschini, L., Yamashita, A., Gilquin, B., Lambert, E., Perot, J., Shichino, Y., Nazaret, N. & Boyault, C. 2012, "Mmi1 RNA surveillance machinery directs RNAi complex RITS to specific meiotic genes in fission yeast", *The EMBO journal,* vol. 31, no. 10, pp. 2296-2308.

Hjelmeland, A.B., Wu, Q., Heddleston, J., Choudhary, G., MacSwords, J., Lathia, J., McLendon, R., Lindner, D., Sloan, A. & Rich, J.N. 2010, "Acidic stress promotes a glioma stem cell phenotype", *Cell Death & Differentiation,* vol. 18, no. 5, pp. 829-840.

Hofstetrova, K., Uzlikova, M., Tumova, P., Troell, K., Svard, S.G. & Nohynkova, E. 2010, "Giardia intestinalis: aphidicolin influence on the trophozoite cell cycle", *Experimental parasitology,* vol. 124, no. 2, pp. 159-166.

Horton, N. & Mathew, P. 2013, "Extracellular Proliferating Cell Nuclear Antigen is a novel marker for cancer stem cells and facilitates evasion of Natural Killer cell effector function (P2133)", *The Journal of Immunology,* vol. 190, pp. 170.23.

Hrkach, J., Von Hoff, D., Mukkaram Ali, M., Andrianova, E., Auer, J., Campbell, T., De Witt, D., Figa, M., Figueiredo, M., Horhota, A., Low, S., McDonnell, K., Peeke, E., Retnarajan, B., Sabnis, A., Schnipper, E., Song, J.J., Song, Y.H., Summa, J., Tompsett, D., Troiano, G., Van Geen Hoven, T., Wright, J., LoRusso, P., Kantoff, P.W., Bander, N.H., Sweeney, C., Farokhzad, O.C., Langer, R. & Zale, S. 2012, "Preclinical development and clinical translation of a PSMA-targeted docetaxel nanoparticle with a differentiated pharmacological profile", *Science translational medicine,* vol. 4, no. 128, pp. 128ra39.

Hu, Z., Huang, G., Sadanandam, A., Gu, S., Lenburg, M.E., Pai, M., Bayani, N., Blakely, E.A., Gray, J.W. & Mao, J. 2010, "The expression level of HJURP has an independent prognostic impact and predicts the sensitivity to radiotherapy in breast cancer", *Breast Cancer Res,* vol. 12, no. 2, pp. R18.

Hung, M.C. & Link, W. 2011, "Protein localization in disease and therapy", *Journal of cell science,* vol. 124, no. Pt 20, pp. 3381-3392.

Hyka-Nouspikel, N., Desmarais, J., Gokhale, P.J., Jones, M., Meuth, M., Andrews, P.W. & Nouspikel, T. 2012, "Deficient DNA damage response and cell cycle checkpoints lead to accumulation of point mutations in human embryonic stem cells", *Stem cells (Dayton, Ohio),* vol. 30, no. 9, pp. 1901-1910.

Ikeno, M. & Suzuki, N. 2011, "Construction and use of a bottom-up HAC vector for transgene expression" in *Mammalian Chromosome Engineering* Springer, , pp. 101-110.

Im, M.J., Russell, M.A. & Feng, J.F. 1997, "Transglutaminase II: a new class of GTP-binding protein with new biological functions", *Cellular signalling,* vol. 9, no. 7, pp. 477-482.

Ip, S.C., Rass, U., Blanco, M.G., Flynn, H.R., Skehel, J.M. & West, S.C. 2008, "Identification of Holliday junction resolvases from humans and yeast", *Nature,* vol. 456, no. 7220, pp. 357-361.

Iwasaki, H. 2014, "Leukemia stem cell", *Gan to kagaku ryoho.Cancer & chemotherapy,* vol. 41, no. 3, pp. 280-284.

Jaco, I., Canela, A., Vera, E. & Blasco, M.A. 2008, "Centromere mitotic recombination in mammalian cells", *The Journal of cell biology,* vol. 181, no. 6, pp. 885.

Jansen, L.E., Black, B.E., Foltz, D.R. & Cleveland, D.W. 2007, "Propagation of centromeric chromatin requires exit from mitosis", *The Journal of cell biology,* vol. 176, no. 6, pp. 795-805.

Kamakaka, R.T. & Biggins, S. 2005, "Histone variants: deviants?", *Genes & development,* vol. 19, no. 3, pp. 295-310.

Kanwar, S.S., Yu, Y., Nautiyal, J., Patel, B.B. & Majumdar, A.P. 2010, "The Wnt/β-catenin pathway regulates growth and maintenance of colonospheres", *Molecular cancer,* vol. 9, no. 1, pp. 212.

Kasparek, T.R. & Humphrey, T.C. 2011, "DNA double-strand break repair pathways, chromosomal rearrangements and cancer", *Seminars in cell & developmental biology*Elsevier, , pp. 886.

Kastan, M.B. & Bartek, J. 2004, "Cell-cycle checkpoints and cancer", *Nature,* vol. 432, no. 7015, pp. 316-323.

Kato, T., Sato, N., Hayama, S., Yamabuki, T., Ito, T., Miyamoto, M., Kondo, S., Nakamura, Y. & Daigo, Y. 2007, "Activation of Holliday junction recognizing protein involved in the chromosomal stability and immortality of cancer cells", *Cancer research,* vol. 67, no. 18, pp. 8544-8553.

Kelland, K. 2014, *Archaeologists discover earliest example of human with cancer*, Reuters, London.

Kidder, B.L., Hu, G. & Zhao, K. 2014, "KDM5B focuses H3K4 methylation near promoters and enhancers during embryonic stem cell self-renewal and differentiation", *Genome biology,* vol. 15, no. 2, pp. R32-2014-15-2-r32.

Killen, M.W., Stults, D.M., Adachi, N., Hanakahi, L. & Pierce, A.J. 2009, "Loss of Bloom syndrome protein destabilizes human gene cluster architecture", *Human molecular genetics,* vol. 18, no. 18, pp. 3417-3428.

Kim, J.B., Greber, B., Araúzo-Bravo, M.J., Meyer, J., Park, K.I., Zaehres, H. & Schöler, H.R. 2009, "Direct reprogramming of human neural stem cells by OCT4", *Nature,* vol. 461, no. 7264, pp. 649-653.

Kim, S.M., Dubey, D.D. & Huberman, J.A. 2003, "Early-replicating heterochromatin", *Genes & development*, vol. 17, no. 3, pp. 330.

Kim, Y., Spitz, G.S., Veturi, U., Lach, F.P., Auerbach, A.D. & Smogorzewska, A. 2013, "Regulation of multiple DNA repair pathways by the Fanconi anemia protein SLX4", *Blood*, vol. 121, no. 1, pp. 54-63.

Kitagishi, Y., Kobayashi, M. & Matsuda, S. 2013, "DNA Repair Molecules and Cancer Therapeutical Responses", *Oncogene and Cancer-From Bench to Clinic*, , pp. 117.

Koledova, Z., Kafkova, L.R., Krämer, A. & Divoky, V. 2010, "DNA Damage-Induced Degradation of Cdc25A Does Not Lead to Inhibition of Cdk2 Activity in Mouse Embryonic Stem Cells", *Stem cells*, vol. 28, no. 3, pp. 450-461.

Kops, G.J., Weaver, B.A. & Cleveland, D.W. 2005, "On the road to cancer: aneuploidy and the mitotic checkpoint", *Nature Reviews Cancer*, vol. 5, no. 10, pp. 773-785.

Kormann, M.S., Hasenpusch, G., Aneja, M.K., Nica, G., Flemmer, A.W., Herber-Jonat, S., Huppmann, M., Mays, L.E., Illenyi, M. & Schams, A. 2011, "Expression of therapeutic proteins after delivery of chemically modified mRNA in mice", *Nature biotechnology*, vol. 29, no. 2, pp. 154-157.

Kouprina, N., Earnshaw, W.C., Masumoto, H. & Larionov, V. 2013, "A new generation of human artificial chromosomes for functional genomics and gene therapy", *Cellular and Molecular Life Sciences*, vol. 70, no. 7, pp. 1135-1148.

Kouprina, N., Samoshkin, A., Erliandri, I., Nakano, M., Lee, H., Fu, H., Iida, Y., Aladjem, M., Oshimura, M. & Masumoto, H. 2012, "Organization of synthetic alphoid DNA array in human artificial chromosome (HAC) with a conditional centromere", *ACS synthetic biology*, vol. 1, no. 12, pp. 590-601.

Krejci, L., Altmannova, V., Spirek, M. & Zhao, X. 2012, "Homologous recombination and its regulation", *Nucleic acids research*, vol. 40, no. 13, pp. 5795-5818.

Krokan, H.E. & Bjoras, M. 2013, "Base excision repair", *Cold Spring Harbor perspectives in biology*, vol. 5, no. 4, pp. a012583.

Kronja, I. & Orr-Weaver, T.L. 2011, "Translational regulation of the cell cycle: when, where, how and why?", *Philosophical transactions of the Royal Society of London.Series B, Biological sciences*, vol. 366, no. 1584, pp. 3638-3652.

Kuo, L.J. & Yang, L.X. 2008, "Gamma-H2AX - a novel biomarker for DNA double-strand breaks", *In vivo (Athens, Greece)*, vol. 22, no. 3, pp. 305-309.

Ladomery, M. 2013, "Aberrant alternative splicing is another hallmark of cancer", *International journal of cell biology*, vol. 2013.

LaFave, M.C. & Sekelsky, J. 2009, "Mitotic Recombination: Why? When? How? Where?", *PLoS Genetics,* vol. 5, no. 3, pp. e1000411.

Larissa, J.V., Jakub, K.F. & Gordon, K. 2011, "hZwint-1 bridges the inner and outer kinetochore: identification of the kinetochore localization domain and the hZw10-interaction domain", *Biochemical Journal,* vol. 436, no. 1, pp. 157-168.

Larsson, L. 2011, "Oncogene-and tumor suppressor gene-mediated suppression of cellular senescence", *Seminars in cancer biology*Elsevier, , pp. 367.

Lee, J., Smith, E. & Shilatifard, A. 2010, "The language of histone crosstalk", *Cell,* vol. 142, no. 5, pp. 682-685.

Lee, A.J. & Swanton, C. 2012, "Tumour heterogeneity and drug resistance: personalising cancer medicine through functional genomics", *Biochemical pharmacology,* vol. 83, no. 8, pp. 1013-1020.

Lehmann, A.R. 2011, "DNA polymerases and repair synthesis in NER in human cells", *DNA repair,* vol. 10, no. 7, pp. 730-733.

Li, H., Collado, M., Villasante, A., Strati, K., Ortega, S., Cañamero, M., Blasco, M.A. & Serrano, M. 2009, "The Ink4/Arf locus is a barrier for iPS cell reprogramming", *Nature,* vol. 460, no. 7259, pp. 1136-1139.

Li, P., Kuo, T., Chang, J., Yeh, J. & Chan, W. 2010, "Induction of cytotoxicity and apoptosis in mouse blastocysts by silver nanoparticles", *Toxicology letters,* vol. 197, no. 2, pp. 82-87.

Li, Y. & Zhang, T. 2014, "Targeting cancer stem cells by curcumin and clinical applications", *Cancer letters,* vol. 346, no. 2, pp. 197-205.

Lieber, M.R., Lu, H., Gu, J. & Schwarz, K. 2007, "Flexibility in the order of action and in the enzymology of the nuclease, polymerases, and ligase of vertebrate non-homologous DNA end joining: relevance to cancer, aging, and the immune system", *Cell research,* vol. 18, no. 1, pp. 125-133.

Liebman, S.W., Symington, L.S. & Petes, T.D. 1988, "Mitotic recombination within the centromere of a yeast chromosome", *Science (New York, N.Y.),* vol. 241, no. 4869, pp. 1074-1077.

Lin, S. & Ying, S. 2013, "Mechanism and method for generating tumor-free iPS cells using intronic microRNA miR-302 induction" in *MicroRNA Protocols* Springer, , pp. 295-312.

Liu, Y., Gaines, W.A., Callender, T., Busygina, V., Oke, A., Sung, P., Fung, J.C. & Hollingsworth, N.M. 2014a, "Down-regulation of Rad51 activity during meiosis in yeast prevents competition with Dmc1 for repair of double-strand breaks", *PLoS genetics,* vol. 10, no. 1, pp. e1004005.

Liu, Y., Nielsen, C.F., Yao, Q. & Hickson, I.D. 2014b, "The origins and processing of ultra fine anaphase DNA bridges", *Current opinion in genetics & development,* vol. 26, pp. 1-5.

Liu, J.C., Lerou, P.H. & Lahav, G. 2014, "Stem cells: balancing resistance and sensitivity to DNA damage", *Trends in cell biology,* vol. 24, no. 5, pp. 268-274.

Liu, X., Weaver, E.M. & Hummon, A.B. 2013, "Evaluation of therapeutics in three-dimensional cell culture systems by MALDI imaging mass spectrometry", *Analytical Chemistry,* vol. 85, no. 13, pp. 6295-6302.

Lord, C.J. & Ashworth, A. 2012, "The DNA damage response and cancer therapy", *Nature,* vol. 481, no. 7381, pp. 287-294.

Lossaint, G., Besnard, E., Fisher, D., Piette, J. & Dulic, V. 2011, "Chk1 is dispensable for G2 arrest in response to sustained DNA damage when the ATM/p53/p21 pathway is functional", *Oncogene,* vol. 30, no. 41, pp. 4261-4274.

Luger, K., Dechassa, M.L. & Tremethick, D.J. 2012, "New insights into nucleosome and chromatin structure: an ordered state or a disordered affair?", *Nature Reviews Molecular Cell Biology,* vol. 13, no. 7, pp. 436-447.

Lundholm, L., Hååg, P., Zong, D., Juntti, T., Mörk, B., Lewensohn, R. & Viktorsson, K. 2013, "Resistance to DNA-damaging treatment in non-small cell lung cancer tumor-initiating cells involves reduced DNA-PK/ATM activation and diminished cell cycle arrest", *Cell death & disease,* vol. 4, no. 1, pp. e478.

Mahaney, B.L., Hammel, M., Meek, K., Tainer, J.A. & Lees-Miller, S.P. 2013, "XRCC4 and XLF form long helical protein filaments suitable for DNA end protection and alignment to facilitate DNA double strand break repair 1", *Biochemistry and Cell Biology,* vol. 91, no. 1, pp. 31-41.

Malanchi, I. 2013, "Tumour cells coerce host tissue to cancer spread", *BoneKEy reports,* vol. 2.

Malik, N. & Rao, M.S. 2013, "A review of the methods for human iPSC derivation" in *Pluripotent Stem Cells* Springer, , pp. 23-33.

Mandal, P.K. & Rossi, D.J. 2013, "Reprogramming human fibroblasts to pluripotency using modified mRNA", *Nature protocols,* vol. 8, no. 3, pp. 568-582.

Mani, S.A., Guo, W., Liao, M., Eaton, E.N., Ayyanan, A., Zhou, A.Y., Brooks, M., Reinhard, F., Zhang, C.C. & Shipitsin, M. 2008, "The epithelial-mesenchymal transition generates cells with properties of stem cells", *Cell,* vol. 133, no. 4, pp. 704-715.

Mankouri, H.W., Huttner, D. & Hickson, I.D. 2013, "How unfinished business from S-phase affects mitosis and beyond", *The EMBO journal,* vol. 32, no. 20, pp. 2661-2671.

Marechal, A. & Zou, L. 2013, "DNA damage sensing by the ATM and ATR kinases", *Cold Spring Harbor perspectives in biology,* vol. 5, no. 9, pp. 10.1101/cshperspect.a012716.

Mariño-Ramírez, L., Kann, M.G., Shoemaker, B.A. & Landsman, D. 2005, "Histone structure and nucleosome stability", .

Marshall, O.J., Chueh, A.C., Wong, L.H. & Choo, K. 2008, "Neocentromeres: new insights into centromere structure, disease development, and karyotype evolution", *The American Journal of Human Genetics,* vol. 82, no. 2, pp. 261-282.

Marteijn, J.A., Lans, H., Vermeulen, W. & Hoeijmakers, J.H. 2014, "Understanding nucleotide excision repair and its roles in cancer and ageing", *Nature Reviews Molecular Cell Biology,* vol. 15, no. 7, pp. 465-481.

Mathews, L.A., Cabarcas, S.M. & Farrar, W.L. 2011, "DNA repair: the culprit for tumor-initiating cell survival?", *Cancer and metastasis reviews,* vol. 30, no. 2, pp. 185-197.

Mathews, L.A., Cabarcas, S.M. & Hurt, E.M. 2013, *DNA repair of cancer stem cells,* Springer.

Maugeri-Sacca, M., Bartucci, M. & De Maria, R. 2012, "DNA damage repair pathways in cancer stem cells", *Molecular cancer therapeutics,* vol. 11, no. 8, pp. 1627-1636.

Maynard, S., Swistowska, A.M., Lee, J.W., Liu, Y., Liu, S., Da Cruz, A.B., Rao, M., de Souza-Pinto, N.C., Zeng, X. & Bohr, V.A. 2008, "Human embryonic stem cells have enhanced repair of multiple forms of DNA damage", *Stem cells,* vol. 26, no. 9, pp. 2266-2274.

Mazin, A.V., Mazina, O.M., Bugreev, D.V. & Rossi, M.J. 2010, "Rad54, the motor of homologous recombination", *DNA repair,* vol. 9, no. 3, pp. 286-302.

McFarlane, R.J. & Humphrey, T.C. 2010, "A role for recombination in centromere function", *Trends in genetics,* vol. 26, no. 5, pp. 209-213.

McGranahan, N., Burrell, R.A., Endesfelder, D., Novelli, M.R. & Swanton, C. 2012, "Cancer chromosomal instability: therapeutic and diagnostic challenges", *EMBO reports,* vol. 13, no. 6, pp. 528-538.

McMurray, C.T. 2010, "Mechanisms of trinucleotide repeat instability during human development", *Nature Reviews Genetics,* vol. 11, no. 11, pp. 786-799.

McVey, M., Larocque, J.R., Adams, M.D. & Sekelsky, J.J. 2004, "Formation of deletions during double-strand break repair in Drosophila DmBlm mutants occurs after strand invasion", *Proceedings of the National Academy of Sciences of the United States of America,* vol. 101, no. 44, pp. 15694-15699.

Mehta, G.D., Agarwal, M.P. & Ghosh, S.K. 2010, "Centromere identity: a challenge to be faced", *Molecular Genetics and Genomics*, vol. 284, no. 2, pp. 75-94.

Mehta, A. & Haber, J.E. 2014, "Sources of DNA Double-Strand Breaks and Models of Recombinational DNA Repair", *Cold Spring Harbor perspectives in biology,* vol. 6, no. 9, pp. 10.1101/cshperspect.a016428.

Middel, V. & Blattner, C. 2011, *DNA Repair in Embryonic Stem Cells*, INTECH Open Access Publisher.

Mignone, J.L., Kreutziger, K.L., Paige, S.L. & Murry, C.E. 2010, "Cardiogenesis from human embryonic stem cells", *Circulation journal : official journal of the Japanese Circulation Society*, vol. 74, no. 12, pp. 2517-2526.

Mohanty, C., Fayad, W., Olofsson, M.H., Larsson, R., De Milito, A., Fryknäs, M. & Linder, S.T. 2013, "Massive induction of apoptosis of multicellular tumor spheroids by a novel compound with a calmodulin inhibitor-like mechanism", *journal of cancer therapeutics and research,* vol. 2, no. 1, pp. 19.

Momcilovic, O., Knobloch, L., Fornsaglio, J., Varum, S., Easley, C. & Schatten, G. 2010, "DNA damage responses in human induced pluripotent stem cells and embryonic stem cells", *PloS one,* vol. 5, no. 10, pp. e13410.

Momcilovic, O., Choi, S., Varum, S., Bakkenist, C., Schatten, G. & Navara, C. 2009, "Ionizing radiation induces ataxia telangiectasia mutated-dependent checkpoint signaling and G(2) but not G(1) cell cycle arrest in pluripotent human embryonic stem cells", *Stem cells (Dayton, Ohio),* vol. 27, no. 8, pp. 1822-1835.

Moralli, D., Jefferson, A., Volpi, E.V. & Monaco, Z.L. 2013, "Comparative study of artificial chromosome centromeres in human and murine cells", *European Journal of Human Genetics,* vol. 21, no. 9, pp. 948-956.

Moynahan, M.E. & Jasin, M. 2010, "Mitotic homologous recombination maintains genomic stability and suppresses tumorigenesis", *Nature reviews Molecular cell biology*, vol. 11, no. 3, pp. 196-207.

Mukherjee, S., Wright, W.D., Ehmsen, K.T. & Heyer, W.D. 2014, "The Mus81-Mms4 structure-selective endonuclease requires nicked DNA junctions to undergo conformational changes and bend its DNA substrates for cleavage", *Nucleic acids research,* vol. 42, no. 10, pp. 6511-6522.

Muller, P.A. & Vousden, K.H. 2013, "p53 mutations in cancer", *Nature cell biology,* vol. 15, no. 1, pp. 2-8.

Munoz, P., Iliou, M.S. & Esteller, M. 2012, "Epigenetic alterations involved in cancer stem cell reprogramming", *Molecular oncology,* vol. 6, no. 6, pp. 620-636.

Munz, P., Amstutz, H., Kohli, J. & Leupold, U. 1982, "Recombination between dispersed serine tRNA genes in Schizosaccharomyces pombe", .

Neganova, I., Vilella, F., Atkinson, S.P., Lloret, M., Passos, J.F., von Zglinicki, T., O'Connor, J., Burks, D., Jones, R. & Armstrong, L. 2011, "An important role for CDK2 in G1 to S checkpoint activation and DNA damage response in human embryonic stem cells", *Stem cells,* vol. 29, no. 4, pp. 651-659.

Nickson, C.M. & Parsons, J.L. 2014, "Monitoring regulation of DNA repair activities of cultured cells in-gel using the comet assay", *Frontiers in genetics,* vol. 5.

Nimonkar, A.V., Özsoy, A.Z., Genschel, J., Modrich, P. & Kowalczykowski, S.C. 2008, "Human exonuclease 1 and BLM helicase interact to resect DNA and initiate DNA repair", *Proceedings of the National Academy of Sciences,* vol. 105, no. 44, pp. 16906-16911.

Nishimura, Y., Mieda, H., Ishii, J., Ogino, C., Fujiwara, T. & Kondo, A. 2013, "Targeting cancer cell-specific RNA interference by siRNA delivery using a complex carrier of affibody-displaying bio-nanocapsules and liposomes", *Journal of nanobiotechnology,* vol. 11, pp. 19-3155-11-19.

O'Farrell, P.H. 2011, "Quiescence: early evolutionary origins and universality do not imply uniformity", *Philosophical transactions of the Royal Society of London.Series B, Biological sciences,* vol. 366, no. 1584, pp. 3498-3507.

OGURO, M., SUZUKI-HORI, C., NAGANO, H., MANO, Y. & Ikegami, S. 1979, "The mode of inhibitory action by aphidicolin on eukaryotic DNA polymerase α", *European Journal of Biochemistry,* vol. 97, no. 2, pp. 603-607.

Oltean, S. & Bates, D. 2013, "Hallmarks of alternative splicing in cancer", *Oncogene,* .

Oum, J.H., Seong, C., Kwon, Y., Ji, J.H., Sid, A., Ramakrishnan, S., Ira, G., Malkova, A., Sung, P., Lee, S.E. & Shim, E.Y. 2011, "RSC facilitates Rad59-dependent homologous recombination between sister chromatids by promoting cohesin loading at DNA double-strand breaks", *Molecular and cellular biology,* vol. 31, no. 19, pp. 3924-3937.

Ouyang, K.J., Yagle, M.K., Matunis, M.J. & Ellis, N.A. 2013, "BLM SUMOylation regulates ssDNA accumulation at stalled replication forks", *Frontiers in genetics,* vol. 4.

Padmanabhan, R., Chen, K.G., Gillet, J., Handley, M., Mallon, B.S., Hamilton, R.S., Park, K., Varma, S., Mehaffey, M.G. & Robey, P.G. 2012, "Regulation and Expression of the ATP-Binding Cassette Transporter ABCG2 in Human Embryonic Stem Cells", *Stem cells,* vol. 30, no. 10, pp. 2175-2187.

Pampaloni, F., Stelzer, E.H. & Masotti, A. 2009, "Three-dimensional tissue models for drug discovery and toxicology", *Recent patents on biotechnology,* vol. 3, no. 2, pp. 103-117.

Park, C. & Kim, K. 2012, "Apoptotic Phosphorylation of Histone H3 on Ser-10 by Protein Kinase Cδ", *PloS one,* vol. 7, no. 9, pp. e44307.

Park, C.Y., Tseng, D. & Weissman, I.L. 2009, "Cancer stem cell–directed therapies: recent data from the laboratory and clinic", *Molecular Therapy,* vol. 17, no. 2, pp. 219-230.

Pasi, C.E., Dereli-Oz, A., Negrini, S., Friedli, M., Fragola, G., Lombardo, A., Van Houwe, G., Naldini, L., Casola, S., Testa, G., Trono, D., Pelicci, P.G. & Halazonetis, T.D. 2011, "Genomic instability in induced stem cells", *Cell death and differentiation,* vol. 18, no. 5, pp. 745-753.

Pauleau, A. & Erhardt, S. 2011, "Centromere regulation: new players, new rules, new questions", *European journal of cell biology,* vol. 90, no. 10, pp. 805-810.

Peitz, M., Münst, B., Thummer, R.P., Helfen, M. & Edenhofer, F. 2014, "Cell-permeant recombinant Nanog protein promotes pluripotency by inhibiting endodermal specification", *Stem cell research,* vol. 12, no. 3, pp. 680-689.

Peña-Diaz, J. & Jiricny, J. 2012, "Mammalian mismatch repair: error-free or error-prone?", *Trends in biochemical sciences,* vol. 37, no. 5, pp. 206-214.

Peng, G. & Lin, S.Y. 2011, "Exploiting the homologous recombination DNA repair network for targeted cancer therapy", *World journal of clinical oncology,* vol. 2, no. 2, pp. 73-79.

Pepe, A. & West, S.C. 2014, "MUS81-EME2 Promotes Replication Fork Restart", *Cell reports,* vol. 7, no. 4, pp. 1048-1055.

Peserico, A. & Simone, C. 2011, "Physical and functional HAT/HDAC interplay regulates protein acetylation balance", *Journal of biomedicine & biotechnology,* vol. 2011, pp. 371832.

Peter W. Andrews 2006, "TERA2 and Its NTERA2 Subline: Pluripotent Human Embryonal Carcinoma Cells", *Cell Biology: A Laboratory Handbook,* vol. 1, pp. 183.

Petruseva, I., Evdokimov, A. & Lavrik, O. 2014, "Molecular Mechanism of Global Genome Nucleotide Excision Repair", *Acta naturae,* vol. 6, no. 1, pp. 23.

Pidoux, A.L. & Allshire, R.C. 2005, "The role of heterochromatin in centromere function", *Philosophical transactions of the Royal Society of London.Series B, Biological sciences,* vol. 360, no. 1455, pp. 569-579.

Podhorecka, M., Skladanowski, A. & Bozko, P. 2010, "H2AX Phosphorylation: Its Role in DNA Damage Response and Cancer Therapy", *Journal of nucleic acids*, vol. 2010, pp. 10.4061/2010/920161.

Polo, S.E. & Jackson, S.P. 2011, "Dynamics of DNA damage response proteins at DNA breaks: a focus on protein modifications", *Genes & development*, vol. 25, no. 5, pp. 409-433.

Price, J.D., Park, K.Y., Chen, J., Salinas, R.D., Cho, M.J., Kriegstein, A.R. & Lim, D.A. 2014, "The ink4a/arf locus is a barrier to direct neuronal transdifferentiation", *The Journal of neuroscience : the official journal of the Society for Neuroscience*, vol. 34, no. 37, pp. 12560-12567.

Puglisi, M.A., Tesori, V., Lattanzi, W., Gasbarrini, G.B. & Gasbarrini, A. 2013, "Colon cancer stem cells: Controversies and perspectives", *World journal of gastroenterology: WJG*, vol. 19, no. 20, pp. 2997.

Qin, H., Yu, T., Qing, T., Liu, Y., Zhao, Y., Cai, J., Li, J., Song, Z., Qu, X., Zhou, P., Wu, J., Ding, M. & Deng, H. 2007, "Regulation of apoptosis and differentiation by p53 in human embryonic stem cells", *The Journal of biological chemistry*, vol. 282, no. 8, pp. 5842-5852.

Rao, G., Liu, H., Li, B., Hao, J., Yang, Y., Wang, M., Wang, X., Wang, J., Jin, H. & Du, L. 2013, "Establishment of a human colorectal cancer cell line P6C with stem cell properties and resistance to chemotherapeutic drugs", *Acta Pharmacologica Sinica*, vol. 34, no. 6, pp. 793-804.

Rawlinson, R. & Massey, A.J. 2014, "gammaH2AX and Chk1 phosphorylation as predictive pharmacodynamic biomarkers of Chk1 inhibitor-chemotherapy combination treatments", *BMC cancer*, vol. 14, no. 1, pp. 483.

Regnier, V., Vagnarelli, P., Fukagawa, T., Zerjal, T., Burns, E., Trouche, D., Earnshaw, W. & Brown, W. 2005, "CENP-A is required for accurate chromosome segregation and sustained kinetochore association of BubR1", *Molecular and cellular biology*, vol. 25, no. 10, pp. 3967.

Rimoin, D.L., Pyeritz, R.E. & Korf, B. 2013, *Emery and Rimoin's principles and practice of medical genetics*, Academic Press.

Robertson, A., Klungland, A., Rognes, T. & Leiros, I. 2009, "DNA repair in mammalian cells", *Cellular and Molecular Life Sciences*, vol. 66, no. 6, pp. 981-993.

Robinton, D.A. & Daley, G.Q. 2012, "The promise of induced pluripotent stem cells in research and therapy", *Nature*, vol. 481, no. 7381, pp. 295-305.

Rocha, C.R.R., Lerner, L.K., Okamoto, O.K., Marchetto, M.C. & Menck, C.F.M. 2013, "The role of DNA repair in the pluripotency and differentiation of human stem cells", *Mutation Research/Reviews in Mutation Research*, vol. 752, no. 1, pp. 25-35.

Rochette, P.J., Bastien, N., Lavoie, J., Guerin, S.L. & Drouin, R. 2005, "SW480, a p53 double-mutant cell line retains proficiency for some p53 functions", *Journal of Molecular Biology*, vol. 352, no. 1, pp. 44-57.

Rodriguez-Rocha, H., Garcia-Garcia, A., Panayiotidis, M.I. & Franco, R. 2011, "DNA damage and autophagy", *Mutation Research/Fundamental and Molecular Mechanisms of Mutagenesis*, vol. 711, no. 1, pp. 158-166.

Rogakou, E.P., Boon, C., Redon, C. & Bonner, W.M. 1999, "Megabase chromatin domains involved in DNA double-strand breaks in vivo", *The Journal of cell biology*, vol. 146, no. 5, pp. 905-916.

Rountree, M. & Selker, E. 2010, "DNA methylation and the formation of heterochromatin in Neurospora crassa", *Heredity*, vol. 105, no. 1, pp. 38-44.

Rousseaux, S., Debernardi, A., Jacquiau, B., Vitte, A.L., Vesin, A., Nagy-Mignotte, H., Moro-Sibilot, D., Brichon, P.Y., Lantuejoul, S., Hainaut, P., Laffaire, J., de Reynies, A., Beer, D.G., Timsit, J.F., Brambilla, C., Brambilla, E. & Khochbin, S. 2013, "Ectopic activation of germline and placental genes identifies aggressive metastasis-prone lung cancers", *Science translational medicine*, vol. 5, no. 186, pp. 186ra66.

Rusche, L.N. & Rine, J. 2010, "Switching the mechanism of mating type switching: a domesticated transposase supplants a domesticated homing endonuclease", *Genes & development*, vol. 24, no. 1, pp. 10-14.

Sammut, J., Wakeman, J., Stuart, N. & McFarlane, R. 2013, "Cancer/Testis Antigens and Colorectal Cancer", *J Genet Syndr Gene Ther*, vol. 4, no. 149, pp. 2.

Sanchez-Pulido, L., Pidoux, A.L., Ponting, C.P. & Allshire, R.C. 2009, "Common ancestry of the CENP-A chaperones Scm3 and HJURP.", *Cell*, vol. 137, no. 7, pp. 1173.

Sarbajna, S. & West, S.C. 2014, "Holliday junction processing enzymes as guardians of genome stability", *Trends in biochemical sciences*, .

Saretzki, G., Walter, T., Atkinson, S., Passos, J.F., Bareth, B., Keith, W.N., Stewart, R., Hoare, S., Stojkovic, M. & Armstrong, L. 2008, "Downregulation of multiple stress defense mechanisms during differentiation of human embryonic stem cells", *Stem cells*, vol. 26, no. 2, pp. 455-464.

Sartori, A.A., Lukas, C., Coates, J., Mistrik, M., Fu, S., Bartek, J., Baer, R., Lukas, J. & Jackson, S.P. 2007, "Human CtIP promotes DNA end resection", *Nature*, vol. 450, no. 7169, pp. 509-514.

Sarvi, S., Mackinnon, A.C., Avlonitis, N., Bradley, M., Rintoul, R.C., Rassl, D.M., Wang, W., Forbes, S.J., Gregory, C.D. & Sethi, T. 2014, "CD133+ cancer stem-like cells in small cell lung cancer are highly tumorigenic and chemoresistant but sensitive to a novel neuropeptide antagonist", *Cancer research*, vol. 74, no. 5, pp. 1554-1565.

Schueler, M.G. & Sullivan, B.A. 2006, "Structural and functional dynamics of human centromeric chromatin", *Annu.Rev.Genomics Hum.Genet.*, vol. 7, pp. 301-313.

Scott, A.M., Wolchok, J.D. & Old, L.J. 2012, "Antibody therapy of cancer", *Nature Reviews Cancer*, vol. 12, no. 4, pp. 278-287.

Scott, K.C., White, C.V. & Willard, H.F. 2007, "An RNA polymerase III-dependent heterochromatin barrier at fission yeast centromere 1", *PLoS One*, vol. 2, no. 10, pp. e1099.

Sekulic, N., Bassett, E.A., Rogers, D.J. & Black, B.E. 2010, "The structure of (CENP-A-H4) 2 reveals physical features that mark centromeres", *Nature*, vol. 467, no. 7313, pp. 347-351.

Sela, Y., Molotski, N., Golan, S., Itskovitz-Eldor, J. & Soen, Y. 2012, "Human embryonic stem cells exhibit increased propensity to differentiate during the G1 phase prior to phosphorylation of retinoblastoma protein", *Stem cells (Dayton, Ohio)*, vol. 30, no. 6, pp. 1097-1108.

Shammas, M.A., Shmookler Reis, R.J., Koley, H., Batchu, R.B., Li, C. & Munshi, N.C. 2009, "Dysfunctional homologous recombination mediates genomic instability and progression in myeloma", *Blood*, vol. 113, no. 10, pp. 2290-2297.

Shimono, Y., Zabala, M., Cho, R.W., Lobo, N., Dalerba, P., Qian, D., Diehn, M., Liu, H., Panula, S.P. & Chiao, E. 2009, "Downregulation of miRNA-200c links breast cancer stem cells with normal stem cells", *Cell*, vol. 138, no. 3, pp. 592-603.

Siegel, R., Naishadham, D. & Jemal, A. 2013, "Cancer statistics, 2013", *CA: a cancer journal for clinicians*, vol. 63, no. 1, pp. 11-30.

Singh, A.M. & Dalton, S. 2014, "Cell Cycle Regulation of Pluripotent Stem Cells", *Stem Cells: From Basic Research to Therapy: Basic Stem Cell Biology, Tissue Formation during Development, and Model Organisms*, vol. 1, pp. 3.

Sliwkowski, M.X. & Mellman, I. 2013, "Antibody therapeutics in cancer", *Science (New York, N.Y.)*, vol. 341, no. 6151, pp. 1192-1198.

Soltysova, A., Altanerova, V. & Altaner, C. 2005, "Cancer stem cells", *Neoplasma*, vol. 52, no. 6, pp. 435.

Sonoda, E., Sasaki, M.S., Morrison, C., Yamaguchi-Iwai, Y., Takata, M. & Takeda, S. 1999, "Sister chromatid exchanges are mediated by homologous recombination in vertebrate cells", *Molecular and cellular biology*, vol. 19, no. 7, pp. 5166-5169.

Sorensen, C.S. & Syljuasen, R.G. 2012, "Safeguarding genome integrity: the checkpoint kinases ATR, CHK1 and WEE1 restrain CDK activity during normal DNA replication", *Nucleic acids research*, vol. 40, no. 2, pp. 477-486.

Stellfox, M.E., Bailey, A.O. & Foltz, D.R. 2013, "Putting CENP-A in its place", *Cellular and Molecular Life Sciences*, vol. 70, no. 3, pp. 387-406.

Stern, C. 1936, "Somatic crossing over and segregation in Drosophila melanogaster", *Genetics*, vol. 21, no. 6, pp. 625.

Stowell, A., Hamilton, N., Hitchin, J., Blagg, J., Burke, R., Burns, S., Cockerill, M.J., Fairweather, E., Hutton, C. & Jordan, A. 2013, "Abstract B98: Development and evaluation of selective, reversible LSD1 inhibitors from fragment startpoints.", *Molecular Cancer Therapeutics*, vol. 12, no. 11 Supplement, pp. B98-B98.

Stults, D.M., Killen, M.W. & Pierce, A.J. 2014, "The Sister Chromatid Exchange (SCE) Assay" in *Molecular Toxicology Protocols* Springer, , pp. 439-455.

Stults, D.M., Killen, M.W., Shelton, B.J. & Pierce, A.J. 2011, "Recombination phenotypes of the NCI-60 collection of human cancer cells", *BMC molecular biology*, vol. 12, pp. 23-2199-12-23.

Sullivan, Y.B., Narahari, J., Hughes, D.E. & Webb, B.L. 2008, "Validation of antibody specificity using RNA Interference", *The FASEB Journal*, vol. 22, pp. 1070.25.

Tabar, V. & Studer, L. 2014, "Pluripotent stem cells in regenerative medicine: challenges and recent progress", *Nature Reviews Genetics*, vol. 15, no. 2, pp. 82-92.

Tachiwana, H., Kagawa, W., Shiga, T., Osakabe, A., Miya, Y., Saito, K., Hayashi-Takanaka, Y., Oda, T., Sato, M. & Park, S. 2011, "Crystal structure of the human centromeric nucleosome containing CENP-A", *Nature*, vol. 476, no. 7359, pp. 232-235.

Takahashi, K. & Yamanaka, S. 2006, "Induction of pluripotent stem cells from mouse embryonic and adult fibroblast cultures by defined factors", *Cell*, vol. 126, no. 4, pp. 663-676.

Takahashi, K. & Yamanaka, S. 2013, "Induced pluripotent stem cells in medicine and biology", *Development (Cambridge, England)*, vol. 140, no. 12, pp. 2457-2461.

Takahashi, R.U., Miyazaki, H. & Ochiya, T. 2014, "The role of microRNAs in the regulation of cancer stem cells", *Frontiers in genetics*, vol. 4, pp. 295.

Takebe, N., Harris, P.J., Warren, R.Q. & Ivy, S.P. 2011, "Targeting cancer stem cells by inhibiting Wnt, Notch, and Hedgehog pathways", *Nature reviews Clinical oncology*, vol. 8, no. 2, pp. 97-106.

Talbert, P.B. & Henikoff, S. 2010, "Histone variants—ancient wrap artists of the epigenome", *Nature reviews Molecular cell biology*, vol. 11, no. 4, pp. 264-275.

Tamm, C., Bower, N. & Anneren, C. 2011, "Regulation of mouse embryonic stem cell self-renewal by a Yes-YAP-TEAD2 signaling pathway downstream of LIF", *Journal of cell science,* vol. 124, no. Pt 7, pp. 1136-1144.

Tannock, I.F., Lee, C.M., Tunggal, J.K., Cowan, D.S. & Egorin, M.J. 2002, "Limited penetration of anticancer drugs through tumor tissue: a potential cause of resistance of solid tumors to chemotherapy", *Clinical cancer research : an official journal of the American Association for Cancer Research,* vol. 8, no. 3, pp. 878-884.

Tesauro, C., Morozzo della Rocca, B., Ottaviani, A., Coletta, A., Zuccaro, L., Arno, B., D'Annessa, I., Fiorani, P. & Desideri, A. 2013, "Molecular mechanism of the camptothecin resistance of Glu710Gly topoisomerase IB mutant analyzed in vitro and in silico", *Molecular cancer,* vol. 12, no. 1, pp. 100-4598-12-100.

Tichy, E.D., Pillai, R., Deng, L., Liang, L., Tischfield, J., Schwemberger, S.J., Babcock, G.F. & Stambrook, P.J. 2010, "Mouse embryonic stem cells, but not somatic cells, predominantly use homologous recombination to repair double-strand DNA breaks", *Stem cells and development,* vol. 19, no. 11, pp. 1699-1711.

Tichy, E.D. & Stambrook, P.J. 2008, "DNA repair in murine embryonic stem cells and differentiated cells", *Experimental cell research,* vol. 314, no. 9, pp. 1929-1936.

Tirino, V., Desiderio, V., Paino, F., De Rosa, A., Papaccio, F., La Noce, M., Laino, L., De Francesco, F. & Papaccio, G. 2013, "Cancer stem cells in solid tumors: an overview and new approaches for their isolation and characterization", *FASEB journal : official publication of the Federation of American Societies for Experimental Biology,* vol. 27, no. 1, pp. 13-24.

Todaro, M., Francipane, M.G., Medema, J.P. & Stassi, G. 2010, "Colon cancer stem cells: promise of targeted therapy", *Gastroenterology,* vol. 138, no. 6, pp. 2151-2162.

Turinetto, V., Orlando, L., Sanchez-Ripoll, Y., Kumpfmueller, B., Storm, M.P., Porcedda, P., Minieri, V., Saviozzi, S., Accomasso, L. & Cibrario Rocchietti, E. 2012, "High Basal γH2AX Levels Sustain Self-Renewal of Mouse Embryonic and Induced Pluripotent Stem Cells", *Stem cells,* vol. 30, no. 7, pp. 1414-1423.

Uringa, E.J., Youds, J.L., Lisaingo, K., Lansdorp, P.M. & Boulton, S.J. 2011, "RTEL1: an essential helicase for telomere maintenance and the regulation of homologous recombination", *Nucleic acids research,* vol. 39, no. 5, pp. 1647-1655.

van Kouwenhove, M., Kedde, M. & Agami, R. 2011, "MicroRNA regulation by RNA-binding proteins and its implications for cancer", *Nature Reviews Cancer,* vol. 11, no. 9, pp. 644-656.

Van Vliet, P., Wu, S.M., Zaffran, S. & Puceat, M. 2012, "Early cardiac development: a view from stem cells to embryos", *Cardiovascular research,* vol. 96, no. 3, pp. 352-362.

Ventura, A., Kirsch, D.G., McLaughlin, M.E., Tuveson, D.A., Grimm, J., Lintault, L., Newman, J., Reczek, E.E., Weissleder, R. & Jacks, T. 2007, "Restoration of p53 function leads to tumour regression in vivo", *Nature,* vol. 445, no. 7128, pp. 661-665.

Verdaasdonk, J.S. & Bloom, K. 2011, "Centromeres: unique chromatin structures that drive chromosome segregation", *Nature Reviews Molecular Cell Biology,* vol. 12, no. 5, pp. 320-332.

Vincent, A. & Van Seuningen, I. 2012, "On the epigenetic origin of cancer stem cells", *Biochimica et Biophysica Acta (BBA)-Reviews on Cancer,* vol. 1826, no. 1, pp. 83-88.

Voss, M.H., Feldman, D.R., Bosl, G.J. & Motzer, R.J. 2011, "A review of second-line chemotherapy and prognostic models for disseminated germ cell tumors", *Hematology/oncology clinics of North America,* vol. 25, no. 3, pp. 557-576.

Wang, D. & Lippard, S.J. 2005, "Cellular processing of platinum anticancer drugs", *Nature reviews Drug discovery,* vol. 4, no. 4, pp. 307-320.

Wang, J., Chen, J. & Gong, Z. 2013, "TopBP1 controls BLM protein level to maintain genome stability", *Molecular cell,* vol. 52, no. 5, pp. 667-678.

Wang, Y.C., Peterson, S.E. & Loring, J.F. 2014, "Protein post-translational modifications and regulation of pluripotency in human stem cells", *Cell research,* vol. 24, no. 2, pp. 143-160.

Warren, L., Manos, P.D., Ahfeldt, T., Loh, Y., Li, H., Lau, F., Ebina, W., Mandal, P.K., Smith, Z.D. & Meissner, A. 2010, "Highly efficient reprogramming to pluripotency and directed differentiation of human cells with synthetic modified mRNA", *Cell stem cell,* vol. 7, no. 5, pp. 618-630.

Waters, C.A., Strande, N.T., Wyatt, D.W., Pryor, J.M. & Ramsden, D.A. 2014, "Nonhomologous end joining: A good solution for bad ends", *DNA repair,* vol. 17, pp. 39-51.

Watt, F.M. & Driskell, R.R. 2010, "The therapeutic potential of stem cells", *Philosophical transactions of the Royal Society of London.Series B, Biological sciences,* vol. 365, no. 1537, pp. 155-163.

Wechsler, T., Newman, S. & West, S.C. 2011, "Aberrant chromosome morphology in human cells defective for Holliday junction resolution", *Nature,* vol. 471, no. 7340, pp. 642-646.

Wen, K., Fu, Z., Wu, X., Feng, J., Chen, W. & Qian, J. 2013, "Oct-4 is required for an antiapoptotic behavior of chemoresistant colorectal cancer cells enriched for

cancer stem cells: effects associated with STAT3/Survivin", *Cancer letters*, vol. 333, no. 1, pp. 56-65.

Werengowska-Ciećwierz, K., Wiśniewski, M., Terzyk, A.P., Gurtowska, N., Olkowska, J., Kloskowski, T., Drewa, T.A., Kiełkowska, U. & Drużyński, S. 2014, "Nanotube-mediated efficiency of cisplatin anticancer therapy", *Carbon*, vol. 70, pp. 46-58.

Whitby, M.C. 2005, "Making crossovers during meiosis", *Biochemical Society transactions*, vol. 33, no. Pt 6, pp. 1451-1455.

Williams, G.H. & Stoeber, K. 2012, "The cell cycle and cancer", *The Journal of pathology*, vol. 226, no. 2, pp. 352-364.

Win, A.K., Young, J.P., Lindor, N.M., Tucker, K.M., Ahnen, D.J., Young, G.P., Buchanan, D.D., Clendenning, M., Giles, G.G., Winship, I., Macrae, F.A., Goldblatt, J., Southey, M.C., Arnold, J., Thibodeau, S.N., Gunawardena, S.R., Bapat, B., Baron, J.A., Casey, G., Gallinger, S., Le Marchand, L., Newcomb, P.A., Haile, R.W., Hopper, J.L. & Jenkins, M.A. 2012, "Colorectal and other cancer risks for carriers and noncarriers from families with a DNA mismatch repair gene mutation: a prospective cohort study", *Journal of clinical oncology : official journal of the American Society of Clinical Oncology*, vol. 30, no. 9, pp. 958-964.

Wood, V., Gwilliam, R., Rajandream, M., Lyne, M., Lyne, R., Stewart, A., Sgouros, J., Peat, N., Hayles, J. & Baker, S. 2002, "The genome sequence of Schizosaccharomyces pombe", *Nature*, vol. 415, no. 6874, pp. 871-880.

Wu, H. & Choudhry, H. 2013, *Next Generation Sequencing in Cancer Research*, Springer.

Wu, K., House, L., Liu, W. & Cho, W. 2012, "Personalized targeted therapy for lung cancer", *International journal of molecular sciences*, vol. 13, no. 9, pp. 11471-11496.

Wu, J., Clingen, P.H., Spanswick, V.J., Mellinas-Gomez, M., Meyer, T., Puzanov, I., Jodrell, D., Hochhauser, D. & Hartley, J.A. 2013, "gamma-H2AX foci formation as a pharmacodynamic marker of DNA damage produced by DNA cross-linking agents: results from 2 phase I clinical trials of SJG-136 (SG2000)", *Clinical cancer research : an official journal of the American Association for Cancer Research*, vol. 19, no. 3, pp. 721-730.

Wyatt, H.D., Sarbajna, S., Matos, J. & West, S.C. 2013, "Coordinated actions of SLX1-SLX4 and MUS81-EME1 for Holliday junction resolution in human cells", *Molecular cell*, vol. 52, no. 2, pp. 234-247.

Xiang, S., Fruehauf, J. & Li, C.J. 2006, "Short hairpin RNA–expressing bacteria elicit RNA interference in mammals", *Nature biotechnology*, vol. 24, no. 6, pp. 697-702.

Xu, D., Muniandy, P., Leo, E., Yin, J., Thangavel, S., Shen, X., Ii, M., Agama, K., Guo, R. & Fox, D. 2010, "Rif1 provides a new DNA-binding interface for the Bloom syndrome complex to maintain normal replication", *The EMBO journal,* vol. 29, no. 18, pp. 3140-3155.

Yu, Z., Pestell, T.G., Lisanti, M.P. & Pestell, R.G. 2012, "Cancer stem cells", *The international journal of biochemistry & cell biology,* vol. 44, no. 12, pp. 2144-2151.

Zakharyevich, K., Tang, S., Ma, Y. & Hunter, N. 2012, "Delineation of joint molecule resolution pathways in meiosis identifies a crossover-specific resolvase", *Cell,* vol. 149, no. 2, pp. 334-347.

Zangi, L., Lui, K.O., von Gise, A., Ma, Q., Ebina, W., Ptaszek, L.M., Später, D., Xu, H., Tabebordbar, M. & Gorbatov, R. 2013, "Modified mRNA directs the fate of heart progenitor cells and induces vascular regeneration after myocardial infarction", *Nature biotechnology,* vol. 31, no. 10, pp. 898-907.

Zasadzińska, E., Barnhart-Dailey, M.C., Kuich, P.H.J. & Foltz, D.R. 2013, "Dimerization of the CENP-A assembly factor HJURP is required for centromeric nucleosome deposition", *The EMBO journal,* vol. 32, no. 15, pp. 2113-2124.

Zhang, Y. & Hunter, T. 2014, "Roles of Chk1 in cell biology and cancer therapy", *International journal of cancer.Journal international du cancer,* vol. 134, no. 5, pp. 1013-1023.

Zhao, Y., Alakhova, D.Y. & Kabanov, A.V. 2013, "Can nanomedicines kill cancer stem cells?", *Advanced Drug Delivery Reviews,* vol. 65, no. 13, pp. 1763-1783.

Zhou, H., Wu, S., Joo, J.Y., Zhu, S., Han, D.W., Lin, T., Trauger, S., Bien, G., Yao, S. & Zhu, Y. 2009, "Generation of induced pluripotent stem cells using recombinant proteins", *Cell stem cell,* vol. 4, no. 5, pp. 381-384.

Zhou, Y. & Zeng, F. 2013, "Integration-free methods for generating induced pluripotent stem cells", *Genomics, proteomics & bioinformatics,* vol. 11, no. 5, pp. 284-287.

Appendix

8.1 Testing specificity of CENP-A

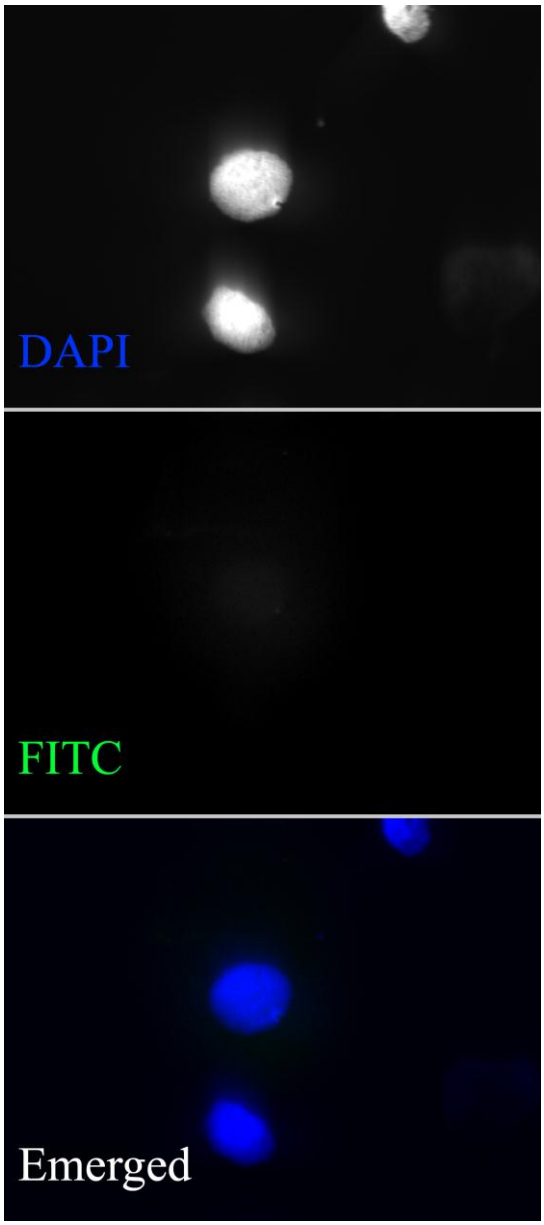

Figure 8:1 Testing specificity of CENP-A

The specificity of this antibody was confirmed by immunostaining of NT2 cells with the secondary antibody without incubate them with anti-CENP-A.

8.2 BLM siRNA target sequences:

Product name	Cat. No	Target sequenc	Gene ID
Hs_BLM_4	SI00000959	gacgctagacagataagttta	GS641
Hs_BLM_5	SI03033387	aagcgacatcaggagccaata	GS641
Hs_BLM_1	SI00000938	ccgaatctcaatgtacataga	GS641
Hs_BLM_2	SI00000945	ctgaccatctgtgactataaa	GS641

Homo sapiens Bloom syndrome, RecQ helicase-like (BLM), transcript variant 1, mRNA

NCBI Reference Sequence: NM_000057.3

Blue highlight is indicating alternate exons.

Yellow highlight is indicate siRNA sequence

AATCGGAATAGGCAAGCTTCCGGCGGGAAGTGAGCCAGGGCTTGGCGCGGCGGCCGTGGTTGCGGCGCGG
GAAGTTTGGATCCTGGTTCCGTCCGCTAGGAGTCTGCGTGCGAGGATTATGGCTGCTGTTCCTCAAAATA
ATCTACAGGAGCAACTAGAACGTCACTCAGCCAGAACACTTAATAATAAATTAAGTCTTTCAAAACCAAA
ATTTTCAGGTTTCACTTTTAAAAAGAAAACATCTTCAGATAACAATGTATCTGTAACTAATGTGTCAGTA
GCAAAAACACCTGTATTAAGAAATAAAGATGTTAATGTTACCGAAGACTTTTCCTTCAGTGAACCTCTAC
CCAACACCACAAATCAGCAAAGGGTCAAGGACTTCTTTAAAAATGCTCCAGCAGGACAGGAAACACAGAG
AGGTGGATCAAAATCATTATTGCCAGATTTCTTGCAGACTCCGAAGGAAGTTGTATGCACTACCCAAAAC
ACACCAACTGTAAAGAAATCCCGGGATACTGCTCTCAAGAAATTAGAATTTAGTTCTTCACCAGATTCTT
TAAGTACCATCAATGATTGGGATGATATGGATGACTTTGATACTTCTGAGACTTCAAAATCATTTGTTAC
ACCACCCCAAAGTCACTTTGTAAGAGTAAGCACTGCTCAGAAATCAAAAAAGGGTAAGAGAAACTTTTTT
AAAGCACAGCTTTATACAACAAACACAGTAAAGACTGATTTGCCTCCACCCTCCTCTGAAAGCGAGCAAA
TAGATTTGACTGAGGAACAGAAGGATGACTCAGAATGGTTAAGCAGCGATGTGATTTGCATCGATGATGG
CCCCATTGCTGAAGTGCATATAAATGAAGATGCTCAGGAAAGTGACTCTCTGAAAACTCATTTGGAAGAT
GAAAGAGATAATAGCGAAAAGAAGAAGAATTTGGAAGAAGCTGAATTACATTCAACTGAGAAAGTTCCAT
GTATTGAATTTGATGATGATGATTATGATACGGATTTTGTTCCACCTTCTCCAGAAGAAATTATTTCTGC
TTCTTCTTCCTCTTCAAAATGCCTTAGTACGTTAAAGGACCTTGACACCTCTGACAGAAAAGAGGATGTT
CTTAGCACATCAAAAGATCTTTTGTCAAAACCTGAGAAAATGAGTATGCAGGAGCTGAATCCAGAAACCA
GCACAGACTGTGACGCTAGACAGATAAGTTTACAGCAGCAGCTTATTCATGTGATGGAGCACATCTGTAA
ATTAATTGATACTATTCCTGATGATAAACTGAAACTTTTGGATTGTGGGAACGAACTGCTTCAGCAGCGG
AACATAAGAAGGAAACTTCTAACGGAAGTAGATTTTAATAAAAGTGATGCCAGTCTTCTTGGCTCATTGT
GGAGATACAGGCCTGATTCACTTGATGGCCCTATGGAGGGTGATTCCTGCCCTACAGGGAATTCTATGAA
GGAGTTAAATTTTTCACACCTTCCCTCAAATTCTGTTTCTCCTGGGGACTGTTTACTGACTACCACCCTA
GGAAAGACAGGATTCTCTGCCACCAGGAAGAATCTTTTTGAAAGGCCTTTATTCAATACCCATTTACAGA
AGTCCTTTGTAAGTAGCAACTGGGCTGAAACACCAAGACTAGGAAAAAAAAATGAAAGCTCTTATTTCCC
AGGAAATGTTCTCACAAGCACTGCTGTGAAAGATCAGAATAAACATACTGCTTCAATAAATGACTTAGAA
AGAGAAACCCAACCTTCCTATGATATTGATAATTTTGACATAGATGACTTTGATGATGATGATGACTGGG
AAGACATAATGCATAATTTAGCAGCCAGCAAATCTTCCACAGCTGCCTATCAACCCATCAAGGAAGGTCG
GCCAATTAAATCAGTATCAGAAAGACTTTCCTCAGCCAAGACAGACTGTCTTCCAGTGTCATCTACTGCT
CAAAATATAAACTTCTCAGAGTCAATTCAGAATTATACTGACAAGTCAGCACAAAATTTAGCATCCAGAA
ATCTGAAACATGAGCGTTTCCAAAGTCTTAGTTTTCCTCATACAAAGGAAATGATGAAGATTTTTCATAA

AAAATTTGGCCTGCATAATTTTAGAACTAATCAGCTAGAGGCGATCAATGCTGCACTGCTTGGTGAAGAC
TGTTTTATCCTGATGCCGACTGGAGGTGGTAAGAGTTTGTGTTACCAGCTCCCTGCCTGTGTTTCTCCTG
GGGTCACTGTTGTCATTTCTCCCTTGAGATCACTTATCGTAGATCAAGTCCAAAAGCTGACTTCCTTGGA
TATTCCAGCTACATATCTGACAGGTGATAAGACTGACTCAGAAGCTACAAATATTTACCTCCAGTTATCA
AAAAAAGACCCAATCATAAAACTTCTATATGTCACTCCAGAAAAGATCTGTGCAAGTAACAGACTCATTT
CTACTCTGGAGAATCTCTATGAGAGGAAGCTCTTGGCACGTTTTGTTATTGATGAAGCACATTGTGTCAG
TCAGTGGGGACATGATTTTCGTCAAGATTACAAAAGAATGAATATGCTTCGCCAGAAGTTTCCTTCTGTT
CCGGTGATGGCTCTTACGGCCACAGCTAATCCCAGGGTACAGAAGGACATCCTGACTCAGCTGAAGATTC
TCAGACCTCAGGTGTTTAGCATGAGCTTTAACAGACATAATCTGAAATACTATGTATTACCGAAAAAGCC
TAAAAAGGTGGCATTTGATTGCCTAGAATGGATCAGAAAGCACCACCCATATGATTCAGGGATAATTTAC
TGCCTCTCCAGGCGAGAATGTGACACCATGGCTGACACGTTACAGAGAGATGGGCTCGCTGCTCTTGCTT
ACCATGCTGGCCTCAGTGATTCTGCCAGAGATGAAGTGCAGCAGAAGTGGATTAATCAGGATGGCTGTCA
GGTTATCTGTGCTACAATTGCATTTGGAATGGGGATTGACAAACCGGACGTGCGATTTGTGATTCATGCA
TCTCTCCCTAAATCTGTGGAGGGTTACTACCAAGAATCTGGCAGAGCTGGAAGAGATGGGGAAATATCTC
ACTGCCTGCTTTTCTATACCTATCATGATGTGACCAGACTGAAAAGACTTATAATGATGGAAAAAGATGG
AAACCATCATACAAGAGAAACTCACTTCAATAATTTGTATAGCATGGTACATTACTGTGAAAATATAACG
GAATGCAGGAGAATACAGCTTTTGGCCTACTTTGGTGAAAATGGATTTAATCCTGATTTTTGTAAGAAAC
ACCCAGATGTTTCTTGTGATAATTGCTGTAAAACAAAGGATTATAAAACAAGAGATGTGACTGACGATGT
GAAAAGTATTGTAAGATTTGTTCAAGAACATAGTTCATCACAAGGAATGAGAAATATAAAACATGTAGGT
CCTTCTGGAAGATTTACTATGAATATGCTGGTCGACATTTTCTTGGGGAGTAAGAGTGCAAAAATCCAGT
CAGGTATATTTGGAAAAGGATCTGCTTATTCACGACACAATGCCGAAAGACTTTTTAAAAAGCTGATACT
TGACAAGATTTTGGATGAAGACTTATATATCAATGCCAATGACCAGGCGATCGCTTATGTGATGCTCGGA
AATAAAGCCCAAACTGTACTAAATGGCAATTTAAAGGTAGACTTTATGGAAACAGAAAATTCCAGCAGTG
TGAAAAAACAAAAAGCGTTAGTAGCAAAAGTGTCTCAGAGGGAAGAGATGGTTAAAAAATGTCTTGGAGA
ACTTACAGAAGTCTGCAAATCTCTGGGGAAAGTTTTTGGTGTCCATTACTTCAATATTTTTAATACCGTC
ACTCTCAAGAAGCTTGCAGAATCTTTATCTTCTGATCCTGAGGTTTTGCTTCAAATTGATGGTGTTACTG
AAGACAAACTGGAAAAATATGGTGCGGAAGTGATTTCAGTATTACAGAAATACTCTGAATGGACATCGCC
AGCTGAAGACAGTTCCCCAGGGATAAGCCTGTCCAGCAGCAGAGGCCCCGGAAGAAGTGCCGCTGAGGAG
CTCGACGAGGAAATACCCGTATCTTCCCACTACTTTGCAAGTAAAACCAGAAATGAAAGGAAGAGGAAAA
AGATGCCAGCCTCCCAAAGGTCTAAGAGGAGAAAAACTGCTTCCAGTGGTTCCAAGGCAAAGGGGGGGTC
TGCCACATGTAGAAAGATATCTTCCAAAACGAAATCCTCCAGCATCATTGGATCCAGTTCAGCCTCACAT
ACTTCTCAAGCGACATCAGGAGCCAATAGCAAATTGGGGATTATGGCTCCACCGAAGCCTATAAATAGAC
CGTTTCTTAAGCCTTCATATGCATTCTCATAACAACCGAATCTCAATGTACATAGACCCTCTTTCTTGTT
TGTCAGCATCTGACCATCTGTGACTATAAAGCTGTTATTCTTGTTATACCATTTGAAGTTTTTACTCGTC
TCTATTAATATTTAAATAAATGCTGGGGGGTGATAGTTCTTCTTTTTAAAATAAACATTTTCTTTTGAAT
AAGCA

8.3 Bloom protein half-life

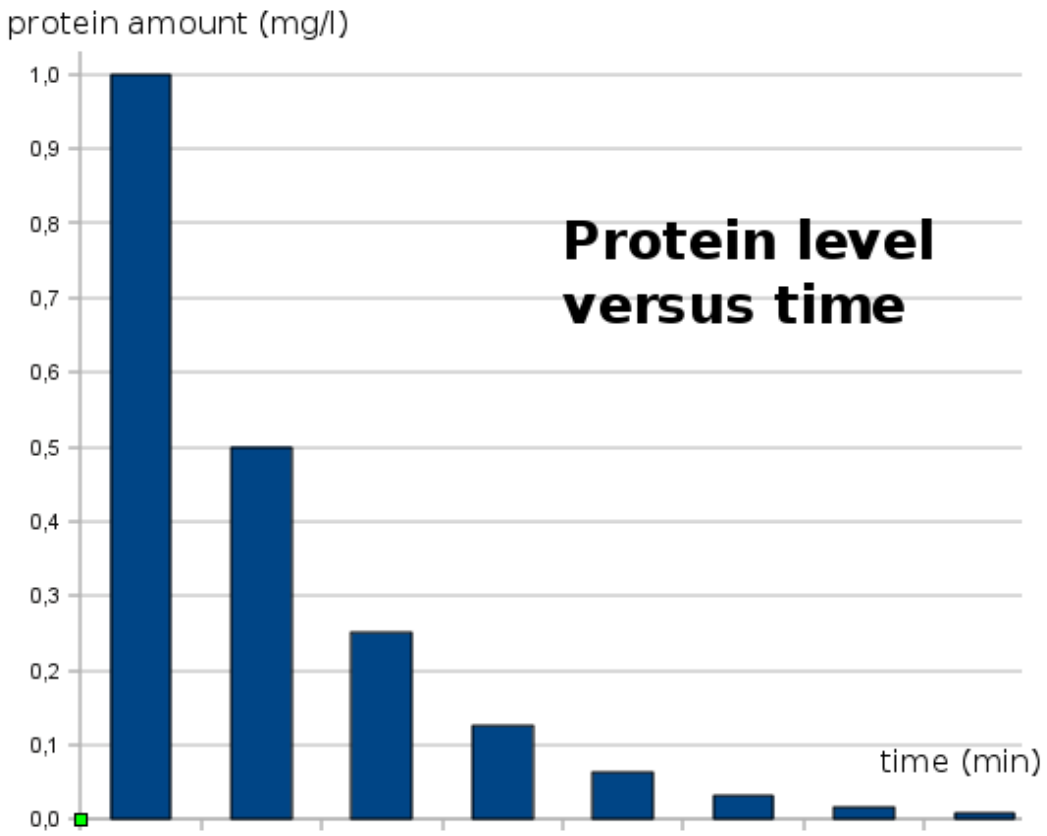

Figure 8:2 Bloom protein half-life

Bloom protein half-life was calcuated by ProtParam. It is a tool which allows the computation of various physical and chemical parameters for a given protein stored in Swiss-Prot or TrEMBL or for a user entered sequence.

Protein has 1417 amino acids.

Molecular mass: 161.83 kDa

Protein half-life is ~ 30 hour